Neuroprotection after perinatal asphyxia:

Mitochondrial and inflammatory targets

Hilde Bonestroo

Neuroprotection after perinatal asphyxia: mitochondrial and inflammatory targets
PhD thesis University of Utrecht, Utrecht, The Netherlands

Author	Hilde Joanne Charlotte Bonestroo
Cover	mus-atelier.nl
Layout/print	Gildeprint, Enschede
ISBN	978-90-393-6222-8

The publication of this thesis had been kindly supported by the Division of Perinatology, University Medical Center Utrecht, Gilles Hondius Foundation, Pfizer BV, Nutricia Benelux BV, ChipSoft BV, Toshiba Medical Systems Nederland, Chiesi Pharmaceuticals BV, BMA BV (Mosos), the Surgical Company, Noldus Information Technology BV and ABN Amro.

Neuroprotection after perinatal asphyxia:

Mitochondrial and inflammatory targets

Neuroprotectie na perinatale asfyxie:
mitochondriële en inflammatoire targets
(met een samenvatting in het Nederlands)

Proefschrift

ter verkrijging van de graad van doctor aan de Universiteit Utrecht
op gezag van de rector magnificus, prof. dr. G.J. van der Zwaan,
ingevolge het besluit van het college voor promoties
in het openbaar te verdedigen op
maandag 24 november 2014 des middags te 12.45 uur

door

Hilde Joanne Charlotte Bonestroo
geboren op 9 oktober 1984 te Heerlen

Promotoren:
Prof. dr. C.J. Heijnen
Prof. dr. F. van Bel

Copromotor:
Dr. C.H.A. Nijboer

Financial support by the Dutch Heart Foundation for the publication of this thesis is gratefully acknowledged.

Voor mijn kleine en grote held

Contents


HI

1

General introduction

Perinatal asphyxia or neonatal hypoxia-ischemia (HI) is a severe condition and defined as a period of insufficient blood gas exchange leading to progressive hypoxia, hypercapnia, metabolic and/or respiratory acidosis and eventually ischemia before during or early after birth. It is one of the primary causes of early neonatal mortality worldwide. The prevalence of neonatal HI is about 2-6 per 1000 live term births in Western countries. Neonatal HI results in death or severe adverse outcome in 1-2 per 1000 live term births. In less-developed countries the incidence is much higher and results in more than 900.000 deaths each year.[1-4]

Neonatal HI affects different organ systems and can cause *e.g.* myocardial ischemia, persistent pulmonary hypertension, acute tubular necrosis, disseminated intravascular coagulation and/or necrotizing enterocolitis. However, due to its high metabolic rate and energy need, the brain is one of the most vulnerable organs with limited regenerative capacity and HI can cause severe neonatal encephalopathy.[5,6] Neonatal encephalopathy causes severe morbidity in surviving children, with life-lasting neurological disabilities that have an enormous impact on the child, family and society.[7] A wide range of disorders can cause neonatal encephalopathy and the designation hypoxic-ischemic encephalopathy (HIE) is only used when a clear HI insult causes the encephalopathy. Despite the wide range of animal studies exploring new therapeutic approaches for neonatal HIE, currently the only standard care for HIE in humans is hypothermia (see below). Further research to decipher the pathophysiological pathways involved in the development of HIE is crucial, because this will lead to development of new therapeutic treatments and better prospects for patients affected by this severe illness.

In this thesis, by using experimental animal models of neonatal HI, we focus on 1) the mechanisms contributing to neonatal HIE, especially the influence of inflammation and apoptotic cell death and 2) promising neuroprotective strategies to combat neonatal HIE by protecting mitochondrial integrity.

This thesis will start with an introduction on the clinical background of neonatal HIE, followed by the underlying mechanisms involved in the development of brain damage after neonatal HI, promising treatment options and information about the animal models used in this thesis. The introduction will conclude with the outline of this thesis.

Clinical Background

Clinical presentation

Neonatal HI can be diagnosed shortly after birth based on several criteria: 1) the persistence of a low Apgar score ($\leq$ 3) for more than 5 min postpartum which is composed of a score for activity (muscle tone), pulse (higher or lower than 100 beats per min), reflex irritability (grimas), appearance (skin color) and respiration (strong/crying, irregular/gasping or absent) at 1, 5 and 10 min postpartum,[8] 2) a blood pH less than 7.00, and base excess smaller than -12 mmol/L assessed in umbilical arterial cord blood; 3) a lactate higher than 10 mmol/L; 4) the need for ventilation for more than 10 min; 5) resuscitation directly postpartum; and

6) moderate to severe encephalopathy or multi-organ system dysfunction. Furthermore, neonatal HI can be suspected after a history of fetal distress (*e.g.* decelerating fetal heart rate, meconium-stained amniotic fluid) or a clear sentinel event during labor (*e.g.* uterus rupture, placental abruption, birth trauma).[3, 9] These criteria are especially useful to assess the condition of the baby directly after birth, however, they have poor predictive value for long-term outcome.

Clinical signs of encephalopathy following neonatal HI appear within 7 days postpartum and consist of respiratory problems with signs of periodic breathing with apneas or bradycardia, feeding difficulties, an altered muscle tone (hypotonia), absent primary reflexes, decreased consciousness and often seizures.[10,11] HIE can be classified into 3 stages: mild, moderate and severe according to the criteria of Sarnat and Sarnat modified by Fenichel (Table 1).[11,12] Although there is a strong relation between the severity of neonatal HIE and neurodevelopmental outcome, the prognosis in especially newborns with moderate HIE is hard to predict since there is a wide range of motor and cognitive outcomes observed in these children.[7,9,11,12]

Table 1: Classification for hypoxia-ischemia induced encephalopathy

Symptoms	Stage 1: Mild	Stage 2: Moderate	Stage 3: Severe
Duration	< 24 hours	2 - 14 days	hours - weeks
Consciousness	(hyper)alert/irritability	lethargy	stupor/coma
Muscle tone	normal/hypertonia	hypotonia	flaccidity
Stretch reflexes	increase	increase	decrease/absent
Myoclonus	present	present	absent
Suck reflex	weak	weak/absent	absent
Moro reflex	normal/exaggerated	incomplete	absent
Oculovestibular reflex	normal	overactive	weak/absent
Heart rate	increase	decrease	variable
Respiration	tachypnea	occasional apnea	severe apnea
Seizures	none	present	frequent

Risk factors

Several potential risk factors for the development of neonatal HI have been identified and these factors can be divided into prepartum, intrapartum and postpartum risk factors. Prepartum factors that increase the risk of neonatal HI are *e.g.* maternal disease like hypotension or hypertension, hypothyroidism, diabetes, intrauterine growth retardation, chorioamnionitis, chronic villitis, prolonged rupture of membranes, placental insufficiency, gestational age >42 weeks or multiple gestation. Intrapartum risk factors consist of placental abruption, uterus rupture, abnormal uterine contractions, umbilical cord compression, umbilical cord prolapse or knot, birth trauma, persistent occipito-posterior presentation, maternal fever or conditions that cause a decrease in maternal blood pressure or oxygenation of the maternal blood during labor. Examples of postpartum factors are severe neonatal respiratory distress, cardiac failure, sepsis or shock. The causes of neonatal HIE are often heterogeneous and frequently

there is no clear evidence of an (intrapartum) insult detectable. However, most insults are related to prepartum and/or intrapartum events, postpartum events occur in less than 10% of the cases.[13-18]

Patterns of brain damage

Besides the duration and the severity of the HI incident, the timing of the insult is an important factor that influences the pattern of brain damage and clinical outcome. Depending on the maturational stage of the brain, different patterns of cerebral damage are observed. In near- or full-term infants an acute severe HI insult mainly induces damage to the central gray nuclei, the basal ganglia and thalamus, hippocampus and brain stem. Cerebral injury is located bilaterally in most cases with relative cortical sparing. A moderate HI insult more often induces cortical and white matter injury in the watershed areas.[10,19] In preterm infants, HI-induced brain damage is mostly characterized by focal or diffuse white matter injury (periventricular leukomalacia) or periventricular hemorrhagic infarction (PVHI) and only in more severe cases the overlying cortex is also affected.[19,20] Preterm infants are more susceptible to white matter injury due to the fact that myelination is still underdeveloped and the immature oligodendrocyte precursors are more vulnerable for HI-induced excitotoxicity, free radical attack and inflammation than mature oligodendrocytes.[5,21-24]

Neurodevelopmental outcome

As mentioned before, HIE is associated with a high mortality and morbidity. Severe prepartum or intrapartum insults can lead to fetal death *in utero* or during delivery (stillbirths) and these numbers are mostly not included in the estimation of the incidence of birth asphyxia. After birth approximately 20% of the affected newborns die in the neonatal period, mostly within the first week after birth. Of the surviving infants over 25% have long-lasting motor and/or cognitive deficits. Newborns with a severe grade of HIE have a worrisome prognosis; these children will either die or develop severe disabilities like spastic cerebral palsy, severe developmental delay, mental retardation, neural deafness, cortical blindness and/or epilepsy. Short-term follow-up studies showed that following moderate neonatal HIE, 32% of the infants have an adverse outcome (death, cognitive and/or sensori-motor impairments), while those with a mild stage HIE appear to have quite normal neurocognitive outcome.[25] However, data on long-term outcome have shown that also following moderate HIE more than 80% of the infants developed cognitive deficits and/or difficulties in behavior (regardless of motor impairment). Examples of cognitive deficits are impairments in language, attention, planning, memory and visual motoric and perceptive dysfunction. Furthermore, a relation between HIE and psychological problems like attention-deficit hyperactivity disorder (ADHD), autism and schizophrenia have been suggested.[25-31]

As a clinical assessment to differentiate between good and poor outcome within the first hours after birth, nowadays the Thompson score is used. This score is based on the Sarnat and Sarnat criteria. However, on its own the Thompson score based on clinical

symptoms is not very reliable for predicting long-term outcome, especially not in moderately affected neonates.[32] To establish the degree of neonatal HIE and to predict long-term neurodevelopmental outcome several diagnostic tools can be used. The most important neuroimaging and electro-physiologic methods that provide prognostic information are magnetic resonance neuroimaging (MRI), magnetic resonance spectroscopy (MRS), cranial ultrasound, continuous amplitude-integrated electroencephalogram (aEEG) monitoring and near-infrared spectroscopy (NIRS).[33,34]

Neurodevelopmental outcome after HIE is strongly dependent on the patterns of injury observed with neonatal MRI. Lesions in the basal ganglia and thalami are associated with severe motor and learning disabilities and epilepsy, whereas children with a watershed pattern of injury show a much better outcome, although behavioral problems and impaired cognition are common.[35,36] Long-term follow-up of children with neonatal encephalopathy is important for the assessment and support of neurodevelopment, cognitive and behavioral problems that may become visible later in life.

The focus of the second part of this introduction will be on the complex mechanisms underlying the development of brain injury following HI. This part of the introduction is based on several important reviews.[10,37-49]

Pathophysiological mechanisms

The (newborn) brain has an extremely high energy need compared to other organs, making the brain more sensitive for a reduction in oxygenation. Glucose is the main energy source of the brain and since the brain cannot store its energy, it requires a continuous supply of glucose. Glucose is mainly metabolized during aerobic glycolysis, in which glucose is converted into pyruvate. Subsequently in the mitochondria, pyruvate is metabolized to acetyl-CoA that can enter the citric acid cycle. Eventually, energy (adenosine triphosphate (ATP)) is formed in the mitochondrial respiratory chain during oxidative phosphorylation.

During neonatal HI the essential processes of oxygen and glucose supply to the brain and the possibility to produce ATP are strongly disrupted. HIE is not induced by a single event but is a process that evolves over time. Different mechanisms are involved in the primary and secondary phases of cerebral damage after HI.

Primary phase of injury

During a HI insult the decrease in oxygen results in a cascade of biochemical intracellular events, including a reduction in oxidative phosphorylation in the mitochondria and a decrease in high energy phosphate levels. To compensate for the decreased energy levels, glycogenolysis is stimulated and anaerobic glycolysis takes place, resulting in a rapid decline in brain glucose and glycogen concentrations, with a concomitant increase in lactate levels and decrease in pH. The decrease in ATP results in disturbance of normal energy-dependent

homeostatic functions, like the ATP-dependent Na^+-K^+ channel. Under basal conditions the Na^+-K^+ channels are responsible for maintaining a negative cell membrane potential, which is essential for normal cellular functions. A decrease in ATP levels therefore affects cell membrane function and membrane depolarization, leading to three closely interrelated events involved in neuronal cell death during the primary phase of injury. Firstly, membrane depolarization causes influx of Na^+ and Cl^- ions into the cytoplasm followed by water entry, cell edema and cell lysis. Secondly, voltage-sensitive Ca^{2+} channels open with an increased influx of Ca^{2+} ions into the cytoplasm and decreased removal of Ca^{2+} by the Na^+-Ca^{2+} pump; and thirdly membrane depolarization leads to release of presynaptic glutamate (an excitotoxic neurotransmitter) into the synaptic cleft. Moreover, the extracellular levels of glutamate are increased due to impaired removal of glutamate from the synaptic cleft by astrocytes and presynaptic nerve terminals. The accumulation of extracellular glutamate causes activation of *N*-methyl-D-Aspartate (NMDA) channels, α-amino-3-hydroxy-5-methyl-4-isoxazole-propionic acid (AMPA) and kainate receptors, and opening of Na^+-K^+ channels which contributes to acute cell swelling. Besides, it induces intense NMDA receptor-mediated seizure activity, increases metabolism and creates an imbalance in cell metabolism and blood circulation. Additionally, the activation of NMDA and AMPA receptors further increases Ca^{2+} influx into the cell. The increase in intracellular Ca^{2+} activates a plethora of Ca^{2+}-dependent enzymes like proteases, phospholipases and endonucleases, leading to the proteolytic degradation of multiple cellular structures. Thereby, Ca^{2+} plays an important role in the formation of reactive oxygen species (ROS) in the mitochondria. All these factors contribute to cellular damage, and if severe enough, to cell death. However, most of the injury after neonatal HI evolves in the secondary phase of injury.

Secondary phase of injury

Secondary energy failure is started 6-48 h after the acute HI insult, creating a time window of opportunity (therapeutic window) for protective treatments. Restoration of blood flow and reoxygenation after HI is of course necessary to limit the amount of cerebral damage. However, the reperfusion period is also responsible for an exacerbation of cell damage, known as reperfusion injury. The mechanisms involved in this phase mainly include the formation of ROS, an inflammatory response and persistent glutamate excitotoxicity and all these factors can eventually contribute to delayed apoptotic cell death.

Formation of reactive oxygen species

During the neonatal HI insult the increase in intracellular Ca^{2+} is involved in the formation and accumulation of superoxide, hydrogen peroxide (H_2O_2) and activation of nitric oxide synthases (NOS). NOS is an enzyme responsible for the generation of the highly neurotoxic reactive oxygen molecule nitric oxide (NO). ROS possess an unpaired electron leading to donation of electrons from/to other molecules and induction of damage. The increased oxygen levels during reperfusion are accompanied by leakage of superoxide from damaged mitochondria

which interact with NO resulting in the generation of peroxynitrite (ONOO-), an even more potent neurotoxic ROS. ROS can oxidize cellular components for example membrane lipids, proteins, and DNA resulting in additional cellular damage and accumulation of mitochondrial injury. The released free fatty acids are involved in activation of cyclooxygenase (COX), implicated in the formation of prostaglandins and subsequently ROS. In addition, the HI-induced decrease in pH and damage to iron-binding proteins results in the accumulation of non-protein bound or free iron. Free iron can react with superoxide in the Fenton reaction, producing the highly toxic hydroxyl radical ($OH^{\cdot}$).
In conclusion, the neonatal brain is very sensitive to oxidative damage due to high oxygen consumption, low levels of anti-oxidant defense enzymes (for example glutathione peroxidase and catalase), high concentration of unsaturated fatty acids and high availability of free redox-active iron involved in production of ROS.

Inflammation

Another key phenomenon in the secondary phase of injury is neuroinflammation consisting of, activation of resident glial cells, influx of inflammatory cells in the brain and production of inflammatory molecules. The increase in intracellular Ca^{2+}, ROS formation and hypoxia all contribute to the activation of different transcription factors *e.g.* nuclear factor-κB (NF-κB), c-Jun N-terminal kinase (JNK), hypoxia inducible factor 1 (HIF-1) and interferon regulatory factor 1 (IRF-1). These transcription factors regulate the expression of many inflammatory target genes and thereby cell death and survival. The inflammatory response following neonatal HI is characterized by a time-dependent activation of microglia and astrocytes, influx of neutrophils, recruitment of macrophages/monocytes, T cells, excretion/upregulation of cytokines and chemokines by activated and damaged cells and activation of the complement pathway.

Glial cells

Microglia, the resident macrophages of the brain and spinal cord are important first line immune cells in the central nervous system and are involved in maintaining homeostasis. Microglia protect the brain from injury by destroying bacteria, clearing cellular debris, and repairing tissue. However, uncontrolled activation of microglia can cause damage to neighboring neurons and oligodendrocytes. In the early phase of HI, microglia/macrophages are the main source of cytotoxic molecules, like pro-inflammatory cytokines, chemokines, reactive oxygen species, proteases, complement factors and excitotoxic neurotransmitters. When microglia are in a pro-inflammatory state they are designated as M1-type microglia. Within a few days, peripheral macrophages and monocytes migrate into the damaged area further increasing the inflammatory response. In a later phase of HI microglia/macrophages are involved in phagocytosis of neutrophils, promotion of repair by the secretion of anti-inflammatory cytokines and growth factors, and by inhibition of the production of NO and pro-inflammatory cytokines. In this later phase of HI, microglia express an anti-inflammatory M2 phenotype.

Astrocytes, another type of glial cells, play a crucial role in the brain. These cells are key in regulating *e.g.* secretion/absorption of neurotransmitters, transmission of electrical impulses, maintenance of the blood-brain-barrier (BBB), providing nutrients to neuronal tissue and are involved in glial scar formation after damage. After neonatal HI reactive astrocytes are also an important source of pro-inflammatory cytokines that affect neurons.

Neutrophilic granulocytes and lymphocytes

Due to an increased expression of adhesion molecules on endothelial cells (*e.g.* P-, E-selectin, inter-cellular adhesion molecule 1 (ICAM-1)) and excretion of chemokines by damaged and activated local cells, neutrophilic granulocytes (polymorphonuclear leukocytes or neutrophils) are activated and move from the circulation into the ischemic area within 6 hours post-HI. Locally-produced cytokines in the damaged area further activate these neutrophils. Neutrophils are important immune cells that can phagocytose micro-organisms and particles. However, when activated they also synthesize ROS and pro-inflammatory cytokines and chemokines that can aggravate cerebral damage. Moreover, neutrophils can increase ischemic damage by microvascular obstruction.

The recruitment of lymphocytes (predominantly T-cells) to the injured brain takes place in a later stage after HI, starting within 1-2 weeks and still present 3 months post-insult. The exact contribution of lymphocytes to neonatal HI brain injury is not clear; cytotoxic $CD8^+$ T-cells are thought to induce brain damage by releasing cytotoxic granules, whereas $CD4^+$ T-helper 1 and 2 cells can modulate the cerebral inflammatory response by producing pro- and anti-inflammatory cytokines.

Cytokines and chemokines

After neonatal HI, activated and damaged cells present in the brain *e.g.* microglia, astrocytes, neutrophils, neurons and endothelial cells produce pro-inflammatory cytokines like tumor necrosis factor (TNF)-α and interleukin (IL)-1 and -6. These cytokines can affect the brain by inducing direct harm to oligodendrocyte (precursors) and neuronal cells, by activating astrocytes and microglia, enhancing glutamate excitotoxicity and inducing necrotic or apoptotic cell death. Anti-inflammatory factors (IL-4, -10 and transforming growth factor (TGF)-β) are molecules that can antagonize the pro-inflammatory response. Furthermore, the above mentioned activated cells also release chemokines, (for example cytokine-induced neutrophil chemoattractant (CINC-)1 and monocyte chemotactic protein (MCP)-1), which are signal molecules responsible for the recruitment of peripheral immune cells (*e.g.* neutrophils and macrophages/monocytes) into the damaged brain.

Complement

The complement system is an important part of innate immunity, consisting of a number of circulating and membrane-bound small proteins. Complement activation occurs via three pathways: the classic, alternative and lectin pathways. Activated complement proteins

are important in the defense against invading pathogens by inducing opsonization (C3b), chemotaxis (C3a, C5a), cell lysis (membrane attack complex C5b-C9) and agglutination of pathogens. Interestingly, complement activation is also observed in blood, cerebral spinal fluid and cerebral post-mortem tissue of neonates who suffered from neonatal HIE.[50-52] Activated complement proteins amplify the inflammatory response and can induce direct damage to cerebral tissue, thereby aggravating HI brain damage.[53]

In conclusion, the inflammatory response which is activated after neonatal HI has a dual role: it is necessary for clearance of damaged and death cells, initiating growth, repair and neurogenesis and thereby contributes to limitation of cerebral damage. However, the cerebral immune response can also contribute to exacerbation of damage after neonatal HI by *e.g.* activation and recruitment of peripheral immune cells towards the site of injury and the production of neurotoxic molecules.

Apoptotic cell death

Apoptosis is a strictly regulated, balanced, energy-requiring process which is essential for normal brain development since it refines cellular connections.[54] Apoptosis is characterized by blebbing, cell shrinkage, chromatin condensation, DNA and nuclear fragmentation. The cellular membrane remains intact until the last stage of cell death, which is in clear contrast to cell death via necrosis. Ultimately apoptotic cells are removed by phagocytic cells. A neonatal HI insult results in a disturbance of the apoptotic balance with a major increase in neuronal cell death. Cysteine-dependent aspartate-specific proteases (caspases) play a central role in transducing apoptotic signals and eventually causing the degradation of cellular organelles via proteolysis/cleavage of different essential cellular structures.[55] Apoptosis can be activated via an extrinsic or intrinsic route (Fig 1).

Intrinsic route of apoptosis

The intrinsic route of apoptosis or the mitochondria-mediated pathway is activated after DNA damage or other types of cellular stress, for example hypoxia. A severe HI insult results in an increase in mitochondrial outer membrane permeability (MOMP) which leads to release of mitochondrial apoptotic effector molecules from the inside of mitochondria into the cytosol. Examples of these molecules include cytochrome *c,* apoptosis-inducing factor (AIF) and Smac/DIABLO (second mitochondria-derived activator of caspases/direct inhibitor of apoptosis protein-binding protein with Low PI). Cytochrome *c*, when released into the cytosol, binds to apoptotic protease activating factor-1 (Apaf-1), ATP and pro-caspase 9 leading to the formation of the apoptosome that results in cleavage and activation of pro-caspase 9 and downstream activation of the effector/executioner caspase 3. Effector caspases 3 and 6 activate caspase activated DNAses (CADs) which are responsible for cleavage of cellular structures leading to DNA fragmentation, membrane blebbing and cell shrinkage leading to cell death. AIF, when released from the mitochondria by *e.g.* poly (ADP-ribose) polymerase (PARP-1) is translocated directly to the nucleus and induces fragmentation of nuclear DNA

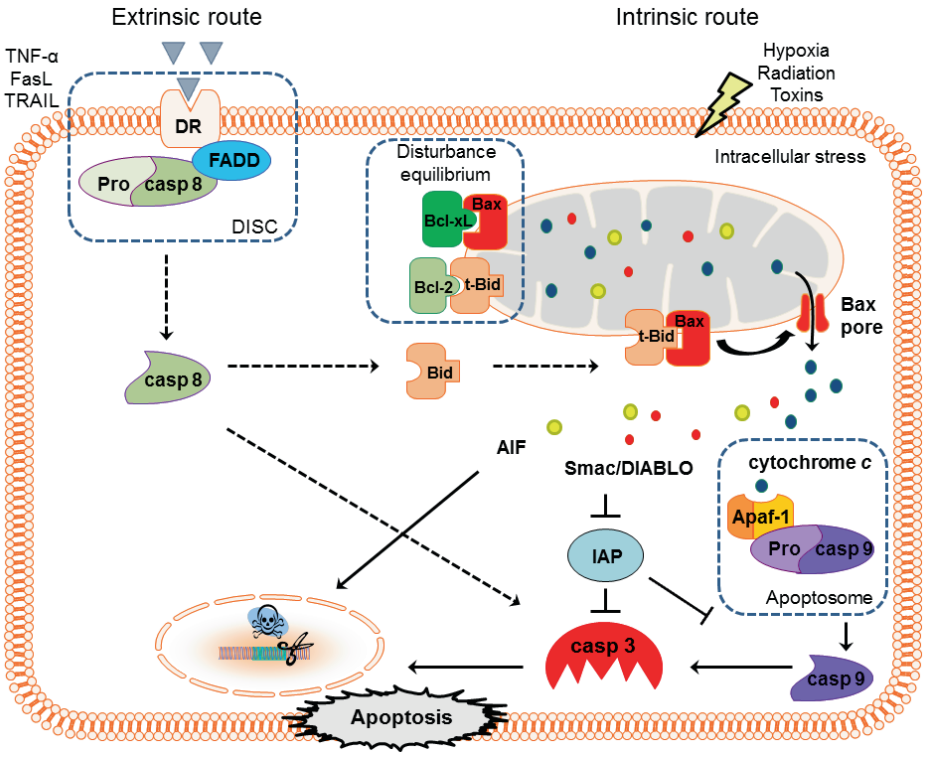

Figure 1: Schematic diagram of the extrinsic and intrinsic routes of apoptosis
Apoptotic cell death can be activated via two main routes: 1) the extrinsic or death receptor-mediated pathway is activated after binding of death ligands (TNF-α, FasL and TRAIL are depicted as examples) to death receptors. Downstream of the activated death receptor the DISC is formed consisting of the death receptor, FADD and pro-caspase 8. As a result caspase 8 is cleaved/activated which subsequently activates caspase 3. Additionally, cleaved caspase 8 activates the intrinsic apoptotic pathway via cleavage of Bid into t-Bid (truncated Bid). 2) The intrinsic or mitochondria-mediated pathway is activated after stress stimuli that disturb the balance between mitochondrial anti- and pro-apoptotic proteins (*e.g.* Bcl-xL/Bcl-2 and t-Bid/Bax respectively), which under basal conditions form dimers. Tipping over the balance to a pro-apoptotic state leads to mitochondrial outer membrane permeability, *e.g.* by Bax pore formation, with the subsequent release of mitochondrial apoptotic effector molecules (cytochrome *c*, Smac/DIABLO and AIF are depicted as examples) into the cytosol that either activate caspase 3 (cytochrome *c* and Smac/DIABLO) or have caspase-independent nuclear effects (AIF). As depicted both pathways result in caspase 3 activation, which executes apoptosis by activating DNAses. The dotted black lines represent the extrinsic route, whereas the straight black lines represent the intrinsic route.
AIF: apoptosis-inducing factor; Apaf-1: apoptotic protease activating factor-1; Casp: caspase; DISC: death-inducing signaling complex; DR: death receptor; FADD: Fas associated death domain; FasL: Fas ligand; IAP: inhibitor of apoptosis protein; Smac/DIABLO: second mitochondria-derived activator of caspases/direct inhibitor of apoptosis protein-Binding protein with low PI; TRAIL: TNF related apoptosis-inducing ligand.

in a caspase *independent* manner.[48,55] Another factor released from the mitochondrium is Smac/DIABLO which binds and deactivates inhibitor of apoptosis proteins (IAPs) which are endogenous inhibitors of caspases, thereby indirectly promoting apoptosis.

Extrinsic route of apoptosis

The extrinsic or receptor-mediated apoptotic pathway signaling starts at the cellular membrane. The pro-inflammatory cytokine TNF-α, first apoptosis signal (Fas) ligand and TNF-related apoptosis-inducing ligand (TRAIL) play a key role in binding and activating cell surface death receptors (TNF-R1, Fas, DR4, DR5) causing the formation of the death-inducing signaling complex (DISC) on the intracellular site of the receptor. Subsequently, DISC activates a cascade of intracellular events including the proteolytic cleavage and activation of pro-caspase 8 into caspase 8 and activation of downstream caspase 3, caspase 6, caspase 7. Furthermore caspase 8 can activate the intrinsic apoptotic pathway by cleavage of Bid into truncated Bid (t-Bid), a Bcl-2 family member (see below) which is involved in mitochondrial membrane permeability.

Mitochondrial outer membrane permeability (MOMP)

The process of MOMP is affected by different apoptotic proteins that target the mitochondria, causing the formation of pores in the outer mitochondrial membrane. These pores increase MOMP and leakage of mitochondrial apoptotic proteins into the cytosol. The formation of pores in the outer mitochondrial membrane is regulated by several proteins, encoded by the Bcl-2 family. Pro-apoptotic proteins that promote pore formation are Bax, Bid, Bak and Bad, while anti-apoptotic Bcl-2 and Bcl-xL inhibit pore formation.[56]

During and after neonatal HI various transcription factors regulate the expression of target genes involved in cell death following HI. In this thesis, we will focus on two important proteins involved in the regulation of apoptotic cell death: transcription factor p53 and the mitogen activated protein kinase (MAPK) JNK.

p53

p53 is a tumor suppressor protein, which regulates expression of proteins associated with growth control, cell cycle checkpoints and apoptosis. p53 protein levels are strongly upregulated as a result of various injuries *e.g.* oxidative stress, Ca^{2+} overload, hypoxia and DNA damage. After HI, p53 is upregulated and accumulates in the nucleus and mitochondrium, thereby activating apoptotic cell death at multiple levels. Nuclear p53 can induce apoptosis by transactivating pro-apoptotic genes (PUMA, Noxa, Bax) and inhibiting transcription of anti-apoptotic genes of the Bcl-2 family. Furthermore, we have shown before that HI triggers the translocation of p53 to the mitochondria where it promotes MOMP by inducing mitochondrial translocation and activation of Bax and inhibits activity of Bcl-2/Bcl-xL in a transcription-independent manner.[57-63]

c-Jun N-Terminal Kinase (JNK) pathway

JNK (also termed stress-activated protein kinase) is a member of the MAPK family consisting of numerous protein kinases (*e.g.* ERK, p38), involved in the regulation of cell growth, proliferation, differentiation and apoptosis. When a cell is stressed, for example after neonatal HI, the JNK MAPK pathway is activated and JNK is phosphorylated by its upstream MAPKK-4 and -7. JNK can only be phosphorylated when it is bound to one of its scaffold proteins, for example JNK-interacting protein (JIP). There are 3 isoforms of JNK (JNK1-3), JNK1 and 2 are widely expressed, whereas JNK3 is mainly expressed in the brain. JNK itself phosphorylates/activates more than 50 nuclear and non-nuclear substrates involved in *e.g.* inflammation and apoptosis. One of these substrates is c-Jun, the dominant component of the transcription factor activator protein 1 (AP-1), which regulates expression of multiple genes, including several pro-apoptotic genes (*e.g.* TNF-α, Fas-L, Bak). Furthermore, JNK can induce apoptosis via 1) cleavage of the pro-apoptotic protein Bid into t-Bid which at its turn translocates to the mitochondria, activates Bax pore formation and MOMP; 2) phosphorylation of pro-apoptotic proteins Bim and Bad, causing them to bind to and thereby inhibit the anti-apoptotic properties of Bcl-xL and Bcl-2, which subsequently activates Bax pore formation, and 3) phosphorylation of anti-apoptotic Bcl-2 and Bcl-xL, thereby reducing the interaction with their pro-apoptotic partners. In addition, JNK is involved in phosphorylation of p53 and thereby reduces degradation of p53. This JNK-mediated increased stability of p53 contributes to apoptotic cell death (For an overview of the subcellular functions of the JNK pathway after HI see Fig 2).[64-67]

Necroptosis

In the past decades, apoptosis was looked upon as the one and only form of programmed cell death and necrosis as an uncontrolled unregulated form of cell death. However, it has been suggested that in the presence of an increased amount of caspase inhibitors (induced by severe mitochondrial dysfunction and ATP depletion) activation of death receptors does not result in apoptosis but in a phenomenon called necroptosis, or programmed cell necrosis. After activation of death receptors in a severe energy-insufficient environment a receptor interacting protein (RIP)-1/RIP-3 complex is formed, which is called the necrosome. The necrosome promotes the production of mitochondrial ROS that attack the mitochondrial, lysosomal and plasma membranes, resulting in cell death with coexisting morphological and biochemical characteristics of necrosis and apoptosis (*i.e.* chromatin organized in regular aggregates, partial dissolution of the nuclear membrane, preservation of the cytoplastic membrane with condensed cytoplasma, with or without swelling of cytoplasmatic organelles).[68-70] Inhibition of RIP-1 kinase activity by necrostatin-1 provides cerebral neuroprotection following neonatal HI in the mouse model.[69] Further research is necessary to clarify the role and importance of necroptosis in neonatal HI-induced brain damage.

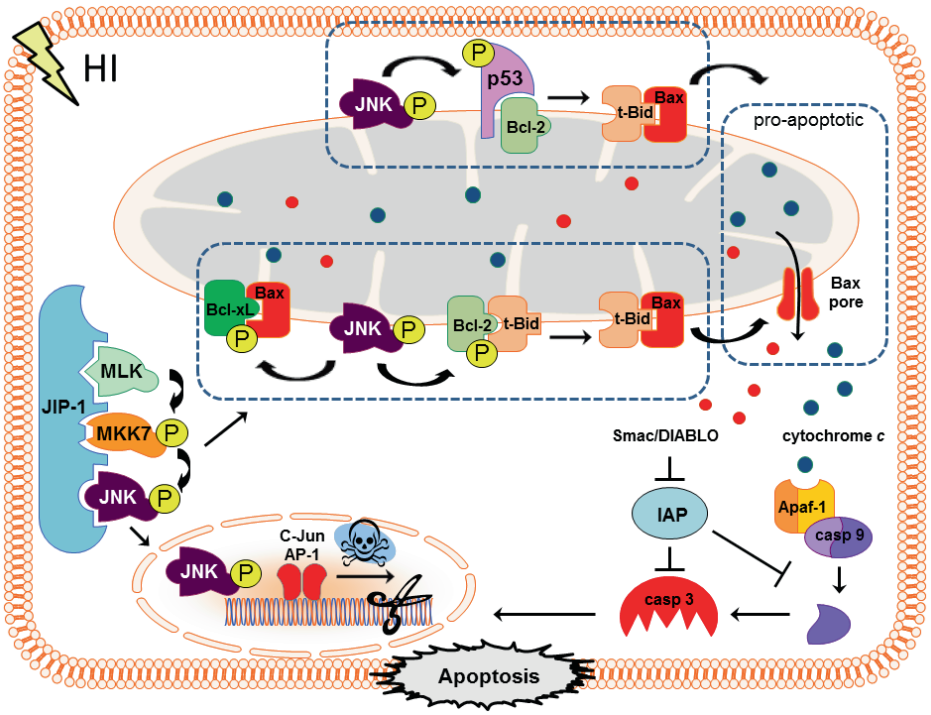

Figure 2: Overview of the subcellular functions of the JNK pathway after HI
JNK is a member of the mitogen activated protein kinase (MAPK) family that is activated by different cellular stressors. Phosphorylation/activation of JNK is regulated via two upstream kinases that bind together with JNK to the scaffold protein JIP-1 (left). Activated JNK can phosphorylate multiple proteins of which several examples are shown in this figure. In the nucleus, JNK can phosphorylate c-Jun, which is part of the transcription factor AP-1 dimer, thereby regulating transcription of multiple genes involved in *e.g.* inflammation and apoptosis. At the mitochondria activated JNK can induce apoptosis by phosphorylation of anti- and pro-apoptotic mitochondrial proteins (lower part of mitochondrium) and the presumed phosphorylation of p53 (upper part of mitochondrium). Both effects of JNK at mitochondrial level promote Bax pore formation and activation of the intrinsic apoptotic pathway (see also figure 1).
AP-1: activator protein 1; Apaf-1: apoptotic protease activating factor-1; Casp: caspase; HI: hypoxia-ischemia; IAP: inhibitor of apoptosis protein; JIP-1: JNK interacting protein-1; JNK: c-Jun N-terminal kinase; MKK: mitogen activated protein kinase kinase; MLK: mitogen activated protein kinase kinase kinase; P: phosphorylation; Smac/DIABLO: second mitochondria-derived activator of caspases/direct inhibitor of apoptosis protein-Binding protein with low PI.

Therapeutic options

HI brain damage evolves over time in a period of hours to weeks which creates a window of opportunity. However, therapeutic options to improve the outcome of neonates who suffer from HIE are still very limited. Supportive care consists of adequate respiratory support, optimizing blood gases and blood pressure, normalizing fluid-electrolyte balance and blood glucose levels, and treatment of seizures. Currently, hypothermia is the only established neuroprotective intervention with modest protective effect if started within 6 hours after the insult.

Hypothermia

During hypothermia the body temperature is decreased to 33-34 °C for 72 hours. Hypothermia has to be started before the development of the secondary phase of injury, suggesting a potential time window for treatment up to 6 hours post-insult.[71] There are two methods to induce hypothermia: selective head cooling (using a cap with circulating cold water) or total body cooling (using a cooling blanket or mattress wrapped around the child's body, circulated with cold air). Hypothermia is associated with a modest reduction in neurological impairment and improvement in survival in moderately but not severely-affected infants following neonatal HI.[72-77] Hypothermia is thought to be neuroprotective via reducing a broad number of cellular processes involved in the secondary phase of injury and cell death evoked by HI. Proposed neuroprotective mechanisms are a reduction in cerebral metabolism and oxygen consumption, a reduction in free radical levels and NO efflux, a decrease in excitatory amino acids, prevention of intracellular ion and water entry, a reduction in apoptotic cell death and suppression of the secondary inflammatory cascade.[78] Hypothermia is a relatively safe treatment; the main observed adverse effects are bradycardia and thrombocytopenia.[72-74] However, since hypothermia only provides a partial protective effect when started within 6 hours following moderate neonatal HI, the development of additional therapies is of crucial importance. A selection of promising strategies for experimental neonatal HI is provided in short below.[38,55,77,79-83]

Glutamate inhibitors and calcium blockers

Increased levels of extracellular glutamate and intracellular Ca^{2+} are key processes in the development of injury after neonatal HI, as mentioned above. Reduction in glutamate excitotoxicity could therefore be a promising strategy. Magnesium and Xenon (a noble anesthetic gas) are NMDA receptor antagonists; both have neuroprotective properties in different neonatal HI animal models.[84,85] However, in human term neonates treatment with magnesium showed no protective effects and resulted in even strong hemodynamic adverse effects.[86,87] In addition, different calcium blockers (flunarizine, nimodipine and nicardipine) have been proven to be neuroprotective after experimental HI. However, in humans limiting effects have been observed and some of these agents were associated with severe cardiovascular adverse side effects.[88-90]

Reducing ROS formation

The formation of ROS also has a prominent contribution to the development of cerebral injury. A number of ROS inhibitors or scavengers have been shown to be protective in experimental model of neonatal HI, for example allopurinol (xanthine-oxidase inhibitor),[91-93] vitamin C/E, N-acetylcysteine (ROS scavengers), deferoxamine (iron chelator), indomethacin (cyclooxygenase inhibitor), 7-nitroindazole, aminoguanidine, JI-8 and HJ619 (selective NOS inhibitors).[94-102]

Anti-inflammatory strategies

As described above, the neuroinflammatory response after neonatal HI strongly aggravates neuronal damage. Treatments aimed at preventing or decreasing the inflammatory response could possibly reduce cerebral damage. Examples of some promising anti-inflammatory treatments are: Etanercept (TNF-α inhibitor), IL-1 receptor antagonist, the use of monoclonal antibodies to inhibit leukocyte adhesion molecules or deplete neutrophils, and inhibition of specific complement proteins.[53,103-106] Furthermore, minocycline has been shown to inhibit microglia activation and caspase 3 activation, and melatonin has been shown to exert inhibitory effects on microglia activation, ROS formation and apoptosis.[107-109]

Apoptotic targets

Multiple pathways eventually lead to activation of the apoptotic cascade and delayed cell death. Reducing apoptosis could therefore be a promising neuroprotective treatment. Neuroprotective effects have been described after the use of pan or broad spectrum caspase inhibitors in experimental neonatal HI models.

The importance of the transcription factor NF-κB, p53 and the JNK pathway in apoptotic cell death and cerebral damage following neonatal HI has been shown in previous studies by our group. First of all, Nijboer et al. (2008) showed that TAT-NBD, a selective NF-κB inhibitor (consisting of the NEMO Binding Domain coupled to the protein transduction sequence of HIV-TAT to facilitate cellular uptake), had a strong neuroprotective effect (80% reduction in infarct volume) after intra-peritoneal injection in a neonatal HI rat model.[58] The protective effect of TAT-NBD involved the prevention of p53 upregulation and nuclear and mitochondrial localization, upregulation of anti-apoptotic Bcl-2 family members and prevention of the apoptotic cascade with no effect on cytokine production. TAT-NBD has a therapeutic window of at least 6 hours.[58] The major disadvantage of this treatment is, however, that administration at a later time point (18/21 hours post-insult) aggravated brain damage.[57] Secondly, a small molecule inhibitor pifithrin-μ (PFT-μ) was tested in a model of neonatal HI in order to selectively inhibit mitochondrial p53 association. PFT-μ significantly reduced cerebral damage (80%) following neonatal HI and improved sensorimotor function and cognition at the long-term.[60] Neuroprotection after PFT-μ was associated with prevention of MOMP, reduction in oxidative stress and caspase 3 activation. PFT-μ administration at 18/21 hours post insult did not have a significant neuroprotective effect, however, more importantly, it did not aggravate brain damage as was observed after TAT-NDB treatment, making it more useful as a clinical application.[60]

Thirdly, the neuroprotective effect of a JNK peptide inhibitor, consisting of the JNK Binding Domain (JBD) of JIP-1 coupled to TAT (which was named L-JNKi) was investigated. Administration of L-JNKi at 0 and 3 hours post-insult resulted in a long-lasting neuroprotective effect (30-50% reduction in infarct volume), with a potent improvement in sensorimotor and cognitive function. L-JNKi treatment prevented the HI-induced activation of cerebral AP-1 and reduced the increase in Smac/DIABLO and caspase 3 activation.[110]

Regenerative treatment

Treatment with erythropoietin (EPO), a glycoprotein hormone, has multiple neuroregenerative and neuroprotective effects following experimental neonatal HI.[55,111,112] EPO stimulates expression of different neurotrophic factors (*i.e.* vascular endothelial growth factor (VEGF) and brain-derived neurotrophic factor (BDNF)) and thereby promotes neurogenesis and angiogenesis.[95] Furthermore EPO has an inhibitory effect on excitotoxicity, inflammation and apoptotic cell death.[113,114]

The use of neural or mesenchymal stem cells (NSCs or MSCs) to regenerate the brain following HI is one of the most promising regenerative therapies at this moment.[115-120] The major advantage of this treatment is the wide therapeutic window. We have shown before that MSC treatment still reduces the HI lesion size when administered 10 days post-insult in neonatal mice. The regenerative effects of stem cells are likely due to the secretion of neurotrophic factors that stimulate and maintain neurogenesis of the endogenous neuronal stem cell population in the affected areas, increasing cell proliferation, differentiation and functional integration. Examples of secreted neurotrophic factors are: BDNF, VEGF, basis fibroblast growth factor (bFGF), nerve growth factor (NGF), and colony-stimulating factor (CSF-) 1.[117] Some clinical trials will be started in the near future to investigate the effect of MSC treatment in human term neonates suffering from HIE.

Although many agents have been described to have a protective effect in neonatal HI animal models, studies in human term newborns have not confirmed convincing neuroprotective effects for most of these agents following neonatal HI. The combination of different treatments with hypothermia is probably necessary to achieve proper neuroprotection after neonatal HI. Further research and translation from fundamental research to the clinical setting is crucial to improve the outcome and quality-of-life for children with neonatal HIE in the future.

Animal model

The use of animal models is crucial to study underlying mechanisms of diseases and to investigate new therapeutic approaches. Most of our current knowledge of the pathophysiology of neonatal HIE has evolved from animal (rodent) studies. In former days, brain growth based on weight changes over time was used to assess which postnatal rodents age was most equivalent to human brain development.[121] In the last decade more advanced techniques have been used to investigate the different stages of brain development in humans and rodents. They showed that in postnatal day 7-10 (P7-10) rodents the main events in brain maturation (timing neurogenesis, synaptogenesis, gliogenesis, oligodendrocyte maturation and innate and adaptive immunity) are largely comparable with (near-) term human neonates.[122] Furthermore, the cerebral damage patterns observed with histology in rodent animals after a HI insult are remarkably similar compared to the patterns observed

with MRI in human term neonates following severe HI.[123,22] Although a simplification of the complex situation in humans, the rodent neonatal HI model is well suited for preclinical research to study pathophysiologic mechanisms involved in neonatal HIE, and the potential of new therapeutic approaches on long-term neurological and behavioral outcomes, dose response curves and time window assessment. However, before promising experimental treatments can be translation into clinical practice, investigations in larger animal models (for example piglets, lamb or primates) are often necessary.

Neonatal HI rodent model

In this thesis we used the neonatal HI rodent model originally published by Rice and Vannucci. In this model brain damage is induced by permanent occlusion of the right common carotid artery under isoflurane anesthesia in P7 rat pups or P9 mice pups, followed by systemic hypoxia. The duration of systemic hypoxia and oxygen concentration depends on the species and the strain of the animals.[124] HI brain damage induced in this model is unilateral and restricted to the (right) hemisphere ipsilateral to the occluded carotid artery, and primarily affects the hippocampal area, but also the cerebral cortex, subcortical and periventricular white matter and striatum/thalamus.

Combined perinatal inflammation and HI rodent model

We also combined the above described neonatal HI model with a preceding inflammatory stimulus (lipopolysaccharide: LPS) to investigate the effect of infection/inflammation on neonatal HI brain damage. A maternal-fetal infection is a well-known risk factor for neonatal HIE. Especially chorioamnionitis, an infection of the placental membranes, is associated with an increased risk of neonatal HI, since placental inflammation can lead to disturbance of placental gas exchange and blood flow. Importantly, the combined exposure to an inflammatory environment *in utero* and a neonatal HI insult dramatically increases the risk of cerebral brain damage and is associated with a worse outcome, probably due to an increase in immune cells and intrapartum fever.[125-131] To mimic this clinical situation, we injected LPS intraperitoneally 14 hours before the HI insult in P9 mice pups.[132,133] LPS is a structural component of most gram-negative bacteria and a strong inducer of innate immunity. Effects are mediated through interaction with a member of the toll-like receptor (TRL) family including TLR-4. TLR-4 is an integral membrane glycoprotein receptor, expressed on immune cells (macrophages, dendritic cells, B/T cells) and non-immune cells (*e.g.* fibroblasts and epithelial cells).[133,134] Binding of LPS to TLR-4 activates signal-transduction pathways with activation of protein kinases (ERK1/2, p38, JNK, NF-kB) and transcription factors (IRF5, AP1, IRF3) that induce the expression of genes coding for inflammatory mediators.[133,135] Low doses of LPS mimic subclinical infections and cause no apparent brain injury as such. Understanding the underlying mechanisms involved in the development of cerebral damage following (inflammation and) neonatal HI is an essential step in the development of future treatment strategies to combat this serious condition. Furthermore, it is important to investigate the

outcome of promising treatments in a model in which inflammation and HI are combined, since the effect of treatments might differ depending on the presence of inflammation.

Aim of this thesis

Nowadays, no effective neuroprotective treatment is available for neonates who are exposed to HI and are at risk for developing encephalopathy. Therefore, neonatal HIE is still a severe illness with a high mortality and morbidity. The research described in this thesis focuses on exploring two key pathophysiological pathways involved in the development of HIE: inflammation and apoptosis. Knowledge about these pathways is crucial since this can eventually lead to the development of new neuroprotective treatments to combat HIE. Within the apoptotic pathway, we focus in detail on promising strategies aimed at guarding mitochondrial integrity to protect the neonatal brain after HI.

In **Chapter 2** we determine the inflammatory response in the liver in comparison to inflammation in the brain after HI in P7 rats. The expression of different cytokines and chemokines in the liver and brain is investigated. Additionally, we describe the influence of neonatal HI on the polarization of macrophages/microglia to a M1/M2 phenotype and influx of neutrophils in the brain.

Chapter 3 describes the potent neuroprotective effect of two small peptides, D-JNKi and Sab_{KIM1}, that inhibit HI-induced mitochondrial JNK activation in P7 rats. The therapeutic window of D-JNKi treatment and the effects on long-term motor function and cognition are studied. Moreover, the effects of D-JNKi treatment on several markers involved in the JNK pathway, inflammation, mitochondrial integrity and apoptotic cell death are investigated.

In **Chapter 4** we explore the interaction between JNK and p53 in P7 rats after HI, by using the TAT-P7-pi peptide. TAT-P7-pi is a peptide that prevents p53-JNK association and thereby phosphorylation of p53. Besides the effect on neuronal damage and functional behavior, we studied the dose-response, time window and biochemical effects of TAT-P7-pi treatment after experimental neonatal HI.

Chapter 5 illustrates the sensitizing effect of inflammation (LPS) on the development of HI-induced cerebral gray and white matter injury over time in P9 mice. Additionally, the influence of combined exposure to inflammation and neonatal HI on white matter integrity, oligodendrocyte maturation and the cerebral inflammatory response is shown.

In **Chapter 6** the effect of D-JNKi treatment and inhibition of TNF-α on HI brain damage after LPS-sensitization in P9 mice pups is studied. We focus specifically on markers involved in apoptotic cell death, the JNK pathway, mitochondrial integrity, TNF-α and its receptors TNF-R1 and -R2.

In **Chapter 7** of this thesis we study the effect of osteopontin peptide treatment on HI brain damage and sensori-motor impairment in P9 mice. We have investigated intranasal, intraperitoneal and intracerebral administration of osteopontin peptide in different dosages and diverse (repetitive) treatment schedules.

References

1. Lawn JE, Cousens S, Zupan J, Lancet Neonatal Survival Steering Team. 4 million neonatal deaths: when? Where? Why? *Lancet*. 2005;365:891-900.
2. Spector JM, Daga S. Preventing those so-called stillbirths. *Bull World Health Organ*. 2008;86:315-316.
3. Graham EM, Ruis KA, Hartman AL, Northington FJ, Fox HE. A systematic review of the role of intrapartum hypoxia-ischemia in the causation of neonatal encephalopathy. *Am J Obstet Gynecol*. 2008;199:587-595.
4. Thornberg E, Thiringer K, Odeback A, Milsom I. Birth asphyxia: incidence, clinical course and outcome in a Swedish population. *Acta Paediatr*. 1995;84:927-932.
5. Pasternak JF, Gorey MT. The syndrome of acute near-total intrauterine asphyxia in the term infant. *Pediatr Neurol*. 1998;18:391-398.
6. Dammann O, Ferriero D, Gressens P. Neonatal encephalopathy or hypoxic-ischemic encephalopathy? Appropriate terminology matters. *Pediatr Res*. 2011;70:1-2.
7. Volpe JJ. *Neurology of the Newborn*. 4th ed. Philadelphia: W.B. Saunders; 2001.
8. APGAR V. A proposal for a new method of evaluation of the newborn infant. *Curr Res Anesth Analg*. 1953;32:260-267.
9. Carter BS, Haverkamp AD, Merenstein GB. The definition of acute perinatal asphyxia. *Clin Perinatol*. 1993;20:287-304.
10. Ferriero DM. Neonatal brain injury. *N Engl J Med*. 2004;351:1985-1995.
11. Sarnat HB, Sarnat MS. Neonatal encephalopathy following fetal distress. A clinical and electroencephalographic study. *Arch Neurol*. 1976;33:696-705.
12. Fenichel GM. Hypoxic-ischemic encephalopathy in the newborn. *Arch Neurol*. 1983;40:261-266.
13. Adamson SJ, Alessandri LM, Badawi N, Burton PR, Pemberton PJ, Stanley F. Predictors of neonatal encephalopathy in full-term infants. *BMJ*. 1995;311:598-602.
14. Badawi N, Kurinczuk JJ, Keogh JM, et al. Intrapartum risk factors for newborn encephalopathy: the Western Australian case-control study. *BMJ*. 1998;317:1554-1558.
15. Badawi N, Kurinczuk JJ, Keogh JM, et al. Antepartum risk factors for newborn encephalopathy: the Western Australian case-control study. *BMJ*. 1998;317:1549-1553.
16. Cowan F, Rutherford M, Groenendaal F, et al. Origin and timing of brain lesions in term infants with neonatal encephalopathy. *Lancet*. 2003;361:736-742.
17. Ellis M, Manandhar N, Manandhar DS, Costello AM. Risk factors for neonatal encephalopathy in Kathmandu, Nepal, a developing country: unmatched case-control study. *BMJ*. 2000;320:1229-1236.
18. Milsom I, Ladfors L, Thiringer K, Niklasson A, Odeback A, Thornberg E. Influence of maternal, obstetric and fetal risk factors on the prevalence of birth asphyxia at term in a Swedish urban population. *Acta Obstet Gynecol Scand*. 2002;81:909-917.
19. Folkerth RD. Periventricular leukomalacia: overview and recent findings. *Pediatr Dev Pathol*. 2006;9:3-13.
20. Back SA. Perinatal white matter injury: the changing spectrum of pathology and emerging insights into pathogenetic mechanisms. *Ment Retard Dev Disabil Res Rev*. 2006;12:129-140.
21. Khwaja O, Volpe JJ. Pathogenesis of cerebral white matter injury of prematurity. *Arch Dis Child Fetal Neonatal Ed*. 2008;93:F153-61.
22. Okereafor A, Allsop J, Counsell SJ, et al. Patterns of brain injury in neonates exposed to perinatal sentinel events. *Pediatrics*. 2008;121:906-914.
23. Miller SP, Ramaswamy V, Michelson D, et al. Patterns of brain injury in term neonatal encephalopathy. *J Pediatr*. 2005;146:453-460.

24. Volpe JJ, Kinney HC, Jensen FE, Rosenberg PA. Reprint of "The developing oligodendrocyte: key cellular target in brain injury in the premature infant". *Int J Dev Neurosci*. 2011;29:565-582.
25. Pin TW, Eldridge B, Galea MP. A review of developmental outcomes of term infants with post-asphyxia neonatal encephalopathy. *Eur J Paediatr Neurol*. 2009;13:224-234.
26. Lindstrom K, Hallberg B, Blennow M, Wolff K, Fernell E, Westgren M. Moderate neonatal encephalopathy: pre- and perinatal risk factors and long-term outcome. *Acta Obstet Gynecol Scand*. 2008;87:503-509.
27. Gonzalez FF, Miller SP. Does perinatal asphyxia impair cognitive function without cerebral palsy? *Arch Dis Child Fetal Neonatal Ed*. 2006;91:F454-9.
28. Marlow N, Rose AS, Rands CE, Draper ES. Neuropsychological and educational problems at school age associated with neonatal encephalopathy. *Arch Dis Child Fetal Neonatal Ed*. 2005;90:F380-7.
29. Armstrong-Wells J, Bernard TJ, Boada R, Manco-Johnson M. Neurocognitive outcomes following neonatal encephalopathy. *NeuroRehabilitation*. 2010;26:27-33.
30. de Haan M, Wyatt JS, Roth S, Vargha-Khadem F, Gadian D, Mishkin M. Brain and cognitive-behavioural development after asphyxia at term birth. *Dev Sci*. 2006;9:350-358.
31. van Handel M, Swaab H, de Vries LS, Jongmans MJ. Long-term cognitive and behavioral consequences of neonatal encephalopathy following perinatal asphyxia: a review. *Eur J Pediatr*. 2007;166:645-654.
32. Thompson CM, Puterman AS, Linley LL, et al. The value of a scoring system for hypoxic ischaemic encephalopathy in predicting neurodevelopmental outcome. *Acta Paediatr*. 1997;86:757-761.
33. van Bel F, Lemmers P, Naulaers G. Monitoring neonatal regional cerebral oxygen saturation in clinical practice: value and pitfalls. *Neonatology*. 2008;94:237-244.
34. de Vries LS, Cowan FM. Evolving understanding of hypoxic-ischemic encephalopathy in the term infant. *Semin Pediatr Neurol*. 2009;16:216-225.
35. Himmelmann K, Hagberg G, Wiklund LM, Eek MN, Uvebrant P. Dyskinetic cerebral palsy: a population-based study of children born between 1991 and 1998. *Dev Med Child Neurol*. 2007;49:246-251.
36. Krageloh-Mann I, Helber A, Mader I, et al. Bilateral lesions of thalamus and basal ganglia: origin and outcome. *Dev Med Child Neurol*. 2002;44:477-484.
37. Busl KM, Greer DM. Hypoxic-ischemic brain injury: pathophysiology, neuropathology and mechanisms. *NeuroRehabilitation*. 2010;26:5-13.
38. Thornton C, Rousset CI, Kichev A, et al. Molecular mechanisms of neonatal brain injury. *Neurol Res Int*. 2012;2012:506320.
39. Fatemi A, Wilson MA, Johnston MV. Hypoxic-ischemic encephalopathy in the term infant. *Clin Perinatol*. 2009;36:835-58, vii.
40. Badr Zahr LK, Purdy I. Brain injury in the infant: the old, the new, and the uncertain. *J Perinat Neonatal Nurs*. 2006;20:163-75; quiz 176-7.
41. Vannucci SJ, Hagberg H. Hypoxia-ischemia in the immature brain. *J Exp Biol*. 2004;207:3149-3154.
42. Vexler ZS, Ferriero DM. Molecular and biochemical mechanisms of perinatal brain injury. *Semin Neonatol*. 2001;6:99-108.
43. Inder TE, Volpe JJ. Mechanisms of perinatal brain injury. *Semin Neonatol*. 2000;5:3-16.
44. Berger R, Garnier Y. Pathophysiology of perinatal brain damage. *Brain Res Brain Res Rev*. 1999;30:107-134.
45. Dirnagl U, Iadecola C, Moskowitz MA. Pathobiology of ischaemic stroke: an integrated view. *Trends Neurosci*. 1999;22:391-397.
46. Jin R, Yang G, Li G. Inflammatory mechanisms in ischemic stroke: role of inflammatory cells. *J Leukoc Biol*. 2010;87:779-789.
47. Dammann O, O'Shea TM. Cytokines and perinatal brain damage. *Clin Perinatol*. 2008;35:643-63, v.

48. Broughton BR, Reutens DC, Sobey CG. Apoptotic mechanisms after cerebral ischemia. *Stroke*. 2009;40:e331-9.
49. Hamrick SE, Ferriero DM. The injury response in the term newborn brain: can we neuroprotect? *Curr Opin Neurol*. 2003;16:147-154.
50. Sonntag J, Wagner MH, Strauss E, Obladen M. Complement and contact activation in term neonates after fetal acidosis. *Arch Dis Child Fetal Neonatal Ed*. 1998;78:F125-8.
51. Schultz SJ, Aly H, Hasanen BM, et al. Complement component 9 activation, consumption, and neuronal deposition in the post-hypoxic-ischemic central nervous system of human newborn infants. *Neurosci Lett*. 2005;378:1-6.
52. Aly H, Khashaba MT, Nada A, et al. The role of complement in neurodevelopmental impairment following neonatal hypoxic-ischemic encephalopathy. *Am J Perinatol*. 2009;26:659-665.
53. Lassiter HA. The role of complement in neonatal hypoxic-ischemic cerebral injury. *Clin Perinatol*. 2004;31:117-127.
54. Blaschke AJ, Staley K, Chun J. Widespread programmed cell death in proliferative and postmitotic regions of the fetal cerebral cortex. *Development*. 1996;122:1165-1174.
55. Fan X, Kavelaars A, Heijnen CJ, Groenendaal F, van Bel F. Pharmacological neuroprotection after perinatal hypoxic-ischemic brain injury. *Curr Neuropharmacol*. 2010;8:324-334.
56. Chipuk JE, Green DR. How do BCL-2 proteins induce mitochondrial outer membrane permeabilization? *Trends Cell Biol*. 2008;18:157-164.
57. Nijboer CH, Heijnen CJ, Groenendaal F, May MJ, van Bel F, Kavelaars A. A dual role of the NF-kappaB pathway in neonatal hypoxic-ischemic brain damage. *Stroke*. 2008;39:2578-2586.
58. Nijboer CH, Heijnen CJ, Groenendaal F, May MJ, van Bel F, Kavelaars A. Strong neuroprotection by inhibition of NF-kappaB after neonatal hypoxia-ischemia involves apoptotic mechanisms but is independent of cytokines. *Stroke*. 2008;39:2129-2137.
59. Nijboer CH, Heijnen CJ, Groenendaal F, van Bel F, Kavelaars A. Alternate pathways preserve tumor necrosis factor-alpha production after nuclear factor-kappaB inhibition in neonatal cerebral hypoxia-ischemia. *Stroke*. 2009;40:3362-3368.
60. Nijboer CH, Heijnen CJ, van der Kooij MA, et al. Targeting the p53 pathway to protect the neonatal ischemic brain. *Ann Neurol*. 2011;70:255-264.
61. Vousden KH, Prives C. Blinded by the Light: The Growing Complexity of p53. *Cell*. 2009;137:413-431.
62. Morrison RS, Kinoshita Y, Johnson MD, Guo W, Garden GA. P53-Dependent Cell Death Signaling in Neurons. *Neurochem Res*. 2003;28:15-27.
63. Green DR, Kroemer G. Cytoplasmic functions of the tumour suppressor p53. *Nature*. 2009;458:1127-1130.
64. Fuchs SY, Adler V, Pincus MR, Ronai Z. MEKK1/JNK signaling stabilizes and activates p53. *Proc Natl Acad Sci U S A*. 1998;95:10541-10546.
65. Bogoyevitch MA, Ngoei KR, Zhao TT, Yeap YY, Ng DC. c-Jun N-terminal kinase (JNK) signaling: recent advances and challenges. *Biochim Biophys Acta*. 2010;1804:463-475.
66. Dhanasekaran DN, Reddy EP. JNK signaling in apoptosis. *Oncogene*. 2008;27:6245-6251.
67. Raivich G, Behrens A. Role of the AP-1 transcription factor c-Jun in developing, adult and injured brain. *Prog Neurobiol*. 2006;78:347-363.
68. Chavez-Valdez R, Martin LJ, Northington FJ. Programmed Necrosis: A Prominent Mechanism of Cell Death following Neonatal Brain Injury. *Neurol Res Int*. 2012;2012:257563.
69. Northington FJ, Chavez-Valdez R, Martin LJ. Neuronal cell death in neonatal hypoxia-ischemia. *Ann Neurol*. 2011;69:743-758.
70. Vandenabeele P, Galluzzi L, Vanden Berghe T, Kroemer G. Molecular mechanisms of necroptosis: an ordered cellular explosion. *Nat Rev Mol Cell Biol*. 2010;11:700-714.

71. Gunn AJ, Bennet L, Gunning MI, Gluckman PD, Gunn TR. Cerebral hypothermia is not neuroprotective when started after postischemic seizures in fetal sheep. *Pediatr Res*. 1999;46:274-280.

72. Azzopardi DV, Strohm B, Edwards AD, et al. Moderate hypothermia to treat perinatal asphyxial encephalopathy. *N Engl J Med*. 2009;361:1349-1358.

73. Gluckman PD, Wyatt JS, Azzopardi D, et al. Selective head cooling with mild systemic hypothermia after neonatal encephalopathy: multicentre randomised trial. *Lancet*. 2005;365:663-670.

74. Shankaran S, Laptook AR, Ehrenkranz RA, et al. Whole-body hypothermia for neonates with hypoxic-ischemic encephalopathy. *N Engl J Med*. 2005;353:1574-1584.

75. Edwards AD, Brocklehurst P, Gunn AJ, et al. Neurological outcomes at 18 months of age after moderate hypothermia for perinatal hypoxic ischaemic encephalopathy: synthesis and meta-analysis of trial data. *BMJ*. 2010;340:c363.

76. Guillet R, Edwards AD, Thoresen M, et al. Seven- to eight-year follow-up of the CoolCap trial of head cooling for neonatal encephalopathy. *Pediatr Res*. 2012;71:205-209.

77. Wachtel EV, Hendricks-Munoz KD. Current management of the infant who presents with neonatal encephalopathy. *Curr Probl Pediatr Adolesc Health Care*. 2011;41:132-153.

78. Drury PP, Bennet L, Gunn AJ. Mechanisms of hypothermic neuroprotection. *Semin Fetal Neonatal Med*. 2010;15:287-292.

79. Perlman JM. Intervention strategies for neonatal hypoxic-ischemic cerebral injury. *Clin Ther*. 2006;28:1353-1365.

80. Peeters C, van Bel F. Pharmacotherapeutical reduction of post-hypoxic-ischemic brain injury in the newborn. *Biol Neonate*. 2001;79:274-280.

81. Robertson NJ, Tan S, Groenendaal F, et al. Which neuroprotective agents are ready for bench to bedside translation in the newborn infant? *J Pediatr*. 2012;160:544-552.e4.

82. Kelen D, Robertson NJ. Experimental treatments for hypoxic ischaemic encephalopathy. *Early Hum Dev*. 2010;86:369-377.

83. van Bel F, Groenendaal F. Long-term pharmacologic neuroprotection after birth asphyxia: where do we stand? *Neonatology*. 2008;94:203-210.

84. Ma D, Hossain M, Chow A, et al. Xenon and hypothermia combine to provide neuroprotection from neonatal asphyxia. *Ann Neurol*. 2005;58:182-193.

85. Cetinkaya M, Alkan T, Ozyener F, Kafa IM, Kurt MA, Koksal N. Possible neuroprotective effects of magnesium sulfate and melatonin as both pre- and post-treatment in a neonatal hypoxic-ischemic rat model. *Neonatology*. 2011;99:302-310.

86. Groenendaal F, Rademaker CM, Toet MC, de Vries LS. Effects of magnesium sulphate on amplitude-integrated continuous EEG in asphyxiated term neonates. *Acta Paediatr*. 2002;91:1073-1077.

87. Whitelaw A, Thoresen M. Clinical trials of treatments after perinatal asphyxia. *Curr Opin Pediatr*. 2002;14:664-668.

88. Berger R, Lehmann T, Karcher J, Garnier Y, Jensen A. Low dose flunarizine protects the fetal brain from ischemic injury in sheep. *Pediatr Res*. 1998;44:277-282.

89. Kittaka M, Giannotta SL, Zelman V, et al. Attenuation of brain injury and reduction of neuron-specific enolase by nicardipine in systemic circulation following focal ischemia and reperfusion in a rat model. *J Neurosurg*. 1997;87:731-737.

90. Levene MI, Gibson NA, Fenton AC, Papathoma E, Barnett D. The use of a calcium-channel blocker, nicardipine, for severely asphyxiated newborn infants. *Dev Med Child Neurol*. 1990;32:567-574.

91. Kaandorp JJ, Derks JB, Oudijk MA, et al. Antenatal allopurinol reduces hippocampal brain damage after acute birth asphyxia in late gestation fetal sheep. *Reprod Sci*. 2014;21:251-259.

92. Kaandorp JJ, van Bel F, Veen S, et al. Long-term neuroprotective effects of allopurinol after moderate perinatal asphyxia: follow-up of two randomised controlled trials. *Arch Dis Child Fetal Neonatal Ed*. 2012;97:F162-6.

93. Torrance HL, Benders MJ, Derks JB, et al. Maternal allopurinol during fetal hypoxia lowers cord blood levels of the brain injury marker S-100B. *Pediatrics*. 2009;124:350-357.

94. Palmer C, Towfighi J, Roberts RL, Heitjan DF. Allopurinol administered after inducing hypoxia-ischemia reduces brain injury in 7-day-old rats. *Pediatr Res*. 1993;33:405-411.

95. Wang L, Zhang Z, Wang Y, Zhang R, Chopp M. Treatment of stroke with erythropoietin enhances neurogenesis and angiogenesis and improves neurological function in rats. *Stroke*. 2004;35:1732-1737.

96. Liu JQ, Lee TF, Chen C, Bagim DL, Cheung PY. N-acetylcysteine improves hemodynamics and reduces oxidative stress in the brains of newborn piglets with hypoxia-reoxygenation injury. *J Neurotrauma*. 2010;27:1865-1873.

97. Daneyemez M, Kurt E, Cosar A, Yuce E, Ide T. Methylprednisolone and vitamin E therapy in perinatal hypoxic-ischemic brain damage in rats. *Neuroscience*. 1999;92:693-697.

98. Papazisis G, Pourzitaki C, Sardeli C, Lallas A, Amaniti E, Kouvelas D. Deferoxamine decreases the excitatory amino acid levels and improves the histological outcome in the hippocampus of neonatal rats after hypoxia-ischemia. *Pharmacol Res*. 2008;57:73-78.

99. Ishida A, Trescher WH, Lange MS, Johnston MV. Prolonged suppression of brain nitric oxide synthase activity by 7-nitroindazole protects against cerebral hypoxic-ischemic injury in neonatal rat. *Brain Dev*. 2001;23:349-354.

100. Tsuji M, Higuchi Y, Shiraishi K, Kume T, Akaike A, Hattori H. Protective effect of aminoguanidine on hypoxic-ischemic brain damage and temporal profile of brain nitric oxide in neonatal rat. *Pediatr Res*. 2000;47:79-83.

101. van den Tweel ER, Peeters-Scholte CM, van Bel F, Heijnen CJ, Groenendaal F. Inhibition of nNOS and iNOS following hypoxia-ischaemia improves long-term outcome but does not influence the inflammatory response in the neonatal rat brain. *Dev Neurosci*. 2002;24:389-395.

102. Taskin E, Ozcan K, Canacankatan N, Satar M, Yapicioglu HY, Erdogan S. The effects of indomethacin on caspases, glutathione level and lipid peroxidation in the newborn rats with hypoxic-ischemic cerebral injury. *Brain Res*. 2009;1289:118-123.

103. Hudome S, Palmer C, Roberts RL, Mauger D, Housman C, Towfighi J. The role of neutrophils in the production of hypoxic-ischemic brain injury in the neonatal rat. *Pediatr Res*. 1997;41:607-616.

104. Nijboer CH, Kavelaars A, Vroon A, Groenendaal F, van Bel F, Heijnen CJ. Low endogenous G-protein-coupled receptor kinase 2 sensitizes the immature brain to hypoxia-ischemia-induced gray and white matter damage. *J Neurosci*. 2008;28:3324-3332.

105. Girard S, Sebire H, Brochu ME, Briota S, Sarret P, Sebire G. Postnatal administration of IL-1Ra exerts neuroprotective effects following perinatal inflammation and/or hypoxic-ischemic injuries. *Brain Behav Immun*. 2012;26:1331-1339.

106. Palmer C, Roberts RL, Young PI. Timing of neutrophil depletion influences long-term neuroprotection in neonatal rat hypoxic-ischemic brain injury. *Pediatr Res*. 2004;55:549-556.

107. Welin AK, Svedin P, Lapatto R, et al. Melatonin reduces inflammation and cell death in white matter in the mid-gestation fetal sheep following umbilical cord occlusion. *Pediatr Res*. 2007;61:153-158.

108. Wixey JA, Reinebrant HE, Spencer SJ, Buller KM. Efficacy of post-insult minocycline administration to alter long-term hypoxia-ischemia-induced damage to the serotonergic system in the immature rat brain. *Neuroscience*. 2011;182:184-192.

109. Buller KM, Carty ML, Reinebrant HE, Wixey JA. Minocycline: a neuroprotective agent for hypoxic-ischemic brain injury in the neonate? *J Neurosci Res*. 2009;87:599-608.

110. Nijboer CH, van der Kooij MA, van Bel F, Ohl F, Heijnen CJ, Kavelaars A. Inhibition of the JNK/AP-1 pathway reduces neuronal death and improves behavioral outcome after neonatal hypoxic-ischemic brain injury. *Brain Behav Immun*. 2010;24:812-821.

111. Chang YS, Mu D, Wendland M, et al. Erythropoietin improves functional and histological outcome in neonatal stroke. *Pediatr Res*. 2005;58:106-111.

112. Traudt CM, McPherson RJ, Bauer LA, et al. Concurrent erythropoietin and hypothermia treatment improve outcomes in a term nonhuman primate model of perinatal asphyxia. *Dev Neurosci*. 2013;35:491-503.

113. Xiong T, Qu Y, Mu D, Ferriero D. Erythropoietin for neonatal brain injury: opportunity and challenge. *Int J Dev Neurosci*. 2011;29:583-591.

114. Juul S. Neuroprotective role of erythropoietin in neonates. *J Matern Fetal Neonatal Med*. 2012;25 Suppl 4:105-107.

115. Bennet L, Tan S, Van den Heuij L, et al. Cell therapy for neonatal hypoxia-ischemia and cerebral palsy. *Ann Neurol*. 2012;71:589-600.

116. Donega V, Nijboer CH, van Tilborg G, Dijkhuizen RM, Kavelaars A, Heijnen CJ. Intranasally administered mesenchymal stem cells promote a regenerative niche for repair of neonatal ischemic brain injury. *Exp Neurol*. 2014.

117. Donega V, van Velthoven CT, Nijboer CH, Kavelaars A, Heijnen CJ. The endogenous regenerative capacity of the damaged newborn brain: boosting neurogenesis with mesenchymal stem cell treatment. *J Cereb Blood Flow Metab*. 2013;33:625-634.

118. Donega V, van Velthoven CT, Nijboer CH, et al. Intranasal mesenchymal stem cell treatment for neonatal brain damage: long-term cognitive and sensorimotor improvement. *PLoS One*. 2013;8:e51253.

119. van Velthoven CT, Kavelaars A, Heijnen CJ. Mesenchymal stem cells as a treatment for neonatal ischemic brain damage. *Pediatr Res*. 2012;71:474-481.

120. van Velthoven CT, Sheldon RA, Kavelaars A, et al. Mesenchymal stem cell transplantation attenuates brain injury after neonatal stroke. *Stroke*. 2013;44:1426-1432.

121. Dobbing J, Sands J. Comparative aspects of the brain growth spurt. *Early Hum Dev*. 1979;3:79-83.

122. Semple BD, Blomgren K, Gimlin K, Ferriero DM, Noble-Haeusslein LJ. Brain development in rodents and humans: Identifying benchmarks of maturation and vulnerability to injury across species. *Prog Neurobiol*. 2013;106-107:1-16.

123. Nakajima W, Ishida A, Lange MS, et al. Apoptosis has a prolonged role in the neurodegeneration after hypoxic ischemia in the newborn rat. *J Neurosci*. 2000;20:7994-8004.

124. Rice JE,3rd, Vannucci RC, Brierley JB. The influence of immaturity on hypoxic-ischemic brain damage in the rat. *Ann Neurol*. 1981;9:131-141.

125. Wu YW, Escobar GJ, Grether JK, Croen LA, Greene JD, Newman TB. Chorioamnionitis and cerebral palsy in term and near-term infants. *JAMA*. 2003;290:2677-2684.

126. Blume HK, Li CI, Loch CM, Koepsell TD. Intrapartum fever and chorioamnionitis as risks for encephalopathy in term newborns: a case-control study. *Dev Med Child Neurol*. 2008;50:19-24.

127. Nelson KB, Grether JK. Potentially asphyxiating conditions and spastic cerebral palsy in infants of normal birth weight. *Am J Obstet Gynecol*. 1998;179:507-513.

128. Bartha AI, Foster-Barber A, Miller SP, et al. Neonatal encephalopathy: association of cytokines with MR spectroscopy and outcome. *Pediatr Res*. 2004;56:960-966.

129. Shalak LF, Laptook AR, Jafri HS, Ramilo O, Perlman JM. Clinical chorioamnionitis, elevated cytokines, and brain injury in term infants. *Pediatrics*. 2002;110:673-680.

130. Aly H, Khashaba MT, El-Ayouty M, El-Sayed O, Hasanein BM. IL-1beta, IL-6 and TNF-alpha and outcomes of neonatal hypoxic ischemic encephalopathy. *Brain Dev*. 2006;28:178-182.

131. Impey L, Greenwood C, MacQuillan K, Reynolds M, Sheil O. Fever in labour and neonatal encephalopathy: a prospective cohort study. *BJOG*. 2001;108:594-597.

132. Eklind S, Mallard C, Leverin AL, et al. Bacterial endotoxin sensitizes the immature brain to hypoxic--ischaemic injury. *Eur J Neurosci*. 2001;13:1101-1106.

133. Wang X, Rousset CI, Hagberg H, Mallard C. Lipopolysaccharide-induced inflammation and perinatal brain injury. *Semin Fetal Neonatal Med*. 2006;11:343-353.

134. Akira S. TLR signaling. *Curr Top Microbiol Immunol*. 2006;311:1-16.

135. Mallard C. Innate immune regulation by toll-like receptors in the brain. *ISRN Neurol*. 2012;2012:701950.

2

Cerebral and hepatic inflammatory response after neonatal hypoxia-ischemia in newborn rats

Hilde J.C. Bonestroo
Cora H. Nijboer
Cindy T.J. van Velthoven
Annemieke Kavelaars
Erik C. Hack
Frank van Bel
Cobi J. Heijnen

Developmental Neuroscience **2013;35:197-211.**

Abstract

Background Neonatal encephalopathy induced by perinatal asphyxia is a serious condition associated with high mortality and morbidity. Inflammation after the insult is thought to contribute to brain injury. This inflammatory response to hypoxia-ischemia (HI) may not only occur in the brain but also in peripheral organs. The aim of the present study was to investigate the effect of neonatal HI on the inflammatory response in the liver in comparison to inflammation in the brain.

Methods HI was induced in postnatal day (P)7 Wistar rats by unilateral carotid artery occlusion and hypoxia. Cytokine and chemokine mRNA levels were determined in brain and liver by quantitative PCR. Polarization of brain macrophages to the M1/M2-like phenotype and infiltration of neutrophils were characterized by immunohistochemistry.

Results At 3 h post-HI, an upregulation of the pro-inflammatory cytokines TNF-α and IL-1β and anti-inflammatory IL-10 was observed in the ipsilateral hemisphere of the brain compared to mRNA levels in sham-operated animals. Additionally, cerebral CINC-1 and MCP-1 mRNA expression were increased. We also observed increased numbers of macrophages/microglia of the M1-like phenotype as well as a small increase in granulocyte influx in the ipsilateral hemisphere. Conversely, in the liver at 3 h post-HI a downregulation of TNF-α, IL-1β, and MCP-1 and a trend towards an upregulation of IL-10 were observed compared to mRNA levels of sham-operated animals. However, hepatic CINC-1 expression was increased compared to levels in sham-operated animals. Following systemic hypoxia only, no significant changes in the expression of TNF-α, CINC-1 or MCP-1 were observed in the liver compared to sham-operated littermates, except for an upregulation in hepatic IL-1β expression at 3 h after hypoxia.
Twenty-four hours post-insult, cerebral ipsilateral TNF-α, MCP-1 and CINC-1 mRNA expression was still increased, together with an increase in TGF-β expression. Moreover, an increase in macrophages/microglia of the M1-like phenotype was observed together with the appearance of macrophages/microglia of the M2-like phenotype around the cerebral lesion as well as an increase in granulocyte influx in comparison to 3 h post-HI. In the liver, at 24 h after HI, cytokine and chemokine responses were similar to mRNA levels in sham-operated animals except for a decrease in IL-10 and MCP-1.

Conclusion We describe for the first time that brain damage following neonatal HI induces an early downregulation of the pro-inflammatory response in the liver. HI induces an early pro-inflammatory response in the brain with a concomitant increase in influx of neutrophils and polarization of macrophages/microglia to the M1-like phenotype starting at 3 h and increasing up to 24 h after HI. The inflammatory state of the brain changes after 24 h, with an increase in the anti-inflammatory cytokine TGF-β together with the appearance of macrophages/microglia of the M2-like phenotype. The downregulation of pro-inflammatory cytokines in the liver is not due to systemic hypoxia only, but is induced by the cerebral damage.

Introduction

Neonatal encephalopathy due to perinatal asphyxia or hypoxia-ischemia (HI) is an important cause of mortality in the neonatal period and is associated with high morbidity, mainly characterized by neurological deficits as cerebral palsy, seizures, and sensory and cognitive limitations.[1-5] The prevalence of neonatal HI is about 2-6 per 1000 live term births in Western countries.[1,6,7] Therapeutic options to improve the outcome of neonates with HI brain injury are still very limited. At the moment, hypothermia is the only established intervention with modest therapeutic effects if started within 6 h after the insult.[8-10] Hypothermia is thought to be neuroprotective via reducing cellular metabolism, a decrease in glutamate excitotoxicity and apoptotic cell death and a suppression of the inflammatory cascade.[11-18]

Inflammation is a complex process consisting of an intrinsic network of multiple subsets of immune cells. Neonatal HI induces a cerebral inflammatory response including the production of cerebral inflammatory cytokines and chemokines and activation and recruitment of neutrophils and macrophages from the circulation to the brain.[19-29] This inflammatory response to neonatal HI is thought to result in additional cerebral damage.[30,31] Several studies have shown that inhibition of IL-1β (IL-1ra) and TNF-α (etanercept), neutralization of MCP-1 or neutrophil depletion leads to a reduction of brain injury.[19,20,22,32,33] Anthony et al. (2012) described in a recent review that brain injury in adult rodent models often results in an increased inflammatory response in peripheral organs, especially in the liver.[34-40] For instance, after middle cerebral artery occlusion (MCAO) in adult mice, hepatic pro-inflammatory cytokines and chemokines increased within 4 h.[40] Additionally, intracerebral microinjection of IL-1β in adult mice resulted in an early activation of the transcription factor NF-κB and a change in the expression of hundreds of genes in the liver, which subsequently led to mobilization of circulating leukocytes to the brain.[39,41] Inhibition of peripheral TNF-α by etanercept, which does not cross the blood-brain barrier in this model, reduced the influx of neutrophils in the brain as well.[41] Therefore it has been suggested that inhibition of the hepatic inflammatory response may lead to a reduced inflammatory response in the central nervous system (CNS) thereby dampening the development of brain damage.[34]

The inflammatory response of peripheral organs after brain injury has been primarily studied in adult animal models and little is known on the role of the peripheral inflammatory response after *neonatal* HI. Since perinatal HI also involves a systemic hypoxia due to diminished blood perfusion and oxygenation of the fetus/neonate, we studied the peripheral inflammatory response in comparison to the cerebral inflammatory response in a model of neonatal HI, on the level of cytokine and chemokine expression. In addition, we investigated neutrophil influx and polarization of macrophages/microglia to the M1/M2-like phenotype in the brain at 3 and 24 h after HI.

Materials and methods

Animals

All experiments were performed according to international guidelines and approved by the local experimental animal committee. Postnatal day 7 (P7) Wistar rat pups of both genders were subjected to HI by permanent occlusion of the right common carotid artery under isoflurane anesthesia, followed by systemic hypoxia for 90 min at 8% O_2. Animals that only underwent hypoxia (hypoxia-only group) were subjected to anesthesia and incision, followed by 90 min of systemic hypoxia (8% O_2). Sham-control animals underwent anesthesia and incision only. Naive animals did not undergo any of the experimental procedures and were included to investigate the possible effects of anesthesia.

For quantitative PCR analysis animals were sacrificed by decapitation at 3 or 24 h after insult, and contra- and ipsilateral brain hemispheres and the liver were collected and stored at -80 °C.

For immunohistochemistry, animals were sacrificed by pentobarbital overdose at 3 or 24 h after insult, and rat pups were perfused with 4% paraformaldehyde in phosphate buffered saline (PBS). Brains were post-fixed and either cryoprotected in sucrose and embedded in OCT freezing medium (Tissue-Teck, Sakura Finetek Europe, Zoeterwoude, The Netherlands), or embedded in paraffin.

Histology

Coronal paraffin section (8 µm) were cut at hippocampal level and incubated with mouse-anti-microtubule-associated protein 2 (MAP2) (Sigma-Aldrich, Steinheim, Germany) followed by biotinylated horse anti-mouse (Vector Laboratories, Burlingame, CA) antibody. Visualization was performed using Vectastain ABC kit (Vector Laboratories) and diaminobenzamidine. Full section images were captured with a Nikon D1 digital camera (Nikon, Tokyo, Japan). The brain areas were outlined manually using image processing tools in Adobe Photoshop CS5 (Adobe Systems Inc., San Jose, CA). Ipsilateral MAP2 area loss was calculated as follows: 1-(area ipsilateral MAP2 staining/area contralateral MAP2 staining) x 100%.

Coronal frozen sections (10 µm) were cut at hippocampal level and incubated with rabbit-anti-polymorphonuclear granulocytes (PMN) (Accurate Chemical & Scientific Corporation, Westbury, NY) followed by AlexaFluor 488-conjugated secondary antibody (Molecular Probes, Eugene, OR). Fluorescent images were obtained using a Zeiss Axio Observer inverted microscope (Zeiss, Oberkochen, Germany).

For M1 and M2 staining, frozen sections were incubated with M1 macrophage marker mouse anti-iNOS (Santa Cruz Biotechnology, Santa Cruz, CA) and M2 macrophage marker goat anti-CD206 (R&D systems, Minneapolis, MN). Both were double-stained with rabbit anti-ionized calcium binding adaptor molecule (Iba-)1 (Wako Chemicals, Richmond, VA) followed by AlexaFluor 488- and 594-conjugated secondary antibodies (both Molecular Probes, Eugene, OR). Fluorescent images were obtained using an EVOS digital inverted fluorescence

microscope (Advanced Microscopy Group, Bothell, WA). M1 and M2 microglia/macrophages were quantified in the whole hemisphere by counting iNOS$^+$- or CD206$^+$- Iba-1$^+$ (double positive) cells using ImageJ software (Rasband WS, ImageJ, U.S. National Institutes of Health, Bethesda, MD, USA; http://rsb.info.nih.gov/ij/, 1997-2006).

Quantitative real time reverse transcriptase PCR

Total RNA was isolated from brain and liver by using TRIzol® (Invitrogen, Paisley, UK) according to manufacturer's protocol. cDNA was synthesized with SuperScript Reverse Transcriptase (Invitrogen). The PCR reaction was performed with iQ5 Real-Time PCR Detection System (Bio-Rad laboratories, Veenendaal, The Netherlands) for IL-1β, TNF-α, IL-10, TGF-β, IL-4, IL-6, MCP-1, CINC-1 and arginase-1 (for primer sequences see Table 1). To confirm appropriate amplification, size of PCR products was verified on gel. Expression of glyceraldehydes-3-phosphate dehydrogenase (GAPDH) was used for normalization of expression in brain and expression of hypoxanthine-guanine phosphoribosyltransferase (HPRT) was used for normalization of expression in liver.

Table 1: Primer sequences used for quantitative real time reverse transcriptase PCR.

Marker	Forward primer	Reverse primer
GAPDH	CACGGCAAGTTCAACGGCACAG	GACTCCACGACATACTCAGCACCAG
HPRT	TCCTCCTCAGACCGCTTTT	CCTGGTTCATCATCGCTAATC
IL-1β	CTCTGTGACTCGTGGGATGATG	CACTTGTTGGCTTATGTTCTGTCC
TNF-α	CCCAGACCCTCACACTCAGATCAT	GCAGCCTTGTCCCTTGAAGAGAA
IL-6	AACGAAAGTCAACTCCATCTG	GGTATCCTCTGTGAAGTCTCC
IL-10	CCTTACTGCAGGACTTTAAGGGTTA	TTTCTGGGCCATGGTTCTCT
IL-4	GCAACAAGGAACACCACGGAGAAC	CTTCAAGCACGGAGGTACATCACG
TGF-β	TGAGTGGCTGTCTTTTGACGTC	CCTGTATTCCGTCTCCTTGGTT
MCP-1	CAGAAACCAGCCAACTCTCA	GTGGGGCATTAACTGCATCT
CINC-1	CCAAAAGATGCTAAAGGGTGTCC	CAGAAGCCAGCGTTCACCA
Arginase-1	CATATCTGCCAAGGACATCG	GGTCTCTTCCATCACTTTGC

Neutrophil infiltration

Neutrophil infiltration was determined using a myeloperoxidase (MPO) assay as described earlier.[42] In short, pulverized brain was homogenized in 50 mM HEPES buffer (pH 8.0), centrifuged and pellets were rehomogenized in H_2O/0.5% cetyltrimethylammonium chloride (CTAC) (Merck, Darmstadt, Germany). After centrifugation, supernatants were diluted in 10 mM citrate buffer (pH 5.0)/0.22% CTAC and substrate solution (3 mM 3', 5,5'-tetramethylbenzidine dihydrochloride (Sigma-Aldrich), 120 µM resorcinol (Merck) and 2.2 mM H_2O_2 in distilled water) was added. These reaction mixtures were incubated for 30 min at 37 °C and stopped by addition of H_2SO_4. Optical density (OD) at 450 nm was determined. Cerebral MPO activity was determined using a standard with known MPO activity (10 units/ml). Protein concentration of samples was determined with bicinchoninic acid (BCA) protein assay (Pierce Biotechnology, Rockford, IL) using bovine serum albumin (BSA) as a standard.

Statistical analysis

All data are expressed as mean ± SEM. Data were compared by Student's t-test for two comparisons and one-way ANOVA with Bonferroni post hoc tests was used for multiple comparisons. p <0.05 was considered statistically significant.

Results

Gray matter damage

HI brain damage was induced in P7 rat pups by unilateral occlusion of the carotid artery and 90 min of hypoxia (8% O_2), which resulted in severe neuronal damage with 79.9% MAP2 loss at 3 h and 86.0% MAP2 loss at 24 h after HI, without detectable damage in the contralateral hemisphere (Fig 1).

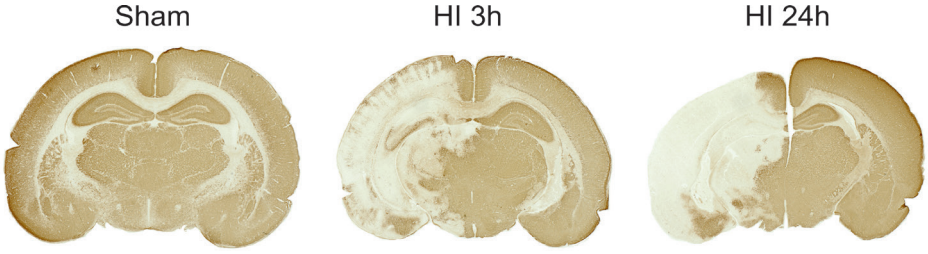

Figure 1: Early neuronal damage after HI
Rat pups were subjected to HI at P7 and early neuronal damage was measured by analyzing staining for microtubule-associated protein 2 (MAP2) in the contra- and ipsilateral hemisphere. Representative photographs of MAP2 staining in brains of sham-operated rats (Sham) and rats that underwent HI, terminated at 3 (HI 3 h) or 24 h (HI 24 h) after HI.

Cerebral and hepatic cytokine and chemokine expression at 3 hours after HI

Three hours after insult, HI induced an upregulation of the pro-inflammatory cytokines TNF-α and IL-1β (5.8 and 3.2 fold respectively) in the ipsilateral hemisphere compared to levels in sham-operated animals (Fig 2A). The anti-inflammatory cytokine IL-10 was also significantly upregulated at 3 h post-HI (Fig 2A). We did not observe an upregulation of TGF-β, IL-4 or IL-6 at this time point in the brain (Fig 2A and data not shown). Cerebral CINC-1 mRNA expression, an important chemokine for recruitment of neutrophils, was increased in the ipsilateral hemisphere at 3 h after insult (Fig 3A). Similarly, the ipsilateral level of MCP-1 mRNA, a chemokine involved in monocyte recruitment, was increased at this time point (Fig 3A). Cytokine and chemokine mRNA expression levels in the contralateral hemisphere were not significantly increased compared to the levels in sham-operated littermates (Fig 2A and Fig 3A).

In contrast, in the liver, TNF-α and IL-1β mRNA levels were significantly downregulated compared to sham-operated animals at 3 h after HI (Fig 2B). Additionally, a trend towards an upregulation of IL-10 was observed in the liver of HI-treated rats compared to levels in sham-

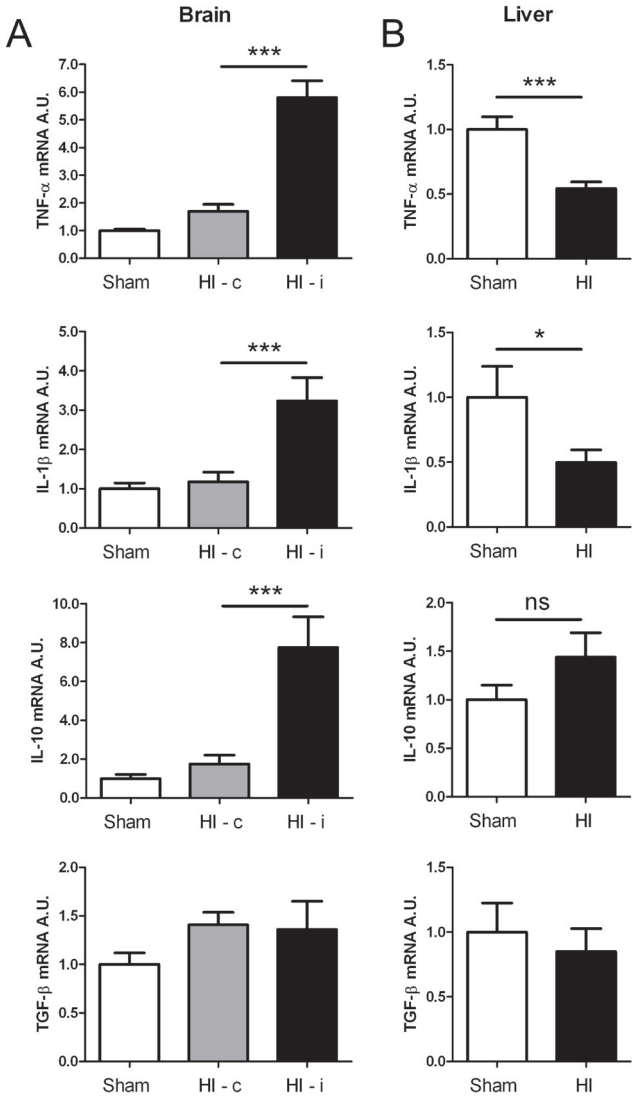

Figure 2: HI-induced expression of cytokines in the brain and liver at 3 h after HI.
Effect of HI on expression of TNF-α, IL-1β, IL-10 and TGF-β in the brain (**A**) and liver (**B**) as determined by quantitative real time reverse transcriptase PCR at 3 h after HI. n=14 animals for HI group and 10 animals for sham-operated (Sham) group. HI did not induce a significant increase in cytokine expression in the contralateral hemisphere compared to sham-operated littermates. * p <0.05, *** p <0.001. Expression levels in the contra- (HI-c) and ipsilateral (HI-i) hemisphere or liver in HI animals are relative to levels in sham-operated animals which were put at 1. A.U.: arbitrary units; ns: non-significant.

operated littermates (Fig 2B). No changes in TGF-β, IL-4 or IL-6 were observed in the liver at this time point (Fig 2B and data not shown). However, HI induced an increase in CINC-1 mRNA at 3 h after insult in the liver (Fig 3B). In contrast, hepatic expression of MCP-1 mRNA was decreased at this time point (Fig 3B).

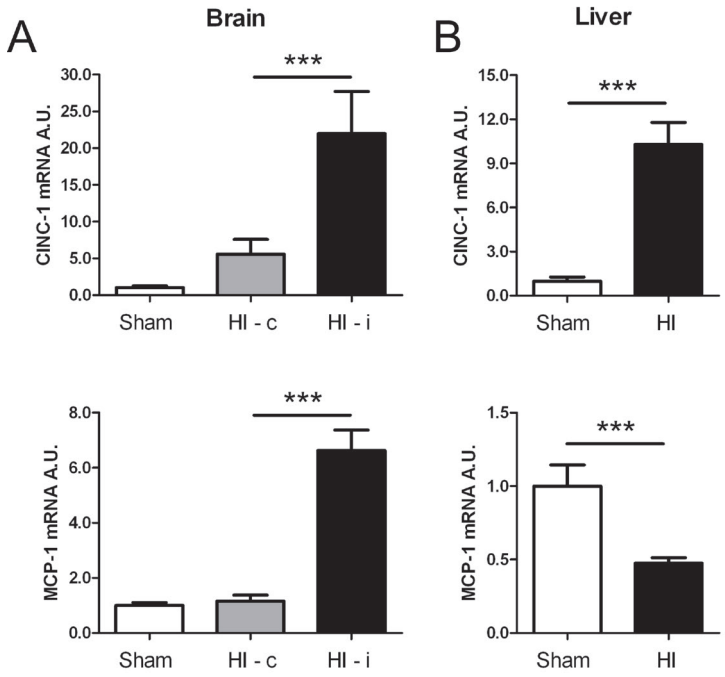

Figure 3: HI-induced expression of chemokines in the brain and liver at 3 h after HI.
Effect of HI on expression of CINC-1 and MCP-1 in the brain (**A**) and liver (**B**) as determined by quantitative real time reverse transcriptase PCR at 3 h after HI. n=14 animals for HI group and 10 animals for sham-operated (Sham) group. HI did not induce a significant increase in chemokine expression in the contralateral hemisphere compared to sham-operated littermates. *** p <0.001. Expression levels in the contra- (HI-c) and ipsilateral (HI-i) hemisphere or liver in HI animals are relative to levels in sham-operated animals which were put at 1. A.U.: arbitrary units.

Cerebral and hepatic cytokine and chemokine expression at 24 hours after HI

Twenty-four hours after insult, TNF-α, MCP-1 and CINC-1 mRNA expression were still increased in the ipsilateral hemisphere, although expression was less pronounced than at 3 h after HI (2.6 vs 5.8, 4.4 vs 6.6 and 7.0 vs 22.0 fold, 24 h vs 3 h respectively) (Fig 4A, 5A). The observed HI-induced changes in IL-1β and IL-10 mRNA expression at 3 h after HI were normalized at 24 h after HI. Interestingly, ipsilateral expression of TGF-β mRNA was increased at 24 h after HI compared to sham-operated animals (Fig 4A). No significant changes were observed in IL-4 or IL-6 mRNA expression in the brain at 24 h after HI.

In the liver, no differences in mRNA expression of any of the measured pro-inflammatory, anti-inflammatory cytokines or chemokines were observed anymore between HI-treated and sham-operated animals, except for a significant decrease in IL-10 and MCP-1 expression at 24 h after HI (Fig 4B, 5B).

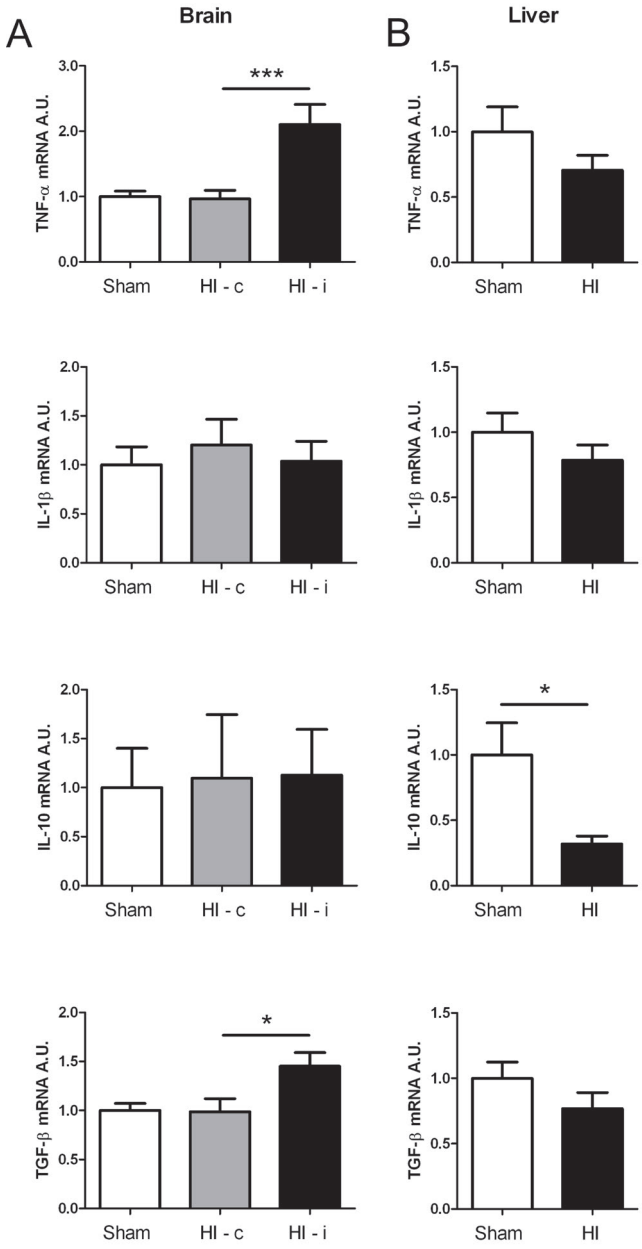

Figure 4: HI-induced expression of cytokines in the brain and liver at 24 h after HI.
Effect of HI on expression of TNF-α, IL-1β, IL-10 and TGF-β in the brain (**A**) and liver (**B**) as determined by quantitative real time reverse transcriptase PCR at 24 h after HI. n=11 animals for HI group and 10 animals for sham-operated (Sham) group. HI did not induce a significant increase in cytokine expression in the contralateral hemisphere compared to sham-operated littermates. * p <0.05, *** p <0.001. Expression levels in the contra- (HI-c) and ipsilateral (HI-i) hemisphere or liver in HI animals are relative to levels in sham-operated animals which were put at 1. A.U.: arbitrary units.

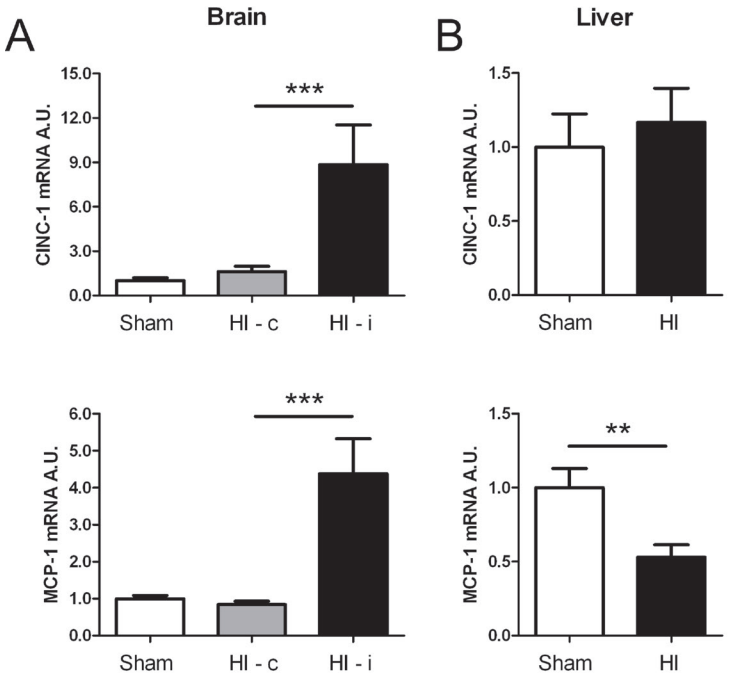

Figure 5: HI-induced expression of chemokines in the brain and liver at 24 h after HI.
Effect of HI on expression of CINC-1 and MCP-1 in the brain (**A**) and liver (**B**) as determined by quantitative real time reverse transcriptase PCR at 24 h after HI. n=11 animals for HI group and 10 animals for sham-operated (Sham) group. HI did not induce a significant increase in chemokine expression in the contralateral hemisphere compared to sham-operated littermates. ** p <0.01, *** p <0.001. Expression levels in the contra- (HI-c) and ipsilateral (HI-i) hemisphere or liver in HI animals are relative to levels in sham-operated animals which were put at 1. A.U.: arbitrary units.

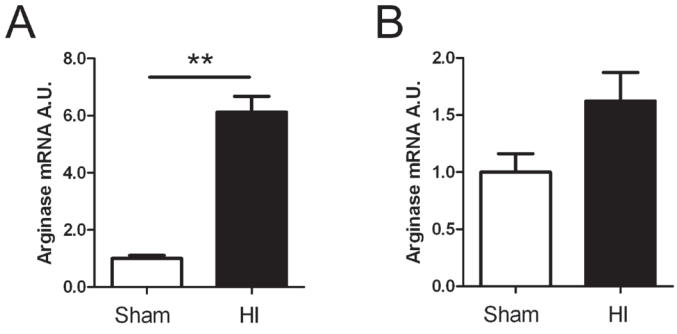

Figure 6: Hepatic arginase expression at 3 and 24 h after HI.
Effect of HI on expression of arginase in the liver as determined by quantitative real time reverse transcriptase PCR at 3 h (**A**) and 24 h (**B**) after HI. **A.** n=14 animals for HI group and 10 animals for sham-operated (Sham) group. **B.** n=11 animals for HI group and 10 animals for sham-operated group. ** p <0.01. Expression levels in the HI animals are relative to levels in sham-operated animals which were put at 1. A.U.: arbitrary units.

Hepatic metabolism

The data in figure 2B, 3B and 5B show that hepatic cytokine/chemokine expression is downregulated compared to levels in sham-operated animals. To investigate whether metabolic activity in the liver was downregulated by systemic hypoxia as such, we analyzed hepatic arginase expression. Arginase is a hepatic enzyme involved in the urea cycle and is responsible for the detoxification of ammonia released after tissue injury. Interestingly, a significant increase in hepatic arginase was observed at 3 h after HI (Fig 6A). These data indicate that hepatic metabolism is increased following HI. Twenty-four hours after HI, arginase mRNA levels were not significantly increased compared to levels in sham-operated animals, indicating that HI induces an early increase in hepatic metabolism (Fig 6A, B).

Effects of systemic hypoxia on cytokine and chemokine mRNA expression in the liver

To determine the contribution of HI-induced brain damage to the observed downregulation of cytokine and chemokine responses in the liver, we compared the expression of hepatic inflammatory cytokines and chemokines in HI animals versus animals that underwent systemic hypoxia-only or sham-operation. We analyzed hepatic expression of cytokines/chemokines that were strongly altered at 3 h after HI (Fig 2, 3), *i.e.* TNF-α, IL-1β, CINC-1 and MCP-1. For comparison reasons, we have added the hepatic cytokine/chemokine mRNA levels of sham-operated and HI-treated animals shown in figure 2 and 3 also to figure 7. Systemic hypoxia without occlusion of the carotid artery did not result in cerebral gray matter damage, since we could not observe any loss in MAP2 staining at 24 h after hypoxia (Fig 7A). Three hours after insult, no significant changes were observed in TNF-α, CINC-1 or MCP-1 expression in the liver following hypoxia-only treatment (Fig 7B). Hypoxia-only treatment induced a significant upregulation in IL-1β expression in the liver compared to levels in sham-operated littermates (Fig 7B). The effects of hypoxia-only treatment on hepatic cytokine/chemokine expression differs from the effects observed following HI, as HI induced a strong downregulation in hepatic IL-1β, TNF-α and MCP-1 expression and a significant upregulation in CINC-1 expression compared to sham-operated littermates. These data indicate that the early observed changes in hepatic cytokine/chemokine expression following HI are not induced by systemic hypoxia only.

To examine the possible effect of isoflurane anesthesia on hepatic cytokine/chemokine mRNA expression, the hepatic responses of naive animals on TNF-α, IL-1β, CINC-1 and MCP-1 mRNA expression were compared to sham-control littermates. Figure 7B shows that anesthesia did not induce significant changes in hepatic TNF-α or CINC-1 expression. In contrast, anesthesia induces a significant downregulation in hepatic IL-1β and MCP-1 expression compared to levels in naive animals, indicating that isoflurane anesthesia might influence expression of some hepatic cytokines/chemokines expression.

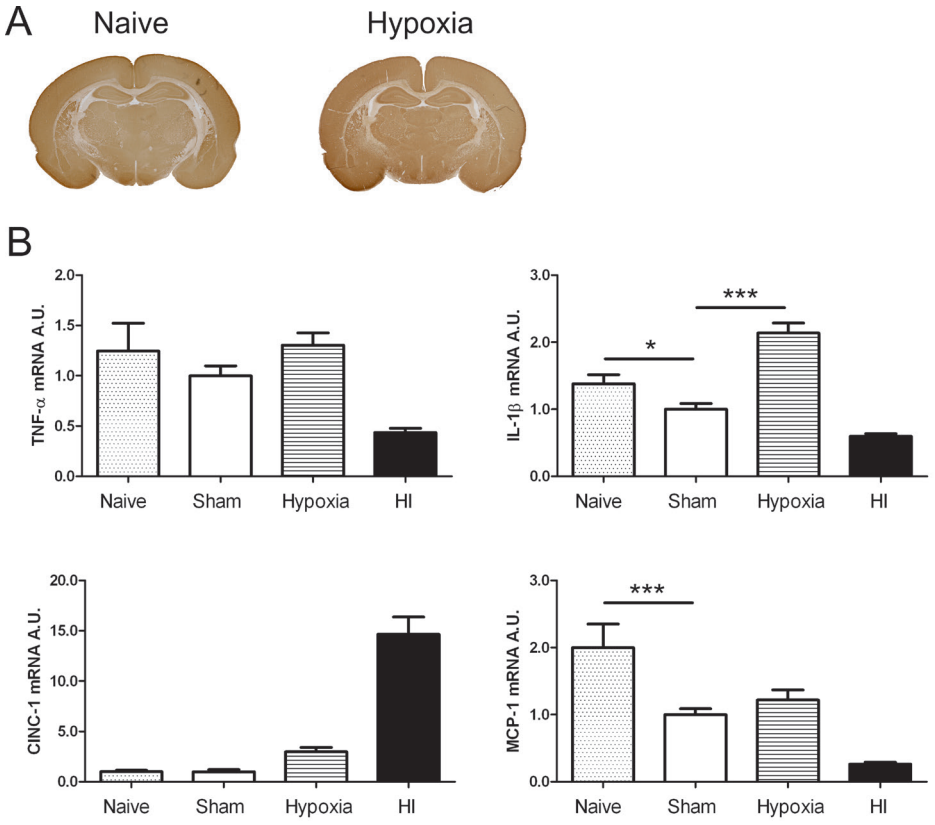

Figure 7: Effects of systemic hypoxia and anesthesia on MAP2 staining and hepatic cytokines/ chemokines mRNA expression at 3 h after hypoxia.
No neuronal damage was measured by analyzing staining for microtubule-associated protein 2 (MAP2) in the contra- and ipsilateral hemisphere of naive animals (Naive) and rats following systemic hypoxia only (Hypoxia), terminated at 24 h after insult (**A**). Effects of hypoxia and anesthesia on hepatic expression of TNF-α, IL-1β, CINC-1 and MCP-1 (**B**), as determined by quantitative real time reverse transcriptase PCR at 3 h after insult, in comparison to the expression in HI-treated and sham-operated animals (data also shown in Fig 2B and 3B). Animal numbers: n=6 naive rats, n=10 sham-operated rats (Sham), n=8 hypoxia-only treated rats and n = 14 HI-treated rats. * p <0.05, *** p <0.001. Expression levels in the liver in naive, hypoxia and HI animals are relative to levels in sham-operated animals which were put at 1. A.U.: arbitrary units.

Influx of granulocytes

Next we determined whether an influx of neutrophils into the brain was associated with the increase in cerebral CINC-1. To determine neutrophil influx in the brain, we performed a MPO assay and stained for the presence of neutrophils at 3 and 24 h after HI (Fig 8). Figure 8A shows a small, non-significant increase in neutrophil influx, determined as cerebral MPO activity, in the ipsilateral hemisphere of HI-animals as compared to MPO activity in sham-operated animals at 3 h after HI. Twenty-four hours after HI, neutrophil infiltration was significantly increased in the ipsilateral hemisphere compared to 3 h after HI (Fig 8A; p <0.001). MPO activity in contralateral hemispheres was comparable to levels in sham-operated animals.

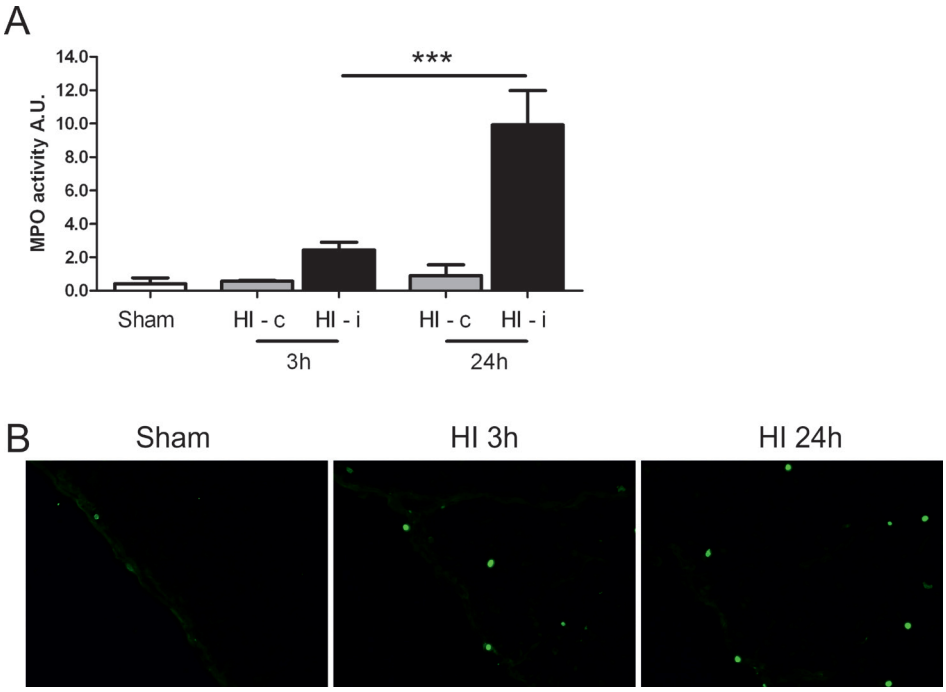

Figure 8: Influx of neutrophils in the brain at 3 and 24 h after HI.
A. Cerebral MPO activity was determined in brain homogenates of sham-operated (Sham) rat pups and in the contra- (HI-c) and ipsilateral (HI-i) hemisphere of HI-treated littermates at 3 h and 24 h after HI as a measure of neutrophil mobilization to the brain. *** p <0.001. n=6-8 animals per group. **B.** Representative examples of immunofluorescent polymorphonuclear granulocytes (PMN) staining, showing presence of one neutrophil within the meninges of sham-operated (Sham) brain (left panel), presence of neutrophils within the meninges in the ipsilateral hemisphere of a HI-treated animal at 3 h after HI (middle panel) and clear neutrophil influx in the ipsilateral cortical parenchyma at 24 h after HI (right panel). A.U.: arbitrary units.

A PMN staining was performed to determine the localization of neutrophilic granulocytes in the brain. In sham-operated animals, neutrophils were scarcely observed, and if observed, only within the meninges (Fig 8B; left panel). Three hours after HI, a slight increase in presence of neutrophils was observed within the meninges and within the cortex of the ipsilateral hemisphere (Fig 8B; middle panel). Twenty-four hours after insult, neutrophils were observed at the same locations as at 3 h, along with an increase of neutrophils throughout the cortical and hippocampal parenchyma of the ipsilateral hemisphere (Fig 8B; right panel).

Polarization of macrophages/microglia

To address whether HI induces a polarization of macrophages/microglia to the M1/M2-like phenotype in the brain, we examined the expression of specific macrophage/microglia markers at 3 and 24 h after HI. iNOS staining was used as a marker for the classical activated pro-inflammatory phenotype of macrophages/microglia (M1). Alternatively, the (anti-inflammatory) M2-like phenotype of macrophages/microglia was investigated using CD206. In sham-operated animals no clear iNOS staining could be observed in Iba-1$^+$ cells (Fig 9A,

B). Three hours after HI, a small number of iNOS$^+$-Iba-1$^+$ cells were present in the cortical region of the ipsilateral hemisphere (Fig 9A, B). However, 24 h after HI a significant increase in iNOS$^+$-Iba-1$^+$ cells was observed throughout the ipsilateral cortex, striatum, thalamus and ventromedial hypothalamic nucleus with a small increase in hippocampal region (Fig 9A, B). In the contralateral hemisphere no significant increase in iNOS$^+$-Iba-1$^+$ cells was observed.
Only very few M2-like macrophages/microglia were observed in the meninges surrounding the brain and hippocampus and capsula interna in sham-operated animals (Fig 10A, B). In HI-treated animals, no significant increase in CD206$^+$-Iba-1$^+$ cells was detected at 3 h after HI (Fig 10A, B). However, at 24 h after HI a significant increase in the amount of CD206$^+$-Iba-1$^+$ cells was observed in the ipsilateral hemisphere, especially in cortex, thalamus and hippocampus (Fig 10A, B). In the contralateral hemisphere no significant increase in CD206$^+$-Iba-1$^+$ cells was observed.

Discussion

In the present study, we demonstrate for the first time that early after induction of a neonatal HI insult, the liver responds with a downregulation of pro-inflammation whereas a pro-inflammatory response is induced in the brain, as shown by changes in hepatic and cerebral cytokine expression, cerebral neutrophil influx and polarization of cerebral macrophages/microglia to the M1-like phenotype. The hepatic response to neonatal HI is short-lasting since at 24 h most hepatic cytokine/chemokine expression levels had normalized to levels in sham-operated animals. In the brain, 24 h after HI, the early pro-inflammatory cytokine response and ipsilateral neutrophil influx was followed by a switch towards a more anti-inflammatory state of the brain exemplified by less pronounced upregulation of pro-inflammatory cytokines/chemokines and an increased expression of TGF-β 24 h after HI. Additionally an increase in the expression of the (anti-inflammatory) M2-like macrophages/microglia phenotype was observed at 24 h after HI in the ipsilateral hemisphere. However, the presence of M1-like macrophages/microglia still increased over time. The latter results may indicate that the function of M1 macrophages/microglia is actively suppressed by the action of M2 macrophages/microglia.
The hepatic response after neonatal HI differs from the peripheral response described in adult animal models of cerebral injury. In general, an increased inflammatory hepatic response has been described after brain damage. Moreover, it has been described that the pro-inflammatory state in the brain may induce the hepatic pro-inflammatory response. For instance, the group of Campbell and co-workers showed that in an adult model of local brain injury, a pronounced pro-inflammatory response was observed in the liver including an increase in hepatic chemokine expression and leukocytosis.[36,39-41] In contrast, in our neonatal model of HI, we did not observe a pro-inflammatory response in the liver after cerebral ischemic injury. There are some important differences between our study and the studies by Campbell et al. Firstly, there are clear differences in developmental stage of the animals

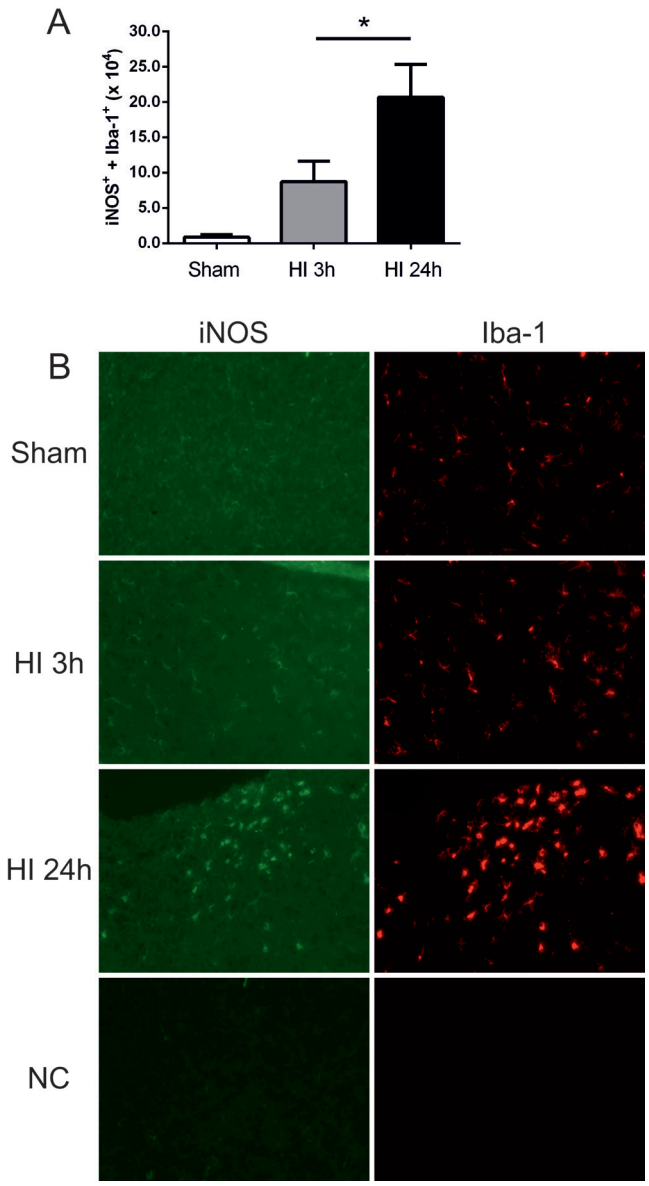

Figure 9: M1 macrophage/microglia activation in the brain at 3 and 24 h after HI.
To determine the presence and inflammatory status of macrophages/microglia in the brain, the expression of M1-like (iNOS$^+$) macrophages/microglia were examined by fluorescent immunohistochemistry at 3 and 24 h after HI. Iba-1 staining was used as a control for detection of the macrophage/microglia cell type. **A.** M1-like macrophage/microglia expression was quantified in the whole hemisphere by counting iNOS and Iba-1 double positive cells in the ipsilateral hemisphere of sham-operated (Sham) and HI-treated animals at 3 and 24 h after HI. * p <0.05. n=3 animals per group. **B.** Representative photographs of iNOS$^+$-Iba-1$^+$ staining in the ipsilateral cortex of sham-operated (Sham) animals and HI-treated animals at 3 and 24 h after HI. A negative control (NC) was used in which the primary antibodies were omitted in sections of a HI-treated animal at 24 h after HI.

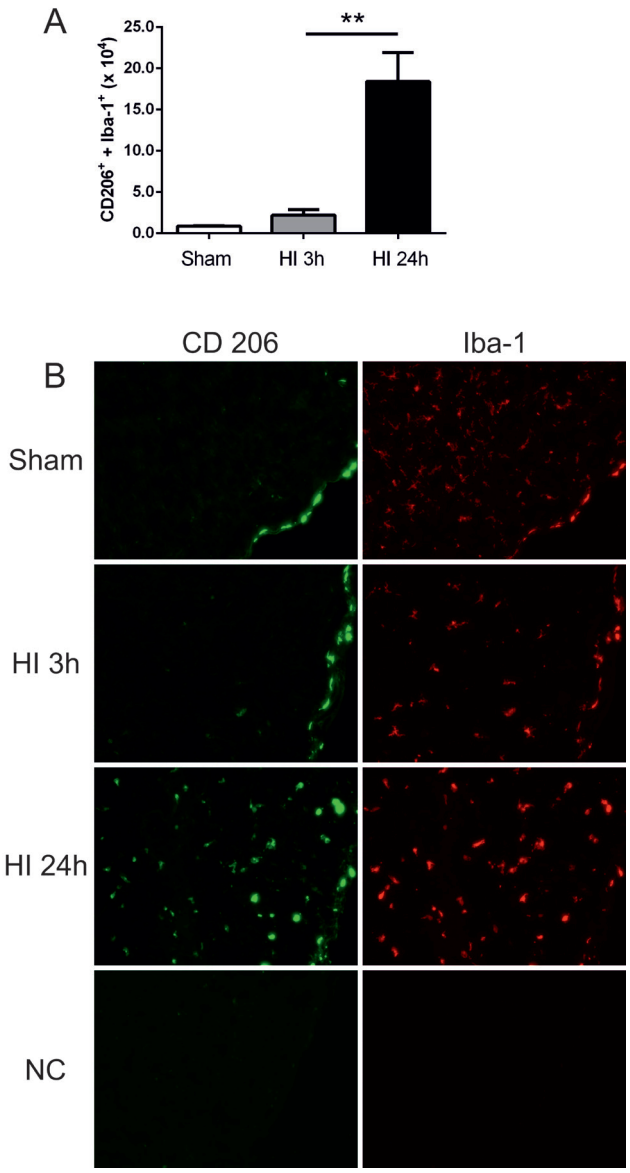

Figure 10: M2 type macrophage/microglia activation in the brain at 3 and 24 h after HI.
To determine the presence and inflammatory status of macrophages/microglia in the brain, the expression of M2-like ($CD206^+$) macrophages/microglia were examined by fluorescent immunohistochemistry at 3 and 24 h after HI. Iba-1 staining was used as a control for detection of the macrophage/microglia cell type. **A.** M2-like macrophage/microglia expression was quantified in the whole hemisphere by counting CD206 and Iba-1 double positive cells in the ipsilateral hemisphere of sham-operated (Sham) and HI-treated animals at 3 and 24 h after HI. ** p <0.01. n=3 per group. **B.** Representative photographs of $CD206^+$-$Iba\text{-}1^+$ staining in the ipsilateral cortex of sham-operated (Sham) animals and HI-treated animals at 3 and 24 h after HI. Note the $CD206^+$-staining in the meninges in sham-operated animals and HI-treated animals at 3h after HI. A negative control (NC) was used in which the primary antibodies were omitted in sections of a HI-treated animal at 24 h after HI

as we have used a model of *neonatal* HI using P7 rats whereas Campbell et al. have used a model of local brain injury (intracerebral IL-1β injection) in *adult* mice.[36-39,41] Secondly, the type of brain injury that is induced in the studies of Campbell et al. (2003) differs as we used a combination of cerebral ischemia and systemic hypoxia, whereas Campbell et al. have induced brain injury by injecting a high (non-physiological) dose of IL-1β in the brain. It is possible that this high dose of IL-1β injected locally in the brain causes a spillover into the bloodstream via which it may have affected the hepatic inflammatory response. Our model of combined cerebral ischemia and systemic hypoxia may have more clinical relevance, since the human neonate is also often subjected to systemic hypoxia in case of a cerebral insult.

Although systemic hypoxia might be responsible for the decreased pro-inflammatory response in the liver after cerebral ischemia, in the literature hypoxia is mostly associated with an induction of pro-inflammatory responses. For instance, Ashdown et al. (2008) described an increase in hepatic IL-1β and IL-6 protein levels following 15 min of global hypoxia in a neonatal rat model.[43] Furthermore, several studies show that hypoxic conditions induce activation of several transcriptional pathways including HIF-1α, NF-κB and JNK, which together regulate the transcription of more than 100 genes involved in inflammation.[44-48] To address the role of systemic hypoxia following neonatal HI in hepatic inflammatory responses, we included rats which underwent systemic hypoxia only without occlusion of the carotid artery. As was shown in figure 7B, systemic hypoxia did not change hepatic expression of TNF-α, CINC-1 or MCP-1 mRNA, whereas IL-1β mRNA expression was significantly increased instead of decreased as observed after HI. These data clearly indicate that systemic hypoxia as such is not primarily responsible for the downregulation of the hepatic pro-inflammatory response 3 h after insult. We suggest that the damage signal originating from the cerebral injury regulates downregulation of the hepatic pro-inflammatory cytokine response.

Direct damage to the brain and/or subsequent cerebral production of pro-inflammatory cytokines can cause a downregulation of the peripheral inflammatory response due to stimulation of the (para)sympathetic nervous system or the hypothalamic pituitary adrenal (HPA) axis.[49-52] Glucocorticoids, catecholamines and acetylcholamine released after brain injury might inhibit the systemic expression of pro-inflammatory cytokines IL-1β and TNF-α and increase the secretion of anti-inflammatory IL-10 and IL-4.[53-55] This phenomenon of local brain damage affecting peripheral inflammatory responses is in adult brain injury models known as stroke- or CNS injury-induced immunodepression syndrome. In this syndrome, local brain damage is responsible for the systemic downregulation of innate and adaptive immunity.[49,51,52,56] The downregulation of systemic pro-inflammatory cytokines and the increase in IL-10 by stimulation of the (para)sympathetic nervous system and HPA axis are in line with our hepatic cytokine data.

We did not observe an overall downregulation of hepatic cytokine activity at 3 h after HI, since IL-10 and CINC-1 were increased. Moreover, there is an increase in metabolic activity in the liver since arginase was profoundly increased. Arginase is involved in the last step of the urea cycle in which toxic ammonia is converted to urea, which takes plays in the cytoplasm

of the liver.[57-59] We suggest that the increase in hepatic arginase could be used as a marker for increased hepatic metabolism after HI.

In the literature, it has been described that (isoflurane) anesthesia can affect cerebral and systemic cytokine/chemokine expression and inflammatory responses.[60-62] To determine the effect of brief isoflurane anesthesia on the hepatic cytokine and chemokine expression, we compared the expression of TNF-α, IL-1β, CINC-1 and MCP-1 in the liver of naive and sham-operated animals. Anesthesia did not affect hepatic expression of TNF-α and CINC-1, whereas it downregulated hepatic IL-1β and MCP-1 mRNA expression, indicating that isoflurane anesthesia or minor surgery influences hepatic cytokine and chemokine expression. However, since there was no difference in anesthesia dosage or duration between sham-operated animals and HI animals, the differences in cytokine/chemokine expression between both groups cannot be explained by the influence of anesthesia.

Besides a decrease in pro-inflammatory cytokines, we observed an increase in CINC-1 expression in the liver. Campbell et al. (2003) have described that the chemokine CINC-1 can be viewed upon as an acute phase protein, which is upregulated in the liver following brain injury.[36] Furthermore, Devlin et al. (2005) described an upregulation of hepatic acute phase proteins (complement factors C9 and C3 mRNA) following neonatal HI.[63] Taken these data together, we conclude that neonatal HI induces an acute phase response in the liver. Interestingly, the selective increased CINC-1 expression in the liver might be another indication for sympathetic regulation of the hepatic response to neonatal HI. We have previously shown that stimulation of β2-adrenergic receptors on freshly isolated human peripheral blood monocytes and a premonocytic cell line results in enhanced IL-8 (homologue of CINC-1 in the rat) production.[64] From these data, we are inclined to speculate that sympathetic activation might be the important regulator of the inflammatory response in the liver after neonatal HI. CINC-1 is an important chemokine involved in the recruitment of neutrophils to sites of injury.[65,66] An increase in hepatic CINC-1 has been observed in adult murine models of stroke and cerebral IL-1β micro-injection, in which an increase in CINC-1 was associated with increased neutrophil numbers within the liver and the circulation.[36,40] Hepatic CINC-1 expression could be partly responsible for the mobilization of neutrophils from the bone marrow to the circulation and secondary to the brain. Within 3 h after the insult, a small increase in the presence of neutrophils was observed in the ipsilateral hemisphere, which further increased at 24 h after insult. Neutrophilic granulocytes are known to play a role in clearing cellular debris after tissue damage. However, these cells can negatively affect the development of tissue damage as neutrophils can produce *e.g.* reactive oxygen species, release cytotoxic agents and reduce microvascular flow. By neutrophil depletion studies, we and others have shown the detrimental effects of infiltrating neutrophils into the brain for cerebral damage.[19,20,22,42] We propose that inhibition of peripheral CINC-1 could reduce the massive influx of neutrophils to the circulation and brain and could be a novel therapeutic option for neonatal HI.

Besides the influx of neutrophils, HI also induces recruitment of macrophages to the brain. In our study, an increase in MCP-1, a crucial chemokine for monocyte recruitment, was observed in the ipsilateral hemisphere within 3 h after the insult. Monocytes/macrophages are known to be recruited to the site of injury where they locally contribute to the inflammatory process by producing cytokines and chemokines.[67,68] Resident microglia may also be activated to regulate local injury. Immune activation can polarize macrophages/microglia to express a pro-inflammatory (M1) or an anti-inflammatory (M2) phenotype.[69] Interferon-γ, LPS and TNF-α are factors known to induce the pro-inflammatory M1 phenotype and these macrophages are characterized by expression of pro-inflammatory factors, iNOS and IL-1β. In contrast, IL-4, IL-13 and IL-10 are known inducers of the anti-inflammatory M2 macrophage type, which induce anti-inflammatory cytokines like IL-10 and TGF-β. Moreover, M2 macrophages can inhibit NO production and pro-inflammatory cytokines and are involved in tissue repair and regeneration.[68,70-72]

Although we used a single marker to determine the M1 (iNOS) and M2 (CD206) macrophages, we show here for the first time that neonatal HI also induces polarization of macrophages/microglia to the M1-like or M2-like phenotype in the brain. Going along with the pro-inflammatory state of the brain at 3 h after HI, an increase in the presence of M1-like macrophages (iNOS$^+$-Iba-1$^+$) was observed in the ipsilateral hemisphere at this time point, further increasing at 24 h after HI. For M2-like macrophages, an increase in CD206$^+$-Iba-1$^+$ cells was observed in the ipsilateral hemisphere 24 h after HI, along with normalization of the pro-inflammatory state and an upregulation of TGF-β expression in the ipsilateral hemisphere. Both M1-like and M2-like macrophages/microglia were particularly observed in the most damaged areas of the ipsilateral hemisphere as demonstrated with MAP2 staining. The presence of the M2-like cells in the meninges indicates that the recruitment of macrophages partially takes place via the meningeal circulation.

Conclusions

In conclusion, in the present study we show that neonatal HI induces an early downregulation of the pro-inflammatory response in the liver. We propose that this downregulation might be induced by activation of the (para)sympathetic nervous system due to brain damage and/or the cerebral inflammatory response following HI. In contrast to the liver, in the brain an early pro-inflammatory response is induced with a concomitant increase in ipsilateral expression of pro-inflammatory cytokines/chemokines, influx of neutrophils and polarization of macrophages/microglia to the M1-like phenotype. This pro-inflammatory state of the brain changes after 24 h, with normalization of pro-inflammatory cytokine/chemokine expression, an increase of anti-inflammatory TGF-β and an increase in expression of M2-like macrophages/microglia in the ipsilateral hemisphere.

References

1. de Haan M, Wyatt JS, Roth S, Vargha-Khadem F, Gadian D, Mishkin M. Brain and cognitive-behavioural development after asphyxia at term birth. *Dev Sci* 2006;9:350-358.
2. Gonzalez FF, Miller SP. Does perinatal asphyxia impair cognitive function without cerebral palsy? *Arch Dis Child Fetal Neonatal Ed* 2006;91:F454-9.
3. van Handel M, Swaab H, de Vries LS, Jongmans MJ. Long-term cognitive and behavioral consequences of neonatal encephalopathy following perinatal asphyxia: a review. *Eur J Pediatr* 2007;166:645-654.
4. Armstrong-Wells J, Bernard TJ, Boada R, Manco-Johnson M. Neurocognitive outcomes following neonatal encephalopathy. *NeuroRehabilitation* 2010;26:27-33.
5. Glass HC, Hong KJ, Rogers EE, et al. Risk factors for epilepsy in children with neonatal encephalopathy. *Pediatr Res* 2011;70:535-540.
6. Wyatt JS, Gluckman PD, Liu PY, et al. Determinants of outcomes after head cooling for neonatal encephalopathy. *Pediatrics* 2007;119:912-921.
7. Graham EM, Ruis KA, Hartman AL, Northington FJ, Fox HE. A systematic review of the role of intrapartum hypoxia-ischemia in the causation of neonatal encephalopathy. *Am J Obstet Gynecol* 2008;199:587-595.
8. Shankaran S, Laptook AR, Ehrenkranz RA, et al. Whole-body hypothermia for neonates with hypoxic-ischemic encephalopathy. *N Engl J Med* 2005;353:1574-1584.
9. Gluckman PD, Wyatt JS, Azzopardi D, et al. Selective head cooling with mild systemic hypothermia after neonatal encephalopathy: multicentre randomised trial. *Lancet* 2005;365:663-670.
10. Azzopardi DV, Strohm B, Edwards AD, et al. Moderate hypothermia to treat perinatal asphyxial encephalopathy. *N Engl J Med* 2009;361:1349-1358.
11. Cao J, Xu J, Li W, Liu J. Influence of selective brain cooling on the expression of ICAM-1 mRNA and infiltration of PMNLs and monocytes/macrophages in rats suffering from global brain ischemia/reperfusion injury. *Biosci Trends* 2008;2:241-244.
12. Gunn AJ, Wyatt JS, Whitelaw A, et al. Therapeutic hypothermia changes the prognostic value of clinical evaluation of neonatal encephalopathy. *J Pediatr* 2008;152:55-8, 58.e1.
13. Gonzalez-Ibarra FP, Varon J, Lopez-Meza EG. Therapeutic hypothermia: critical review of the molecular mechanisms of action. *Front Neurol* 2011;2:4.
14. Williams GD, Dardzinski BJ, Buckalew AR, Smith MB. Modest hypothermia preserves cerebral energy metabolism during hypoxia-ischemia and correlates with brain damage: a 31P nuclear magnetic resonance study in unanesthetized neonatal rats. *Pediatr Res* 1997;42:700-708.
15. Zhao H, Shimohata T, Wang JQ, et al. Akt contributes to neuroprotection by hypothermia against cerebral ischemia in rats. *J Neurosci* 2005;25:9794-9806.
16. Baker AJ, Zornow MH, Grafe MR, et al. Hypothermia prevents ischemia-induced increases in hippocampal glycine concentrations in rabbits. *Stroke* 1991;22:666-673.
17. Lin S, Rhodes PG, Cai Z. Whole body hypothermia broadens the therapeutic window of intranasally administered IGF-1 in a neonatal rat model of cerebral hypoxia-ischemia. *Brain Res* 2011;1385:246-256.
18. Robertson NJ, Bhakoo K, Puri BK, Edwards AD, Cox IJ. Hypothermia and amiloride preserve energetics in a neonatal brain slice model. *Pediatr Res* 2005;58:288-296.
19. Palmer C, Roberts RL, Young PI. Timing of neutrophil depletion influences long-term neuroprotection in neonatal rat hypoxic-ischemic brain injury. *Pediatr Res* 2004;55:549-556.
20. Hagberg H, Gilland E, Bona E, et al. Enhanced expression of interleukin (IL)-1 and IL-6 messenger RNA and bioactive protein after hypoxia-ischemia in neonatal rats. *Pediatr Res* 1996;40:603-609.
21. Silverstein FS, Barks JD, Hagan P, Liu XH, Ivacko J, Szaflarski J. Cytokines and perinatal brain injury. *Neurochem Int* 1997;30:375-383.

22. Hudome S, Palmer C, Roberts RL, Mauger D, Housman C, Towfighi J. The role of neutrophils in the production of hypoxic-ischemic brain injury in the neonatal rat. *Pediatr Res* 1997;41:607-616.
23. Silveira RC, Procianoy RS. Interleukin-6 and tumor necrosis factor-alpha levels in plasma and cerebrospinal fluid of term newborn infants with hypoxic-ischemic encephalopathy. *J Pediatr* 2003;143:625-629.
24. Hedtjarn M, Mallard C, Hagberg H. Inflammatory gene profiling in the developing mouse brain after hypoxia-ischemia. *J Cereb Blood Flow Metab* 2004;24:1333-1351.
25. van den Tweel ER, Kavelaars A, Lombardi MS, et al. Bilateral molecular changes in a neonatal rat model of unilateral hypoxic-ischemic brain damage. *Pediatr Res* 2006;59:434-439.
26. Aly H, Khashaba MT, El-Ayouty M, El-Sayed O, Hasanein BM. IL-1beta, IL-6 and TNF-alpha and outcomes of neonatal hypoxic ischemic encephalopathy. *Brain Dev* 2006;28:178-182.
27. Bona E, Andersson AL, Blomgren K, et al. Chemokine and inflammatory cell response to hypoxia-ischemia in immature rats. *Pediatr Res* 1999;45:500-509.
28. Dammann O, O'Shea TM. Cytokines and perinatal brain damage. *Clin Perinatol* 2008;35:643-63.
29. Nijboer CH, Heijnen CJ, Groenendaal F, May MJ, van Bel F, Kavelaars A. Strong neuroprotection by inhibition of NF-kappaB after neonatal hypoxia-ischemia involves apoptotic mechanisms but is independent of cytokines. *Stroke* 2008;39:2129-2137.
30. Jones TB, McDaniel EE, Popovich PG. Inflammatory-mediated injury and repair in the traumatically injured spinal cord. *Curr Pharm Des* 2005;11:1223-1236.
31. Lucas SM, Rothwell NJ, Gibson RM. The role of inflammation in CNS injury and disease. Br J *Pharmacol* 2006;147 Suppl 1:S232-40.
32. Nijboer CH, Heijnen CJ, Groenendaal F, van Bel F, Kavelaars A. Alternate pathways preserve tumor necrosis factor-alpha production after nuclear factor-kappaB inhibition in neonatal cerebral hypoxia-ischemia. *Stroke* 2009;40:3362-3368.
33. Greenhalgh AD, Galea J, Denes A, Tyrrell PJ, Rothwell NJ. Rapid brain penetration of interleukin-1 receptor antagonist in rat cerebral ischaemia: pharmacokinetics, distribution, protection. Br J *Pharmacol* 2010;160:153-159.
34. Anthony DC, Couch Y, Losey P, Evans MC. The systemic response to brain injury and disease. *Brain Behav Immun* 2012;26:534-540.
35. Wilcockson DC, Campbell SJ, Anthony DC, Perry VH. The systemic and local acute phase response following acute brain injury. *J Cereb Blood Flow Metab* 2002;22:318-326.
36. Campbell SJ, Hughes PM, Iredale JP, et al. CINC-1 is an acute-phase protein induced by focal brain injury causing leukocyte mobilization and liver injury. *FASEB J* 2003;17:1168-1170.
37. Campbell SJ, Perry VH, Pitossi FJ, et al. Central nervous system injury triggers hepatic CC and CXC chemokine expression that is associated with leukocyte mobilization and recruitment to both the central nervous system and the liver. *Am J Pathol* 2005;166:1487-1497.
38. Campbell SJ, Zahid I, Losey P, et al. Liver Kupffer cells control the magnitude of the inflammatory response in the injured brain and spinal cord. *Neuropharmacology* 2008;55:780-787.
39. Campbell SJ, Anthony DC, Oakley F, et al. Hepatic nuclear factor kappa B regulates neutrophil recruitment to the injured brain. *J Neuropathol Exp Neurol* 2008;67:223-230.
40. Chapman KZ, Dale VQ, Denes A, et al. A rapid and transient peripheral inflammatory response precedes brain inflammation after experimental stroke. *J Cereb Blood Flow Metab* 2009;29:1764-1768.
41. Campbell SJ, Deacon RM, Jiang Y, Ferrari C, Pitossi FJ, Anthony DC. Overexpression of IL-1beta by adenoviral-mediated gene transfer in the rat brain causes a prolonged hepatic chemokine response, axonal injury and the suppression of spontaneous behaviour. *Neurobiol Dis* 2007;27:151-163.
42. Nijboer CH, Kavelaars A, Vroon A, Groenendaal F, van Bel F, Heijnen CJ. Low endogenous G-protein-coupled receptor kinase 2 sensitizes the immature brain to hypoxia-ischemia-induced gray and white matter damage. *J Neurosci* 2008;28:3324-3332.
43. Ashdown H, Joita S, Luheshi GN, Boksa P. Acute brain cytokine responses after global birth hypoxia in the rat. *J Neurosci Res* 2008;86:3401-3409.

44. Hellwig-Burgel T, Stiehl DP, Wagner AE, Metzen E, Jelkmann W. Review: hypoxia-inducible factor-1 (HIF-1): a novel transcription factor in immune reactions. *J Interferon Cytokine Res* 2005;25:297-310.
45. Copple BL, Bai S, Burgoon LD, Moon JO. Hypoxia-inducible factor-1alpha regulates the expression of genes in hypoxic hepatic stellate cells important for collagen deposition and angiogenesis. *Liver Int* 2011;31:230-244.
46. Wenger RH. Mammalian oxygen sensing, signalling and gene regulation. *J Exp Biol* 2000;203:1253-1263.
47. Stroka DM, Burkhardt T, Desbaillets I, et al. HIF-1 is expressed in normoxic tissue and displays an organ-specific regulation under systemic hypoxia. *FASEB J* 2001;15:2445-2453.
48. McCloskey CA, Kameneva MV, Uryash A, Gallo DJ, Billiar TR. Tissue hypoxia activates JNK in the liver during hemorrhagic shock. *Shock* 2004;22:380-386.
49. Prass K, Meisel C, Hoflich C, et al. Stroke-induced immunodeficiency promotes spontaneous bacterial infections and is mediated by sympathetic activation reversal by poststroke T helper cell type 1-like immunostimulation. *J Exp Med* 2003;198:725-736.
50. Pavlov VA, Wang H, Czura CJ, Friedman SG, Tracey KJ. The cholinergic anti-inflammatory pathway: a missing link in neuroimmunomodulation. *Mol Med* 2003;9:125-134.
51. Meisel C, Schwab JM, Prass K, Meisel A, Dirnagl U. Central nervous system injury-induced immune deficiency syndrome. *Nat Rev Neurosci* 2005;6:775-786.
52. Chamorro A, Urra X, Planas AM. Infection after acute ischemic stroke: a manifestation of brain-induced immunodepression. *Stroke* 2007;38:1097-1103.
53. Woiciechowsky C, Asadullah K, Nestler D, et al. Sympathetic activation triggers systemic interleukin-10 release in immunodepression induced by brain injury. *Nat Med* 1998;4:808-813.
54. Webster JI, Tonelli L, Sternberg EM. Neuroendocrine regulation of immunity. *Annu Rev Immunol* 2002;20:125-163.
55. Borovikova LV, Ivanova S, Zhang M, et al. Vagus nerve stimulation attenuates the systemic inflammatory response to endotoxin. *Nature* 2000;405:458-462.
56. Elenkov IJ, Wilder RL, Chrousos GP, Vizi ES. The sympathetic nerve--an integrative interface between two supersystems: the brain and the immune system. *Pharmacol Rev* 2000;52:595-638.
57. Procianoy RS. Hyperammonemia and perinatal asphyxia. *Pediatrics* 1981;67:578-579.
58. Esque-Ruiz MT, Figueras-Aloy J, Salvia-Roiges MD, Carbonell-Estrany X. Blood ammonia and transaminases in full term infants suffering from perinatal asphyxia. *Rev Neurol* 2003;36:801-805.
59. Lee A, Lingwood BE, Bjorkman ST, et al. Rapid loss of glutamine synthetase from astrocytes in response to hypoxia: implications for excitotoxicity. *J Chem Neuroanat* 2010;39:211-220.
60. Barnum SR, Ames RS, Maycox PR, et al. Expression of the complement C3a and C5a receptors after permanent focal ischemia: An alternative interpretation. *Glia* 2002;38:169-173.
61. Lee HT, Emala CW, Joo JD, Kim M. Isoflurane improves survival and protects against renal and hepatic injury in murine septic peritonitis. *Shock* 2007;27:373-379.
62. Lv X, Yang L, Tao K, et al. Isoflurane preconditioning at clinically relevant doses induce protective effects of heme oxygenase-1 on hepatic ischemia reperfusion in rats. *BMC Gastroenterol* 2011;11:31.
63. Devlin LA, Nguyen MD, Figueroa E, Gordon LE, Feldhoff PW, Lassiter HA. Effects of endotoxin administration and cerebral hypoxia-ischemia on complement activity and local transcriptional regulation in neonatal rats. *Neurosci Lett* 2005;390:109-113.
64. Kavelaars A, van de Pol M, Zijlstra J, Heijnen CJ. Beta 2-adrenergic activation enhances interleukin-8 production by human monocytes. *J Neuroimmunol* 1997;77:211-216.
65. Maher JJ, Scott MK, Saito JM, Burton MC. Adenovirus-mediated expression of cytokine-induced neutrophil chemoattractant in rat liver induces a neutrophilic hepatitis. *Hepatology* 1997;25:624-630.

66. Wittwer AJ, Carr LS, Zagorski J, Dolecki GJ, Crippes BA, De Larco JE. High-level expression of cytokine-induced neutrophil chemoattractant (CINC) by a metastatic rat cell line: purification and production of blocking antibodies. *J Cell Physiol* 1993;156:421-427.

67. Martinez FO, Helming L, Gordon S. Alternative activation of macrophages: an immunologic functional perspective. *Annu Rev Immunol* 2009;27:451-483.

68. Martinez FO. Regulators of macrophage activation. *Eur J Immunol* 2011;41:1531-1534.

69. Martinez FO, Sica A, Mantovani A, Locati M. Macrophage activation and polarization. *Front Biosci* 2008;13:453-461.

70. Mosser DM, Edwards JP. Exploring the full spectrum of macrophage activation. *Nat Rev Immunol* 2008;8:958-969.

71. Gordon S, Martinez FO. Alternative activation of macrophages: mechanism and functions. *Immunity* 2010;32:593-604.

72. Murray PJ, Wynn TA. Obstacles and opportunities for understanding macrophage polarization. *J Leukoc Biol* 2011;89:557-563.

3

Mitochondrial JNK phosphorylation as a novel therapeutic target to inhibit neuroinflammation and apoptosis after neonatal ischemic brain damage

Cora H. Nijboer
Hilde J.C. Bonestroo
Jitske Zijlstra
Annemieke Kavelaars
Cobi J. Heijnen

Neurobiology of Disease 2013;54:432-44.

Abstract

Background Neonatal encephalopathy is associated with high mortality and life-long developmental consequences. Therapeutic options are very limited. We assessed the effects of D-JNKi, a small peptide c-Jun N-terminal kinase (JNK) MAP kinase inhibitor, on neuroinflammation, mitochondrial integrity and neuronal damage in a neonatal rat model of ischemic brain damage.

Methods Hypoxic-ischemic (HI) brain injury was induced in postnatal-day 7 rats by unilateral carotid artery occlusion and hypoxia, and was followed by intraperitoneal D-JNKi treatment.

Results We demonstrate here for the first time that a single intraperitoneal injection with D-JNKi directly after HI strongly reduces neonatal brain damage by >85% with a therapeutic window of at least 6 h. D-JNKi treatment also restored cognitive and motor function as analyzed at 9 weeks post-insult. Neuroprotective D-JNKi treatment inhibited phosphorylation of nuclear c-Jun (P-c-Jun), and consequently reduced activity of the AP-1 transcription factor and production of cerebral cytokines/chemokines as determined at 3 and 24 h post-HI. Inhibition of P-c-Jun by D-JNKi is thought to be mediated via inhibition of the upstream phosphorylation of cytosolic and nuclear JNK and/or by preventing the direct interaction of phosphorylated (P)JNK with c-Jun. Surprisingly, however, HI did not induce a detectable increase in P-JNK in cytosol or nucleus. Notably, we show here for the first time that HI induces P-JNK only in the mitochondrial fraction, which was completely prevented by D-JNKi treatment. The hypothesis that mitochondrial JNK activation is key to HI brain injury was supported by data showing that treatment of rat pups with Sab_{KIM1} peptide, a specific mitochondrial JNK inhibitor, is also neuroprotective. Inhibition of HI-induced mitochondrial JNK activation was associated with preservation of mitochondrial integrity as evidenced by prevention of ATP loss and inhibition of lipid peroxidation. The HI-induced increase in apoptotic markers (cytochrome *c* release and caspase 3 activation) as analyzed at 24 h post-HI were also strongly reduced by D-JNKi and the mitochondrial anti-apoptotic proteins Bcl-2 and Bcl-xL were upregulated. Neuroprotection was lost after repeated 0+3 h D-JNKi treatment which was associated with complete inhibition of the second peak of AP-1 activity and disability to upregulate mitochondrial Bcl-2 and Bcl-xL.

Conclusion We show here for the first time that D-JNKi treatment efficiently protects the neonatal brain against ischemic brain damage and subsequent cognitive and motor impairment. We propose that inhibition of phosphorylation of mitochondrial JNK is a pivotal step in preventing early loss of mitochondrial integrity leading to reduced neuroinflammation and inhibition of apoptotic neuronal loss. Moreover we show the crucial role of upregulation of mitochondrial anti-apoptotic proteins to maintain neuroprotection.

Introduction

The consequences of neonatal encephalopathy include high mortality and, in the surviving infants, life-long consequences like cerebral palsy and cognitive deficits.[1,2] At present, hypothermia is the only clinical intervention available and additional neuroprotective strategies to combat perinatal brain injury are urgently needed.[3,4]

Key players in the pathophysiology of neonatal cerebral injury are excitotoxicity, oxidative stress, and inflammation leading to apoptotic and necrotic neuronal death.[5] Upon cellular stress, mitogen-activated protein (MAP) kinases, including the c-Jun N-terminal kinase (JNK), are activated. Activated JNK regulates several cellular processes like apoptosis, DNA repair and inflammation via phosphorylation of c-Jun, the dominant component of the activator protein (AP-)1 transcription factor.[6,7] JNK also phosphorylates non-nuclear proteins, including members of the Bcl-2 family that reside at the mitochondria and regulate apoptosis.[8]

JNK activation occurs in a complex consisting of the scaffold protein JIP1 (JNK-interacting protein 1) which binds JNK and upstream kinases such as MKK4/7 and MEK-1.[9-11] A conserved kinase-interaction motif (KIM) has been identified in JIP1 and other proteins that interact with JNK. The JNK-inhibiting peptides L-JNKI and its more stable retro-inverso peptide D-JNKi have been developed based on the structure of the KIM of JIP1.[9-11] L-JNKi and D-JNKi are thought to bind JNK thereby competitively inhibiting JNK interaction with JIP1 as well as with the KIM of upstream kinases and JNK-substrates, including c-Jun.[9-12]

D-JNKi has been shown to be a powerful neuroprotectant in *in vitro* models of excitotoxicity and *in vivo* models of adult cerebral ischemia.[13-17] Previously we showed a modest neuroprotective effect of repeated L-JNKi administration (10 mg/kg intraperitoneal (i.p.), 0+3 h post-insult) after neonatal hypoxia ischemia (HI) in newborn rats. However, Ginet et al. (2009) showed that repeated D-JNKi treatment (0.3 mg/kg i.p. at 30 min prior to and 3, 5, 8, 12 and 20 h post-HI) failed to reduce HI brain injury in neonatal rats.[18]

The aim of the current study was to determine whether D-JNKi reduces brain damage and prevents cognitive and motor impairment in a model of neonatal HI brain damage when given as a single injection at a dose of 10 mg/kg. We also studied the underlying mechanism of treatment with the D-JNKi peptide on the JNK/AP-1 pathway and on neuroinflammation, mitochondrial integrity and apoptotic cell death after neonatal HI.

Materials and Methods

Animals

Experiments were approved by the UMC Utrecht-animal ethical committee. Seven-day-old (P7) Wistar rats were anesthetized with isoflurane (5% induction, 1.5% maintenance in O_2:N_2O (1:1)) for <5 min during which the right common carotid artery was exposed and occluded by thermocauterization. Pups recovered for at least 1 h before undergoing hypoxia

for 120 min at 8% O_2 in N_2. Sham-controls underwent anesthesia and incision only. All analyses were performed in blinded set-up. Pups of both genders were used and we did not observe any gender differences in any of the measured parameters.

D-JNKi (dqsrpvqpflnlttprkpr-pp-rrrqrrkkrg; all D-amino acids retro-inverso form; underlined amino acids represent HIV-TAT shuttle domain) was provided by Xigen SA (Epalinges, Switzerland). Sab_{KIM1} peptide (gfeslsvpspldlsgprvva-pp-rrrqrrkkrg; all D-amino acids retro-inverso form) and scrambled TAT-containing retro-inverso D-peptide (SCR) (lpsvfgdvgapsrlpevsls-pp-rrrqrrkkrg; all D-amino acids retro-inverso form) were synthetized at W.M. Keck facility (Yale University, New Haven, CT, USA). Peptides were dissolved in PBS (vehicle) and administered i.p. at 10 mg/kg or 20 mg/kg.

Histology

Rats were sacrificed by pentobarbital overdose and perfused with 4% paraformaldehyde in PBS. Brains were post-fixed and either embedded in paraffin, or cryoprotected in 30% sucrose in PBS and embedded in OCT freezing medium (Tissue-Teck, Sakura Finetek Europe, Zoeterwoude, the Netherlands).

Coronal paraffin sections (8 µm; -3.20 mm from bregma in adult brain) were stained with hematoxylin-eosin (HE) or with mouse-anti-microtubule-associated protein 2 (MAP2) (Sigma-Aldrich, Steinheim, Germany) followed by biotin-labeled horse-anti-mouse antibody (Vector-Labs, Burlingame, CA) and revealed using Vectastain ABC kit (Vector-Labs) and diaminobenzamidine. MAP2 staining was used as an early marker of neuronal damage at 48 h post-HI and HE staining was used to study long-term infarct size at 9 weeks post-HI. Full section images were captured with a Nikon D1 digital camera (Nikon, Tokyo, Japan). We analyzed HE- or MAP2-stained sections as described previously.[19,20] In short, MAP2-positive area of ipsi- and contralateral hemispheres was outlined manually with image processing tools in Adobe Photoshop (Adobe Systems Inc, San Jose, CA) and lesion size was calculated by the ratio of ipsilateral to contralateral areas. Areas of contralateral and ipsilateral hemispheres were measured on HE-stained sections at 9 weeks post-HI using Adobe Photoshop and ipsilateral volume loss was calculated as 1- (ipsi-/contralateral HE-positive area).

For immunofluorescent double-staining's, coronal frozen sections (8 µm; -3.20 mm from bregma in adult brain) were incubated with rabbit-anti-phospho-c-Jun (Ser63II) (Cell Signaling, Danvers, MA) and double-stained with mouse-anti-neuronal nuclei (NeuN) (Millipore, Darmstadt, Germany), mouse-anti-glial fibrillary acidic protein (GFAP) (Acris, Herford, Germany) or rat-anti-CD11b (BD Biosciences Pharmingen, San Jose, CA) followed by AlexaFluor 488- and 594-conjugated secondary antibodies (both Molecular Probes, Eugene, OR). Sections were counterstained with DAPI (Sigma-Aldrich) and embedded with Fluorsave (Calbiochem, Darmstadt, Germany). Fluorescent images were obtained using a Zeiss Apotome microscope and were processed using ImageJ software (Rasband WS, ImageJ, U.S. National Institutes of Health, Bethesda, MD, USA; http://rsb.info.nih.gov/ij/, 1997-2006).

Cognitive and sensorimotor function

At 7 weeks post-HI, cognitive function was tested in the novel object recognition task (NORT) as described.[20,21] In short, rats were exposed to two identical objects for 10 min. One hour later, rats were re-exposed to one familiar and a novel object. Preference for the novel object was calculated as (time with novel object)/(total time with both objects) x 100%.

At 8 weeks post-HI, sensorimotor function was analyzed by determining paw preference in the cylinder rearing test (CRT) for 3 min. The preference to use the non-impaired forepaw was calculated as: (right-left)/(right+left+both) x 100%.[19,20,22]

Western blotting

Pups were decapitated at 3 or 24 h post-HI, cerebellum was removed and left and right hemispheres were frozen in liquid nitrogen. Hemispheres were pulverized using a liquid nitrogen-cooled mortar and pestle, and stored at -80 °C. Cytosolic, mitochondrial and nuclear protein fractions were prepared from pulverized whole contra- and ipsilateral hemispheres as extensively described previously.[23] Quality of subcellular fractionation was confirmed by exclusive presence of COX-IV in mitochondrial, predominant expression of β-actin in cytoplasmic and histone H1 expression restricted to nuclear fractions (see figure 5 right panel). For loading control, cytosolic protein membranes were reprobed with β-actin and nuclear protein membranes were reprobed with histone H1. Mitochondrial protein membranes were reprobed with β-actin as COX-IV expression was reduced after HI and β-actin expression correlated well with loading controls based on Ponceau S staining.

The same amount of protein for each sample was separated by SDS-PAGE, transferred to Hybond-C membranes (Amersham, Buckinghamshire, UK) and incubated with mouse-anti-cytochrome c (BD Biosciences Pharmingen), rabbit-anti-cleaved-caspase 3, rabbit-anti-Bcl-2, rabbit-anti-Bcl-xL, rabbit-anti-phospho-JNK (Thr183/Tyr185), rabbit-anti-JNK, rabbit-anti-c-Jun, rabbit-anti-phospho-c-Jun (Ser63) (all Cell Signaling, Danvers, MA), goat-anti-β-actin, mouse-anti-histone H1 (both Santa Cruz Biotechnology, Santa Cruz, CA) and mouse-anti-COX-IV (Molecular Probes) followed by peroxidase-labeled secondary antibodies, revealed by enhanced chemiluminescence (Amersham) and analyzed with a GS-700 Imaging Densitometer (Bio-Rad, Hercules, CA).

Electromobility shift assays

Electromobility shift assays (EMSA) on nuclear brain extracts of contra- and ipsilateral hemispheres were performed using ^{32}P labeled AP-1 (Promega, Madison, WA; sequence 5'-CGCTTGATGAGTCAGCCGGAA-3') as described.[24,25]

Quantitative real time reverse transcriptase PCR

Total RNA was isolated from pulverized contra- and ipsilateral hemispheres using TRIzol® (Invitrogen, Paisley, UK). cDNA was synthesized with SuperScript Reverse Transcriptase (Invitrogen). The PCR reaction was performed with iQ5 Real-Time PCR Detection System

(Bio-Rad) using primers for TNF-α (forward: CCCAGACCCTCACACTCAGATCAT; reverse: GCAGCCTTGTCCCTTGAAGAGAA), IL-1β (forward: CTCTGTGACTCGTGGGATGATG; reverse: CACTTGTTGGCTTATGTTCTGTCC), MIP-2 (forward: TTGTCTCAACCCTGAAGCCC; reverse: TGCCCGTTGAGGTACAGGAG) and CINC-1/IL-8 (forward: CCAAAAGATGCTAAAGGGTGTCC; reverse: CAGAAGCCAGCGTTCACCA). Data were individually normalized to the mean of the relative expression of β-actin and GAPDH (for primer sequences see Nijboer et al. (2008)).[25]

ATP measurement

Contra- and ipsilateral hemispheres were homogenized in PBS and deproteinized by PCA precipitation using a deproteinizing Sample Preparation Kit according to manufacturer's protocol (Biovision, Mountain View, CA). Deproteinized samples were neutralized with neutralization buffer (provided by kit) and PCA was precipitated. ATP levels were measured using the ATP colorimetric Assay Kit (Biovision) according to manufacturer's protocol. In short, the deproteinized samples were diluted 1:1 in ATP assay buffer and ATP reaction mix (both provided by kit) was added 1:1. Samples were mixed and incubated for 30 min at room temperature (RT) protected from light after which the optical density was measured at 570 nm. An ATP standard was used to obtain a reference curve.

Oxidative stress

As a measure of oxidative stress, a TBARS (thiobarbituric acid reactive substances) assay was used according to manufacturer's protocol (Oxiselect TBARS Assay Kit; Cell Biolabs, San Diego, CA). In short, ipsi- and contralateral hemispheres were homogenized in PBS/0.05% butylated hydroxytoluene (BHT), centrifuged at 10.000 g for 5 min and supernatants were collected. Supernatants were 1:1 mixed with SDS lysis solution (provided by kit) and incubated for 5 min at RT, after which TBA reagent was added (provided by kit). Samples were incubated for 60 min at 95 °C after which they were quickly cooled to RT and spun at 1000 g for 15 min. Supernatants were 1:1 mixed with n-butanol to prevent interference with hemoglobin, thoroughly vortexed and centrifuged for 5 min at 10.000 g. The butanol fraction was used for absorbance measurement at 532 nm. A MDA standard curve was used as a reference. Samples were normalized for protein concentration.

Statistical analysis

Data were normally distributed, are presented as mean and SEM, and were analyzed by one-way ANOVA with Bonferroni post-tests.

Results

Neuroprotective effect and therapeutic window of D-JNKi

HI was induced in P7 rats by unilateral carotid artery occlusion followed by hypoxia. At 48 h post-HI, marked neuronal damage, as analyzed by loss of MAP2, was observed in the ipsilateral hemisphere (Fig 1A, B). Intraperitoneal treatment with 10 mg/kg D-JNKi directly after HI (0 h) resulted in 86 ± 7.7% reduction in MAP2 loss compared to vehicle-treated rats. When we examined the effect of repeated dosing of D-JNKi (10 mg/kg at 0 and 3 h after HI) on neonatal HI brain damage, we no longer observed a significant neuroprotective effect (Fig 1A, B). The therapeutic window for treatment with a single dose of D-JNKi was at least 6 h; MAP2 loss was reduced by 70 ± 19.7% and 52 ± 12.8% after a single D-JNKi injection at 3 or 6 h post-insult respectively (Fig 1A, B). The neuroprotective effect was specific for the D-JNKi sequence since treatment with a D-TAT-scrambled peptide did not have any effect on brain damage (Fig 1A, B).

Effects of D-JNKi treatment on long-term anatomical and behavioral outcome

The observed neuroprotective effects of 0 h D-JNKi treatment were long-lasting as HI-induced ipsilateral volume loss determined at 9 weeks after the insult was markedly reduced in rats treated with D-JNKi (Fig 2A).

To determine whether the neuroprotective effects of 0 h D-JNKi treatment were associated with functional improvements, we assessed cognitive and sensorimotor function. Cognitive impairment was measured by using the NORT at 7 weeks post-HI. As anticipated, sham-control rats spent more time with the novel than the familiar object (Fig 2B). Vehicle-treated HI rats did not show any preference (app. 54%) for the novel object. D-JNKi-treated rats showed a significant restoration of novel object preference indicative for improved cognition (Fig 2B). The total interaction time with both objects did not differ between the groups.

Additionally, we examined the effect of D-JNKi on lateralizing motor deficits in the CRT at 8 weeks post-HI. HI-vehicle rats showed a significant preference to use their non-impaired paw to initiate vertical exploration (Fig 2C). D-JNKi treatment reduced the HI-induced preference for using the non-impaired forepaw by app. 80% (Fig 2C). Sham-operated rats did not show any paw preference during rearing in the CRT.

The data in figure 2 together show that D-JNKi treatment significantly improved both motor and cognitive function after HI and that functional improvements were associated with a large reduction in HI-induced brain damage.

Effects of HI and D-JNKi on c-Jun and AP-1 activation and pro-inflammatory cytokine/chemokine expression

JNK activation is thought to lead to c-Jun phosphorylation and thereby activation of the transcription factor AP-1, a dimer of which c-Jun is the main component.[8,26] In line with

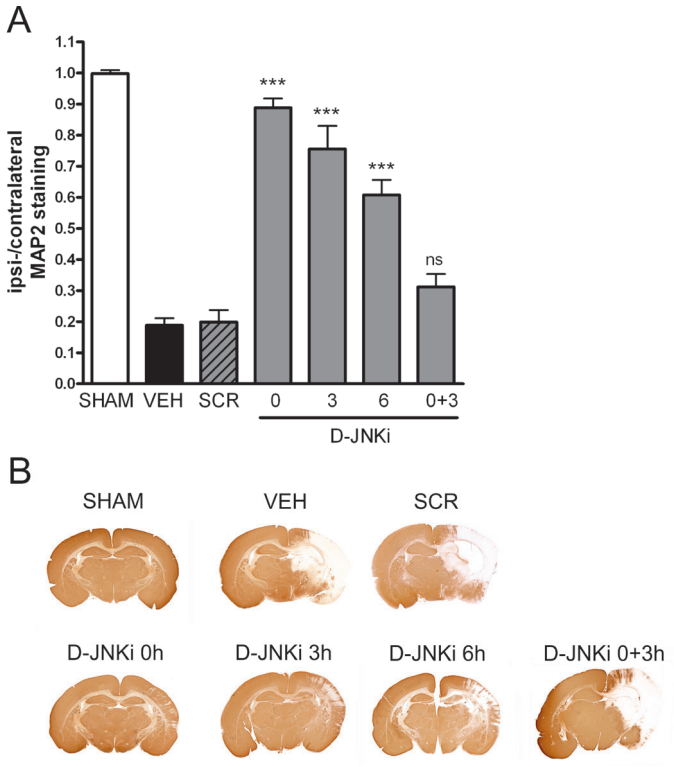

Figure 1: Neuroprotective effect and therapeutic window of D-JNKi
Rats were subjected to HI at P7 and neuronal damage was measured by analyzing staining for microtubule-associated-protein 2 (MAP2) in the contra- and ipsilateral hemisphere at 48 h post-insult. **A**: Ratio ipsi-/contralateral MAP2-positive area at 48 h post-HI in sham-operated (SHAM) rat pups, vehicle-treated (VEH) HI rat pups, D-TAT-scrambled peptide (SCR)-treated HI rat pups or D-JNKi-treated (D-JNKi) HI littermates. D-JNKi was given i.p. as a single injection at 0, 3 or 6 h post-HI or double injections at 0+3 h post-insult at a dose of 10 mg/kg, D-TAT-scrambled peptide was given i.p. at 0 h post-HI at 10 mg/kg. No MAP2 loss was observed in the contralateral hemisphere of HI animals or in sham-operated animals. SHAM n=8, VEH n=16, SCR n=8, D-JNKi 0h, 3 h, 6 h and 0+3 h: all n=8. *** p <0.001 vs vehicle-treatment. ns= not significant. Data were analyzed by one-way ANOVA with Bonferroni post-tests. **B**: Representative photographs of MAP2 staining in sham-operated animals and in HI animals after vehicle, SCR or D-JNKi treatment.

earlier observations,[13,15,16,18,27] HI-induced nuclear P-c-Jun staining was observed in neurons in the ipsilateral hemisphere only and was not detected in the contralateral hemisphere or in sham-operated brains (Fig 3A data not shown). We did not observe nuclear P-c-Jun staining in astrocytes and very scarcely in microglia (data not shown). Additionally, figure 3B shows that HI induced an increase in phosphorylated c-Jun (P-c-Jun) and total c-Jun levels in total brain nuclear fractions at 3 h post-HI. D-JNKi has been described to prevent activation (phosphorylation) of JNK and the downstream interaction of P-JNK with its substrates, including c-Jun.[9,11] In line with this proposed mechanism, the HI-induced increase in nuclear P-c-Jun and total c-Jun was completely prevented by D-JNKi treatment (Fig 3B).

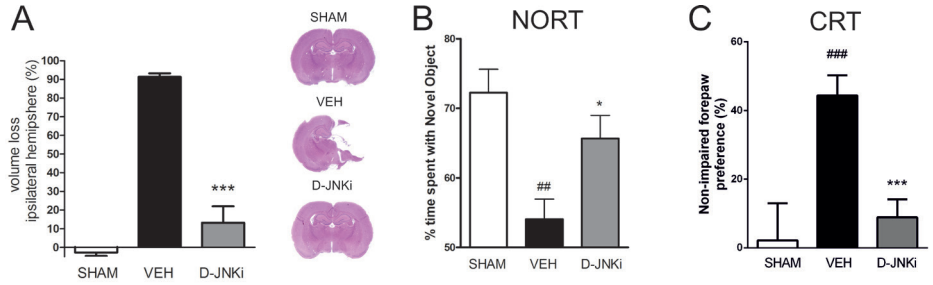

Figure 2: Long-term effects of D-JNKi treatment on behavior and brain damage
Rats were subjected to HI at P7 and were treated with vehicle (VEH) or D-JNKi at 0 h. Brain damage and cognitive and sensorimotor function were analyzed at 7-9 weeks after HI. **A**: HI-induced cerebral volume loss in the ipsilateral hemisphere measured on hematoxylin-eosin (HE) stained sections at app. -3.20 mm from bregma at 9 weeks post-HI. Inset shows representative examples of HE staining. *** p <0.001 vs vehicle-treatment. **B**: The novel object recognition task (NORT) was used to test cognitive function at 7 weeks after HI in sham-operated rats (SHAM) and HI-animals treated with vehicle or D-JNKi. Time spent with the familiar and the novel object was determined during a 5 min test period and the percentage time spent with the novel object is depicted. ## p <0.01 vs sham; * p <0.05 vs vehicle-treatment. **C**: Rats were tested in the cylinder rearing test (CRT) to quantify laterizing sensorimotor deficits at 8 weeks after HI. Use of ipsilateral (impaired) and contralateral (non-impaired) forepaw during full rears was recorded over a 3 min test period and preference (%) for using the non-impaired forepaw is depicted. ### p <0.001 vs sham; *** p <0.001 vs vehicle-treatment. For **A-C**: Sham controls n=8, vehicle n=8, D-JNKi n=12. Data were analyzed by one-way ANOVA with Bonferroni post-tests.

The data in figure 3C demonstrate that the AP-1 transcription factor shows 2 waves of activation; an early activation peak of AP-1 activation at 3 h post-insult as described before and a second peak of AP-1 activity at 24 h post-insult.[19] Here we demonstrate that D-JNKi treatment markedly (>92%) reduced the HI-induced increase in AP-1 activity as determined by EMSA on nuclear extracts at 3 h post-HI (Fig 3D). Treatment with D-JNKi only prevented the first peak of AP-1 activity at 3 h, whereas the second peak at 24 h after HI was not affected (Fig 3E). In contrast, when rats were treated twice with D-JNKi at 0+3 h, AP-1 activity was still completely inhibited at 24 h post-HI (Fig 3E).

The JNK/AP-1 pathway is known to regulate expression of several inflammatory genes. Therefore, we analyzed pro-inflammatory cytokine and chemokine expression in the brain at 3 and 24 h post-HI. HI induced a significant upregulation of TNF-α, IL-1β, CINC-1 (IL-8) and MIP-2 mRNA in the ipsilateral hemisphere at both time points (Fig 4A-H). Treatment with D-JNKi completely abrogated the HI-induced increase in pro-inflammatory cytokine/chemokine expression at 3 h post-HI (Fig 4A-D), which is line with the strong reduction in AP-1 activity at this time point after D-JNKi treatment (Fig 3D). At 24 h post-insult, TNF-α, IL-1β, CINC-1 and MIP-2 mRNA expression were also all strongly reduced after neuroprotective D-JNKi treatment, although AP-1 activity was restored at this time point (Fig 4E-H, 3E). Remarkably, HI-induced TNF-α, IL-1β, CINC-1 and MIP-2 mRNA expression at 24 h post-HI was not reduced after 0+3 h D-JNKi treatment (data not shown).

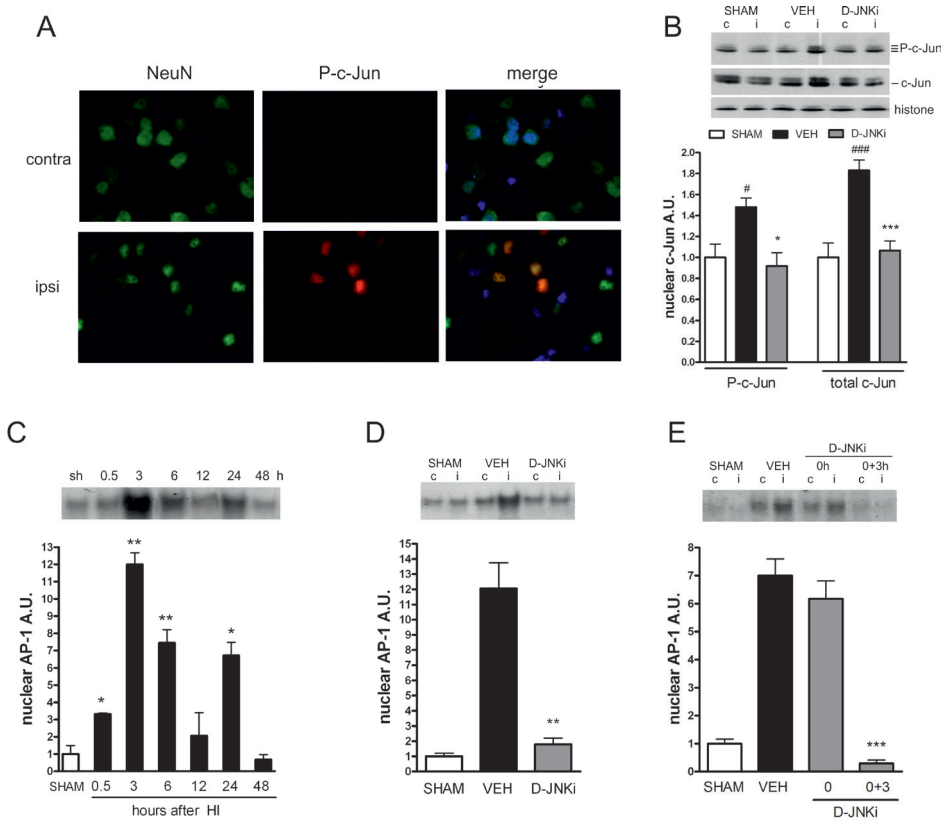

Figure 3: Effects of HI and D-JNKi treatment on phosphorylation of c-Jun and AP-1 activity
P7 rat pups were subjected to HI and were treated with vehicle (VEH) or D-JNKi at 0 h (**B,D,E**) or at 0+3 h (**E**) after the insult. **A:** Representative photographs of immunofluorescent double-labeling of P-c-Jun (red) with NeuN (green) in contra- (contra) and ipsilateral (ipsi) hemispheres at 3 h post-HI. The vast majority of P-c-Jun labeling was observed in neurons and staining was limited to the ipsilateral hemisphere. Photographs were taken in the parietal cortex. **B**: Levels of total c-Jun and P-c-Jun were quantified in contra- (c) and ipsilateral (i) hemispheres at 3 h post-HI by Western Blot in nuclear fractions. Insets show representative examples using histone H1 as loading control. Note that antibody against total c-Jun also recognizes phosphorylated c-Jun (upper band). $^{\#}p$ <0.05, $^{\#\#\#}p$ <0.001 vs sham-operated control levels (SHAM). * p <0.05 and *** p <0.001 vs vehicle-treatment. **C**: Ipsilateral AP-1 activity was determined by EMSA on nuclear brain extracts obtained at different time points after HI. Inset shows representative examples. Animals n=4-6 per time point. * p <0.05, ** p <0.01 vs level in sham-operated (SHAM) animals. **D-E**: Ipsilateral AP-1 activity was determined by EMSA on nuclear extracts obtained at 3 h (**D**) or 24 h (**E**) post-HI. Insets show representative examples. ** p <0.01, *** p <0.001 vs vehicle-treatment. **B-E**: No statistically significant differences were observed between contralateral levels of HI-VEH or HI-D-JNKi animals and levels in sham-operated controls. Levels are relative to levels in sham-operated animals which were put at 1. A.U.: arbitrary units.

Effects of HI and D-JNKi on JNK phosphorylation

It has been described that phosphorylation/activation of c-Jun and AP-1 activation is mediated by translocation of P-JNK from the cytosol to the nucleus. D-JNKi is thought to inhibit phosphorylation of cytosolic JNK by preventing binding of JNK to the JIP-1 scaffold and/or

inhibiting interaction of JNK with upstream kinases thereby inhibiting JNK activation.[8,12,13] To assess whether D-JNKi treatment prevented inhibition of JNK phosphorylation, we determined the effects of HI and D-JNKi treatment on JNK phosphorylation in different subcellular fractions of the brain. Quality of subcellular fractionation was confirmed by Western blot analysis (inset Fig 5).

Using antibodies against JNK1-3 and phospho-JNK1-3, two bands corresponding to the 46 (p46) and a 54 (p54) kDa JNK isoforms were detected.[28] In cytosolic fractions, HI or HI+D-JNKi did not induce detectable changes in phosphorylated p46-JNK (P-JNK-p46) as determined at 3 h post-HI (Fig 5A). Cytosolic P-JNK-p54 was decreased after HI and this reduction was abolished by D-JNKi-treatment (Fig 5B). Total cytosolic JNK-p46 and JNK-p54 levels did not change after HI or D-JNKi (Fig 5A, B). Nuclear P-JNK-p46 and P-JNK-p54 levels were both significantly decreased at 3 h post-HI (Fig 5C, D), the time point when we observed a strong increase in P-c-Jun (Fig 3B). Concomitantly, total nuclear JNK levels were decreased after HI as well. Both the decrease in nuclear P-JNK and total JNK were prevented by D-JNKi treatment. Importantly, in the mitochondrial fraction HI induced a strong increase in JNK phosphorylation; mitochondrial P-JNK-p46 increased 4.9 times and P-JNK-p54 increased 6.4 times at 3 h post-HI (Fig 5E, F). D-JNKi almost completely prevented this HI-induced increase in mitochondrial P-JNK-p46 and P-JNK-p54 (Fig 5E, F). Total level of mitochondrial JNK was not changed after HI or D-JNKi (Fig 5E, F), indicating that the HI-induced increase in mitochondrial P-JNK was not due to translocation of P-JNK to the mitochondria.

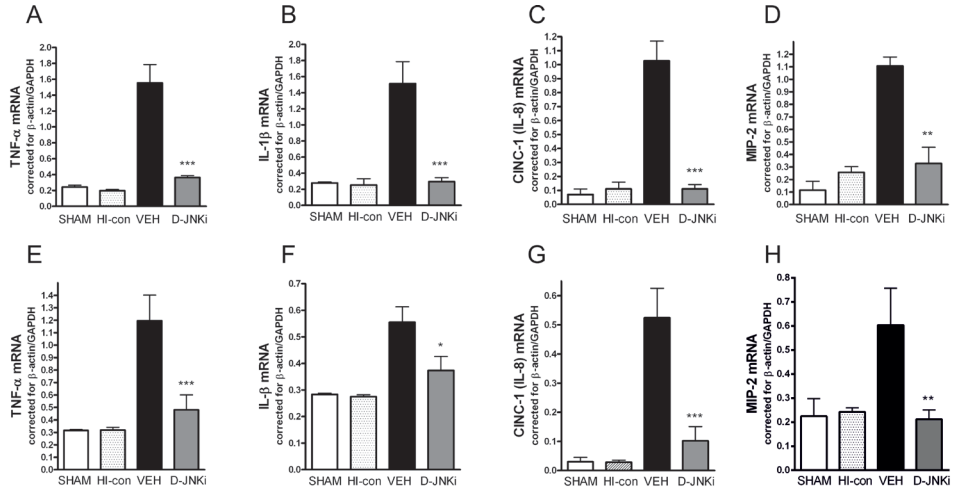

Figure 4: Effects of HI and D-JNKi treatment on neuroinflammation

A-H: Effect of HI and D-JNKi treatment on cytokine/chemokine mRNA expression of TNF-α (**A, E**), IL-1β (**B, F**), CINC-1 (**C, G**) and MIP-2 (**D, H**) as determined by quantitative real time RT-PCR at 3 h (**A-D**) and 24 h (**E-H**) post-HI. Data are normalized for expression of β-actin and GAPDH. No statistically significant differences were observed between contralateral levels of HI-vehicle (VEH) or HI-D-JNKi animals and levels in sham-operated controls (SHAM). * p <0.05, ** p <0.01, *** p <0.001 vs vehicle-treatment. Sham controls n=4, HI-vehicle n=8, HI-D-JNKi n=10 for both time points. Data were analyzed by one-way ANOVA with Bonferroni post-tests.

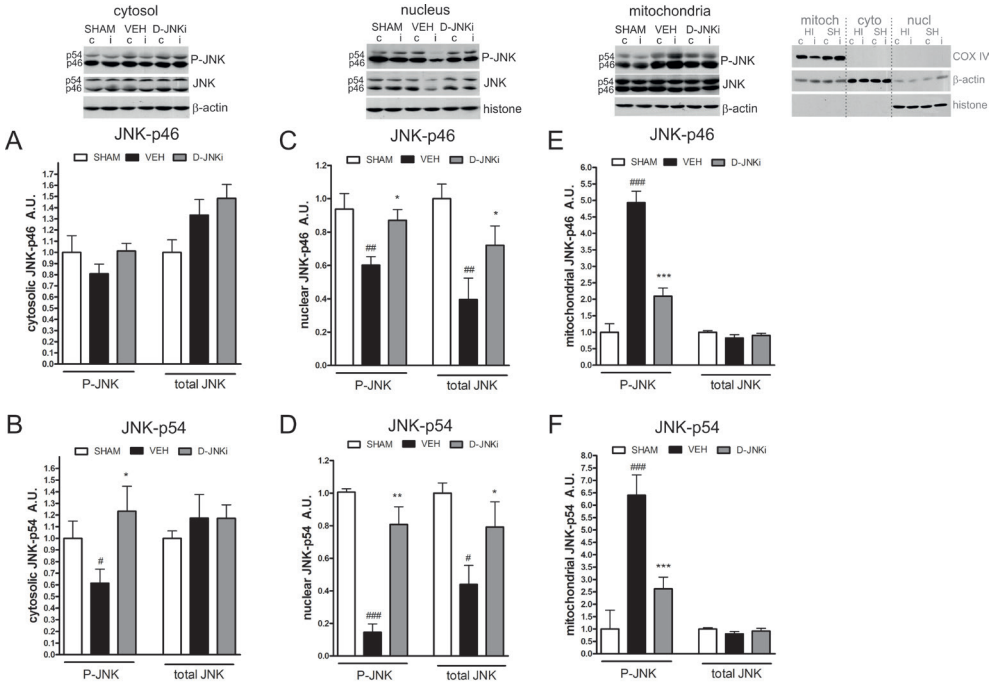

Figure 5: Effects of HI and D-JNKi on phosphorylation of cytosolic, nuclear and mitochondrial JNK

A-F: At P7 HI was induced in rat pups followed by vehicle-treatment (VEH) or D-JNKi-treatment at 0 h post-HI. Phosphorylated and total levels of JNK (P-JNK and total JNK) were determined in cytosolic (**A:** JNK-p46; **B:** JNK-p54), nuclear (**C**: JNK-p46; **D**: JNK-p54) and mitochondrial (**E:** JNK-p46; **F:** JNK-p54) fractions of contra-(c) and ipsilateral (i) hemispheres by Western Blot at 3 h post-HI. Insets show representative examples using β-actin and histone H1 as loading control. $^{\#}p$ <0.05, $^{\#\#}p$ <0.01, $^{\#\#\#}p$ <0.001 vs sham; * p <0.05, ** p <0.01, *** p <0.001 vs vehicle-treatment. There were no statistically significant differences in contralateral levels of HI-VEH or HI-D-JNKi animals compared to levels in sham-operated rats (SHAM). Levels are relative to levels in sham-operated animals which were put at 1. A.U.: Arbitrary units. Sham controls n=4, HI-vehicle n=8, HI-D-JNKi n=10. Data were analyzed by one-way ANOVA with Bonferroni post-tests. Right inset: Confirmation of fractionation quality by Western Blot. Mitochondrial (mitoch), cytosolic (cyto) and nuclear (nucl) fractions of contra-(c) and ipsilateral (i) hemispheres of HI and sham-operated (SH) animals were analyzed for expression of subcellular fraction-specific markers. Blots show exclusive presence of COX-IV in the mitochondria, predominance of β-actin in the cytosol and exclusive presence of histone H1 in the nuclear fractions. Note that COX-IV expression was influenced by HI.

Effects of D-JNKi on mitochondrial integrity and pro- and anti-apoptotic proteins

Next, we determined whether the HI-induced increase in P-JNK at the mitochondria has consequences for mitochondrial functioning. Ischemia and reperfusion induce mitochondrial damage which is associated with loss of mitochondrial membrane potential ($\Delta\psi m$), loss of ATP, increased reactive oxygen species (ROS) generation and calcium influx.[29] These processes ultimately lead to opening of the mitochondrial membrane and release of pro-apoptotic proteins into the cytosol.

Figure 6A demonstrates that HI induced a significant decrease in cerebral ATP levels as measured at 3 h post-insult. D-JNKi treatment completely prevented this HI-induced decrease in ATP (Fig 6A).

To determine the effect of HI and D-JNKi on cerebral oxidative stress, we analyzed TBARS levels, a measure of lipid peroxidation.[20,30] At 3 h after HI, TBARS were significantly increased and this increase was inhibited by D-JNKi (Fig 6B).

Next, we assessed whether the effects of D-JNKi on mitochondrial functioning also had effects on the apoptotic cascade, leakage of mitochondrial cytochrome c to the cytosol and subsequent caspase 3 activation were assessed. As expected, HI induced a strong increase in the levels of cytosolic cytochrome *c* and activated caspase 3 at 24 h post-insult (Fig 6C, D). D-JNKi treatment at 0 h post-HI almost completely inhibited the HI-induced increase in cytosolic cytochrome c and caspase 3 activation (Fig 6C, D). In line with the loss of neuroprotection, repeated D-JNKi treatment at 0+3 h abolished the reduction of cytochrome c release to the cytosol and caspase 3 activation as determined at 24 h post-insult (Fig 6C, D).

We have previously shown that HI reduces mitochondrial levels of the anti-apoptotic proteins Bcl-2 and Bcl-xL at 24 h after the insult and that neuroprotection by nuclear factor kappa B (NF-κB) inhibition is associated with upregulation of these anti-apoptotic factors.[31] In line with our previous data, figures 6E and F show that HI significantly reduced mitochondrial levels of Bcl-2 and Bcl-xL in vehicle-treated HI animals. Interestingly, mitochondrial Bcl-2 and Bcl-xL levels were significantly *increased* after treatment with 0 h D-JNKi, whereas repeated treatment with 0+3 h D-JNKi *reduced* Bcl-2 and Bcl-xL to levels similar to vehicle-treated littermates (Fig 6E, F).

Effects of Sab_{KIM1}, a specific mitochondrial JNK inhibitor, on brain damage after HI

To further investigate the role of mitochondrial JNK after HI, rats were treated with the Sab_{KIM1} peptide. The Sab_{KIM1} peptide (TAT-containing all D-amino acids retro-inverso peptide) has been developed as a specific inhibitor of JNK interaction with its mitochondrial scaffold Sab, thereby specifically reducing binding of JNK to the mitochondria without affecting nuclear JNK-dependent c-Jun phosphorylation.[32,33] Treatment with 10 or 20 mg/kg Sab_{KIM1} peptide i.p. immediately after HI reduced neuronal damage at 48 h post-HI with 36% and 58% respectively (Fig 7A, B). Figures 7C and D show that Sab_{KIM1} strongly reduced HI-induced mitochondrial P-JNK levels. Noteworthy, Sab_{KIM1} treatment also reduced total levels of mitochondrial JNK which is in line with its mode of action, *i.e.* preventing binding of JNK to the mitochondrial scaffold.

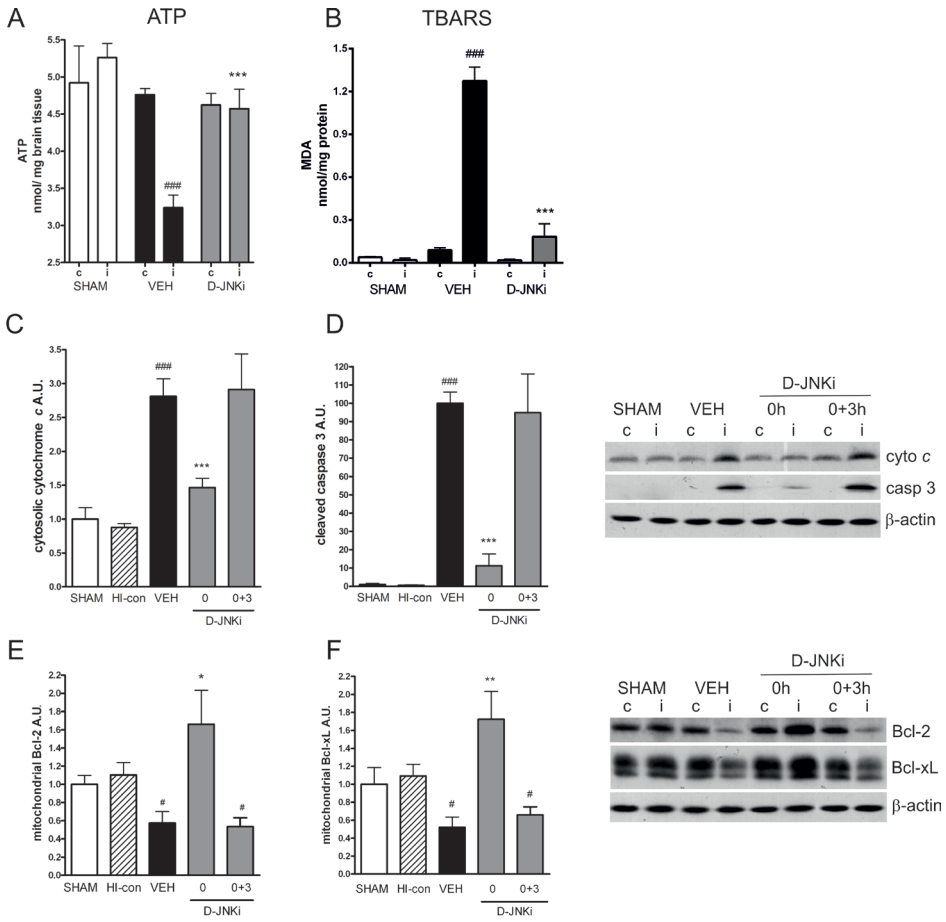

Figure 6: Effects of HI and D-JNKi treatment on ATP levels, oxidative stress and apoptotic markers

Rat pups were subjected to HI at P7 and were treated with vehicle (VEH) or D-JNKi at 0 h (**A-E)** or at 0+3 h (**C-F**) after the insult. **A:** ATP colorimetric assay showing ATP levels (nmol/mg brain tissue) as a measure of mitochondrial respiration at 3 h after induction of HI in contra- (c) and ipsilateral (i) deproteinized brain homogenates of vehicle- and D-JNKi-treated HI rat pups and sham-controls (SHAM). **B**: TBARS assay measuring MDA levels (nmol/mg protein) as a measure of lipid peroxidation at 3 h post-HI in contra- (c) and ipsilateral (i) brain homogenates of rat pups treated with vehicle or D-JNKi directly after HI and sham-controls. **C-D**: Cytosolic fractions of contra- (c) and ipsilateral (i) hemispheres were analyzed by Western Blot at 24 h post-HI for expression of cytochrome *c* **(C)** and cleaved (activated) caspase 3 **(D)**. **E-F**: Mitochondrial brain fractions of both hemispheres were analyzed by Western Blot at 24 h post-HI for expression of Bcl-2 **(E)** and Bcl-xL **(F)**. **A-F:** There were no statistically significant differences in contralateral levels of HI-VEH or HI-D-JNKi animals compared to sham levels. Insets show representative Western Blots with β-actin as loading control. A.U.: arbitrary units. $^{\#}p$ <0.05 and $^{\#\#\#}p$ <0.001 vs contralateral; * p <0.05, ** p <0.01 and *** p <0.001 vs vehicle-treatment. Sham controls n=4, HI-vehicle n=8, HI-D-JNKi n=10. Data were analyzed by one-way ANOVA with Bonferroni post-tests.

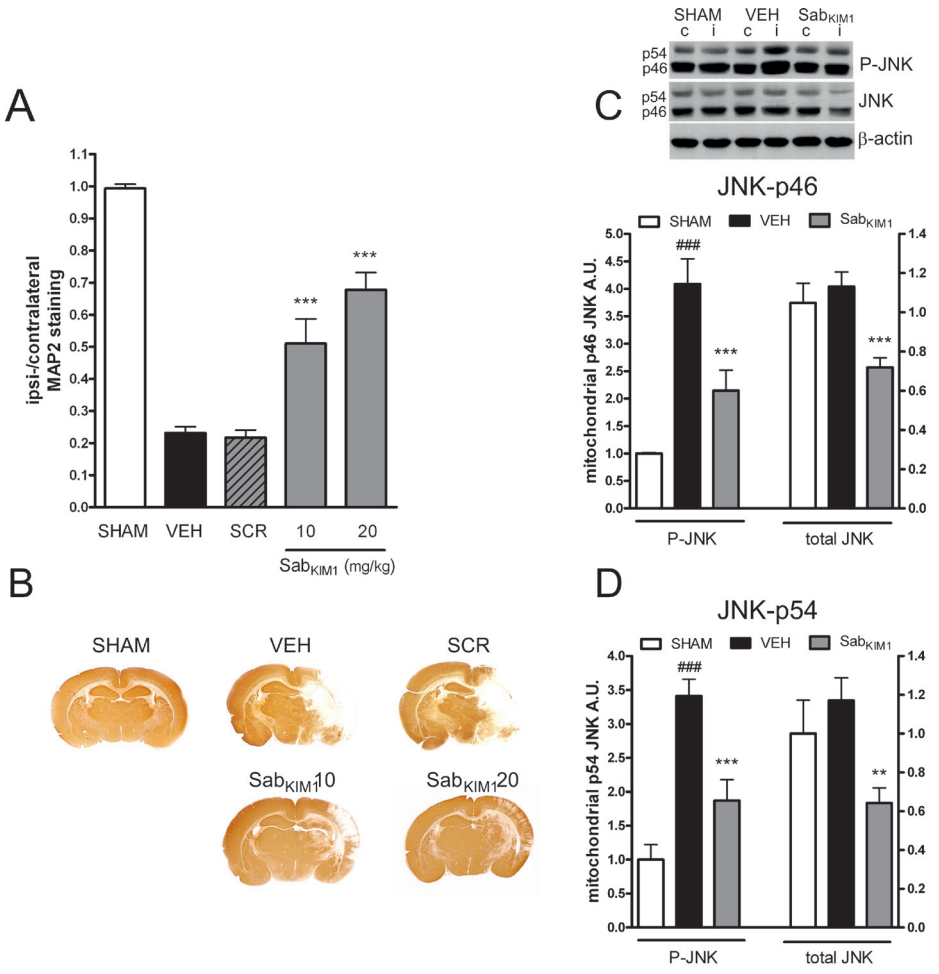

Figure 7: Neuroprotective effect of Sab$_{KIM1}$ peptide

Rats were subjected to HI at P7 and neuronal damage was measured by analyzing staining for MAP2 in the contra- and ipsilateral hemisphere at 48 h post-insult.

A: Ratio ipsi-/contralateral MAP2-positive area at 48 h post-HI in sham-operated rats (SHAM), vehicle-treated (VEH) HI rat pups, D-TAT-scrambled peptide (SCR)-treated HI rat pups or Sab$_{KIM1}$-treated (Sab$_{KIM1}$) HI littermates. Sab$_{KIM1}$ was given i.p. as a single injection at 0 h post-HI at a dose of 10 or 20 mg/kg. D-TAT-scrambled peptide was given i.p. at 0 h post-HI at 20 mg/kg. No MAP2 loss was observed in the contralateral hemisphere of HI animals or in sham-operated animals (SHAM). SHAM n=8, VEH n=9, SCR n=7, Sab$_{KIM1}$ 10 mg/kg n=11, Sab$_{KIM1}$ 20 mg/kg n=11. *** p <0.001 vs vehicle-treatment. Data were analyzed by one-way ANOVA with Bonferroni post-tests. **B**: Representative photographs of MAP2 staining after vehicle, D-TAT-scrambled peptide or Sab$_{KIM1}$ treatment. **C-D**: Phosphorylated and total levels of JNK (P-JNK and total JNK) were determined in mitochondrial fractions (**C:** JNK-p46; **D:** JNK-p54) of contra-(c) and ipsilateral (i) hemispheres by Western Blot at 3 h post-HI. There were no statistically significant differences in contralateral levels of HI-VEH or HI- Sab$_{KIM1}$animals compared to levels in sham-operated rats. Insets show representative examples using β-actin as a loading control. ### p <0.001 vs sham; ** p <0.01, *** p <0.001 vs vehicle-treatment. Levels are relative to levels in sham-operated animals which were put at 1. A.U.: arbitrary units. Sham controls n=5, HI-vehicle n=6, HI- Sab$_{KIM1}$ n=6. Data were analyzed by one-way ANOVA with Bonferroni post-tests.

Discussion

In the neonatal model of severe HI brain injury, we are the first to show the strong neuroprotective effects of JNK inhibition by administration of the D-JNKi peptide. Neuroprotection by D-JNKi is long-lasting and very potent with >85% reduction in infarct size at 9 weeks post-HI. Moreover, neuroprotection by D-JNKi is associated with improved cognitive and sensorimotor behavior during young adulthood. The latter data urge for a more in-depth evaluation on the possibility to use D-JNKi in human asphyxiated newborns.

In search for the underlying mechanism of the neuroprotective effect of D-JNKi, we demonstrate for the first time that the cerebral ischemic insult markedly increased the *mitochondrial* level of P-JNK which was completely blocked by D-JNKi. HI did not induce P-JNK in cytosolic or nuclear fractions. Therefore, we propose that neuroprotection by D-JNKi is mediated via inhibition of JNK activation at the mitochondria. In line with this hypothesis, treatment with Sab_{KIM1}, a peptide inhibiting binding of JNK to mitochondria, also showed potent neuroprotection after HI.

D-JNKi treatment-induced inhibition of mitochondrial JNK activation was associated with preservation of mitochondrial integrity as evidenced by prevention of HI-induced reduction in ATP levels, the increase of ROS production and cytosolic translocation of mitochondrial proteins. We propose that protection of the mitochondria prevents phosphorylation of c-Jun and thus activation of the transcription factor AP-1 and neuroinflammation and ultimately neuronal death. Furthermore we show that upregulation of anti-apoptotic proteins at the mitochondria is a secondary crucial step for neuroprotection, which may depend on restoration of the transcriptional activity of the AP-1 transcription factor after the first wave of AP-1 inhibition by D-JNKi.

A single dose of D-JNKi has also been shown to have moderate to strong (app. 30-90%) neuroprotective effects in the middle cerebral artery occlusion (MCAO) model of ischemic brain damage using adult or P14 rats and in a murine model of intracerebral haemorrhage.[13,14,16,17,34,35] In these studies, the neuroprotective potential of D-JNKi was evaluated within 14 days post-insult. We now show that strong neuroprotection by D-JNKi treatment is maintained until at least 9 weeks post-HI in the neonatal rat. More importantly, our findings that D-JNKi also protects against the HI-induced loss of cognitive and motor function demonstrate that preservation of cerebral tissue by D-JNKi-treatment is associated with preservation of function.

Borsello et al. (2003) demonstrated using an *in vitro* system that D-JNKi specifically inhibited both the activation of JNK by MKK4/7 as well as the activation of c-Jun by JNK in a kinase-assay testing 40 different kinases.[13] However, the mechanism via which D-JNKi protects against brain injury *in vivo* or against neuronal damage *in vitro* is still unclear. For example, Borsello et al. (2003) showed that D-JNKi did not inhibit phosphorylation of JNK as determined in total cell lysates after N-methyl-D-aspartate (NMDA) stimulation of cortical neurons *in vitro* even though D-JNKi did have a neuroprotective effect in this model.[13] *In vivo*, MCAO even

reduced cytosolic P-JNK in the brains of P14 rats and this reduction was not affected by D-JNKi.[35] Nevertheless also in this model D-JNKi was neuroprotective. In our study, we also observed a reduction in cytosolic and nuclear P-JNK post-HI. Similarly, Ginet et al. (2009) described a reduction in P-JNK after neonatal HI *in vivo* in total brain lysates.[18] However, to our knowledge, we are the first to show that HI induces a strong increase in *mitochondrial* P-JNK, which is almost completely abolished by D-JNKi. The increased level of mitochondrial P-JNK combined with reduced cytosolic and nuclear levels of P-JNK might indicate that HI induced a translocation of P-JNK to the mitochondria. Hanawa et al. (2008) suggested that phosphorylation of JNK results in translocation of P-JNK to the mitochondria.[36] However, our data do not support the notion of P-JNK translocating from the cytosol/nucleus to the mitochondria as the *total* JNK level in the mitochondrial fraction did not increase after HI. Therefore, we suggest that D-JNKi inhibits phosphorylation of JNK which is already present at the mitochondria, possibly by prevention of the interaction of upstream kinases MKK4/7 with mitochondrial JNK. In support of our hypothesis, Repici et al. (2009) showed in cell-free systems that D-JNKi inhibited phosphorylation of JNK by MKK4/7.[12] An alternative possibility would be that D-JNKi treatment results in translocation of P-JNK from the mitochondria to the nucleus. Indeed total levels of nuclear JNK (unphosphorylated and phosphorylated) are increased after D-JNKi treatment as well. Even though total JNK levels at the mitochondria do not decrease after D-JNKi treatment, it is possible that a small fraction of JNK does translocate to the nucleus without inducing detectable decreases in mitochondrial JNK.

Interestingly, the neuroprotective effects of treatment with the Sab_{KIM1} peptide, a peptide inhibiting mitochondrial association of JNK, further highlight the important role of mitochondrial JNK activation in HI brain injury. Sab is a scaffold protein associated with the mitochondria and acts as a docking place for activated JNK at this subcellular compartment.[33,37] Sab contains two KIMs of which KIM1 is essential for binding of JNK. Based on this Sab KIM1 motif the small peptide inhibitor Sab_{KIM1} was designed. Chambers et al. (2011) showed that Sab_{KIM1} treatment *in vitro* prevented JNK localization to the mitochondria, which was associated with reduced levels of phosphorylated mitochondrial Bcl-2 and improved cell survival in a model of anisomycin-induced cell death in HeLa cells.[32] Importantly, Sab_{KIM1} treatment did not impact JNK-mediated nuclear events, *i.e.* phosphorylation of c-Jun or nuclear JNK levels.[32] To our knowledge, we are the first to show the potent neuroprotective effects of Sab_{KIM1} in an *in vivo* model of brain injury. The Sab_{KIM1} data strongly support our hypothesis that it is the inhibiton of JNK phosphorylation at the mitochondria that is sufficient to obtain neuroprotection as observed after D-JNKi treatment. Nevertheless, as with any inhibitor, we cannot exclude the possibility that other, potentially off-target effects, contribute to the observed neuroprotective effects of D-JNKi.

Our data show that prevention of the HI-induced increase in mitochondrial P-JNK was associated with preservation of mitochondrial functioning after D-JNKi treatment. D-JNKi prevented the HI-induced reduction in ATP, the increase in lipid peroxidation and the release of mitochondrial proteins into the cytosol. In comparison with earlier data reported by others

the absolute cerebral ATP levels measured in our study were about 2 times higher.[38,39-42] This difference in ATP levels might be due to the termination methods and the analysis of ATP as we used a commercially available kit. Most recently, Chavez-Valdez et al. (2012) reported cerebral ATP levels of 6-8 nmol/mg brain in naive P8-P11 mice, which were quite similar to our data.[43] Nevertheless, we acknowledge that the ATP levels we report here as such might not precisely reflect the absolute ATP concentration in the brain *in vivo*. Nevertheless, we show a clear HI-induced reduction in ipsilateral cerebral ATP, comparable to the study by Gilland et al. (1998), which was completely prevented by D-JNKi treatment.[39]

In vitro and *in vivo* studies have indicated that mitochondrial JNK is involved in regulating mitochondrial integrity, but the exact mechanism how mitochondrial JNK regulates the apoptotic cascade remains to be elucidated.[44-46] There are several potential pathways via which mitochondrial JNK might regulate mitochondrial integrity. P-JNK can phosphorylate anti-apoptotic Bcl-2 and Bcl-xL at the mitochondria, which reduces the interaction of these anti-apoptotic proteins with pro-apoptotic Bcl-2 family members and thereby facilitates induction of apoptotic cell death.[44-46] Since we observed that D-JNKi treatment after HI also led to an increase in mitochondrial Bcl-2 and Bcl-xL levels, the reduced presence of P-JNK and the increased levels of anti-apoptotic proteins at the mitochondria may confer effective neuroprotection.

Additionally, there are some *in vitro* studies indicating that JNK might directly regulate bioenergetics within the mitochondria, *e.g.* via phosphorylation of pyruvate dehydrogenase and/or components of the electron transport chain as well as via induction of the inner mitochondrial transition pore, leading to a collapse of inner membrane potential, ROS production and loss of ATP production.[46-49] *In vivo*, so far the role of mitochondrial JNK has only been described in a liver-injury model, in which it was shown that mitochondrial JNK phosphorylation was associated with mitochondrial permeability transition, a decline in ATP levels and release of cytochrome *c*, which could all be reversed by JNK inhibition.[36]

Notably, JNK has been shown to associate with the mitochondrial outer membrane and does not enter the intermembrane space or matrix.[49] Therefore, direct effects of JNK on proteins within the mitochondrial matrix or inner membrane seem less likely than effects of JNK on targets at the outer mitochondrial membrane. We therefore propose that D-JNKi inhibits JNK-induced effects on targets at this outer membrane, such as Bcl-2 and Bcl-xL which directly regulate permeabilization of the outer membrane. Additionally, other known JNK targets at the outer mitochondrial membrane including Bad, BimL, Bax, p53 and PARP-1 may also participate in protection of mitochondrial integrity by D-JNKi.[6,8]

Previous studies have shown that FITC- or biotin-labeled D-JNKi rapidly distributes to the brain within 1 h after i.p. injection and that within the brain, D-JNKi localizes mainly to neurons.[13,18,35] One of the key mechanisms via which JNK is thought to regulate cellular activity is via phosphorylation of c-Jun and subsequent AP-1 activation. Several studies have shown that ischemia-induced cerebral c-Jun activation takes place primarily in neurons.[13,15,16,18,27] In line with these studies, we show here that activated c-Jun is present in neurons in the

ipsilateral hemisphere. Importantly, we show by using brain homogenates that the activation of c-Jun and the subsequent activation of AP-1 activity is completely inhibited after D-JNKi treatment, indicating that D-JNKi will inhibit these processes in all cerebral cell types in which activation takes place, which will predominantly be neurons. However, we cannot exclude completely that D-JNKi also affects glial cell types or has additional peripheral effects.

Subsequent to the inhibitory effects of D-JNKi on AP-1 activation, the upregulation of AP-1-regulated pro-inflammatory target genes was completely inhibited by D-JNKi treatment at 3 h post-HI. Our present findings support studies that showed inhibitory effects of D-JNKi on phosphorylation of c-Jun in an *in vitro* kinase assay, in NMDA-challenged cortical neurons, in isolated ischemic brain preparations and in *in vivo* studies of MCAO in rodents.[12-16,34] c-Jun is thought to be phosphorylated by nuclear P-JNK.[8] However, the HI-induced increase in P-c-Jun coincided with decreased nuclear P-JNK. In support of our data, Borsello et al. (2003) showed *in vitro* in cortical neurons that D-JNKi strongly inhibited nuclear P-c-Jun levels, whereas nuclear P-JNK levels were not affected.[13] Additionally, Repici et al. (2007) showed an inhibitory effect of D-JNKi on P-c-Jun after MCAO without an effect of D-JNKi on P-JNK levels.[35] Therefore, the question arises how D-JNKi regulates inhibition of phosphorylation of c-Jun when nuclear P-JNK levels are reduced. One possibility is that c-Jun is phosphorylated at the cellular location where HI induces JNK phosphorylation, *i.e.* the mitochondria. However, we could not detect P-c-Jun in the mitochondrial fraction (data not shown). Alternatively, c-Jun can also be phosphorylated by other kinases such as cyclin-dependent kinases, calcium/calmodulin-dependent protein kinases, vaccinia related kinase (VRK) 1 and p38.[50-52] We hypothesize that phosphorylation of c-Jun after HI is mediated by other kinases than JNK and that inhibition of P-c-Jun after D-JNKi is an *indirect* effect of mitochondrial protection which could prevent activation of these alternative kinase pathways mentioned above.

Neuroinflammation after HI is an ongoing process with increasing production of pro-inflammatory cytokine/chemokines starting at 3 h up to 24 h post-insult.[53] Our data show that a single treatment with D-JNKi was effective to inhibit the HI-induced onset of cytokine/chemokine mRNA expression. Importantly, inhibition of neuroinflammation by D-JNKi was long-lasting as also cytokine/chemokine mRNA expression at 24 h was still completely blocked, although AP-1 activity was restored at this later time point, which indicates that cytokine/chemokine production at later time points after HI is not upregulated when neuroprotection has been initiated early after the insult. These data further add to our view that preserving mitochondria integrity is an important upstream step in neuroprotection that prevents activation of early downstream nuclear transcriptional activity and subsequent neuroinflammation.

We show here that D-JNKi is a powerful neuroprotectant in a neonatal model of brain damage. Ginet et al. (2009) evaluated the effect of D-JNKi in the P7 rat HI model earlier, but these authors showed that repeated treatment with D-JNKi (0.3 mg/kg i.p. at 30 min prior to HI and repeated at 3, 5, 8, 12 and 20 h post-HI) was not neuroprotective.[18] Using the same model, we now clearly demonstrate the marked neuroprotective effect of a single

dose of D-JNKi (10 mg/kg) within 6 h post-insult. However, in line with Ginet et al. (2009), we also show that when P7 rats were treated repeatedly with 10 mg/kg D-JNKi at 0+3 h, the neuroprotective effect was abolished.[18] Our therapeutic window data show that a single injection of D-JNKi at 3 h post-HI was strongly neuroprotective, which indicates that it is rather the double dose within 3 h than the time point as such after HI that reduces the neuroprotective effect of D-JNKi. Therefore, we conclude that D-JNKi should only be given once to protect the neonatal brain.

Notably, however, in both the 0 h and 0+3 h treatment schedule, the first dose of D-JNKi was given directly after HI and thus in both treatment schedules, mitochondrial phosphorylation of JNK and AP-1 activity at 3 h post-HI was strongly reduced. Our results on the effects of D-JNKi and Sab_{KIM1} indicate that prevention of mitochondrial JNK activation can be a crucial *first* step in protecting the mitochondria by attenuating detrimental events that set off the apoptotic and inflammatory cascade. The neuroprotective potential of inhibiting *mitochondrial* pro-apoptotic signals after neonatal HI was also shown in our previous studies using the NF-κB inhibitor TAT-NBD (NEMO binding domain) and the mitochondrial p53 inhibitor pifithrin (PFT-)μ.[20,25] Our studies together imply that effective neuroprotective therapies should be targeted first at mitochondrial protection and can only work effectively when given early, within app. 6 h, after the insult.

An important finding in our study is that mitochondrial levels of the anti-apoptotic proteins Bcl-2 and Bcl-xL were upregulated after single, but not after repeated treatment with D-JNKi. These findings indicate that upregulation of these so-called 'guards of mitochondrial integrity' may play a crucial role in maintaining neuroprotection even after the initial preservation of mitochondrial integrity by reducing mitochondrial P-JNK. Notably, we have previously shown that neuroprotection can be lost when anti-apoptotic proteins are not upregulated after HI.[31] The inability to upregulate mitochondrial Bcl-2 and Bcl-xL after 0+3 h D-JNKi treatment might be a consequence of prolonged inhibition of AP-1 transcriptional activity at 24 h post-insult. Although we propose that the effect of the second D-JNKi dose at 3 h post-HI is due to the prolonged inhibition of AP-1 activation downstream of JNK activation, we cannot exclude that potential effects of D-JNKi on other kinases at this higher dose may contribute as well. Moreover, we do not have information on the exact pharmacokinetics of D-JNKi *in vivo* and therefore, we do not know whether the presumed protease-resistance of D-JNKi also prevents clearance (via mechanisms other than degradation) of the peptide. In fact our present data showing that a second dose of D-JNKi has adverse effects could indicate that the peptide is rapidly cleared after one gift (early after HI) and that this is beneficial as it may prevent potential late adverse effects. Alternatively, the peptide is not cleared and the second injection is sufficient to reach a toxic dose.

Our previous studies in which we used the L-isomer of the JNK inhibiting peptide (L-JNKi/TAT-JBD) showed that treatment with L-JNKi had a more moderate neuroprotective effect after HI in P7 rats; repeated injection of 10 mg/kg L-JNKi at 0 and 3 h resulted in app. 29% reduction in MAP2 loss.[19,53] We have additional data that show a comparable neuroprotective effect

(24.1% reduction in MAP2 loss) in rat pups treated with a single dose of L-JNKi at 0 h post-HI. As several studies showed potent neuroprotection using D-JNKi in MCAO models using P14 or adult rodents, we here wanted to explore the neuroprotective potential of D-JNKi treatment in the P7 HI model.[13,15,17,27,35] The data in the present study indeed show a much stronger neuroprotective effect of D-JNKi (>85% neuroprotection).

As was discussed above, we suggest that there are two main mechanisms that contribute to neuroprotection after JNK inhibition; inhibition of early mitochondrial JNK phosphorylation and the ability to upregulate mitochondrial anti-apoptotic proteins like Bcl-2 and Bcl-xL around 24 h post-HI. We have preliminary data showing that L-JNKi treatment does not significantly inhibit HI-induced JNK activation at the mitochondria, which is strongly inhibited by D-JNKi treatment. Furthermore, mitochondrial Bcl-2 or Bcl-xL levels at 24 h post-HI were not strongly upregulated after L-JNKi treatment as was observed after D-JNKi treatment. We feel that the differences in effects of L-JNKi and D-JNKi on mitochondrial JNK activation and mitochondrial anti-apoptotic proteins levels can explain the differences in neuroprotective capability. However, it is not clear at the moment how the configuration of the peptides exactly influences their capacity to regulate these HI-induced processes.

Ischemic injury in the neonatal brain is described to be a continuum between apoptotic and necrotic forms of cell death. Mitochondrial damage, especially induced by calcium, is also operative in necrotic cell death.[54] Therefore the great efficacy of D-JNKi may also be caused by an additional inhibition of necrotic processes. We propose that inhibiting early upstream mitochondrial events together with preserving the ability to upregulate mitochondrial anti-apoptotic proteins might be of great added value for neuroprotection after neonatal HI and should be a focus of translational research.

Conclusions

Collectively, our data indicate that the powerful neuroprotective action of D-JNKi is mediated by inhibition of JNK activity at the mitochondria, leading to preservation of mitochondrial integrity and inhibition of neuroinflammation. Perhaps more importantly, the effects of Sab_{KIM1} peptide treatment showed that specific inhibition of mitochondrial JNK association as such, is sufficient to strongly reduce HI brain damage. Specifically inhibiting mitochondrial JNK activation might develop into a promising therapy for newborns suffering from cerebral ischemia to effectively prevent development of neonatal encephalopathy. As JNK is involved in numerous developmental processes, the use of the more specific Sab_{KIM1} peptide that targets JNK inhibition at the mitochondrial subcellular compartment will probably be preferred as a safe neuroprotective strategy over D-JNKi to avoid or reduce putative side-effects. The present data warrant further studies to determine both acute and long term safety of D-JNKi and Sab_{KIM1} to support the potential clinical translation of these findings.

References

1. Ferriero DM. Neonatal brain injury. *N Engl J Med*. 2004;351:1985-1995.
2. Perlman M, Shah PS. Hypoxic-ischemic encephalopathy: challenges in outcome and prediction. *J Pediatr*. 2011;158:51-54.
3. Azzopardi DV, Strohm B, Edwards AD, et al. Moderate hypothermia to treat perinatal asphyxial encephalopathy. *N Engl J Med*. 2009;361:1349-1358.
4. Johnston MV, Fatemi A, Wilson MA, Northington F. Treatment advances in neonatal neuroprotection and neurointensive care. *Lancet Neurol*. 2011;10:372-382.
5. Grow J, Barks JD. Pathogenesis of hypoxic-ischemic cerebral injury in the term infant: current concepts. *Clin Perinatol*. 2002;29:585-602.
6. Bogoyevitch MA, Kobe B. Uses for JNK: the many and varied substrates of the c-Jun N-terminal kinases. *Microbiol Mol Biol Rev*. 2006;70:1061-1095.
7. Karin M, Gallagher E. From JNK to pay dirt: jun kinases, their biochemistry, physiology and clinical importance. *IUBMB Life*. 2005;57:283-295.
8. Dhanasekaran DN, Reddy EP. JNK signaling in apoptosis. *Oncogene*. 2008;27:6245-6251.
9. Barr RK, Kendrick TS, Bogoyevitch MA. Identification of the critical features of a small peptide inhibitor of JNK activity. *J Biol Chem*. 2002;277:10987-10997.
10. Bogoyevitch MA, Arthur PG. Inhibitors of c-Jun N-terminal kinases: JuNK no more? *Biochim Biophys Acta*. 2008;1784:76-93.
11. Bonny C, Oberson A, Negri S, Sauser C, Schorderet DF. Cell-permeable peptide inhibitors of JNK: novel blockers of beta-cell death. *Diabetes*. 2001;50:77-82.
12. Repici M, Mare L, Colombo A, et al. c-Jun N-terminal kinase binding domain-dependent phosphorylation of mitogen-activated protein kinase kinase 4 and mitogen-activated protein kinase kinase 7 and balancing cross-talk between c-Jun N-terminal kinase and extracellular signal-regulated kinase pathways in cortical neurons. *Neuroscience*. 2009;159:94-103.
13. Borsello T, Clarke PG, Hirt L, et al. A peptide inhibitor of c-Jun N-terminal kinase protects against excitotoxicity and cerebral ischemia. *Nat Med*. 2003;9:1180-1186.
14. Hirt L, Badaut J, Thevenet J, et al. D-JNKI1, a cell-penetrating c-Jun-N-terminal kinase inhibitor, protects against cell death in severe cerebral ischemia. *Stroke*. 2004;35:1738-1743.
15. Liu JR, Zhao Y, Patzer A, et al. The c-Jun N-terminal kinase (JNK) inhibitor XG-102 enhances the neuroprotection of hyperbaric oxygen after cerebral ischaemia in adult rats. *Neuropathol Appl Neurobiol*. 2010;36:211-224.
16. Michel-Monigadon D, Bonny C, Hirt L. c-Jun N-terminal kinase pathway inhibition in intracerebral hemorrhage. *Cerebrovasc Dis*. 2010;29:564-570.
17. Wiegler K, Bonny C, Coquoz D, Hirt L. The JNK inhibitor XG-102 protects from ischemic damage with delayed intravenous administration also in the presence of recombinant tissue plasminogen activator. *Cerebrovasc Dis*. 2008;26:360-366.
18. Ginet V, Puyal J, Magnin G, Clarke PG, Truttmann AC. Limited role of the c-Jun N-terminal kinase pathway in a neonatal rat model of cerebral hypoxia-ischemia. *J Neurochem*. 2009;108:552-562.
19. Nijboer CH, van der Kooij MA, van Bel F, Ohl F, Heijnen CJ, Kavelaars A. Inhibition of the JNK/AP-1 pathway reduces neuronal death and improves behavioral outcome after neonatal hypoxic-ischemic brain injury. *Brain Behav Immun*. 2010;24:812-821.
20. Nijboer CH, Heijnen CJ, van der Kooij MA, et al. Targeting the p53 pathway to protect the neonatal ischemic brain. *Ann Neurol*. 2011;70:255-264.
21. Bevins RA, Besheer J. Object recognition in rats and mice: a one-trial non-matching-to-sample learning task to study 'recognition memory'. *Nat Protoc*. 2006;1:1306-1311.
22. Schallert T, Fleming SM, Leasure JL, Tillerson JL, Bland ST. CNS plasticity and assessment of forelimb sensorimotor outcome in unilateral rat models of stroke, cortical ablation, parkinsonism and spinal cord injury. *Neuropharmacology*. 2000;39:777-787.

23. Nijboer CH, Groenendaal F, Kavelaars A, Hagberg HH, van Bel F, Heijnen CJ. Gender-specific neuroprotection by 2-iminobiotin after hypoxia-ischemia in the neonatal rat via a nitric oxide independent pathway. *J Cereb Blood Flow Metab*. 2007;27:282-292.
24. van den Tweel ER, Kavelaars A, Lombardi MS, Groenendaal F, May M, Heijnen CJ, van Bel F. Selective inhibition of nuclear factor-kappa B activation after hypoxia/ischemia in neonatal rats is not neuroprotective. *Pediatr Res.* 2006;59:232-236.
25. Nijboer CH, Heijnen CJ, Groenendaal F, May MJ, van Bel F, Kavelaars A. Strong neuroprotection by inhibition of NF-kappaB after neonatal hypoxia-ischemia involves apoptotic mechanisms but is independent of cytokines. *Stroke*. 2008a;39:2129-2137.
26. Ham J, Eilers A, Whitfield J, Neame SJ, Shah B. c-Jun and the transcriptional control of neuronal apoptosis. *Biochem Pharmacol*. 2000;60:1015-1021.
27. Benakis C, Bonny C, Hirt L. JNK inhibition and inflammation after cerebral ischemia. *Brain Behav Immun*. 2010;24:800-811.
28. Waetzig V, Herdegen T. Context-specific inhibition of JNKs: overcoming the dilemma of protection and damage. *Trends Pharmacol Sci*. 2005;26:455-461.
29. Kroemer G, Galluzzi L, Brenner C. Mitochondrial membrane permeabilization in cell death. *Physiol Rev*. 2007;87:99-163.
30. Feksa LR, Latini A, Rech VC, et al. Promotion of oxidative stress by L-tryptophan in cerebral cortex of rats. *Neurochem Int*. 2006;49:87-93.
31. Nijboer CH, Heijnen CJ, Groenendaal F, May MJ, van Bel F, Kavelaars A. A dual role of the NF-kappaB pathway in neonatal hypoxic-ischemic brain damage. *Stroke.* 2008b;39:2578-2586.
32. Chambers JW, Cherry L, Laughlin JD, Figuera-Losada M, Lograsso PV. Selective inhibition of mitochondrial JNK signaling achieved using peptide mimicry of the Sab kinase interacting motif-1 (KIM1). *ACS Chem Biol*. 2011;6:808-818.
33. Wiltshire C, Matsushita M, Tsukada S, Gillespie DA, May GH. A new c-Jun N-terminal kinase (JNK)-interacting protein, Sab (SH3BP5), associates with mitochondria. *Biochem J*. 2002;367:577-585.
34. Esneault E, Castagne V, Moser P, Bonny C, Bernaudin M. D-JNKi, a peptide inhibitor of c-Jun N-terminal kinase, promotes functional recovery after transient focal cerebral ischemia in rats. *Neuroscience*. 2008;152:308-320.
35. Repici M, Centeno C, Tomasi S, et al. Time-course of c-Jun N-terminal kinase activation after cerebral ischemia and effect of D-JNKI1 on c-Jun and caspase-3 activation. *Neuroscience*. 2007;150:40-49.
36. Hanawa N, Shinohara M, Saberi B, Gaarde WA, Han D, Kaplowitz N. Role of JNK translocation to mitochondria leading to inhibition of mitochondria bioenergetics in acetaminophen-induced liver injury. *J Biol Chem*. 2008;283:13565-13577.
37. Wiltshire C, Gillespie DA, May GH. Sab (SH3BP5), a novel mitochondria-localized JNK-interacting protein. *Biochem Soc Trans*. 2004;32:1075-1077.
38. Brucklacher RM, Vannucci RC, Vannucci S. Hypoxic preconditioning increases brain glycogen and delays energy depletion from hypoxia-ischemia in the immature rat. *Dev Neurosci*. 2002;24:411-417.
39. Gilland E, Puka-Sundvall M, Hillered L, Hagberg H. Mitochondrial function and energy metabolism after hypoxia-ischemia in the immature rat brain: involvement of NMDA-receptors. *J Cereb Blood Flow Metab*. 1998;18:297-304.
40. Lowry OH, Passonneau JV, Hasselberger FX, Schulz DW. Effect of ischemia on known substrates and cofactors of the glycolytic pathway in brain. *J Biol Chem*. 1964;239:18-30.
41. Vannucci RC, Yager JY, Vannucci S. Cerebral glucose and energy utilization during the evolution of hypoxic-ischemic brain damage in the immature rat. *J Cereb Blood Flow Metab*. 1994;14:279-288.
42. Vannucci RC, Towfighi J, Vannucci S. Secondary energy failure after cerebral hypoxia-ischemia in the immature rat. *J Cereb Blood Flow Metab*. 2004;24:1090-1097.

43. Chavez-Valdez R, Martin LJ, Flock DL, Northington FJ. Necrostatin-1 attenuates mitochondrial dysfunction in neurons and astrocytes following neonatal hypoxia-ischemia. *Neuroscience*. 2012;219:192-203.

44. Fan M, Goodwin M, Vu T, Brantley-Finley C, Gaarde WA, Chambers TC. Vinblastine-induced phosphorylation of Bcl-2 and Bcl-XL is mediated by JNK and occurs in parallel with inactivation of the Raf-1/MEK/ERK cascade. *J Biol Chem*. 2000;275:29980-29985.

45. Kharbanda S, Saxena S, Yoshida K, et al. Translocation of SAPK/JNK to mitochondria and interaction with Bcl-x(L) in response to DNA damage. *J Biol Chem*. 2000;275:322-327.

46. Schroeter H, Boyd CS, Ahmed R, et al. c-Jun N-terminal kinase (JNK)-mediated modulation of brain mitochondria function: new target proteins for JNK signalling in mitochondrion-dependent apoptosis. *Biochem J*. 2003;372:359-369.

47. Chambers JW, Lograsso PV. Mitochondrial c-Jun N-terminal kinase (JNK) signaling initiates physiological changes resulting in amplification of reactive oxygen species generation. *J Biol Chem*. 2011;286:16052-16062.

48. Lee I, Bender E, Kadenbach B. Control of mitochondrial membrane potential and ROS formation by reversible phosphorylation of cytochrome c oxidase. *Mol Cell Biochem*. 2002;234-235:63-70.

49. Zhou Q, Lam PY, Han D, Cadenas E. c-Jun N-terminal kinase regulates mitochondrial bioenergetics by modulating pyruvate dehydrogenase activity in primary cortical neurons. *J Neurochem*. 2008;104:325-335.

50. Besirli CG, Johnson EM, Jr. JNK-independent activation of c-Jun during neuronal apoptosis induced by multiple DNA-damaging agents. *J Biol Chem*. 2003;278:22357-22366.

51. Bessero AC, Chiodini F, Rungger-Brandle E, Bonny C, Clarke PG. Role of the c-Jun N-terminal kinase pathway in retinal excitotoxicity, and neuroprotection by its inhibition. *J Neurochem*. 2010;113:1307-1318.

52. Sevilla A, Santos CR, Barcia R, Vega FM, Lazo PA. c-Jun phosphorylation by the human vaccinia-related kinase 1 (VRK1) and its cooperation with the N-terminal kinase of c-Jun (JNK). *Oncogene*. 2004;23:8950-8958.

53. Nijboer CH, Heijnen CJ, Groenendaal F, van Bel F, Kavelaars A. Alternate pathways preserve tumor necrosis factor-alpha production after nuclear factor-kappaB inhibition in neonatal cerebral hypoxia-ischemia. *Stroke*. 2009;40:3362-3368.

54. Northington FJ, Chavez-Valdez R, Martin LJ. Neuronal cell death in neonatal hypoxia-ischemia. *Ann Neurol*. 2011;69:743-758.

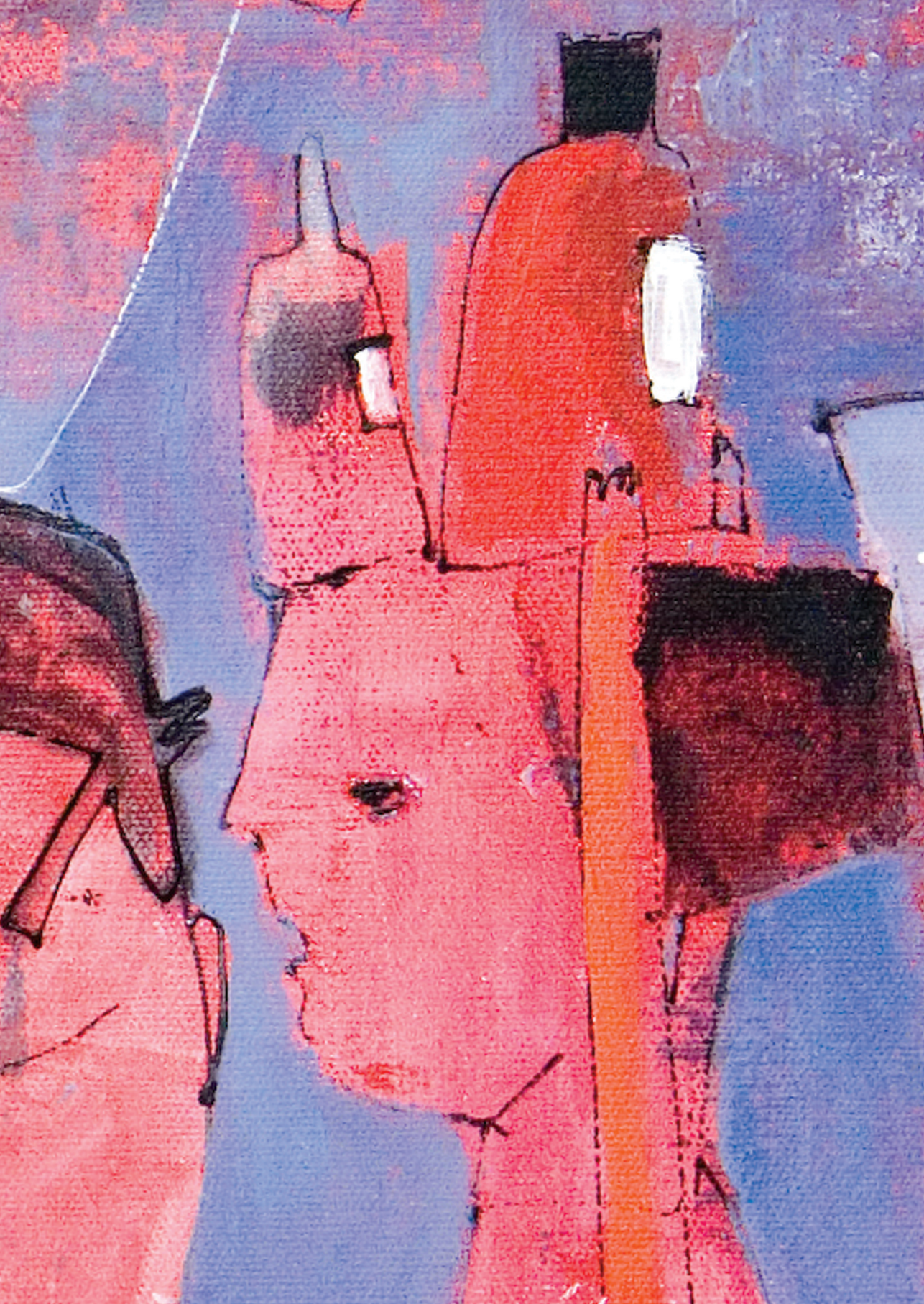

4

Selective inhibition of p53-JNK interaction by TAT-P7-pi strongly protects the neonatal brain against hypoxic-ischemic brain damage

Cora H. Nijboer
Hilde J.C. Bonestroo
Annemieke Kavelaars
Cobi J. Heijnen

Submitted

Abstract

Background Neonatal encephalopathy due to hypoxia-ischemia (HI) remains a major contributor to perinatal mortality and morbidity. At present, therapeutic options are still very limited. We have previously shown that cerebral HI induces mitochondrial translocation of p53 and activation of the MAP kinase c-Jun N-terminal kinase (JNK) at the mitochondrial membrane. Inhibition of mitochondrial p53 translocation by pifithrin (PFT)-μ or inhibition of JNK activation by D-JNKi potently reduced HI-induced apoptotic cell death in the brain. *In vitro* studies have demonstrated a so-called "P7 domain" in the p53 protein which is required for binding to and phosphorylation by JNK. JNK-mediated phosphorylation of p53 results in increased half-life of p53 which boosts apoptosis. Here, we investigated the neuroprotective potential of a small peptide inhibitor of JNK-p53 interaction, *i.e.* the P7 domain-peptide inhibitor (TAT-P7-pi), in a rat model of neonatal HI brain damage.

Methods Seven-day-old Wistar rats were subjected to unilateral carotid artery occlusion and hypoxia (HI) and treated intraperitoneally with TAT-P7-pi. Effective dose and therapeutic window of TAT-P7-pi were assessed at 48 h post-HI. Long-term anatomical and (sensori) motor and cognitive behavioral effects were assessed at 5-9 weeks post-HI. In search for the underlying mechanism, mitochondrial integrity and apoptotic cell death markers were analyzed.

Results A dose-response experiment with intraperitoneal TAT-P7-pi treatment showed that 10 mg/kg was the most effective dose resulting in >81% reduction of HI infarct size. The therapeutic window of 10 mg/kg TAT-P7-pi was at least 6 h. Treatment with TAT-P7-pi had long-term neuroprotective effects on gray and white matter damage and restored long-term cognitive and motor impairment. TAT-P7-pi administration was associated with preservation of mitochondrial integrity as evidenced by prevention of ATP loss and inhibition of lipid peroxidation. HI-induced apoptotic cell death measured by leakage of cytochrome *c*, caspase 3 cleavage, and reduction of anti-apoptotic Bcl-2/Bcl-xL levels, was strongly inhibited by TAT-P7-pi.

Conclusion We show here that TAT-P7-pi treatment protects the neonatal brain against HI injury. Our novel findings indicate that JNK-p53 interaction might be important in regulating mitochondrial damage and subsequent apoptotic cell death after cerebral HI in the newborn brain.

Introduction

Brain injury or encephalopathy in neonates often leads to serious long-lasting neurodevelopmental disabilities that result in a considerable loss of quality of life. Among the severe sequelae of perinatal brain injury are motor impairments, mental retardation, psychological and cognitive problems and the development of seizures.[1-3] Hypoxia-ischemia (HI) is an important cause of neonatal encephalopathy. Despite considerable progress in neonatal care and extensive experimental studies in *in vivo* and *in vitro* models of HI encephalopathy (HIE), effective and clinically-applicable therapies to prevent HIE still remain very scarce to date.[4,5]

HIE results from an intricate interacting network of pathophysiological cascades and in recent years a numerous amount of cellular, molecular and biochemical contributing pathways have been uncovered.[6,7] Understanding how neurons are damaged or die after HI is crucial to develop novel therapeutic strategies to diminish injury in the brain and to improve functional outcome. Recent literature has shown that apoptotic or programmed cell death contributes prominently to neuronal degeneration after HI but other cell death pathways including necrosis, autophagy and other features of the cell death continuum like necroptosis also play a distinguished role.[8] Mitochondria are pivotal organelles for the regulation of cellular energy levels, *i.e.* ATP production. Upon HI, the mitochondrial metabolism changes by *e.g.* excitotoxicity and Ca^{2+} overload which primarily leads to uncoupling of oxidative phosphorylation, decreased energy production and formation of reactive oxygen species (ROS). Importantly, mitochondria also become regulators of cell death in the immature brain after HI.[9-12] One of the hallmarks of mitochondria-regulated cell death is permeabilization of the mitochondrial outer membrane (MOMP) through which mitochondrial proteins leak into the cytosol. As a result, downstream caspases are activated which eventually execute apoptotic cell death. The balance between pro- and anti-apoptotic members of the Bcl-2 family, like Bax and Bid vs Bcl-2 and Bcl-xL respectively, is essential for initiation or prevention of MOMP.[13] Defining which molecules or pathways tip the balance from a dominant protective effect of the mitochondrial Bcl-2 family towards an apoptosis-promoting state is crucial to develop and fine-tune strategies to effectively block neuronal cell death and reduce HIE.

In our previous study we showed for the first time that the tumor-suppressor protein p53 which is well-known for its transcriptional regulation of death genes, was translocated to the mitochondrial membrane in the brain in an *in vivo rat* model of neonatal HI.[14] In another recent study, we discovered that the mitogen-activated protein (MAP) kinase c-Jun N-terminal kinase (JNK) was activated (phosphorylated) at the mitochondria in the brains of neonatal rats after HI.[15] Importantly, we showed that specific inhibitors of p53 mitochondrial translocation (*i.e.* pifithrin-μ (PFT-μ)) or JNK activation at the mitochondria (*i.e.* D-JNKi and Sab_{KIM1} peptides) potently reduced apoptosis and strongly decrease HI-induced infarct size in neonatal rats.[14,15] These previous data highlight the crucial role of p53 and phosphorylated (P)-JNK at the mitochondrial interphase in initiating apoptosis as inhibiting the translocation/

activation of *one* of these proteins results in strong neuroprotection. We hypothesize in the current study that an interaction between p53 and JNK is needed at the mitochondria to induce MOMP. Interestingly, *in vitro* studies have shown that JNK can bind p53 at the so-called P7 domain, which is a requisite for JNK to phosphorylate p53 at a specific threonine residue (Thr 81). JNK-mediated phosphorylation of p53 results in a reduced interaction of p53 with its endogenous inhibitor MDM2 and thereby reduced ubiquitination of p53 which strongly enhances p53's half-life.[16-18] In *in vitro* experiments, addition of a specific peptide called the 'P7 domain peptide' which mimics the JNK-binding domain in p53, was shown to prevent the association of p53 and JNK.[16,18] In the present study we investigated the neuroprotective potential of the P7 domain-peptide inhibitor in an *in vivo* rat model of neonatal HI brain damage.

Materials and Methods

Animals

All animal experiments were approved by the animal ethical committee of the UMC Utrecht (DEC-ABC, UMC Utrecht). Wistar rats were bred at the local animal facility. Seven-day-old Wistar rat pups of both genders were anesthetized with isoflurane (5% induction, 1.5% maintenance) for <5 min. The right common carotid artery was occluded by thermocauterization. Pups recovered for at least 1 h in the home cage before undergoing hypoxia for 120 min at 8% O_2. Sham-control pups underwent anesthesia and incision only. All analyses were performed in blinded set-up.

TAT-P7-pi (YGRKKRRQRR-VPSQKTYQGNYGFHLGFLQSG; underlined amino acids represent HIV-TAT shuttle domain) and mutant (scrambled) peptide (YGRKKRRQRR-SPPVVPSQSKSTSYGQGYRF) were synthetized at W.M. Keck facility (Yale University, New Haven, CT, USA). Peptides were dissolved at 40 mg/ml in dimethylsulfoxide (DMSO) and further diluted in PBS. 2.5% DMSO in PBS was used as vehicle-solution. TAT-P7-pi was administered intraperitoneally (i.p.) at doses of 2, 5 or 10 mg/kg (dose-response experiment). The dose of 10 mg/kg TAT-P7-pi was used in all other experiments. Mutant peptide was administered i.p. at 10 mg/kg.

PFT-μ (Sigma-Aldrich, Steinheim, Germany) was dissolved in DMSO and diluted to 2.5% DMSO in PBS. PFT-μ was administered i.p. at 8 mg/kg as described earlier.[14]

D-JNKi (dqsrpvqpflnlttprkpr-pp-rrrqrrkkrg; all D-amino acids in *retro-inverso* form; underlined amino acids represent HIV-TAT shuttle domain) was synthetized at W.M. Keck facility. D-JNKi was dissolved in PBS and administered i.p. at 10 mg/kg as described earlier.[15]

Histology

Rats were sacrificed by pentobarbital overdose. Animals were transcardially perfused with 4% paraformaldehyde (PFA) in PBS, brains were removed, post-fixed in 4% PFA and

embedded in paraffin. Coronal sections (8 µm; corresponding to -3.20 mm from bregma in adult brain) were stained with mouse-anti-microtubule-associated protein 2 (MAP2; Sigma-Aldrich, Steinheim, Germany) or mouse-anti-myelin basic protein (MBP; Sternberger Monoclonals Incorporated, Lutherville, MD) followed by biotin-labeled horse-anti-mouse antibody (Vector-Labs, Burlingame, CA) and revealed using Vectastain ABC kit (Vector-Labs) and diaminobenzamidine. Other coronal sections were stained with hematoxylin and eosin (HE; Klinipath, Duiven, The Netherlands). MAP2 staining was used to assess neuronal damage at 48 h and 9 weeks post-HI. HE and MBP staining were used to study long-term infarct size and white matter damage at 9 weeks post-HI, respectively. For analyses, full section images were captured with a Nikon D1 digital camera (Nikon, Tokyo, Japan). MAP2-, MBP- and HE-stained sections were analyzed as described previously.[14,15,19] In short, MAP2- or HE-positive areas of ipsi- and contralateral hemispheres were outlined manually with image processing tools in Adobe Photoshop (Adobe Systems Inc, San Jose, CA). The area of MBP staining in both hemispheres was quantified using ImageJ software (http://rsb.info.nih.gov/ij/, 1997-2006). Neuronal damage (MAP2), volume loss (HE) or white matter damage (MBP) is presented as ipsi-/contralateral MAP2-, HE- or MBP-positive area.

For analysis of corpus callosum thickness, photographs were taken with a Zeiss Axio Lab A1 microscope and Icc5 camera and analyzed using ZEN2012 software (both Carl Zeiss, Oberkochen, Germany). MBP-positive fiber coherency was analyzed using the OrientationJ plugin for ImageJ (http://bigwww.epfl.ch/demo/orientation/).

Behavioral tests

Rota-Rod

At 5 weeks after HI, rats were tested for balance, coordination and grip on the Rota-Rod (RTR) (Stoelting Europe, Ireland) according to a standardized protocol.[20] In short, rats were trained for 2 subsequent days to remain on the RTR when rotating with a speed of 5 rpm for a maximum duration of 150 seconds. On day 3 and 4, performance of the rats was tested by measuring the time the animals could stay on the rod when rotation speed was increased from 5-40 rpm for a maximum duration of 300 seconds with increasing steps of 5 rpm. The mean performance of day 3 and 4 was calculated as the time in seconds the animals were able to stay on the rod. The test was performed in the light by a trained observer blinded to treatment.

Cylinder rearing test

At 7 weeks post-HI, forelimb use asymmetry was tested in the cylinder rearing test (CRT). Rats were individually placed in a plexiglas transparent cylinder and observed for 3 min. Initial preference for use of the left (impaired), right (non-impaired) or both forepaw(s) during weight-bearing contacts in full rear with the cylinder were recorded. The % preference to use the non-impaired forepaw was calculated as: (right-left)/(right+left+both) x 100%.[14,15,19,21] The test was performed in the dark by a trained observer blinded to treatment.

Adhesive removal task

The adhesive removal task (ART) was used to test sensorimotor function of the animals. At 8 weeks after HI, stickers (tough-spots, Diversified Biotech, Boston, MA) were placed on the left (impaired) or right (non-impaired) forepaw and the time for adhesive removal was measured. One sticker on each paw was used to habituate the animals to the test, followed by placement of 3 consecutive stickers per forepaw. The order for left/right forepaw sticker placement was alternated between and within animals. The test was recorded on video. The test was performed in the dark by a trained observer blinded to treatment.

We determined the mean "total time for adhesive removal" of the left and right forepaw as described earlier.[19,21,22] Besides the "total time for adhesive removal", we also analyzed "latency to start removal" as a measure for sensory function, and "effective adhesive removal time" as a measure for fine motor coordination between paw and mouth.

Novel object recognition task

At 9 weeks post-HI, cognitive function was tested by exposing the rats to the novel object recognition task (NORT) as described earlier.[14,15,23] In short, rats were allowed to explore two identical objects for 10 min in an empty cage without bedding. One hour later, rats were re-exposed to one familiar and a novel object. Preference for the novel object as a measure of memory was calculated as (time spent with novel object)/(total time spent with both objects) x 100%. The test was performed in the dark by a trained observer blinded to treatment.

Subcellular protein fractionation and Western blotting

At 3 or 24 h post-HI, rat pups were decapitated, brains were quickly removed, cerebellum was discarded and left (contralateral) and right (ipsilateral) hemispheres were separately frozen in liquid nitrogen. Both hemispheres were pulverized using a liquid nitrogen-cooled mortar and pestle, and stored at -80 °C. Cytosolic and mitochondrial protein fractions were prepared from pulverized hemispheres as described previously.[24] In short, pulverized brain was homogenized in buffer (70 mM sucrose, 210 mM mannitol, 5 mM HEPES, 1 mM EDTA and protease/phosphates inhibitors) using a Potter homogenizer. Homogenates were centrifuged at 800 g for 10 min at 4 °C, leading to a nuclear/membrane pellet. Supernatants were centrifuged at 10.000 g for 10 min at 4 °C to obtain a mitochondria-free cytosolic protein fraction in the supernatant and mitochondrial proteins in the pellet. This pellet was sonicated in buffer (50 mM Tris, 5 mM EDTA 150 mM NaCl and protease/phosphatase inhibitors), followed by centrifugation at 10.000 g for 15 min at 4 °C. Supernatant contained mitochondrial proteins. Subcellular fractionation quality was confirmed by predominant expression of β-actin in cytosolic fractions and exclusive presence of COX-IV in mitochondrial fractions.[15,25] To check for equal protein loading, cytosolic protein membranes were reprobed with β-actin. Mitochondrial protein membranes were also reprobed with β-actin as COX-IV expression was reduced after HI.[25] β-Actin expression on mitochondrial protein membranes correlated well with loading controls based on Ponceau S staining.

Similar protein amounts were separated by SDS-PAGE, transferred to Hybond-C membranes (Amersham, Buckinghamshire, UK) and incubated with rabbit-anti-cleaved-caspase 3, rabbit-anti-Bcl-2, rabbit-anti-Bcl-xL (all Cell Signaling, Danvers, MA), mouse-anti-cytochrome *c* (BD Biosciences Pharmingen), goat-anti-β-actin (Santa Cruz Biotechnology) and mouse-anti-COX-IV (Molecular Probes, Eugene, OR) followed by peroxidase-labeled secondary antibodies, revealed by enhanced chemiluminescence (Amersham) and analyzed with a GS-700 Imaging Densitometer (Bio-Rad, Hercules, CA) or Proxima 2750T (Isogen Life Science, De Meern, The Netherlands).

ATP assay

At 3 h post-HI animals were decapitated, brains were very quickly removed (within 15 seconds) and hemispheres were separately frozen in liquid nitrogen. Hemispheres were weighted, homogenized in PBS and deproteinized by using the Deproteinizing Sample Preparation Kit according to manufacturer's protocol (Biovision, Mountain View, CA). ATP levels were measured in deproteinized, neutralized samples using the ATP colorimetric Assay Kit (Biovision) according to manufacturer's protocol. Optical density was measured at 570 nm. An ATP standard was used to obtain a reference curve. Samples were normalized for protein concentration. Protein concentration was measured before deproteination of the samples.

TBARS assay

At 3 h post-HI we measured oxidative stress (lipid peroxidation) by using a TBARS (thiobarbituric acid reactive substances) assay according to the manufacturer's protocol (Oxiselect TBARS Assay Kit; Cell Biolabs, San Diego, CA). In short, both hemispheres were homogenized separately in PBS/0.05% butylated hydroxytoluene (BHT) followed by centrifugation at 10.000 g for 5 min. Supernatants were 1:1 mixed with SDS lysis solution (provided by kit), incubated for 5 min at RT and mixed with TBA reagent (provided by kit). Samples were incubated for 60 min at 95 °C, quickly cooled down to RT and centrifuged at 1.000 g for 15 min. *n*-Butanol was added 1:1 to the supernatants to prevent interference of hemoglobin. Samples were thoroughly vortexed and centrifuged for 5 min at 10.000 g. Absorbance was measured in the butanol fraction at 532 nm. A MDA standard curve was used as a reference. Samples were normalized for protein concentration.

Statistical analysis

Data were normally distributed, are presented as mean and SEM, and were analyzed by one-way ANOVA with Bonferroni post-tests.

Results

Dose-response and therapeutic window of TAT-P7-pi treatment for neonatal HI brain injury

HI brain injury was induced in 7-day-old Wistar rat pups by unilateral carotid artery occlusion followed by systemic hypoxia. Directly after induction of HI (0 h), rats were i.p. treated with vehicle solution or TAT-coupled P7 domain peptide inhibitor (TAT-P7-pi) in doses of 2, 5 or 10 mg/kg. A scrambled TAT-coupled peptide sequence was used as a control (mutant; MUT) at a dose of 10 mg/kg. At 48 h after induction of HI, neuronal damage was assessed by analyzing staining for MAP2 in the contra- and ipsilateral hemispheres. HI induced 78.8 ± 7.9% MAP2 loss in the ipsilateral hemisphere of vehicle-treated rats (Fig 1A). Treatment with TAT-P7-pi at a dose of 2 mg/kg was not significantly neuroprotective (68.9 ± 11.0% ipsilateral MAP2 loss). When rat pups were treated with 5 or 10 mg/kg TAT-P7-pi at 0 h post-HI, ipsilateral MAP2 loss was significantly reduced with 55% and 80% compared to vehicle, respectively (Fig 1A). Treatment with the mutant peptide had no effect on the vast MAP2 loss after HI alone (78.3 ± 7.0%), indicating that the neuroprotective effect of TAT-P7-pi is specific for the peptide sequence and that the TAT sequence as such did not have any effect on HI brain damage. Sham-operated rat pups did not show any MAP2 loss in the ipsi- or contralateral hemisphere and additionally no MAP2 loss was observed in the contralateral hemispheres of HI-treated littermates.

In the next experiment we determined the therapeutic window of TAT-P7-pi. To this end rat pups were treated i.p. with the most effective dose (10 mg/kg) and treatment was postponed for 3, 6 or 9 h after HI. Ipsilateral MAP2 loss at 48 h post-HI was used to assess early neuronal damage. Figure 1B shows that treatment with TAT-P7-pi could be delayed till 6 h after HI: 81% neuroprotection at 0 h versus 82% at 3 h and 49% at 6 h. Ipsilateral MAP2 loss in rats that were treated with TAT-P7-pi at 9 h post-HI was not significantly different from vehicle- or mutant peptide-treated littermates (Fig 1B). No MAP2 loss was observed in sham-operated rats or in contralateral hemispheres of HI-treated animals.

Long-term effects of TAT-P7-pi on motor and cognitive behavior

At 5 weeks after induction of HI brain injury, motor behavior on the Rota-Rod (RTR) was assessed in sham-operated and HI-treated rats. HI induced a significant reduction in the time spent on the rod compared to sham-operation; sham-operated rats spent 131.9 ± 36.3 seconds on the rod while vehicle-treated HI littermates stayed on the rotating rod only for 101.5 ± 33.3 seconds (Fig 2A). Treatment with TAT-P7-pi after HI completely restored performance on the RTR as these rats performed as well as sham-operated animals (Fig 2A). Performance of HI-rats treated with the mutant peptide was similar to vehicle-treated rats (Fig 2A).

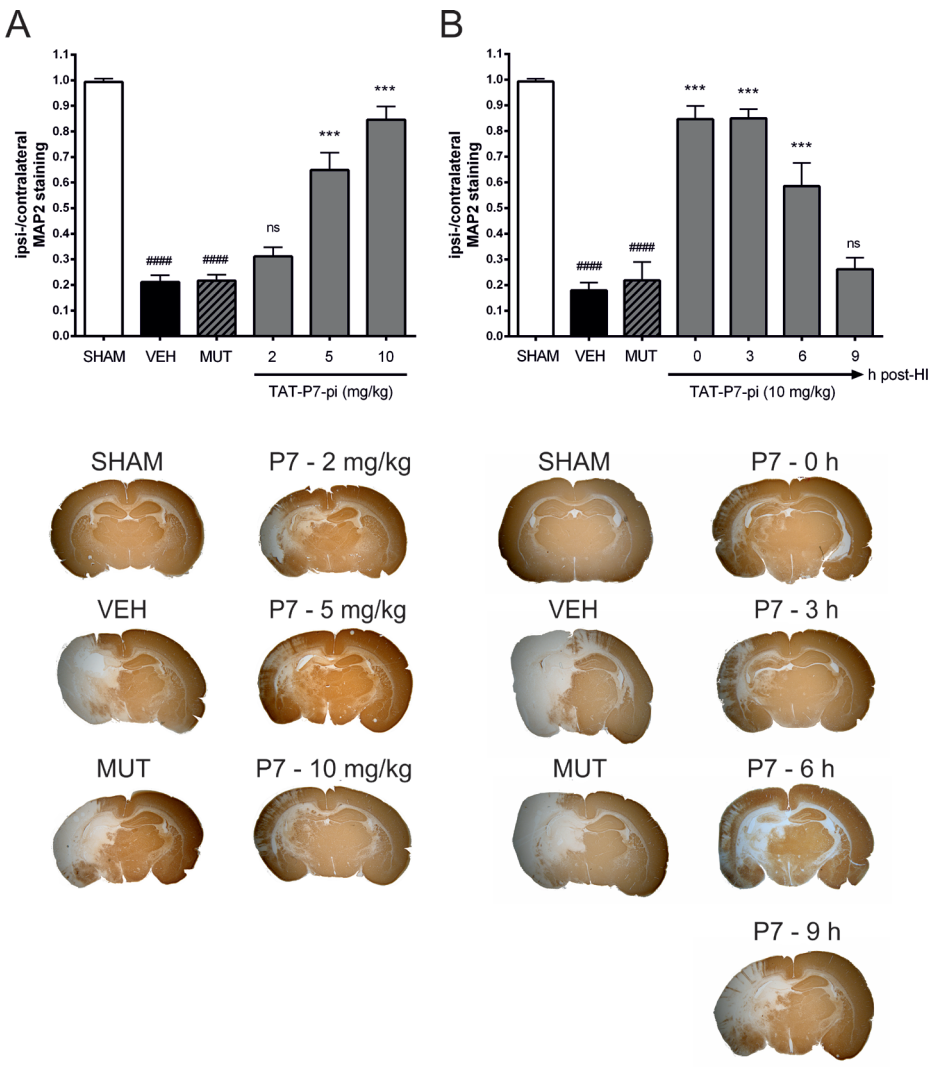

Figure 1: Dose-response and therapeutic window of TAT-P7-pi treatment after HI brain injury
Wistar rat pups were subjected to HI at postnatal day 7. Neuronal damage was assessed at 48 h post-insult by analyzing microtubule-associated protein 2 (MAP2) staining on full brain sections cut at equivalent to app. -3.20 mm from bregma in adult rat brains. **A**: Ratio ipsi-/contralateral MAP2 positive area in sham-operated pups (SHAM), vehicle-treated HI pups (VEH) and pups treated with TAT-P7-pi at a dose of 2, 5 or 10 mg/kg. A TAT-coupled scrambled (mutant) sequence of the peptide was used as a control at 10 mg/kg (MUT). Vehicle and peptides were administered intraperitoneally directly after HI (0 h). SHAM n=8, HI-VEH n=9, HI-MUT n=9, HI-TAT-P7-pi 2 mg/kg n=9, HI-TAT-P7-pi 5 mg/kg n=10, HI-TAT-P7-pi 10 mg/kg n=10. **B**: Ratio ipsi-/contralateral MAP2 positive area in sham-operated, HI-vehicle, HI-mutant peptide and HI-TAT-P7-pi rat pups. Intraperitoneal treatment with TAT-P7-pi (10 mg/kg) was started at 0, 3, 6 or 9 h post-HI. Vehicle solution and mutant peptide were administered at 0 h after HI. SHAM n=7, HI-VEH n=7, HI-MUT n=9, HI-TAT-P7-pi: 0 h n=10, 3 h n=6, 6 h n=6, 9 h n=6. **A-B**: No MAP2 loss was observed in sham-operated pups or in contralateral hemispheres of HI-treated rats. Photographs show representative examples of MAP2 loss in the different experimental groups. Data were analyzed by one-way ANOVA with Bonferroni post-tests. $^{\#\#\#\#}p$ <0.0001 vs sham-control, *** p <0.001 vs vehicle treatment. A.U.: arbitrary units. ns: non-significant.

The preference to use the non-impaired forepaw was tested in the Cylinder Rearing Test (CRT) at 7 weeks post-HI. Sham-operated rats did not show any preference for using the left (impaired) or right (non-impaired) forepaw during vertical rearing in the cylinder (Fig 2B). HI caused a significant 45-48% paw preference for using the non-impaired forepaw in vehicle-treated and mutant peptide-treated rats (Fig 2B). Treatment with TAT-P7-pi (10 mg/kg) strongly reduced paw preference for the non-impaired forepaw (Fig 2B).

At 8 weeks after HI, all animals were subjected to the adhesive removal task (ART) in which the latency to remove a sticker from the impaired and non-impaired forepaw was measured as an indication for sensorimotor function. Rats that underwent sham-operation did not show a difference in "total time for adhesive removal" between the left and right forepaw (app. 12 seconds) (Fig 2C). After induction of HI brain damage, vehicle-treated rats were unilaterally impaired in the ART: "total time for adhesive removal" of the left (impaired) forepaw was significantly (3.4 times) higher than "total time for adhesive removal" of the right (non-impaired) forepaw (Fig 2C). Treatment with TAT-P7-pi showed a strong reduction in the "total time for adhesive removal" of the impaired forepaw (Fig 2C). Mutant peptide treatment after HI showed similar effects as vehicle treatment with a 3.2 times higher "total time for adhesive removal" of the impaired than of the non-impaired forepaw (Fig 2C). The "total time for adhesive removal" of the non-impaired forepaw did not differ between sham-operated and any of the HI-treated groups. We further analyzed the behavior of the rats in the ART by measuring the exploration time spent before the animal started to remove the adhesive patch l ("latency to start removal") as a measure of sensory function, and subsequently how much time the animals actually spent on adhesive removal after sensing it ("effective adhesive removal time") as a measure of fine motor coordination between paw and mouth. Figures 2D and 2E show that both the "latency to start removal" and "effective adhesive removal time" were increased in the impaired forepaw of vehicle- or mutant peptide-treated HI rats, whereas TAT-P7-pi treatment after HI significantly reduced both the time it took the animals to sense and to remove the adhesive patch of the impaired forepaw.

Cognitive behavior of all animals was assessed by using the Novel Object Recognition Task (NORT) at 9 weeks post-HI. The NORT is based on the capacity of rats to discriminate between a novel or a known object and this test can be used to measure short-term memory function. Sham-operated rats spent app. 68% of the total interaction time with the novel object, indicating a clear preference for the novel object (Fig 2F). HI brain injury induced a complete loss of novel object recognition as vehicle-treated rats spent app. 52% of their time with the novel object indicating that these animals could not discriminate between known or novel (Fig 2F). TAT-P7-pi treatment after HI significantly restored novel object recognition, indicating improved memory function (Fig 2F). Treatment with mutant peptide resulted in similar loss of novel object recognition as after vehicle treatment (Fig 2F). Total time of interaction with the two objects did not significantly differ between groups (sham-operated animals: 15.5%; HI-vehicle animals: 14.5%; HI-mutant peptide: 14.2%; HI-TAT-P7-pi: 14.3%).

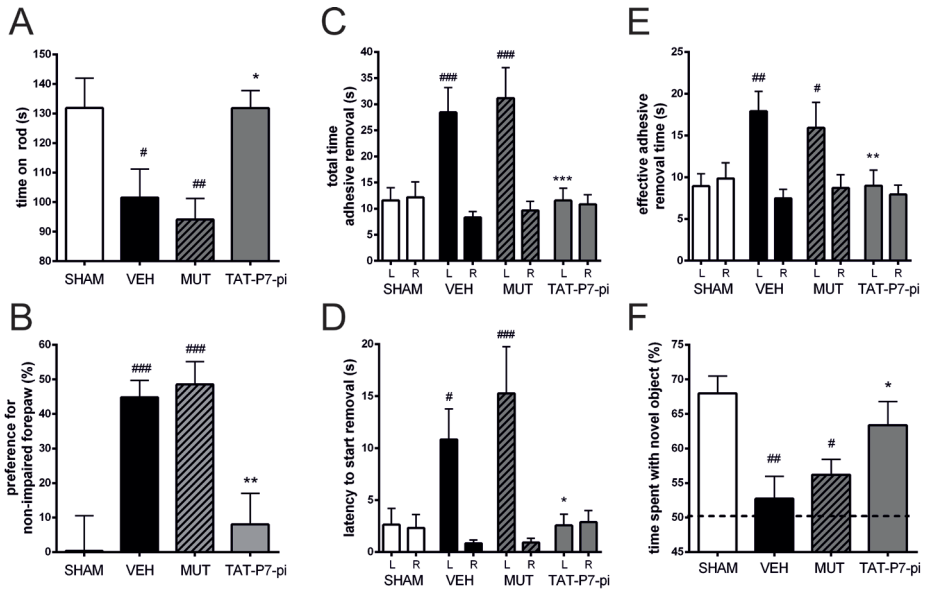

Figure 2: Effects of TAT-P7-pi treatment on motor and cognitive behavior
Rats were subjected to HI at postnatal day 7 followed by intraperitoneal treatment with vehicle (VEH), mutant peptide (MUT) or TAT-P7-pi (10 mg/kg) at 0 h post-insult. Sham-operated animals were used as controls. Performance of all animals was tested on several behavioral paradigms from week 5-9 post-HI. **A**: Rats were tested for their performance on the Rota-Rod (RTR) at 5 weeks after the insult. Rats were trained for 2 days at rotation speed of 5 rpm for 150 seconds. The mean performance on day 3 and 4 is depicted as time (seconds) spent on the rod when rotation speed was increased from 5-40 rpm for a maximum time of 300 seconds with increasing steps of 5 rpm. **B**: Forelimb use asymmetry was tested in the cylinder rearing test (CRT) at 7 weeks post-HI. Preference for use of the left (impaired), right (non-impaired) or both forepaw(s) during weight-bearing contacts in full rear with the cylinder were recorded for 3 min. The % preference to use the non-impaired forepaw was calculated. **C-E**: Sensorimotor behavior was assessed by testing rats in the adhesive removal task (ART) at 8 weeks post-insult. **C**: "Total time for adhesive removal" was measured in seconds for the left (L; impaired) and right (R; non-impaired) forepaw. The mean time of 3 consecutive adhesives per forepaw was calculated. **D**: "Latency to start removal" was measured in seconds, *i.e.* the time it takes the animal before sensing the adhesive, as a measure of sensory function. **E**: "Effective adhesive removal time" was measured in seconds, *i.e.* the time it takes the animal to remove the adhesive after sensing it on its forepaw, as a measure of fine motor coordination. **F**: The novel object recognition task (NORT) was used to test cognitive function at 9 weeks after HI. Time spent with the familiar and novel object was measured for a 5 min time period. Percentage time spent with the novel object is presented. Dotted line represents 50%, *i.e.* equal times are spent with familiar and novel object, indicative for impaired memory. For CRT, ART and NORT: SHAM n=15, HI-VEH n=14, HI-MUT n=15, HI-TAT-P7-pi n=15. For RTR: SHAM n=13, HI-VEH n=12, HI-MUT n=13, HI-TAT-P7-pi n=13, as we did not take into account animals that jumped of the RTR for 3 consecutive times. Data were analyzed by one-way ANOVA with Bonferroni post-tests. $^{\#}p<0.05$, $^{\#\#}p<0.01$, $^{\#\#\#}p<0.001$ vs sham-control; * $p<0.05$, ** $p<0.01$, *** $p<0.001$ vs vehicle treatment. s: seconds.

Effects of TAT-P7-pi treatment on long-term cerebral volume loss and neuronal damage

At 9 weeks after HI large cystic lesions had developed in the ipsilateral hemisphere of HI-treated rats; ipsilateral volume loss as measured on HE-stained brain sections was 68.6 ±

20.0% in vehicle-treated HI rats (Fig 3A). The neuroprotective effect of TAT-P7-pi observed at 48 h post-HI in figure 1 was long-lasting as ipsilateral volume loss at 9 weeks post-insult was still decreased by 85% after TAT-P7-pi treatment (Fig 3A) implying that ipsilateral volume of TAT-P7-pi-treated rats did not significantly differ from sham-operated rats. Besides measuring volume loss in the ipsilateral hemisphere we also determined specific gray matter damage by staining for MAP2 (Fig 3B). TAT-P7-pi treatment resulted in a 65% reduction in HI-induced MAP2 loss at 9 weeks post-insult (Fig 3B), compared to 81% reduction in MAP2 loss at 48 h post-HI. Treatment with mutant peptide resulted in similar ipsilateral volume loss and MAP2 loss as vehicle treatment after HI (Fig 3A, B).

Effect of TAT-P7-pi treatment on HI-induced white matter damage

White matter damage was assessed by staining brains for MBP at 9 weeks post-HI (Fig 4). We first determined HI-induced loss of MBP staining in the whole ipsilateral hemisphere. Vehicle-treated rats displayed 71.7 ± 24.1% MBP loss in the ipsilateral hemisphere after HI (Fig 4A). TAT-P7-pi treatment potently reduced ipsilateral MBP loss by 79% (Fig 4A). Treatment with mutant peptide did not have any effect on HI-induced white matter damage (Fig 4A). No MBP loss was observed in contralateral hemispheres of HI rats compared to sham-controls.

We next determined thickness of the corpus callosum at the midline of the brain at 9 weeks after HI as a measure of possible white matter loss. HI induced a significant thinning of the corpus callosum in vehicle- and mutant peptide-treated rats compared to sham-operated littermates (Fig 4B). TAT-P7-pi treatment after HI significantly restored corpus callosum thickness compared to vehicle treatment (Fig 4B).

We also determined the organization and axonal branching of MBP-positive fibers by determining the lateral arborization of MBP-positive fibers within the cingulum at 9 weeks post-HI. We defined lateral arborization of MBP-positive fibers by measuring fiber coherency. In HI rats treated with vehicle or mutant peptide, fiber coherency in the ipsilateral cingulum was significantly increased, indicating a more linear MBP-positive fiber pattern (less lateral arborization) in comparison to sham-operated littermates (Fig 4C). The HI-induced increase in fiber coherency was significantly reduced after TAT-P7-pi treatment to levels observed in sham-control rats (Fig 4C).

Effects of TAT-P7-pi treatment on mitochondrial integrity and pro- and anti-apoptotic markers

To further explore our hypothesis that TAT-P7-pi acts by protecting against mitochondrial injury and subsequent apoptotic cell death via the prevention of adequate p53-JNK interaction, we first investigated whether the observed neuroprotective effects of TAT-P7-pi treatment after HI were associated with effects on mitochondrial functioning. To this end two important hallmarks of mitochondrial integrity, *i.e.* ATP production and ROS formation, were determined at 3 h post-HI. Figure 5A shows that cerebral HI induced a sharp drop

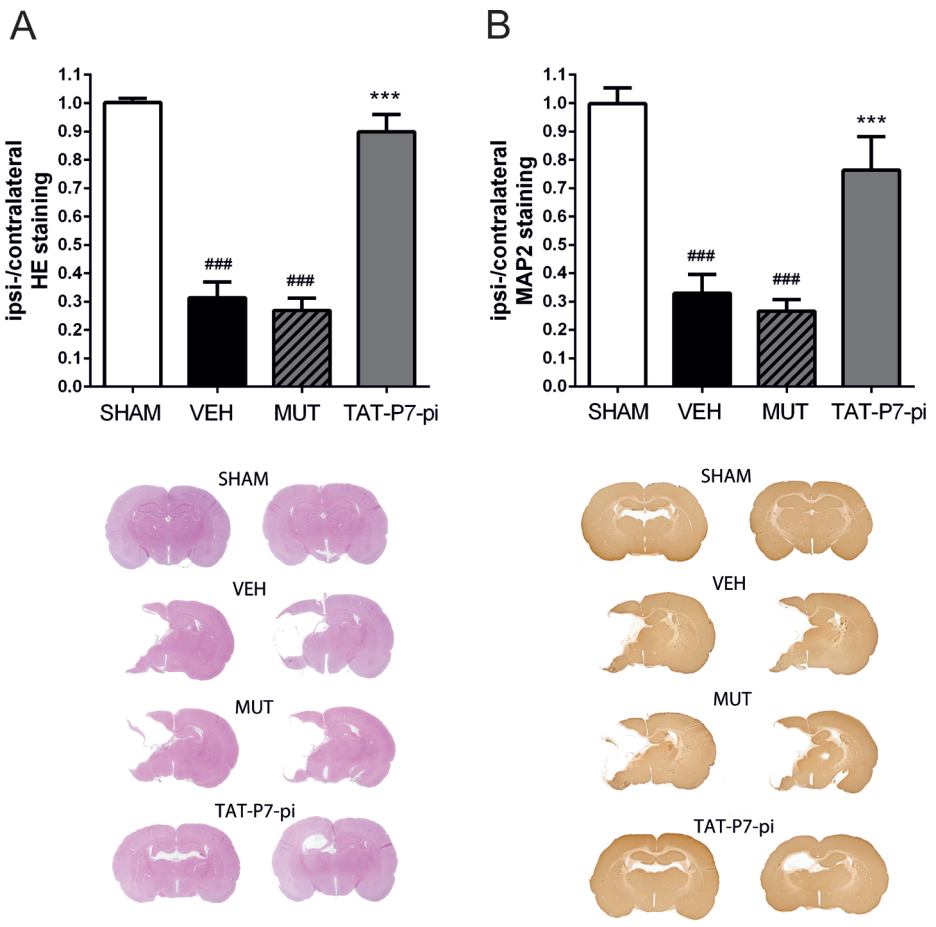

Fig 3: Long-term neuroprotective effects of TAT-P7-pi on HI-induced cerebral volume loss and neuronal damage

Seven-day-old Wistar rats were subjected to HI and treated intraperitoneally with vehicle (VEH), mutant peptide (MUT) or TAT-P7-pi (10 mg/kg) at 0 h post-insult. Sham-operated animals were used as controls. At 9 weeks after induction of HI, brains were stained for hematoxylin-eosin (HE) or microtubule-associated protein 2 (MAP2) at app. -3.20 mm from bregma. **A**: Ratio ipsi-/contralateral HE-positive area as a measure for HI-induced cerebral volume loss in the ipsilateral hemisphere. Photographs show representative examples of all experimental groups. **B**: Ratio ipsi-/contralateral MAP2-positive area as a measure for HI-induced gray matter damage in the ipsilateral hemisphere. Photographs show representative examples of all experimental groups. **A-B**: SHAM n=15, HI-VEH n=14, HI-MUT n=15, HI-TAT-P7-pi n=15. Data were analyzed by one-way ANOVA with Bonferroni post-tests. $^{###}p$ <0.001 vs sham-control; *** p <0.001 vs vehicle treatment.

in ATP production in the ipsilateral hemisphere after vehicle or mutant peptide treatment. Treatment with TAT-P7-pi significantly restored ipsilateral ATP levels by app. 53% (Fig 5A). ATP levels in the contralateral hemispheres of HI animals were not significantly affected when compared to levels in sham-control littermates (Fig 5A).

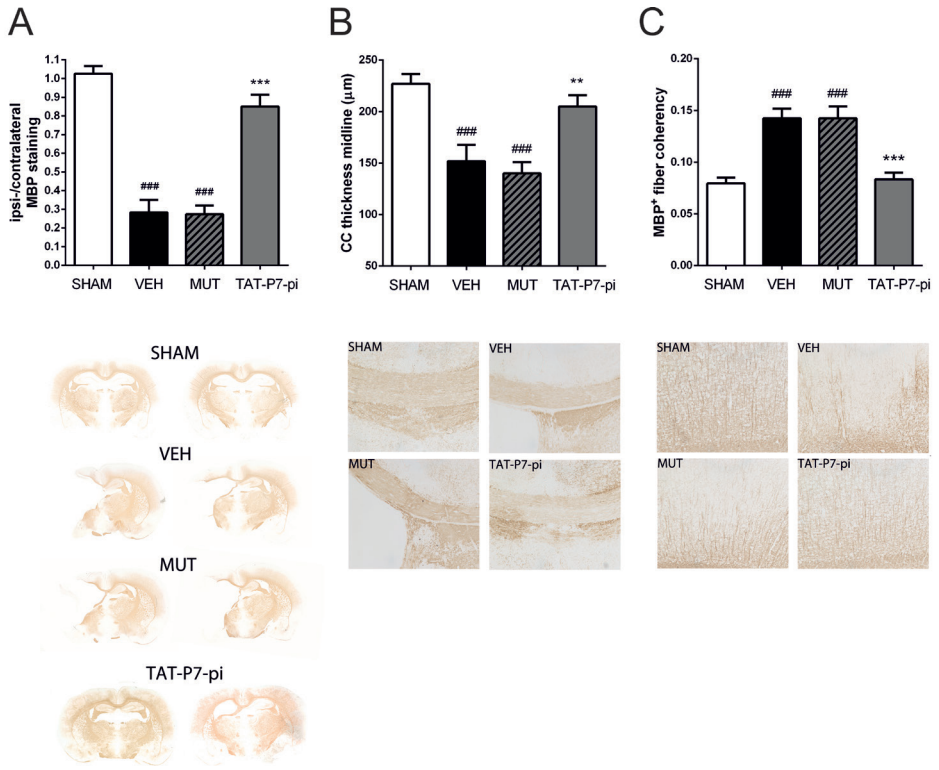

Figure 4: White matter damage, corpus callosum thickness and MBP$^+$ fiber coherency after HI and the effect of TAT-P7-pi treatment

Wistar rat pups were subjected to HI at postnatal day 7 and white matter damage was assessed by analyzing myelin-basic protein (MBP) staining on full brain sections at 9 weeks post-insult. Rats were treated intraperitoneally with vehicle (VEH), mutant peptide (MUT) or TAT-P7-pi (10 mg/kg) at 0 h post-insult and sham-operated littermates were used as controls. Brain sections were cut at app. -3.20 mm from bregma. **A**: Ratio ipsi-/contralateral MBP-positive area as a measure for HI-induced overall white matter damage in the ipsilateral hemisphere. Photographs show representative examples of all experimental groups. **B**: Thickness of the corpus callosum was measured in µm exactly at the midline of the brain on MBP-stained sections. Photographs show representative examples of all experimental groups. **C**: Fiber coherency of MBP-positive fibers was measured in the ipsilateral cingulum as a microstructural measure of white matter organization. An increased fiber coherency correlates to loss of lateral arborization of MBP-positive fibers. Photographs show representative examples of all experimental groups. **B-C**: Coronal brain inset shows areas of analysis: green square for corpus callosum thickness (**B**) and red square for cingulum (**C**). **A-C**: SHAM n=15, HI-VEH n=14, HI-MUT n=15, HI-TAT-P7-pi n=15. Data were analyzed by one-way ANOVA with Bonferroni post-tests. $^{###}p$ <0.001 vs sham-control; ** p <0.01, *** p <0.001 vs vehicle treatment.

To study the effects of TAT-P7-pi on ROS formation, we used a TBARS (*i.e.* malondialdehyde (MDA)) assay. MDA, which is generated during lipid peroxidation, is detected within the TBARS assay and used as an indirect measure of oxidative stress. A strong increase in TBARS/MDA levels was observed in the ipsilateral hemisphere of vehicle-treated HI rats at 3 h post-insult, indicative of cerebral ROS production early after HI (Fig 5B). TAT-P7-pi treatment almost

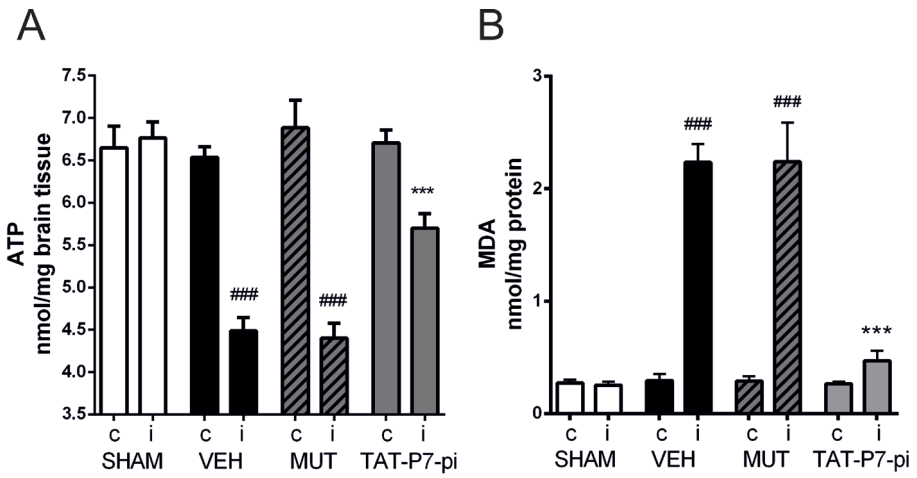

Fig 5: Effects of HI and TAT-P7-pi treatment on markers of mitochondrial integrity
Sham-operated rats and HI rats treated with vehicle (VEH) or TAT-P7-pi (10 mg/kg at 0 h) were euthanized at 3 h post-HI and levels of ATP (**A**) and MDA (**B**) were quantified in contra- (c) and ipsi- (i) lateral hemispheres. Treatment with mutant peptide (MUT) was used as a control. **A**: ATP levels were determined as a measure of mitochondrial respiration in deproteinized brain homogenates by using an ATP colorimetric assay. ATP levels are calculated as nmol/mg brain tissue. SHAM n=5, HI-VEH n=7, HI-MUT n=6, HI-TAT-P7-pi n=9. **B**: TBARS assay measuring MDA levels, a product of lipid peroxidation, in brain homogenates as a measure of oxidative stress. TBARS levels are calculated as nmol/mg protein. All groups n=5. **A-B**: Data were analyzed by one-way ANOVA with Bonferroni post-tests. ### p <0.001 vs sham-control, *** p <0.001 vs vehicle treatment.

completely abolished the HI-induced increase in TBARS/MDA levels (Fig 5B). Treatment with mutant peptide resulted in similar levels as vehicle treatment (Fig 5B). Contralateral TBARS/MDA levels in all HI experimental groups were equal to levels in sham-control littermates.

Next we determined whether the protective effects of TAT-P7-pi treatment could also be observed on markers of apoptotic cell death. Figure 6A shows that neonatal HI induced leakage of cytochrome *c* into the cytosol at 24 h post-insult in the ipsilateral hemisphere of vehicle- and mutant peptide-treated rat pups. A significant reduction of cytochrome *c* release was observed after treatment with TAT-P7-pi (Fig 6A). No cytochrome *c* release was detected in the contralateral hemisphere after HI when compared to sham-control levels (Fig 6A). In line with our observations on cytochrome *c* leakage, TAT-P7-pi treatment potently reduced the HI-induced ipsilateral levels of cleaved caspase 3 as observed in vehicle- and mutant peptide-treated rats at 24 h post-insult (Fig 6B). We did not observe significant caspase 3 cleavage in contralateral hemispheres of HI animals or in sham-controls.

Next we studied whether TAT-P7-pi treatment affected the levels of anti-apoptotic proteins at 24 h post-HI. As we have shown before, neonatal HI induced a significant reduction of mitochondrial Bcl-2 and Bcl-xL levels in the ipsilateral hemisphere after vehicle treatment (Fig 6C, D).[15,26] In clear contrast, after treatment with TAT-P7-pi levels of mitochondrial Bcl-xL were significantly restored in comparison to vehicle treatment. Levels of mitochondrial

Bcl-2 were even *increased* compared to levels in sham-operated rats (Fig 6C, D). Rat pups treated with mutant peptide showed similar reductions in mitochondrial Bcl-2 and Bcl-xL as littermates treated with vehicle (Fig 6C, D). Contralateral levels of Bcl-2 and Bcl-xL were equal to levels in sham-controls.

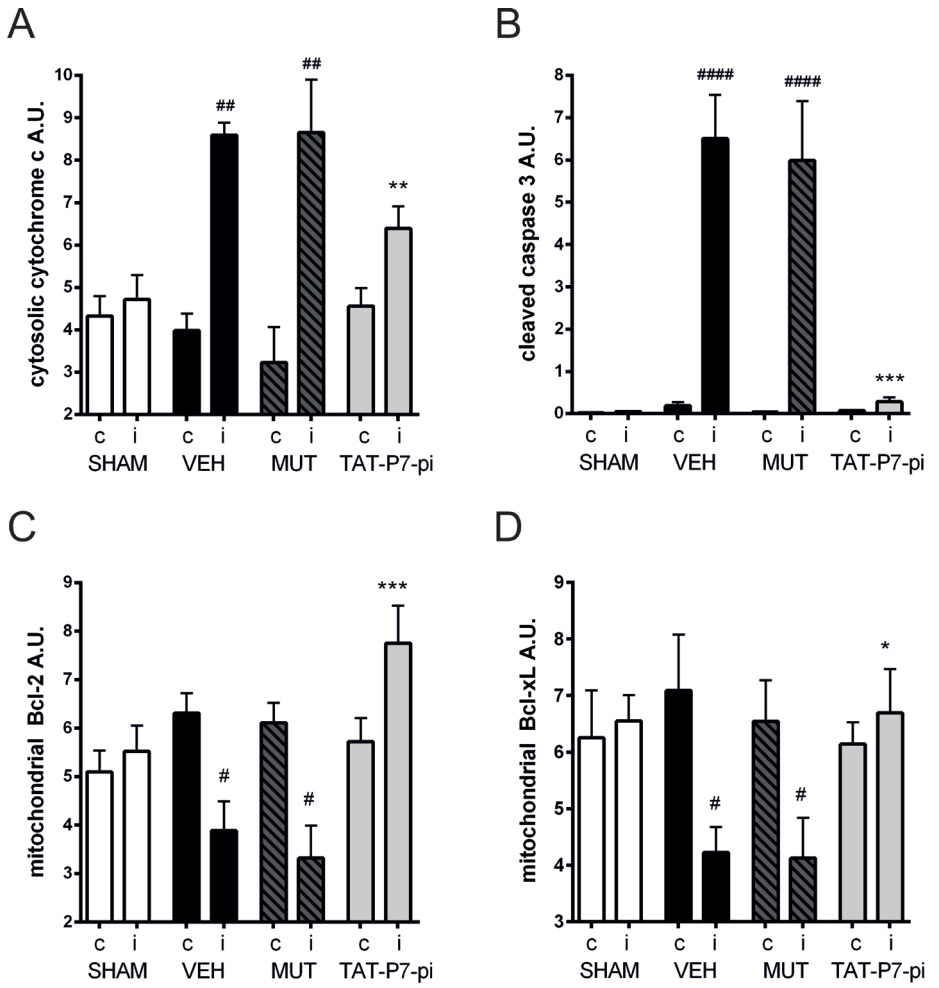

Fig 6: Effects of TAT-P7-pi treatment on pro- and anti-apoptotic proteins after HI
Seven-day-old Wistar rats were subjected to HI and treated intraperitoneally with vehicle (VEH), mutant peptide (MUT) or TAT-P7-pi (10 mg/kg) at 0 h post-insult. Sham-operated animals were used as controls. Protein levels of cytochrome (**A**) and cleaved caspase 3 (**B**) were quantified by Western Blot analysis in cytosolic fractions of contra- (c) and ipsi- (i) lateral hemispheres at 24 h post-HI. Protein levels of Bcl-2 (**C**) and Bcl-xL (**D**) were quantified by Western Blot analysis in mitochondrial fractions of both hemispheres at 24 h post-HI. **A-D**: SHAM n=5, HI-VEH n=7, HI-MUT n=6, HI-TAT-P7-pi n=9. Data were analyzed by one-way ANOVA with Bonferroni post-tests. $^{\#}p$ <0.05, $^{\#\#}p$ <0.01, $^{\#\#\#\#}p$ <0.0001 vs sham-control; * p <0.05, ** p <0.01, *** p <0.001 vs vehicle treatment. A.U.: arbitrary units.

Discussion

In the present study we show in neonatal rats that the inhibitor TAT-P7-pi is a very potent drug to reduce HI brain damage. We demonstrated that the most effective dose of 10 mg/kg reduced neuronal damage by more than 80% when treatment was started within 3 h after the insult. The neuroprotective effect of TAT-P7-pi was long-lasting as ipsilateral volume loss at 9 weeks after the insult was still decreased by 85%. These data indicate that treatment with TAT-P7-pi did not just postpone the onset of damage after HI but effectively prevented occurrence of cerebral tissue injury at an early stage which translated into long-term neuroprotection. Importantly, TAT-P7-pi treatment also improved functional outcome (motor and cognitive behavior) at 9 weeks after induction of HI in a robust way. The behavioral paradigms that we used are of clinical relevance, as children with HIE often develop motor and cognitive disabilities during childhood.[27,28] The assessment of functional outcome is important as it shows that brain areas and connections required for the functional assignments (*i.e.* motor and sensory cortical areas, hippocampus and corticospinal tracts) appear not only anatomically intact but are also functionally preserved. These data together indicate that TAT-P7-pi treatment does not just save neurons which are already damaged and/or that should have died, but preserves functionality of the spared tissue.

We explored in detail the effects of TAT-P7-pi treatment on white matter damage; besides the effect of the peptide on gross white matter injury measured by ipsilateral hemispheric loss of MBP staining, we also assessed white matter damage in areas that were relatively spared by HI like the corpus callosum and cingulum. Reduction of corpus callosum thickness is observed in children with HIE and is associated with impaired motor performance and cognitive development.[29-31] Moreover, corpus callosum thickness is strongly related to total cerebral white matter volume.[32] Also microstructural aberrations in the corpus callosum and cingulum are related to poorer neurodevelopmental outcome.[33] Furthermore, it is known that injury-induced changes to corpus callosum volume are associated with lateralization of motor behavior.[34,35] Our data show that HI rats clearly displayed laterization deficits as observed in the CRT and ART and showed a significant reduction of corpus callosum thickness. Also cognitive performance of the HI rats was clearly affected. Moreover, lateral arborization of MBP-positive fibers in the cingulum was significantly decreased. Treatment with TAT-P7-pi increased corpus callosum thickness and lateral arborization of fibers in the cingulum, together with improved motor and cognitive behavior. These data indicate that TAT-P7-pi treatment also protects against more subtle white matter injury outside the cystic lesion area with significant effects on neurodevelopmental outcome. Whether these protective observations on white matter damage are a direct effect of TAT-P7-pi on oligodendrocyte survival or whether the effects of white matter damage are indirectly caused by protective effects on neuronal tissue remains to be studied.

The tumor suppressor p53 and the MAP kinase JNK are both well-known for their nuclear roles either as a transcription factor (p53) or as the major activator of transcription factor AP-1 (JNK). Both p53 and AP-1 regulate transcription of numerous genes involved in apoptotic cell death, including several pro-apoptotic Bcl-2 family members.[36-39] In recent years, transcription-*independent* functions of p53 and JNK have been elucidated and both proteins have been discovered to also reside at the mitochondrial membrane where they directly regulate apoptosis *e.g.* via interaction with (p53) and phosphorylation of (JNK) pro- and anti-apoptotic Bcl-2 family members.[40-46] The importance of mitochondrial p53 and mitochondrial P-JNK for cerebral cell death after HI became apparent in our previous studies in which we specifically inhibited either mitochondrial translocation of p53 by PFT-μ or JNK activation at the mitochondria by the D-JNKi peptide or Sab_{KIM1} peptide.[14,15] These treatments showed very potent neuroprotective effects on HI brain damage in neonatal rats: i.p. treatment with PFT-μ or D-JNKi (or Sab_{KIM1}) reduced HI brain injury by >65-80%, neuroprotection was long-lasting (>9 weeks) and resulted in behavioral improvements. Inhibition of mitochondrial p53 or P-JNK was associated with a preservation of mitochondrial integrity as measured by an inhibition of HI-induced ROS production and a restoration of the HI-provoked drop in ATP levels. The protective effects on the mitochondria translated into a potent reduction of the apoptotic cascade in the brain after HI.[14,15] As both p53 and P-JNK seemed key regulators of mitochondrial integrity, we have determined whether phosphorylation of JNK was affected when p53 was inhibited by PFT-μ and *vice versa* whether mitochondrial p53 levels were affected by D-JNKi treatment. We have observed that inhibiting either mitochondrial p53 or mitochondrial P-JNK did not affect the level or activation of the other molecule at the mitochondrial membrane (unpublished data). As inhibiting either p53 or JNK phosphorylation at the mitochondrial membrane is sufficient to induce potent neuroprotection without affecting the other molecule, these data indicate that HI-induced apoptosis requires the presence of both P-JNK and p53 at the mitochondria. These data strengthen our hypothesis that p53 and P-JNK might interact, possibly at the mitochondrial membrane which might be key in setting of the apoptotic cascade after HI. Future studies are required to confirm whether p53-JNK interaction indeed takes place after HI in the neonatal brain, whether the interaction takes place at the mitochondrial membrane and whether the interaction is indeed blocked by TAT-P7-pi treatment. Anyway, an interaction between p53 and P-JNK after HI seems to have far-reaching consequences for the development of HI brain injury as the specific inhibition of this interaction by TAT-P7-pi leads to striking neuroprotective effects in the brain.

Ronai and co-workers were the first to propose an interaction between JNK and p53. These authors have shown in *in vitro* models that the P7 domain in p53 (amino acids 97-116) is required for binding of JNK and subsequent JNK-mediated phosphorylation of p53 at Thr81, which greatly enhances half-life of p53. Moreover, they have designed a peptide called the "P7 peptide" that mimics the P7 domain of p53 and thereby blocks off the interaction

between p53 and JNK.[16-18] The promising effects of the P7 peptide on reducing apoptotic cell death in these *in vitro* studies together with our previous *in vivo* results showing that both JNK and p53 reside at the mitochondrial membrane in the HI brain urged us to test the P7 peptide *in vivo*. To facilitate cellular uptake of the peptide in the brain we coupled the P7 sequence used in the *in vitro* studies to a HIV-TAT shuttle and designated the inhibitor as TAT-P7-pi. In the present study we use the TAT-P7 peptide for the first time *in vivo* and show that the interaction between p53-JNK, which was demonstrated before in cell-free systems and cultured cells, is indeed operative in the brain *in vivo*, although it remains to be investigated in which specific cell types of the brain. Two additional research groups have explored the interaction between p53 and JNK: Park et al. (2009) showed a role of JNK-mediated phosphorylation of p53 in autophagic cell death of HCT116 cells *in vitro* and Hong et al. (2012) showed that inhibition of JNK by SP600125 reduced phosphorylation of p53 and decreased autophagic cell death in an *in vivo* model of traumatic brain injury.[47,48]

Being one of the most important death genes, p53's half-life is very short, *i.e.* 5-30 min, under basal unstressed conditions.[49] Half-life and thereby cellular effects of p53 are very tightly regulated. Active p53 is subject to a wide array of post-translational modifications, including phosphorylation, acetylation, methylation, sumoylation, neddylation, poly-ADP ribosylation and (mono- and poly)-ubiquitylation.[50-52] Continuous (poly-)ubiquitylation of p53 by its negative regulator MDM2, an E3 ubiquitin ligase, maintains low levels of p53 in the cell under unstressed conditions as poly-ubiquitinated p53 is targeted to the 26S proteasome.[49,53] In contrast, phosphorylation and acetylation of p53 are generally involved in stabilization and accumulation of p53, mainly by conformational changes of p53. These changes in conformation can lead to suppression of p53's binding to MDM2 (and thereby suppression of ubiquitylation) which is a pivotal event in accumulation of p53 and prolonging p53's half-life from minutes to hours.[49,53] *In vitro* studies show that JNK-mediated phosphorylation of p53 at Thr81 is indeed involved in stabilization of p53.[16-18] Our data show that phosphorylation of p53 by JNK is extremely crucial in starting off the apoptotic cascade after cerebral HI, since using the specific inhibitor TAT-P7-pi induced >80% reduction of brain injury. At this moment the exact location of interaction between JNK and p53 remains to be discovered. It has been described that upon stress, mitochondrial translocation of p53 is dependent on a temporal dissociation of MDM2-p53 complexes.[41,54] We suggest that this dissociation of p53 and MDM2 could be regulated by JNK-mediated phosphorylation of p53. p53, which is mono-ubiquitinated under conditions where MDM2 is dissociated, can now translocate to the mitochondrial membrane where it is de-ubiquitylated by the protein HAUSP. Once de-ubiquitinated, p53 is apoptotically active and can form inhibitory complexes with Bcl-2 and Bcl-xL.[41,54] We have shown before that after HI, JNK is phosphorylated at the mitochondrial membrane and p53 is translocated to the mitochondrial membrane.[14,15] It seems likely that JNK may phosphorylate p53 at the mitochondrial membrane, thereby dissociating MDM2 from p53, leaving p53 ready to be de-ubiquitylated by HAUSP. However, there is evidence

that MDM2 is not escorting p53 to mitochondria, since neither MDM2 nor MDM2-p53 complexes are observed at the mitochondria in different cell lines *in vitro*.[54] As we did not observe active JNK in the cytosol or nucleus upon HI in our previous study,[15] we suggest that JNK phosphorylates p53 in close vicinity of the mitochondria, thereby releasing MDM2 into the cytosol and allowing p53 to reside at the mitochondrial membrane. It is unclear at this moment whether phosphorylation of p53 at Thr81 affects cellular translocation of p53, although in *in vitro* studies it does not seem to affect cytosolic or nuclear presence of p53.[18] In addition, effects of TAT-P7-pi on inhibition of p53-JNK interaction at other subcellular locations than mitochondria could also add to the neuroprotective effects observed.

Our data clearly show a prominent effect of TAT-P7-pi treatment on preservation of mitochondrial integrity early after HI (3 h post-insult). We and other have previously shown that mitochondrial injury is an early upstream process induced after cerebral ischemia that can be reflected by uncoupling of oxidative phosphorylation in the electron transport chain, reduction of mitochondrial membrane potential, formation of ROS, loss of ATP production and eventually MOMP leading to leakage of mitochondrial proteins, *e.g.* cytochrome *c*, into the cytosol and activation of the downstream caspase cascade.[55] The fact that TAT-P7-pi strongly prevented HI-induced ATP loss and lipid peroxidation as a measure of ROS production indicates that p53-JNK interaction occurs upstream of mitochondrial dysfunction and is a very early process after HI.
Induction of MOMP is a hallmark of mitochondria-regulated cell death and has been described as 'a point of no return' during cell death in the brain.[10-12] The anti-apoptotic members of the Bcl-2 family, *e.g.* Bcl-2 and Bcl-xL, are guardians of the outer mitochondrial membrane and act to prevent MOMP by binding pro-apoptotic members of the family.[56-58] It has been shown before that increasing the levels of Bcl-2 or Bcl-xL in the brain reduces injury after different ischemic insults.[59-64] Our present study shows that HI reduced mitochondrial Bcl-2 and Bcl-xL whereas neuroprotective treatment with TAT-P7-pi was associated with a restoration and even an increase in Bcl-2 and Bcl-xL levels at the mitochondria. These data underline the crucial role of upregulation of Bcl-2/xL for neuroprotection after HI as we have proposed earlier. Our previous studies showed that early neuroprotective effects on mitochondria could even be lost when the brain was unable to upregulate levels of Bcl-2/xL at 24 h post-insult, for instance when NF-κB or AP-1 were blocked for longer periods which did not allow transcriptional upregulation of Bcl-2/xL.[15,26] Our data indicate that TAT-P7-pi treatment did not interfere with upregulation of the levels of these crucial proteins.

At the mitochondrial membrane, p53 and JNK can regulate the pro/anti-apoptotic Bcl-2 family balance by directly binding to both pro- and anti-apoptotic Bcl-2 members thereby activating or antagonizing their function.[44-46,58,65-67] Our present study shows that besides the individual effects of p53 and JNK on the members of the Bcl-2 family, the direct interaction between JNK and p53 might have crucial effects on the pro/anti-apoptotic balance by enabling

the prolonged presence of p53 at the mitochondrial site of action. Notably, we observed a therapeutic window of TAT-P7-pi treatment of 6 h post-HI which is in line with our previous data showing that p53 was present at the mitochondria from 0.5-6 h after the insult.[14] Furthermore, this therapeutic window is in line with what we and others observed for several therapies aiming at inhibition of cerebral apoptosis after ischemia.[14,15,25,69,70] Interestingly, it has been described recently that besides having a crucial role in regulating apoptotic cell death, p53 is also involved in regulation of autophagy and necrotic cell death.[71-73] For instance, mitochondrial p53 is directly involved in opening of the mitochondrial permeability transition pore (PTP) by binding to cyclophilin D, a process important during necrotic cell death and the crosstalk between necrotic and apoptotic cell death.[72-77] In conclusion, removing active p53 from the mitochondrial picture by means of TAT-P7-pi treatment could therefore efficiently target multiple cell death routes, which are known to be operative in the brain after HI.[8] The data presented here indicate that JNK-mediated p53 phosphorylation contributes to the apoptotic cascade in the brain after neonatal HI. TAT-P7-pi may develop into a potent and specific therapeutic drug to protect the neonatal brain from HIE to obliterate facing a life-time of disability.

References

1. Volpe JJ. The encephalopathy of prematurity--brain injury and impaired brain development inextricably intertwined. *Semin Pediatr Neurol.* 2009;16:167-178.
2. Ferriero DM. Neonatal brain injury. *N Engl J Med.* 2004;351:1985-1995.
3. Bonifacio SL, Glass HC, Peloquin S, Ferriero DM. A new neurological focus in neonatal intensive care. *Nat Rev Neurol.* 2011;7:485-494.
4. Johnston MV, Fatemi A, Wilson MA, Northington F. Treatment advances in neonatal neuroprotection and neurointensive care. *Lancet Neurol*. 2011;10:372-382.
5. Gonzalez FF, Ferriero DM. Neuroprotection in the newborn infant. *Clin Perinatol*, 2009;36:859-80.
6. Thornton C, Rousset CI, Kichev A, et al. Molecular mechanisms of neonatal brain injury. *Neurol Res Int*. 2012:506320.
7. Fleiss B, Gressens P. Tertiary mechanisms of brain damage: a new hope for treatment of cerebral palsy? *Lancet Neurol*. 2012;11:556-566.
8. Northington FJ, Chavez-Valdez R, Martin LJ. Neuronal cell death in neonatal hypoxia-ischemia. *Ann Neurol*. 2011;69:743-758.
9. Hagberg H, Mallard C, Rousset CI, Thornton C. Mitochondria: hub of injury responses in the developing brain. *Lancet Neurol.* 2014;13:217-232.
10. Hagberg H, Mallard C, Rousset CI, Xiaoyang W. Apoptotic mechanisms in the immature brain: involvement of mitochondria. *J Child Neurol*. 2009;24:1141-1146.
11. Rousset CI, Baburamani AA, Thornton C, Hagberg H, Mitochondria and perinatal brain injury. *J Matern Fetal Neonatal Med*. 2012;25:35-8.
12. Cheng G, Kong RH, Zhang LM, Zhang JN. Mitochondria in traumatic brain injury and mitochondrial-targeted multipotential therapeutic strategies. *Br J Pharmacol*. 2012;167:699-719.
13. Czabotar PE, Lessene G, Strasser A, Adams JM. Control of apoptosis by the BCL-2 protein family: implications for physiology and therapy. *Nat Rev Mol Cell Biol*. 2014;15:49-63.
14. Nijboer CH, Heijnen CJ, van der Kooij, et al. Targeting the p53 pathway to protect the neonatal ischemic brain. *Ann Neurol*. 2011;70:255-264.
15. Nijboer CH, Bonestroo HJ, Zijlstra J, Kavelaars A, Heijnen CJ. Mitochondrial JNK phosphorylation as a novel therapeutic target to inhibit neuroinflammation and apoptosis after neonatal ischemic brain damage. *Neurobiol Dis*. 2013;54:432-44.
16. Adler V, Pincus MR, Minamoto T, et al. Conformation-dependent phosphorylation of p53. *Proc Natl Acad Sci USA.* 1997;94:1686-1691.
17. Fuchs SY, Adler V, Pincus MR, Ronai Z. MEKK1/JNK signaling stabilizes and activates p53. *Proc Natl Acad Sci USA*. 1998;95:10541-10546.
18. Buschmann T, Potapova O, Bar-Shira A, et al. Jun NH2-terminal kinase phosphorylation of p53 on Thr-81 is important for p53 stabilization and transcriptional activities in response to stress. *Mol Cell Biol*. 2001;21:2743-2754.
19. Nijboer CH, van der Kooij MA, van Bel F, Ohl F, Heijnen CJ, Kavelaars A. Inhibition of the JNK/AP-1 pathway reduces neuronal death and improves behavioral outcome after neonatal hypoxic-ischemic brain injury. *Brain Behav Immun*. 2010;24:812-821.
20. Rozas G, Guerra MJ, Labandeira-Garcia JL. An automated rotarod method for quantitative drug-free evaluation of overall motor deficits in rat models of parkinsonism. *Brain Res Brain Res*. 1997;2:75-84.
21. Schallert T, Fleming SM, Leasure JL, Tillerson JL, Bland ST. CNS plasticity and assessment of forelimb sensorimotor outcome in unilateral rat models of stroke, cortical ablation, parkinsonism and spinal cord injury. *Neuropharmacology*. 2000;39:777-787.

22. Grow JL, Liu YQ, Barks JD. Can lateralizing sensorimotor deficits be identified after neonatal cerebral hypoxia-ischemia in rats? *Dev Neurosci.* 2003;25:394-402.

23. Bevins RA, Besheer J. Object recognition in rats and mice: a one-trial non-matching-to-sample learning task to study 'recognition memory'. *Nat Protoc*. 2006;1:1306-1311.

24. Nijboer CH, Groenendaal F, Kavelaars A, Hagberg HH, van Bel F, Heijnen CJ. Gender-specific neuroprotection by 2-iminobiotin after hypoxia-ischemia in the neonatal rat via a nitric oxide independent pathway. *J Cereb Blood Flow Metab*. 2007;27:282-292.

25. Nijboer CH, Heijnen CJ, Groenendaal F, May MJ, van Bel F, Kavelaars A. Strong neuroprotection by inhibition of NF-kappaB after neonatal hypoxia-ischemia involves apoptotic mechanisms but is independent of cytokines. *Stroke*. 2008a;39:2129-2137.

26. Nijboer CH, Heijnen CJ, Groenendaal F, May MJ, van Bel F, Kavelaars A. A dual role of the NF-kappaB pathway in neonatal hypoxic-ischemic brain damage. *Stroke*. 2008a;39:2578-2586.

27. Perlman M, Shah PS. Hypoxic-ischemic encephalopathy: challenges in outcome and prediction. *J Pediatr*. 2011;158:e51-e54.

28. de Vries LS, Jongmans MJ. Long-term outcome after neonatal hypoxic-ischaemic encephalopathy. *Arch Dis Child Fetal Neonatal Ed*. 2010;95:F220-F224.

29. Iai M, Tanabe Y, Goto M, Sugita K, Niimi H. A comparative magnetic resonance imaging study of the corpus callosum in neurologically normal children and children with spastic diplegia. Acta *Paediatr*. 1994;83:1086-1090.

30. van Kooij BJ, Van HM, Uiterwaal CS, Groenendaal F, et al. Corpus callosum size in relation to motor performance in 9- to 10-year-old children with neonatal encephalopathy. *Pediatr Res.* 2008;63:103-108.

31. van Kooij BJ, van PC, Benders MJ, van H, I, de Vries LS, Groenendaal F. Fiber tracking at term displays gender differences regarding cognitive and motor outcome at 2 years of age in preterm infants. *Pediatr Res*. 2011;70:626-632.

32. Panigrahy A, Barnes PD, Robertson RL, Sleeper LA, Sayre JW. Quantitative analysis of the corpus callosum in children with cerebral palsy and developmental delay: correlation with cerebral white matter volume. *Pediatr Radiol.* 2005;35:1199-1207.

33. Counsell SJ, Edwards AD, Chew AT, et al. Specific relations between neurodevelopmental abilities and white matter microstructure in children born preterm. *Brain*. 2008;131:3201-3208.

34. van Velthoven CT, van de LY, Kavelaars A, et al. Mesenchymal stem cells restore cortical rewiring after neonatal ischemia in mice. *Ann Neurol*. 2012;71:785-796.

35. Filgueiras CC, Manhaes AC. Increased lateralization in rotational side preference in male mice rendered acallosal by prenatal gamma irradiation. *Behav Brain Res*. 2005;162:289-298.

36. Yu J, Zhang L. The transcriptional targets of p53 in apoptosis control. *Biochem Biophys Res Commun*. 2005;331:851-858.

37. Haupt S, Berger M, Goldberg Z, Haupt Y. Apoptosis - the p53 network. *J Cell Sci*. 2003;116:4077-4085.

38. Karin M, Gallagher E. From JNK to pay dirt: jun kinases, their biochemistry, physiology and clinical importance. *IUBMB Life*. 2005;57:283-295.

39. Ameyar M, Wisniewska M, Weitzman JB. A role for AP-1 in apoptosis: the case for and against. *Biochimie*. 2003;85:747-752.

40. Moll UM, Wolff S, Speidel D, Deppert W. Transcription-independent pro-apoptotic functions of p53. *Curr Opin Cell Biol*. 2005;17:631-636.

41. Vaseva AV, Moll UM. The mitochondrial p53 pathway. *Biochim Biophys Acta*. 2009;1787:414-420.

42. Hagn F, Klein C, Demmer O, et al. BclxL changes conformation upon binding to wild-type but not mutant p53 DNA binding domain. *J Biol Chem*. 2010;285:3439-3450.

43. Dhanasekaran DN, Reddy EP. JNK signaling in apoptosis. *Oncogene*. 2008;27:6245-6251.

44. Yamamoto K, Ichijo H, Korsmeyer SJ. BCL-2 is phosphorylated and inactivated by an ASK1/Jun N-terminal protein kinase pathway normally activated at G(2)/M. *Mol Cell Biol*. 1999;19:8469-8478.
45. Fan M, Goodwin M, Vu T, Brantley-Finley C, Gaarde WA, Chambers TC. Vinblastine-induced phosphorylation of Bcl-2 and Bcl-XL is mediated by JNK and occurs in parallel with inactivation of the Raf-1/MEK/ERK cascade. *J Biol Chem*. 2000;275:29980-29985.
46. Chambers JW, Cherry L, Laughlin JD, Figuera-Losada M, Lograsso PV. Selective inhibition of mitochondrial JNK signaling achieved using peptide mimicry of the Sab kinase interacting motif-1 (KIM1). *ACS Chem Biol*. 2011;6:808-818.
47. Park KJ, Lee SH, Lee CH, et al. Upregulation of Beclin-1 expression and phosphorylation of Bcl-2 and p53 are involved in the JNK-mediated autophagic cell death. *Biochem Biophys Res Commun*. 2009;382:726-729.
48. Hong MY, Gao JL, Cui JZ, et al. Effect of c-Jun NH(2)-terminal kinase-mediated p53 expression on neuron autophagy following traumatic brain injury in rats. *Chin Med J (Engl)* 2012;125:2019-2024.
49. Moll UM, Petrenko O. The MDM2-p53 interaction. *Mol Cancer Res*. 2003;1:1001-1008.
50. Dotto GP. Crosstalk of Notch with p53 and p63 in cancer growth control. *Nat Rev Cancer*. 2009;9:587-595.
51. Bode AM, Dong Z. Post-translational modification of p53 in tumorigenesis. *Nat Rev Cancer.* 2004;4:793-805.
52. Gu B, Zhu WG. Surf the post-translational modification network of p53 regulation. *Int J Biol Sci*. 2012;8:672-684.
53. Chene P. Inhibiting the p53-MDM2 interaction: an important target for cancer therapy. *Nat Rev Cancer*. 2003;3:102-109.
54. Marchenko ND, Moll UM. The role of ubiquitination in the direct mitochondrial death program of p53. *Cell Cycle*. 2007;6:1718-1723.
55. Kroemer G, Galluzzi L, Brenner C. Mitochondrial membrane permeabilization in cell death. *Physiol Rev*. 2007;87:99-163.
56. Lindsay J, Esposti MD, Gilmore AP. Bcl-2 proteins and mitochondria--specificity in membrane targeting for death. *Biochim Biophys Acta*. 2011;1813:532-539.
57. Shamas-Din A, Brahmbhatt H, Leber B, Andrews DW. BH3-only proteins: Orchestrators of apoptosis. *Biochim Biophys Acta*. 2011;1813:508-520.
58. Speidel D. Transcription-independent p53 apoptosis: an alternative route to death. *Trends Cell Biol*. 2011;20:14-24.
59. Doeppner TR, El AM, Dietz GP, Weise J, Schwarting S, Bahr M. Transplantation of TAT-Bcl-xL-transduced neural precursor cells: long-term neuroprotection after stroke. *Neurobiol Dis*. 2010;40:265-276.
60. Wang F, Jiang Y, Zhang S, Xiao W, Zhu S. Protective effects of overexpression of bcl-xl gene on local cerebral infarction in transgenic mice undergoing permanent occlusion of middle cerebral artery. *J Huazhong Univ Sci Technolog Med Sci*. 2008;28:56-59.
61. Yin W, Cao G, Johnnides MJ, et al. TAT-mediated delivery of Bcl-xL protein is neuroprotective against neonatal hypoxic-ischemic brain injury via inhibition of caspases and AIF. *Neurobiol Dis*. 2006;21:358-371.
62. Kilic E, Dietz GP, Hermann DM, Bahr M. Intravenous TAT-Bcl-Xl is protective after middle cerebral artery occlusion in mice. *Ann Neurol*. 2002;52:617-622.
63. Wong LF, Ralph GS, Walmsley LE, et al. Lentiviral-mediated delivery of Bcl-2 or GDNF protects against excitotoxicity in the rat hippocampus. *Mol Ther*. 2005;11:89-95.
64. Lawrence MS, McLaughlin JR, Sun GH, et al. Herpes simplex viral vectors expressing Bcl-2 are neuroprotective when delivered after a stroke. *J Cereb Blood Flow Metab*. 1997;17:740-744.

65. Lindenboim L, Borner C, Stein R. Nuclear proteins acting on mitochondria. *Biochim Biophys Acta*. 2011;1813:584-596.

66. Wang XT, Pei DS, Xu J, et al. Opposing effects of Bad phosphorylation at two distinct sites by Akt1 and JNK1/2 on ischemic brain injury. *Cell Signal*. 2007;19:1844-1856.

67. Han JY, Jeong EY, Kim YS, et al. C-jun N-terminal kinase regulates the interaction between 14-3-3 and Bad in ethanol-induced cell death. *J Neurosci Res*. 2008;86:3221-3229.

68. Chauvier D, et al. Targeting neonatal ischemic brain injury with a pentapeptide-based irreversible caspase inhibitor. *Cell Death Dis*. 2011;2: 203.

69. Park WS, Sung DK, Kang S, et al. Therapeutic window for cycloheximide treatment after hypoxic-ischemic brain injury in neonatal rats. *J Korean Med Sci.* 2006;21:490-494.

70. Qu Y, Wu J, Chen D, et al. MiR-139-5p inhibits HGTD-P and regulates neuronal apoptosis induced by hypoxia-ischemia in neonatal rats. *Neurobiol Dis*. 2014;63:184-93.

71. Maiuri MC, Galluzzi L, Morselli E, Kepp O, Malik SA, Kroemer G. Autophagy regulation by p53. *Curr Opin Cell Biol*. 2010;22:181-185.

72. Vaseva AV, Marchenko ND, Ji K, Tsirka SE, Holzmann S, Moll UM. p53 opens the mitochondrial permeability transition pore to trigger necrosis. *Cell*. 2012;149:1536-1548.

73. Wang DB, Kinoshita C, Kinoshita Y, Morrison RS. p53 and mitochondrial function in neurons. *Biochim Biophys Acta*. 2014;1842:1186-1197.

74. Galluzzi L, Morselli E, Kepp O, Kroemer G. Targeting post-mitochondrial effectors of apoptosis for neuroprotection. *Biochim Biophys Acta*. 2009;1787:402-413.

75. Kinnally KW, Peixoto PM, Ryu SY, Dejean LM. Is mPTP the gatekeeper for necrosis, apoptosis, or both? *Biochim Biophys Acta*. 2011;1813:616-622.

76. Kroemer G. The mitochondrial permeability transition pore complex as a pharmacological target. An introduction. *Curr Med Chem*. 2003;10:1469-1472.

77. Leung AW, Halestrap AP. Recent progress in elucidating the molecular mechanism of the mitochondrial permeability transition pore. *Biochim Biophys Acta*. 2008;1777:946-952.

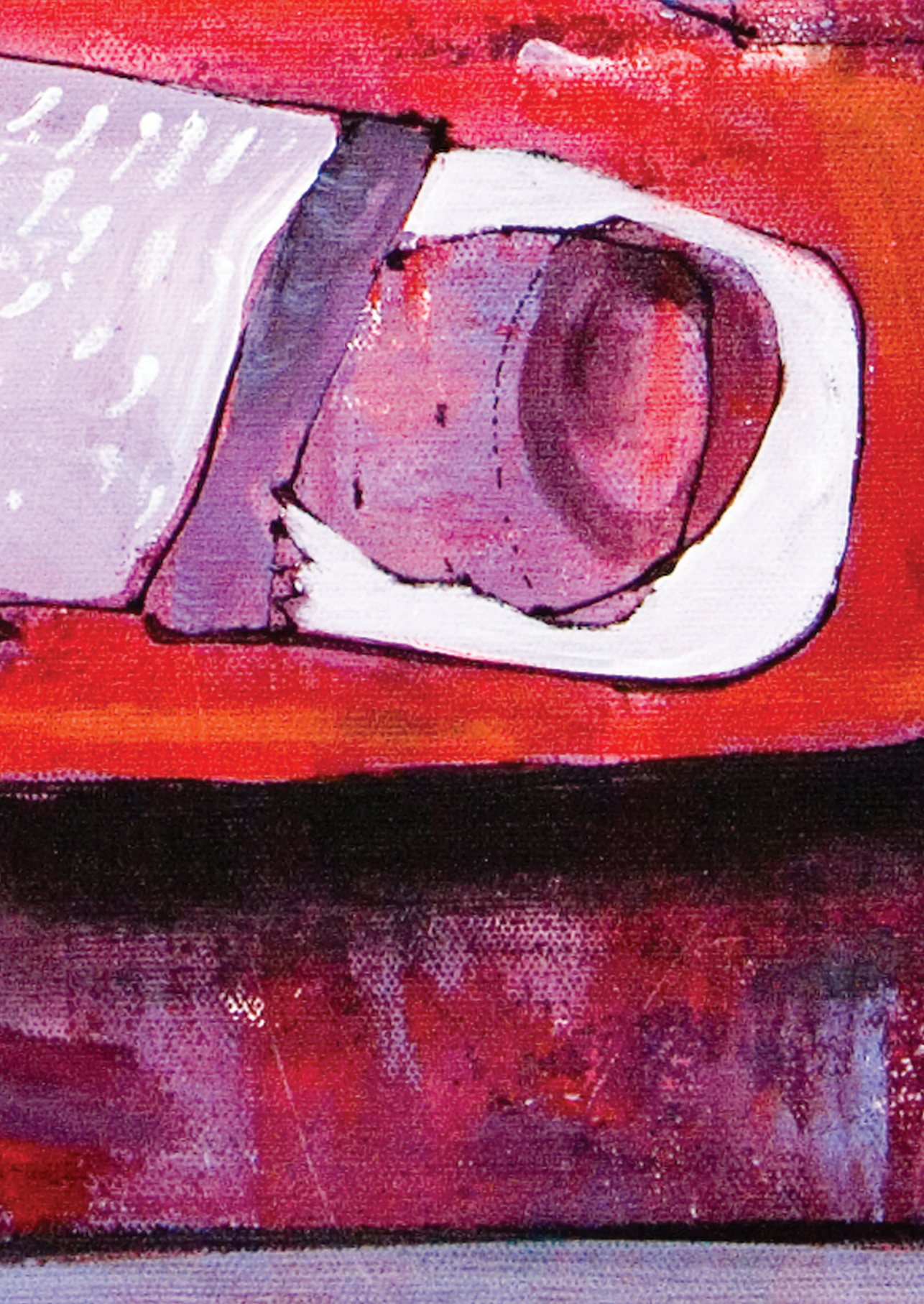

5

Development of cerebral gray and white matter injury and cerebral inflammation over time after inflammatory perinatal asphyxia

Hilde J.C. Bonestroo
Cobi J. Heijnen
Floris Groenendaal
Frank van Bel
Cora H. Nijboer

Developmental Neuroscience **accepted for publication.**

Abstract

Antenatal inflammation is associated with increased severity of hypoxic-ischemic (HI) encephalopathy and adverse outcome in human neonates and experimental rodents. Here, we investigated the effect of lipopolysaccharide (LPS) on the timing of HI-induced cerebral tissue loss and gray matter injury, white matter injury and integrity, and the cerebral inflammatory response.

Postnatal-day-9 mice underwent HI by unilateral carotid artery occlusion followed by systemic hypoxia which resulted in early neuronal damage (MAP2 loss) at 3 h that did not increase up to day 15. LPS injection 14 h before HI (LPS+HI) significantly and gradually aggravated MAP2 loss from 3 h up to day 15, resulting in an a-cellular cystic lesion. LPS+HI increased white matter damage, reduced myelination in the corpus callosum and increased white matter fiber coherency in the cingulum. The number of oligodendrocytes throughout the lineage (Olig2-positive) was increased whereas more mature myelinating (CNPase-positive) oligodendrocytes were strongly decreased after LPS+HI. LPS+HI induced an increased and prolonged expression of cerebral cytokines/chemokines compared to HI. Additionally, LPS+HI increased macrophage/microglia activation and influx of neutrophils in the brain compared to HI.

This study demonstrates the sensitizing effect of LPS on neonatal HI brain injury for an extended time-frame up to 15 days post-insult. LPS before HI induced a gradual increase in gray and white matter deficits including reduced numbers of mature myelinating oligodendrocytes and a decrease in white matter integrity. Moreover, LPS+HI prolonged and intensified the cerebral inflammatory response, including cellular infiltration. In conclusion, as timing of damage and/or involved pathways are changed when HI is preceded by inflammation, experimental therapies might require modifications in time window, dosage or combinations of therapies for efficacious neuroprotection.

Introduction

Neonatal encephalopathy due to perinatal asphyxia continues to be an important cause of mortality and morbidity in the human neonate. Perinatal brain injury often results in severe and long-lasting disabilities, like motor deficits, seizures, severe cognitive, psychological and behavioral problems which represent an enormous burden for the child, its parents and society.[1-3] Importantly, the risk of developing neonatal encephalopathy is strongly increased after maternal intrapartum fever or other antenatal inflammatory conditions like chorioamnionitis.[4-7] Moreover, it is known that exposure of the fetal brain to a pro-inflammatory environment *in utero* is negatively influencing clinical outcome after asphyxia, including an increased risk of development of spastic cerebral palsy.[8-11] In an attempt to mirror this clinical situation, several animal models have been developed over the past decade. Most of these models use lipopolysaccharide (LPS), a structural component of most gram-negative bacteria that binds to Toll-like receptor 4 (TLR4), as the inflammatory stimulus.[12] To investigate the consequences of a pro-inflammatory environment in the neonatal brain, administration of LPS to the pregnant mother (either systemically or locally in the uterus) or direct administration of LPS to the newborn rodent (systemically or locally in the brain) have been tested.[13] With respect to studies on neonatal brain damage, LPS is often combined with hypoxia-ischemia (HI), the latter first described by Rice and Vannucci.[14] The contribution of inflammation to HI brain damage is complex and conflicting results have been obtained when exploring dose and time frame of LPS application before inducing HI. The general view is that inflammation before HI sensitizes the brain and thereby aggravates HI cerebral injury. However, the exact mechanisms underlying pro-inflammatory sensitization are still unclear.[15-21] To date the exact timing of the sensitizing effect of LPS on the intensity of cerebral gray and white matter injury and the formation of an a-cellular cyst after HI have not been investigated in detail. Moreover, most studies only used loss of MBP staining as a marker for white matter injury, whereas the effect of pro-inflammatory environment in the context of HI on white matter integrity and on differentiation of oligodendrocytes remains largely unknown. In addition, it is of great importance to know the effect of combined exposure to LPS and HI on the degree, timing and duration of the cerebral inflammatory response, including the induction of pro-inflammatory or anti-inflammatory cytokines/chemokines, activation of microglia and influx of neutrophils and macrophages into the cerebral parenchyma. Closely mapping the development of injury and the cerebral inflammatory response in the LPS+HI model, that mimics the clinical situation in near-term neonates, is an essential step to allow exploring of future therapeutic strategies for the neonate who faces perinatal asphyxia combined with a pro-inflammatory state.

The data within this paper show the precise timing of development of cerebral tissue loss, gray and white matter damage and integrity in response to LPS+HI over a time window of 3 h up to day (D)15 post-insult. In parallel we determined the effect of LPS+HI on total and mature numbers of oligodendrocytes as well as on the cerebral inflammatory response and infiltration of inflammatory cells into the brain in the first 3 days post-insult.

Materials and Methods

Animals

All experiments were performed according to international guidelines and approved by the local experimental animal committee of the University Medical Center Utrecht (DEC-ABC, Utrecht). Postnatal day 9 (P9) C57Bl/6 mice pups were anaesthetized with isoflurane (4% induction, 2% maintenance), the right common carotid artery was occluded by thermo-cauterization, xylocaine (100mg/ml, AstraZeneca, Zoetermeer, the Netherlands) was applied and incision was closed. After minimal 1 h recovery, pups were exposed to 10% O_2 in N_2 for 45 min and returned to their dams. Sham-control animals underwent anesthesia and incision only. LPS+HI or LPS+sham-control animals received an intraperitoneal (i.p.) injection of lipopolysaccharide (LPS; List biological laboratories, Campbell, CA) at a dose of 0.5 mg/kg 14 h before surgery. Pups of both genders were used. Importantly, we did not observe any significant gender differences in any of the measured parameters. The experimental procedure resulted in a mortality rate of 8.4%, there was no difference in mortality rate between LPS+HI and HI animals. Mortality occurred during the experimental procedure. None of the animals died during follow-up.

For immunohistochemistry, animals were sacrificed by pentobarbital overdose at 3 h or D1, 2, 3, 4, 5, 10 or 15 after the insult followed by transcardial perfusion with 4% paraformaldehyde in phosphate buffered saline (PBS). Brains were post-fixed and embedded in paraffin. For quantitative real time reverse transcriptase PCR analysis, animals were sacrificed by decapitation directly before HI or at 3 h, D1, 2, 3 post-insult. Contra- and ipsilateral brain hemispheres were collected and stored at -80 °C.

Histology

We cut coronal paraffin brain sections (8 µm) at hippocampal and striatal level (equivalent to -1.28 and +0.38 mm from bregma in adult mice). Deparaffinized sections were stained with hematoxylin-eosin (HE; Klinipath, Duiven, the Netherlands) or incubated with mouse anti-microtubule-associated protein 2 (MAP2; Sigma-Aldrich, Steinheim, Germany), mouse anti-myelin basic protein (MBP; Sternberger Monoclonals Incorporated, Lutherville, MD) or rabbit anti-polymorphonuclear neutrophil (PMN; Accurate Antibodies, Westbury, NY) antibodies followed by biotinylated horse anti-mouse or goat anti-rabbit (both Vector Laboratories, Burlingame, CA) antibodies. Visualization was performed using Vectastain ABC kit (Vector Laboratories) and diaminobenzamidine. For HE, MAP2 and MBP staining full-section images were captured with a Nikon D1 digital camera (Nikon, Tokyo, Japan). For HE and MAP2 the brain areas were outlined manually using image processing tools in Adobe Photoshop CS5 (Adobe Systems Inc., San Jose, CA). For quantification of MBP loss, image processing tools in ImageJ software (Rasband WS, Image J, US National Institutes of Health, Bethesda, MD; http://rsb.info.nih.gov/ij/) were used, in which the MBP-positive staining was converted to a binary signal and positive pixels were measured. Ipsilateral area loss was calculated as 1-(area ipsilateral staining/area contralateral staining) x 100%. For analysis of MBP stained

corpus callosum thickness, photographs were taken with a Zeiss Axio Lab A1 microscope and Icc5 camera and analyzed using ZEN2012 software (both Carl Zeiss, Oberkochen, Germany). MBP-positive fiber coherency was analyzed using the OrientationJ plugin for ImageJ (http://bigwww.epfl.ch/demo/orientation/). The fiber coherency was used as a measurement of (dis) organization of MBP positive fibers in the cortex. A higher fiber coherency indicates a more linear MBP positive pattern resulting from a decrease in lateral arborization. PMN staining was quantified by counting area density of positive cells in the ipsilateral hemisphere by a scientist blinded to the experimental conditions.

For immunofluorescent staining, sections were incubated with rabbit anti-oligodendrocyte lineage transcription factor 2 (Olig2; Millipore, Billerica, MA), mouse anti-2'-3'-cyclic nucleotide 3'-phosphodiesterase (CNPase; Abcam, Cambridge, UK) or rabbit anti-ionized calcium binding adapter molecule 1 (Iba-1; Wako Chemicals, Richmond, VA) followed by Alexa Fluor 488-conjugated secondary antibody (Molecular Probes, Eugene, OR). Sections were counterstained with 4',6-diamidino-2-phenylindole (DAPI; Sigma-Aldrich) and embedded using Fluorsave (Calbiochem, Darmstadt, Germany). Fluorescent images were obtained using a Zeiss Axio Observer inverted microscope (Carl Zeiss) and were processed using ImageJ software. Images were analyzed by an observer blinded to the experimental conditions. For Olig2 and CNPase staining 3 microscopic fields were analyzed per infarcted cortex and 5 microscopic fields per corpus callosum and cingulum area at striatal level. The number of Olig2 cells was analyzed using the particle analysis nucleus counter plugin for ImageJ software. Data represent mean value of number of Olig2-positive cells in 3-5 microscopic fields per mm^2. For CNPase staining, mean area of CNPase positive pixels were measured per mm^2 using ImageJ software (threshold, histogram). For Iba-1 staining 6 microscopic fields were analyzed per cortical and hippocampal area and mean area of positive pixels were measured per mm^2 using ImageJ software (threshold, histogram). For CNPase and Iba-1 all images were analyzed with similar threshold per staining.

Quantitative real time reverse transcriptase PCR

Total RNA was isolated from brain samples by using TRIzol® (Invitrogen, Paisley, UK) according to the manufacturer's protocol. cDNA was synthesized with SuperScript Reverse Transcriptase (Invitrogen). PCR was performed using the iQ5 Real-Time PCR Detection System (Bio-Rad Laboratories, Veenendaal, the Netherlands) for TNF-α, IL-1β, IL-6, TGF-β, IL-10, MCP-1 and CINC-1 (for primer sequences, see Table 1). To confirm appropriate amplification, the size of PCR products was verified on gel. Data were individually normalized to the mean of the relative expression of GAPDH and β-actin (for primer sequences, see Table 1).

Statistical analysis

All analyses were performed in a blinded setup. Statistical analyses were performed using SPSS (version 20.0) and GraphPad Prism 5 (GraphPad Software, La Jolla, CA) software. All data are expressed as mean ± SEM and were analyzed by one- or two-way ANOVA with Bonferroni post-tests. $p < 0.05$ was considered statistically significant.

Table 1: Primer sequences used for quantitative real-time reverse transcriptase PCR to measure cytokine/chemokine mRNA expression.

Marker	Forward primer	Reverse primer
GAPDH	TGAAGCAGGCATCTGAGGG	CGAAGGTGGAAGAGTGGGAG
β-Actin	GATGCACAGTAGGTCTAAGTGGAG	CACTCAGGGCAGGTGAAACT
TNF-α	GCGGTGCCTATGTCTCAG	GCCATTTGGGAACTTCTCATC
IL-1β	CAACCAACAAGTGATATTCTCCATG	GATCCACACTCTCCAGCTGCA
IL-6	TCTAATTCATATCTTCAACCAAGAGG	TGGTCCTTAGCCACTCCTTC
TGF-β	GTGACAGCAAAGATAACAAAC	CTGAAGCAATAGTTGGTATCC
IL-10	GCACCCACTTCCCAGTCG	GCATTAAGGAGTCGGTTAGCAG
MCP-1	GGTCCCTGTCATGCTTCTG	CATCTTGCTGGTGAATGAGTAG
CINC-1	AAAAGGTGTCCCCAAGTAACG	GTCAGAAGCCAGCGTTCAC

Results

Cerebral gray matter injury

HI brain damage was induced in P9 mouse pups by unilateral occlusion of the right carotid artery and 45 min of systemic hypoxia (designated as the "HI" group). To investigate the additional effect of a systemic inflammation on HI-induced brain damage, animals in the "LPS+HI" group received an i.p. injection of LPS at a dose of 0.5 mg/kg 14 h before the HI insult. Mice were terminated on several time points after HI, *i.e.* 3 h until D15 to observe the timing of development of brain injury over time after HI or LPS+HI (Fig 1).

First we determined the effect of HI and LPS+HI on cerebral volume loss and possible cyst formation by using HE staining. During the first 2 days after induction of HI, no clear volume loss of the ipsilateral hemisphere was observed in the HI or LPS+HI groups (Fig1A, C). Starting at D3, HI alone caused a small reduction in ipsilateral cortical volume with disintegration of the hippocampal architecture without formation of a cyst (*i.e.* complete loss of tissue/an a-cellular lesion) (Fig1C). No significant increase in ipsilateral volume loss was observed in HI animals between D3 and D15 and consistent with this finding, none of the HI-mice displayed cyst formation (Fig1A, C).

Figure 1: Development of HI-induced cerebral volume loss and neuronal damage at different time points after HI or LPS+HI. ➔

Mouse pups were subjected to HI at P9 (HI). Sham-operated littermates (Sham) were used as controls. Animals received an i.p. LPS injection 14 h before the HI insult or sham-operation (LPS+HI or LPS respectively). **A**: Cerebral tissue loss was measured by analyzing loss of hematoxylin-eosin (HE) staining in the ipsilateral hemisphere from 3 h up to D15 post-insult. Two-way ANOVA: $F_{(2,114)}$= 182.1, p <0.001, time effect $F_{(7,114)}$= 39.1, p <0.001; interaction $F_{(14,114)}$= 15.9, p <0.001. **B:** Neuronal damage in the ipsilateral hemisphere was assessed by measuring loss of microtubule-associated-protein 2 (MAP2) staining at hippocampal level at the indicated time points post-insult. Two-way ANOVA: $F_{(2,120)}$= 160.5, p <0.001. No significant time effect or interaction. **C**: Representative examples of HE and MAP2 staining at hippocampal level in brains of sham-operated, HI and LPS+HI animals at the indicated time points after the insult. **D**: Representative examples of HE and MAP2 staining at hippocampal level in brains of sham-operated and LPS+sham-operated animals at 6 days after injection *i.e.* P14. Sham n=5-8, HI n=6-8, LPS+HI n=6-7 per time point. Data are expressed as mean ± SEM. Data were analyzed using two-way ANOVA with Bonferroni post-tests. ** p <0.01, *** p <0.001: LPS+HI vs HI. # p <0.05, ## p <0.01, ### p <0.001: HI vs sham.

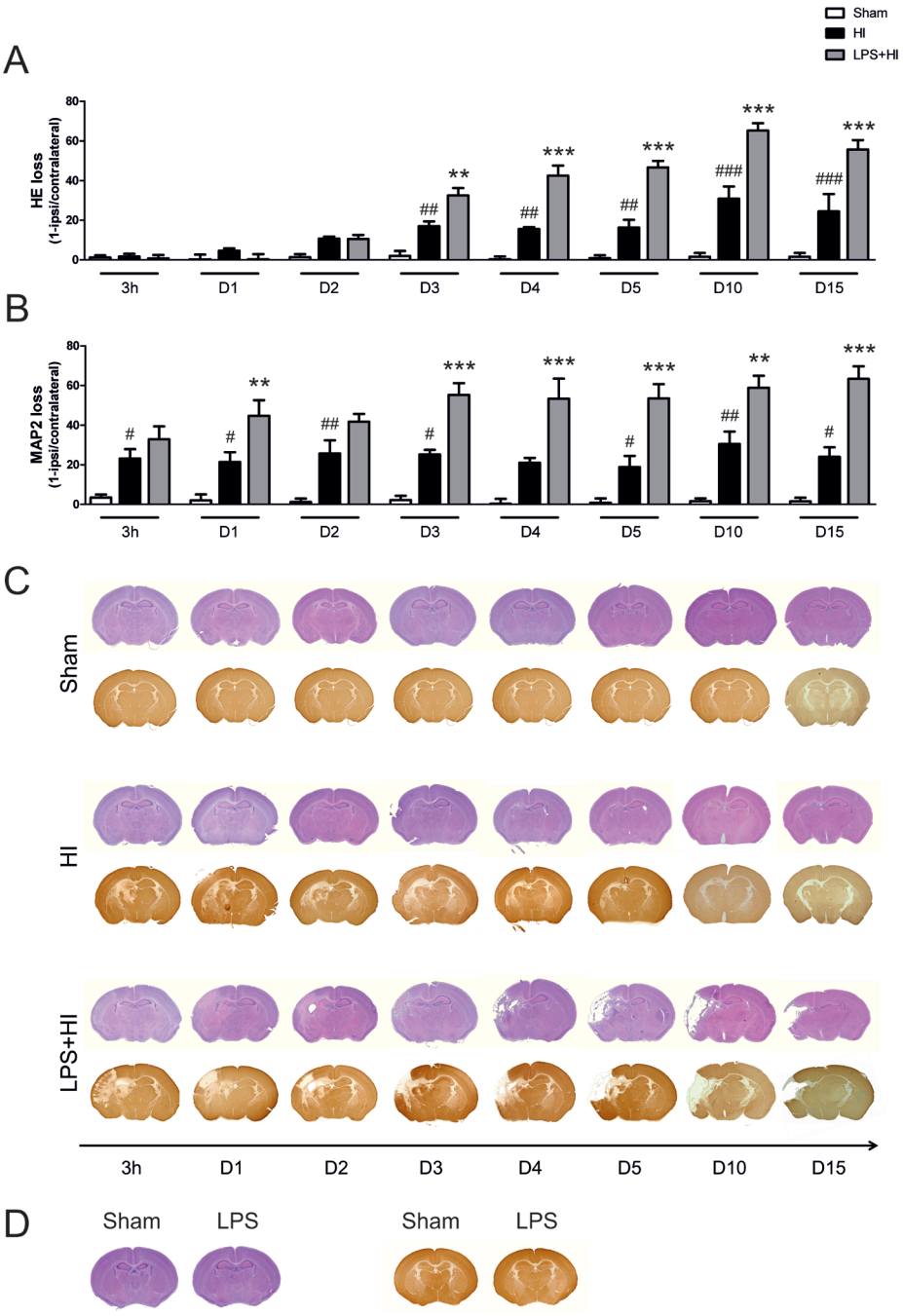
A
Sham
HI
LPS+HI
HE loss
(1-ipsi/contralateral)
80
60
40
20
0
3h
D1
D2
D3
D4
D5
D10
D15
B
MAP2 loss
(1-ipsi/contralateral)
C
Sham
HI
LPS+HI
D
Sham
LPS
Sham
LPS

When HI was preceded by LPS however, a significant increase in ipsilateral volume loss was observed compared to HI littermates starting at D3 post-insult (32.4 ± 3.8% ipsilateral volume loss in LPS+HI mice vs 17.0 ± 2.4% in HI animals) (p <0.01) (Fig 1A, C). After LPS+HI, macroscopically visible cystic lesions developed from D4 onwards, located in the hippocampal and cortical area. Moreover, the amount of ipsilateral volume loss significantly increased over time in LPS+HI vs HI mice; 42.5 ± 5.0% vs 15.5 ± 1.0% at D4, 46.6 ± 3.3% vs 16.3 ± 3.9% at D5, 65.2 ± 3.7% vs 30.8 ± 6.1% at D10 up to 55.7 ± 4.8% vs 24.5 ± 8.7% at D15 (p <0.001 for all time points) (Fig 1A, C). Importantly, no changes in volume loss were observed in the contralateral hemisphere of HI or LPS+HI animals compared to sham-control littermates.

To determine the specific development of gray matter injury after HI and LPS+HI, a MAP2 staining was performed. At 3 h post-insult, HI resulted in ipsilateral MAP2 loss of 23.1 ± 4.7% which was limited to the hippocampal area (Fig 1B, C). Interestingly, no further loss of MAP2 staining was detectable from 3 h until D15 after HI (Fig 1B, C). LPS injection before HI resulted in a significant increase in MAP2 loss, which was located in the ipsilateral hippocampus, cortex and striatum (Fig 1B, C). Enhanced MAP2 loss after LPS+HI was already present as early as D1 post-insult (44.7± 7.9% vs 21.3 ± 5.0%, LPS+HI vs HI) (p <0.01) and showed a gradual increase over time up to 63.3 ± 6.4% vs 24.0 ± 4.8% MAP2 loss at D15 in LPS+HI vs HI animals (p <0.001). Anesthesia and incision only did not result in neuronal damage since we did not observe any MAP2 loss in sham-control animals at any of the measured time points. Importantly, LPS injection alone without HI did not induce any HE or MAP2 loss at D6 after injection compared to sham-operated littermates (Fig 1D).

Cerebral white matter injury

In the first postnatal week of rodent brain development, myelination of the brain is hardly detectable. We first determined at which postnatal day MBP expression was high enough to reliably study effects of HI and LPS+HI on MBP loss as a measure of white matter damage (Fig 2A). To this end we quantitatively measured MBP expression over time in both hemispheres of sham-control animals. Figure 2A shows that MBP expression in the mouse brain was very low until P11. From P12-24, MBP expression gradually increased (Fig 2A). The effects of HI and LPS+HI on MBP loss were therefore measured from D3 (P12) up to D15 (P24) post-insult. HI resulted in stable white matter damage from D3 to D15: *i.e.* we measured 41.9 ± 12.2% ipsilateral MBP loss at D3 without any further increase up to D15 (Fig 2B, C). After combined exposure to LPS+HI, ipsilateral MBP loss was significantly increased compared 69.0 ± 2.7% following LPS+HI vs 41.9 ± 12.2% after HI at D3 post-insult (p <0.05) (Fig 2B, C). Interestingly, also in the LPS+HI group the loss of MBP staining remained constant over the period of D3-D15 (Fig 2B, C). No MBP loss was observed in sham-control littermates or in the contralateral hemisphere of HI or LPS+HI animals. Importantly, LPS injection alone without HI did not induce any MBP loss either at D6 after injection compared to sham-operated littermates (Fig 2D).

Next, we studied the effects of HI and LPS+HI on white matter integrity. It is known that HI can induce changes in corpus callosum volume which is associated with lateralizing motor deficits.[22,23] Therefore, we measured the thickness of the corpus callosum after HI and LPS+HI at striatal level both at the midline and in the contra- and ipsilateral hemisphere at D10 post-insult. HI induced a non-significant thinning of the corpus callosum compared to sham-operated littermates at the midline (83.1 ± 10.4 μm vs 54.6 ± 14.4 μm; HI vs sham) (Fig 3A, C). Administration of LPS prior to HI caused a significant reduction in thickness of the corpus callosum at the midline compared to sham-control levels (39.9 ± 6.2 μm) (p <0.05) (Fig 3A, C). Additionally, in LPS+HI animals loss of MBP staining within the corpus callosum was extending clearly towards the ipsilateral hemisphere, especially in the ventral layer of the corpus callosum. Thickness of the corpus callosum in the ipsilateral hemisphere was 23.1 ± 2.6 μm vs 46.7 ± 9.5 μm, LPS+HI vs sham (p <0.05) (Fig 3A, C). HI alone did not induce significant thinning of the corpus callosum in the ipsilateral hemisphere (Fig 3A, C). No significant differences in corpus callosum thickness were measured in the contralateral hemisphere in sham-operated, HI or LPS+HI animals.

We have shown before that HI can induce a decline in lateral arborization of MBP-positive fibers in the ipsilateral cingulum, defined as an increase in fiber coherency demonstrated by a more linear MBP pattern.[23] Figure 3D and E show that HI did not result in a significant increase in MBP-positive fiber coherency (indicating no significant reduction in lateral arborization of MBP-positive fibers) within the cingulum at D10 post-insult compared to sham-operated littermates. LPS administration before HI however, caused a significant decrease in lateral arborization of MBP-positive fibers, resulting in strongly increased MBP-positive fiber coherency compared to HI and sham at D10 (0.15 ± 0.02% vs 0.07 ± 0.02% or 0.05 ± 0.01%; LPS+HI vs HI or sham) (p <0.05 or p <0.01) (Fig 3D, E).

Next, we examined whether LPS affects oligodendrocyte numbers after HI. Therefore we stained brains of sham-operated, HI and LPS+HI mice with an antibody directed against Olig2 which is expressed throughout the oligodendrocute lineage and thus identifies the entire pool of oligodendrocytes, or with an antibody directed against CNPase that identifies more mature (myelinating) oligodendrocytes. HI significantly increased the number of Olig2-positive cells in the ipsilateral infarct area compared to sham-operated animals at D10 (152.0 ± 17.1 cell/mm^2 vs 79.0 ± 2.4 cell/mm^2) (p <0.001) (Fig 4A, C). HI did not induce changes in the number of Olig2-positive cells in the corpus callosum/cingulum area (Fig 4B). After LPS+HI, significantly higher numbers of Olig2-positive cells were observed in the infarct area compared to HI littermates (221.5 ± 24.1 cell/mm^2 vs 152.0 ± 17.1 cell/mm^2) (p <0.01) (Fig 4A, C), whereas LPS+HI also did not induce changes in the number of Olig2-positive cells in the corpus callosum/cingulum area (Fig 4B). Figure 4D, E and F show that HI caused a significant decrease in more mature myelinating oligodendrocytes measured by a decrease in CNPase-positive signal in the ipsilateral infarct area (p <0.001) and a small, non-significant decrease of CNPase signal in the corpus callosum/cingulum area compared to sham-control

animals. LPS administration before HI however, resulted in a dramatic decrease of CNPase-positive signal in the infarct area (p <0.001) and corpus callosum/cingulum area (p <0.01) compared to HI (Fig 4D, E, F).

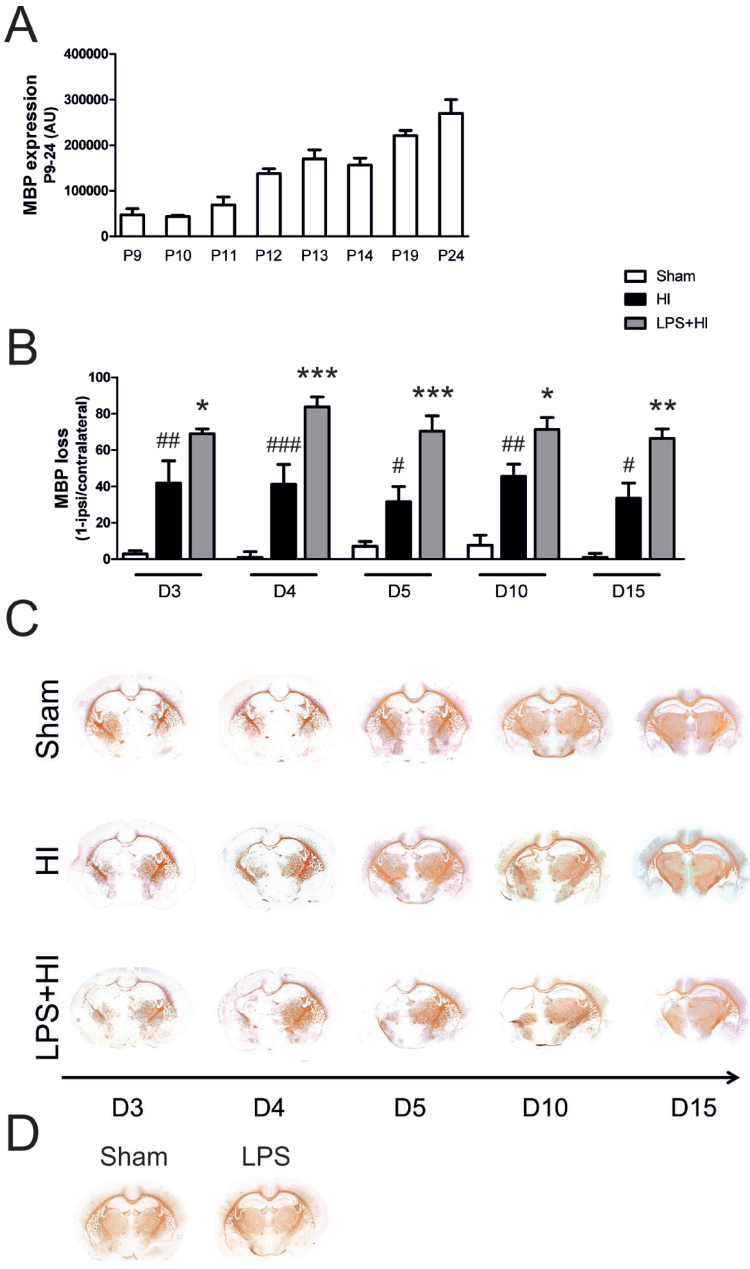

Cerebral inflammatory response

To investigate the effect of LPS on the HI-induced cerebral inflammatory response, we analyzed pro- and anti-inflammatory cytokine and chemokine mRNA expression in the brain at 3 h, D1 (24 h), 2 and 3 post-insult.

Figure 5A shows that HI induced an ipsilateral upregulation of TNF-α mRNA expression compared to sham-control levels within 3 h up to D1 post-HI. The expression of IL-1β and IL-6 mRNA showed a modest, non-significant increase compared to sham-control levels at 3 h and D1 post-insult. At D2 and D3 after HI, TNF-α, IL-1β and IL-6 mRNA expression levels declined to sham-control levels (Fig 5A). When HI was preceded by LPS injection, however, TNF-α mRNA expression was strongly increased compared to HI. In more detail, at 3 h post-insult TNF-α expression increased 34 vs 16 fold in the LPS+HI vs HI animals compared to sham levels (p <0.001). Moreover, TNF-α mRNA expression remained significantly elevated until D3 in LPS+HI mouse pups (Fig 5A). In addition, LPS+HI induced a significant upregulation of IL-1β mRNA expression at 3 h and D1 compared to HI (p <0.01 and p <0.001), which returned to baseline at D2 post-insult. LPS administration before HI significantly enhanced IL-6 expression at D1 (26 fold vs 9 fold; LPS+HI vs HI compared to sham-levels) (p <0.05). IL-6 mRNA levels sharply declined at D2 in both HI and LPS+HI group (Fig 5A). Thus, our data show that LPS+HI resulted in a significant increased and prolonged upregulation of pro-inflammatory cytokines when compared to HI only (Fig 5A).

Next we studied the expression of the anti-inflammatory mediators TGF-β and IL-10 after HI and LPS+HI. HI induced a moderate upregulation of the anti-inflammatory gene TGF-β at D3 post-insult in the ipsilateral hemisphere (p <0.05) (Fig 5B). LPS administration prior to HI resulted in a significant ipsilateral upregulation of TGF-β at D2 and D3 post-insult compared to HI (p <0.0001 and p <0.01) (Fig 5B). For IL-10 mRNA expression, we observed that HI did not induced a statisticant upregulation compared to sham-control levels. LPS+HI induced a strong upregulation of IL-10 expression at 3 h, D1 and D2 which declined to baseline at D3 post-insult. HI-induced IL-10 expression was significantly higher in LPS+HI brains compared to HI at D1 post-insult (p <0.05) (Fig 5B).

← Figure 2: Development of HI-induced cerebral white matter injury at different time points after HI or LPS+HI.

A: Myelin basic protein (MBP) expression in both hemispheres in sham-operated control animals (Sham) from P9 up to P24 (D15 after insult). Mouse pups were subjected to HI at P9 (HI). Sham-operated littermates were used as controls. Animals received an i.p. LPS injection 14 h before the HI insult or sham-operation (LPS+HI or LPS respectively). **B**: Cerebral white matter damage was measured by analyzing loss of MBP staining at hippocampal level in the ipsilateral hemisphere from D3 up to D15 post-insult. Two-way ANOVA: $F_{(2,72)}$= 115.2, p <0.001. No significant time effect or interaction. **C**: Representative examples of MBP staining at hippocampal level in brains of sham-operated, HI and LPS+HI animals at the indicated time points after the insult. **D**: Representative examples of MBP staining at hippocampal level in brains of sham-operated and LPS+sham-operated animals at 6 days after injection *i.e.* P14. Sham n=5-8, HI n=6-8, LPS+HI n=6-7 per time point. Data are expressed as mean ± SEM. Data were analyzed using two-way ANOVA with Bonferroni post-tests. * p <0.05, ** p <0.01, *** p <0.001: LPS+HI vs HI. # p <0.05, ## p <0.01, ### p <0.001: HI vs sham. AU: absorption unit.

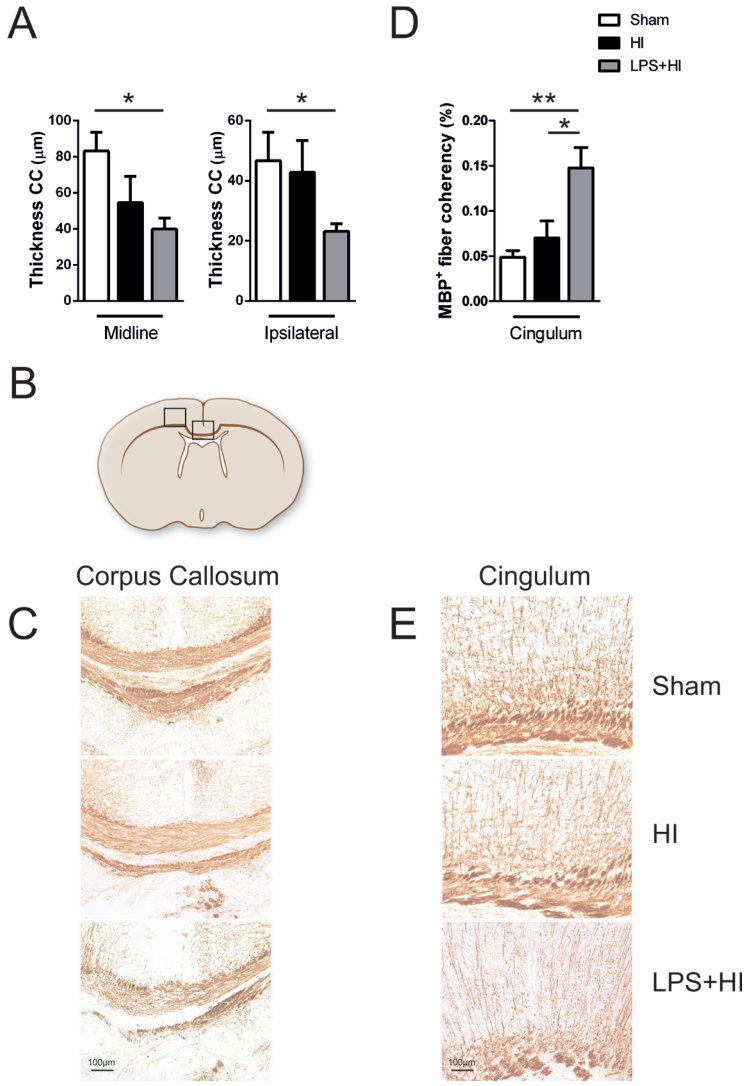

Figure 3: Effects of HI and LPS+HI on thinning of the corpus callosum and arborization of MBP-positive fibers in the cingulum.

Myelination in the corpus callosum and cingulum was measured at striatal level by analyzing staining for MBP at 10 days post-insult. **A**: Corpus callosum thickness in µm measured at the midline and in the ipsilateral part of the corpus callosum in sham-operated, HI and LPS+HI mouse pups. One-way ANOVA: $F_{(2,14)}$= 3.8, p <0.05 and $F_{(2,13)}$= 2.8, p <0.05 midline and ipsilateral part measurements respectively. **B**: Schematic coronal brain view, showing where the MBP photographs were taken in the corpus callosum and cingulum. **C**: Representative photographs of the MBP-stained corpus callosum in the different experimental groups. **D**: MBP-positive fiber coherency in the ipsilateral cingulum, as a measure of (dis) organization of MBP-positive fibers, in sham-operated, HI and LPS+HI mouse pups. Data represent mean value of MBP-positive fiber coherency in the cingulum measured in 4 areas of one microscopic field. One-way ANOVA: $F_{(2,13)}$= 8.0, p <0.01. **E**: Representative pictures of MBP staining in ipsilateral cingulum of sham-operated, HI and LPS+HI animals. Sham n=5, HI n=6, LPS+HI n=6. Data are expressed as mean ± SEM. Data were analyzed using one-way ANOVA with Bonferroni post-tests. * p <0.05, ** p <0.01. CC: corpus callosum.

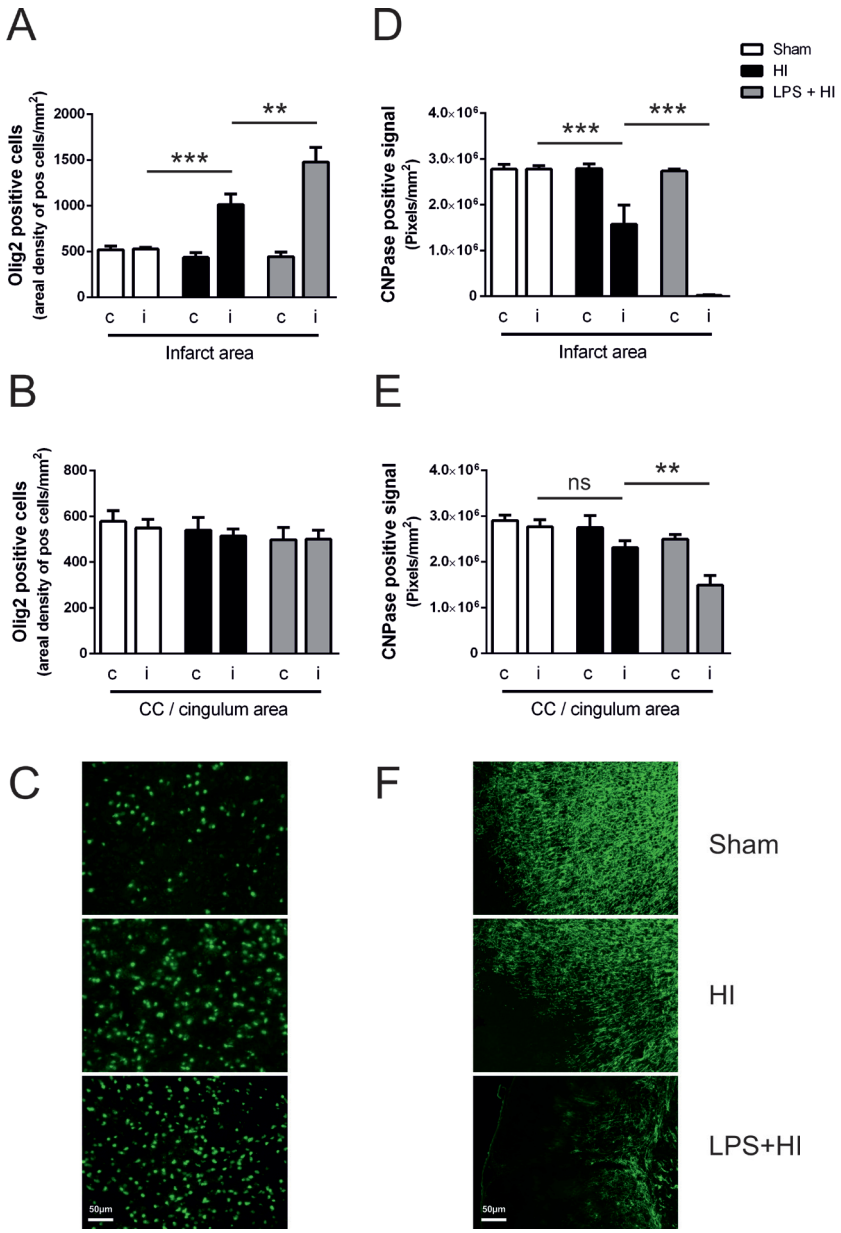

Figure 4: HI- and LPS+HI-induced changes in the number of oligodendrocytes at 10 days post-insult.

The areal density of oligodendrocytes throughout the lineage was measured by analyzing expression of Olig2 staining. CNPase was used as a marker for more mature myelinating oligodendrocytes. **A**: Areal density of Olig2-positive cells in the infarcted cortex at striatal level of sham-operated, HI and LPS+HI mouse pups. Data represent mean value of number of Olig2-positive cells in 3 microscopic fields. Two-way ANOVA: $F_{(2,28)}$= 11.9, p <0.001.**B**: Areal density of Olig2-positive cells in the corpus callosum (CC) and cingulum at striatal level of sham-operated, HI and LPS+HI mouse pups. Data represent mean value of number of Olig2-positive cells in 5 microscopic fields. Two-way ANOVA: $F_{(2,28)}$= 1.2, p = 0.332. **C**: Representative examples of Olig2-positive cells in the infarcted cortex in brains of sham-operated, HI and LPS+HI animals. **D**: CNPase positive signal in the infarcted cortex at striatal level of sham-operated,

HI and LPS+HI mouse pups. Data represent mean value of area of positive signal in 3 microscopic fields. Two-way analysis of variance: $F_{(2,28)}$= 23.5, p <0.001. **E**: CNPase positive signal in the corpus callosum (CC) and cingulum at striatal level of sham-operated, HI and LPS+HI mouse pups. Data represent mean value of area of positive signal in 5 microscopic fields. Two-way analysis of variance: $F_{(2,28)}$= 10.7, p <0.001. **F**: Representative pictures of CNPase staining in the infarcted cortex in brains of sham-operated, HI and LPS+HI animals. Sham n=5, HI n=6, LPS+HI n=6. Data are expressed as mean ± SEM. Data were analyzed using two-way ANOVA with Bonferroni post-tests. ** p <0.01, *** p <0.001. ns = non-significant, c = contralateral hemisphere, i = ipsilateral hemisphere.

Additionally, we determined the effect of HI and LPS+HI on the expression of MCP-1 and CINC-1, two important chemoattractants for influx of macrophages and neutrophils respectively. After HI we observed a 45 and 47 fold increase in cerebral MCP-1 expression at 3 h and D1 post-insult compared to sham-control levels (Fig 5C). The expression of CINC-1 showed a small, non-significant increase at 3 h and D1 (4 fold vs 6 fold; HI compared to sham-levels). When HI was preceded by LPS injection, increased expression of MCP-1 was observed at D1 up to D2 post-insult (p <0.001 and p <0.01), with a peak at D1 (Fig 5C). At D1, LPS+HI induced significantly higher levels of CINC-1 (p <0.001) compared to HI.

The data presented in Figure 5 together show that when HI is preceded by LPS both the pro-inflammatory as well as anti-inflammatory cytokine/chemokine response in the brain is increased and prolonged. Notably, LPS injection without HI resulted in a small but non-significant upregulation of TNF-α, IL-1β, IL-10 and MCP-1 when measured 14 h after the injection ('Pre' groups; Fig 5A-C).

To determine the cerebral activation/influx of microglia/macrophages and neutrophils, we performed an Iba-1 and PMN staining respectively on brain sections of sham-operated, LPS+sham-control, HI and LPS+HI mouse pups. Figure 6A and C show that after HI Iba-1 positive cells displayed a more activated phenotype, but Iba-1 positive signal was not significantly increased. LPS+HI resulted in a significant increase in Iba-1 positive signal with a concomitant increased intensity of Iba-1 staining per cell, indicating an increased activation state of macrophages/microglia, in the ipsilateral cortical and hippocampal area at D2 post-insult (p <0.05) (Fig 6A). The Iba-1 positive signal declined at D15 post-insult (Fig 6A). Figure 6C illustrates that Iba-1 positive cells in sham-operated and LPS+sham-control mice displayed a resting state phenotype with ramified morphology, whereas the Iba-1 positive cells in HI and LPS+HI animals showed a more activated state with amoeboid shape and retracted processes. Importantly, LPS injection alone without HI did not induce an increase in Iba-1 positive signal at D3 after injection compared to sham-operated littermates (Fig 6C).
To assess neutrophil influx into the brain parenchyma, a PMN staining was performed during the first 3 days following the insult. In sham-control animals neutrophils were not detected (Fig 6D, E). Following HI a small number of neutrophils was observed in the right cerebral hemisphere at D1-3. LPS+HI resulted in a massive influx of neutrophils peaking at D1 which was significantly increased compared to HI only (p <0.001). Neutrophil numbers declined but

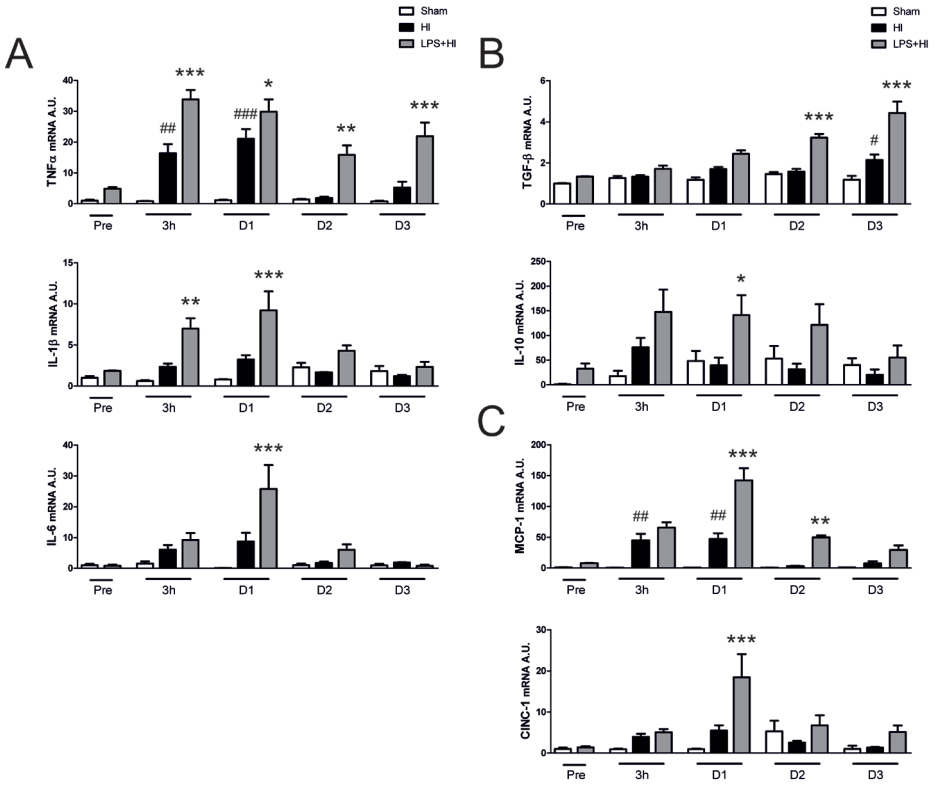

Figure 5: Ipsilateral mRNA expression of pro- and anti-inflammatory cytokines and chemokines at different time points post-insult.

Cerebral mRNA expression of cytokines and chemokines was measured by quantitative real-time reverse transcriptase PCR at the indicated time points. **A**: Ipsilateral mRNA expression of the pro-inflammatory cytokines TNF-α, IL-1β and IL-6. Two-way ANOVA: TNF-α $F_{(2,63)}$= 63.6, p <0.001; IL-1β $F_{(2,57)}$= 19.4, p <0.001; IL-6 $F_{(2,59)}$= 11.9, p <0.001. **B**: Ipsilateral mRNA expression of the anti-inflammatory factors TGF-β and IL-10. Two-way ANOVA: TGF-β $F_{(2,63)}$= 55.0, p <0.001; IL-10 $F_{(2,63)}$= 9.5, p <0.001. **C**: Ipsilateral mRNA expression of the chemokines MCP-1 and CINC-1. Two-way ANOVA: MCP-1 $F_{(2,58)}$= 58.0, p <0.001; CINC-1 $F_{(2,62)}$= 10.5, p <0.001. Data were individually normalized to the mean of the relative expression of GAPDH and β-actin. Expression levels are presented relative to levels in sham-operated animals at time point "Pre" which were put at 1. No significant changes in mRNA expression were observed in the contralateral hemispheres of HI or LPS+HI animals compared to levels in sham-operated littermates. Sham n=5, HI n=6-8, LPS+HI n=6-8 per time point. Data are expressed as mean ± SEM. Data were analyzed using two-way ANOVA with Bonferroni post-tests. * p <0.05, ** p <0.01, *** p < 0.001: LPS+HI vs HI. # p <0.05, ## p <0.01, ### p <0.001: HI vs sham. Pre = animals terminated before hypoxia. A.U. = arbitrary units.

remained slightly elevated until D3 (Fig 6D, E). Neutrophils were specifically observed in the damaged cortex, with minimal numbers in the hippocampal area. A large part of infiltrating neutrophils were observed within the brain parenchyma (outside blood vessels), indicating diapedesis of these cells. LPS injection alone without HI did not induce influx of neutrophils into the brain at D2 after injection compared to sham-operated littermates (Fig 6E).

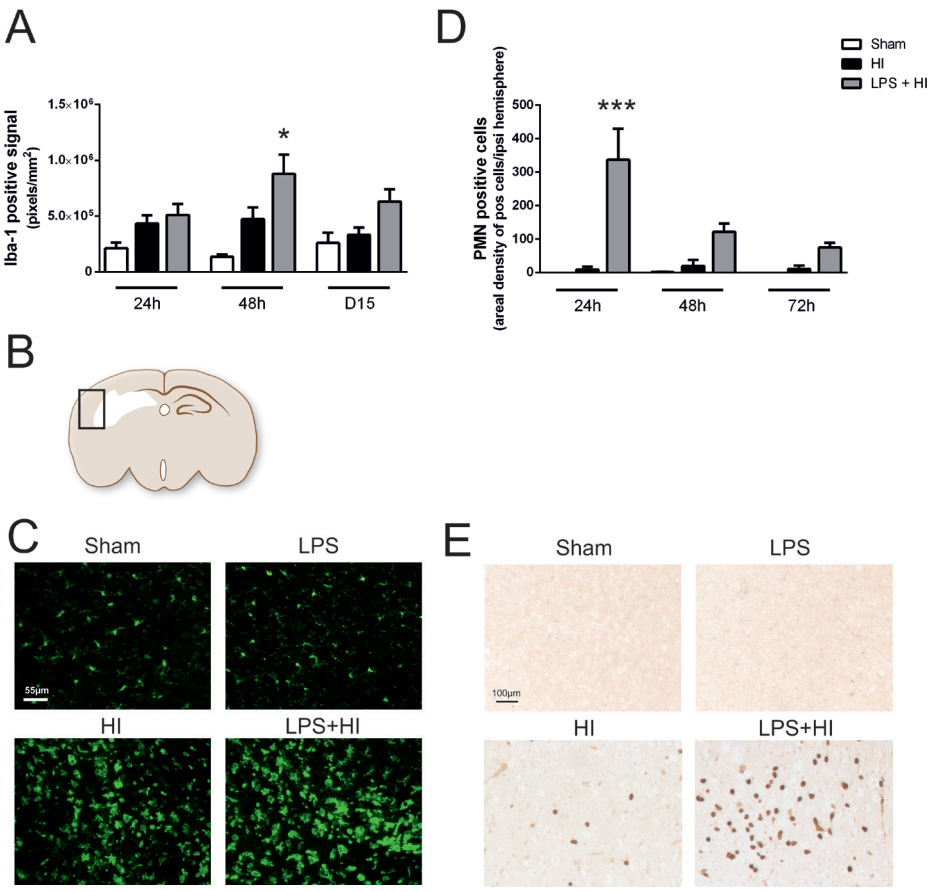

Figure 6: Activation/influx of microglia/macrophages and neutrophils into the brain at different time points post-insult.

The influx/activation of macrophages/microglia was measured by analyzing staining for Iba-1. Staining for polymorphonuclear neutrophils (PMN) was used to assess the presence of neutrophils.

A: Quantification of Iba-1 positive signal in the ipsilateral cortical and hippocampal areas at hippocampal level in sham-operated (Sham), HI and LPS+HI mouse pups at D1, D2 and D15 post-insult. Mean value of area of positive signal in 6 microscopic fields. Two-way ANOVA: $F_{(2,33)}$= 11.1, p <0.001. **B**: Schematic coronal brain view, showing where the Iba-1 and PMN staining photographs were taken in the cortex. **C**: Representative examples of Iba-1 staining within the infarcted area in the cortex of sham-operated, LPS+sham-operated (LPS), HI and LPS+HI animals at D2 post-insult. **D**: Areal density of PMN-positive cells counted in the ipsilateral hemisphere in a coronal section at hippocampal level of sham-operated, HI and LPS+HI mouse pups at D1, D2 and D3 post-insult. **E**: Representative pictures of PMN staining in the (infarcted) cortex of sham-operated, LPS+sham-operated, HI and LPS+HI animals at D1 post-HI. Two-way ANOVA: $F_{(2,35)}$= 25.3, p <0.001. Sham n=3-4, HI n=5-7, LPS+HI n=5-7 per time point. Data are expressed as mean ± SEM. Data were analyzed using two-way ANOVA with Bonferroni post-tests. * p <0.05, *** p <0.001. Pos: positive, ipsi: ipsilateral

Discussion

Over the last years, the role of inflammation in the development of neonatal brain damage has become a matter of great interest. Antenatal infections are recognized as an important risk factor for adverse outcome in term and preterm neonates.[24-29] The combined exposure to perinatal inflammation and neonatal HI results in a complex interplay of various signaling pathways of which the exact underlying mechanism has not been elucidated yet. Experimental peripheral inflammation induced by LPS is known to induce an inflammatory cerebral state leading to sensitization of the brain to HI injury.[15,16,19,21,30,31] Possible mechanisms via which peripheral LPS can sensitize the brain have been described extensively and consist of a) stimulation of endothelial cells of the blood brain barrier (BBB), b) activation/priming of microglia via immune signals produced by endothelial and choroid plexus cells at the level of the BBB, c) direct transport of peripheral inflammatory molecules across the BBB, d) increased permeability of the BBB which enhance the influx of peripheral immune cells into the brain, e) stimulation of the vagal nerve by peripheral cytokines leading to signaling in the brain and f) effects of inflammation on G protein-coupled receptor signaling in the brain.[17,32-35] In the present study, we carefully characterized the sensitizing effect of LPS on the severity, appearance and especially timing of HI-induced brain injury.

We describe here that an inflammatory state before HI not only aggravates neuronal damage measured by MAP2 loss when compared to HI, but is also associated with a gradual increase of neuronal damage from 3 h up to D10 post-insult. In contrast, the total amount of MAP2 loss in HI animals had developed already early, at 3 h post-insult, without further increase over time. Importantly, we observed a clear difference in the timing of acute neuronal damage (MAP2 loss) and actual loss of cerebral tissue, *i.e.* cyst formation after HI and LPS+HI. Whereas MAP2 loss was already present at 3 h post-insult, our data show that volume loss of cerebral tissue does not start before D2-D3 post-insult as shown by HE staining. So, acute neuronal damage measured by MAP2 loss is an early indicator of gray matter damage but is not one-to-one related to direct loss of cerebral tissue, which is delayed for about 2-3 days. Notably, the relatively mild HI insult induced microscopic loss of hippocampal architecture and some loss of cortical volume but did not induce a macroscopically detectable cystic lesion. However, when HI was preceded by LPS, a major cystic lesion developed starting at D3-4 which increased until D10 post-insult. These data are important because they suggest that the time-window for promising pharmacological interventions after HI probably changes when HI is preceded or combined with inflammation. We recently described a treatment strategy to regenerate HI brain injury by administering mesenchymal stem cells (MSCs).[36,37] An advantage of this neuroregenerative strategy is a long therapeutic window; treatment with MSCs leads to repair of the lesion even when started at 10 days after HI. However, since the timing of the 'damage response' to HI changes when HI is accompanied by inflammation, one should take into account that inflammation may considerably shorten the time window of MSC treatment. In particular, the formation of a-cellular cysts that develops from 3-4 days

after LPS+HI might require acceleration of the start of regenerative therapies. Our data may also guide other therapeutic regenerative or neuroprotective strategies currently investigated for neonatal encephalopathy, like erythropoietin (EPO) or melatonin treatment.[38-41]

The influence of combined exposure to inflammation and HI on cerebral white matter injury was measured by loss of MBP staining in the infarct area. As described before, LPS induced a significant increase in HI-induced cerebral white matter damage.[31] Here we show that LPS+HI also affected myelination in white matter structures outside the infarcted area, which can have important consequences for neurodevelopmental outcome. LPS+HI induced thinning of the corpus callosum, an important white matter structure that facilitates communication between both hemispheres. The thickness of the corpus callosum can be influenced by a deficit in myelination and/or axons. In human neonates, a reduction in corpus callosum thickness is associated with cognitive and motor impairment.[42-44] Additionally, arborization of the myelinated fibers in the cingulum was strongly reduced by LPS+HI. Axonal injury in this part of the brain has been shown to be involved in *e.g.* cognition, working-memory performance and motor function.[23,42,45,46]

The observed effects of LPS+HI on myelination urged us to investigate the effect of LPS+HI on oligodendrocytes.[47] Interestingly, after HI the number of Olig2-positive cells was upregulated selectively in the infarcted area. We show that sensitization by LPS led to an even stronger upregulation of Olig2-positive cells in the infarcted area after HI. In line with a decrease in MBP staining, CNPase positive signal, as a marker for more mature myelinating oligodendrocytes, was strongly decreased in the infarcted area after HI and was almost completely absent after LPS+HI. Our data might indicate that HI and LPS+HI induce oligodendrogliogenesis or migration of oligodendrocytes to the site of damage in an attempt to repair myelination of the white matter tracts. However, since there is a decrease in more mature myelinating oligodendrocytes, the development of oligodendrocyte precursors into the final mature myelinating stage, might be delayed or even arrested after LPS+HI. In line with our data, previous animal studies have shown that neonatal HI or systemic inflammation result in proliferation of oligodendrocytes, which is often followed by an arrest in differentiation and maturation into mature oligodendrocytes.[48-51] Importantly, this phenomenon is also described in human neonates following periventricular leukomalacia.[26,52,53] An arrest in oligodendrocyte maturation will eventually result in a decrease in myelin production, white matter damage and axonal injury.

A pro-inflammatory state during the perinatal period can already affect oligodendrocyte precursors and elicit cerebral white matter damage and behavioral deficits as shown in animal models.[48,54-58] However, in a control group we injected LPS (0.5 mg/kg) i.p. without induction of HI, but we did not observe any aberrations in cerebral gray or white matter structures or tissue loss in our neonatal mouse model. The formation of free radicals, excitotoxicity, astrogliosis and release of cytokines by activated microglia are important downstream mechanisms that can damage the developing oligodendrocyte after inflammation and/

or HI.[47,50,59] In particular, TNF-α and IFN-γ are known factors that induce oligodendrocyte death.[47,60,61] Apparently, the changes induced by LPS alone are not sufficient to induce white or gray matter damage in our mouse model. LPS injection prior to HI resulted in increased expression of all measured pro-inflammatory cytokines and chemokines in the ipsilateral hemisphere compared to HI. Besides the *increased* upregulation, levels of TNF-α, TGF-β, IL-10 and MCP-1 were elevated for a *prolonged* time up to D2-3. Particularly TNF-α expression was strongly increased and prolonged following LPS+HI and is likely a crucial factor contributing to the arrest in oligodendrocyte maturation.[47,60-62] We showed earlier that HI-induced changes in cytokine mRNA levels were related to changes in protein levels of these cytokines.[63] Besides the effect on oligodendrocytes, Kendall et al. (2011) showed that TNF-α is a key factor in the LPS-mediated sensitizing effect on HI brain damage, since deletion of the TNF gene cluster prevented the LPS-induced increase in endothelial and microglia activation and the increase in HI brain damage.[16] Consequently, anti-TNF therapies could be promising in neonates were inflammation precedes HI.

Besides the increased upregulation of pro-inflammatory cytokines, we also observed a strong increase in anti-inflammatory TGF-β and IL-10 following LPS+HI. TGF-β was hardly upregulated after HI alone but LPS injection induced elevated and prolonged expression from D2-D3. Besides possible anti-inflammatory effects of TGF-β, Nobuta et al. (2012) showed that TGF-β is also an important inhibitor of oligodendrocyte proliferation and differentiation *in vitro* and that TGF-β is extensively expressed in the white matter following cerebral white matter injury in human neonates.[64] We suggest that the strong and early rise in *e.g.* TNF-α might have an early damaging effect on oligodendrocytes which induces an increase in oligodendrocyte proliferation (increased number of Olig2-positive cells) followed by a possible second hit on maturation caused by increased TGF-β expression at D1-3. TGF-β signaling could therefore also be an interesting target to reduce white matter injury following LPS+HI.

LPS+HI induced an increase in IL-10 mRNA expression at D1 compared to HI only. IL-10 is an anti-inflammatory cytokine capable of suppressing pro-inflammatory cytokine production and IL-10 has been shown to have a protective effect on developing white matter.[65-67] However, our present data indicate that the possible protective effect of IL-10 might become overshadowed by the strong pro-inflammatory response induced by LPS.

Besides the effects of damaging signals like free radical formation, excitotoxicity or cytokine release, maturation and survival of oligodendrocytes is also dependent on the availability of several growth and trophic factors secreted by local cells like microglia, astrocytes and neurons, including insulin-like growth factors (IGFs), nerve growth factor (NGF), ciliary-neurotrophic factor (CNTF), platelet-derived growth factor (PDGF) and fibroblast growth factor (FGF).[68,69] Pang et al. (2010) showed that LPS causes a reduction in microglia-derived growth factors IGF-1 and CNTF which was associated with oligodendrocyte death *in vitro.*[61] However, the exact effects of LPS+HI on these growth factors *in vivo* are still unknown. We feel that ongoing research should also aim at further unraveling the effect of inflammation

on trophic and growth factors involved in differentiation and maturation of oligodendrocytes, so that future therapies can circumvent the arrest in oligodendrocyte maturation to prevent white matter injury in the context of perinatal inflammation.

Microglial activation results in release of harmful molecules including nitric oxide, glutamate and cytokines, which can aggravate brain damage. Several studies have shown that microglia play an important role in the sensitizing effect of LPS on HI brain damage.[31,61,70,71] In this study we observed an increased Iba-1 positive signal and morphologically an increased activation state of microglia/macrophages in the brain at 2 days following LPS+HI when compared to HI only. The increased Iba-1 positive signal is probably caused by infiltration of peripheral macrophages to the site of injury. Interestingly, at D1 after the insult, no significant difference in Iba-1 staining was observed between HI and LPS+HI animals. It could be that LPS induces priming of microglia in an earlier phase without clear morphological changes assessed by Iba-1 staining.[31]
LPS+HI caused a dramatic increase in CINC-1 expression and neutrophil influx into the brain within 1 day post-insult when compared to HI. Besides the increased CINC-1 expression, the early and rapid influx of neutrophils might be explained by the influence of systemic inflammation on adhesion molecule expression on endothelial cells of the BBB, leading to more directed trafficking of immune cells to the lesion site.[17] Furthermore the increase in peripheral cytokines following systemic LPS may influence signaling cascades in leukocytes thereby enhancing their migratory potential.[72,73] Neutrophils play an important role in clearing cellular debris after tissue damage. However after activation they release cytotoxic molecules that can damage surrounding tissue. In line, we and others have previously shown that neutrophil depletion can reduce HI-induced brain damage.[74-76] Prevention of the early influx of neutrophils, by inhibiting chemotactic cues like CINC-1 in the periphery or brain, could be an interesting therapeutic option to prevent the exacerbation of HI brain injury after LPS+HI.

In conclusion, our data show that when a HI insult is preceded by an inflammatory component the timing of brain injury change and additional molecular and/or cellular pathways contribute to the evolvement of the lesion. These changes in timing and pathways are important because they might require modifications in time window, dosage or a combination of promising experimental therapies to result in effective and successful neuroprotection or neuroregeneration after inflammatory perinatal asphyxia. At this moment hypothermia is the only standardized treatment for full term neonates suffering from a HI insult. It is important to realize that exacerbation and prolongation of the 'damage response' induced by inflammation can have important implications for the efficacy of hypothermia treatment after HI. Hypothermia has been shown to be only effective when started within 6 h after HI in term neonates.[77,78] Recently, Osredkar et al. (2014) showed that hypothermia has no neuroprotective effect after LPS-sensitized HI brain injury.[79] Furthermore, Wintermark

et al. (2010) suggested that chorioamnionitis with fetal vasculitis may limit the effectiveness of therapeutic hypothermia following HI in human full term neonates.[9] If the metabolic state of the brain is increased or altered due to (preceding) inflammation, cooling might be less effective. The loss of effectiveness of the only clinically-applied therapy at present in term neonates suffering from inflammatory perinatal asphyxia further highlights the indispensable need to explore novel therapies specifically aimed at dampening the inflammatory component. Moreover, current treatments using anti-inflammatory strategies may have to be continued for a longer period, and/or have to be intensified to suppress the increased and prolonged neuroinflammatory response.

References

1. Perlman M, Shah PS. Hypoxic-ischemic encephalopathy: challenges in outcome and prediction. *J Pediatr*. 2011;158:51-4.
2. Ferriero DM. Neonatal brain injury. *N Engl J Med*. 2004;351:1985-1995.
3. Groenendaal F, Casaer A, Dijkman KP, et al. Introduction of hypothermia for neonates with perinatal asphyxia in the Netherlands and Flanders. *Neonatology*. 2013;104:15-21.
4. Grether JK, Nelson KB. Maternal infection and cerebral palsy in infants of normal birth weight. *JAMA*. 1997;278:207-211.
5. Impey L, Greenwood C, MacQuillan K, Reynolds M, Sheil O. Fever in labour and neonatal encephalopathy: a prospective cohort study. *BJOG*. 2001;108:594-597.
6. Blume HK, Li CI, Loch CM, Koepsell TD. Intrapartum fever and chorioamnionitis as risks for encephalopathy in term newborns: a case-control study. *Dev Med Child Neurol*. 2008;50:19-24.
7. Hayes BC, Cooley S, Donnelly J, et al. The placenta in infants >36 weeks gestation with neonatal encephalopathy: a case control study. *Arch Dis Child Fetal Neonatal Ed*. 2013;98:233-9.
8. Peebles DM, Wyatt JS. Synergy between antenatal exposure to infection and intrapartum events in causation of perinatal brain injury at term. *BJOG*. 2002;109:737-739.
9. Wintermark P, Boyd T, Gregas MC, Labrecque M, Hansen A. Placental pathology in asphyxiated newborns meeting the criteria for therapeutic hypothermia. *Am J Obstet Gynecol*. 2010;203:579.1-579.9.
10. Harteman JC, Nikkels PG, Benders MJ, Kwee A, Groenendaal F, de Vries LS. Placental pathology in full-term infants with hypoxic-ischemic neonatal encephalopathy and association with magnetic resonance imaging pattern of brain injury. *J Pediatr*. 2013;163:968-95.2.
11. Shalak LF, Laptook AR, Jafri HS, Ramilo O, Perlman JM. Clinical chorioamnionitis, elevated cytokines, and brain injury in term infants. *Pediatrics*. 2002;110:673-680.
12. Akira S, Uematsu S, Takeuchi O. Pathogen recognition and innate immunity. *Cell*. 2006;124:783-801.
13. Wang X, Rousset CI, Hagberg H, Mallard C. Lipopolysaccharide-induced inflammation and perinatal brain injury. *Semin Fetal Neonatal Med*. 2006;11:343-353.
14. Rice JE,3rd, Vannucci RC, Brierley JB. The influence of immaturity on hypoxic-ischemic brain damage in the rat. *Ann Neurol*. 1981;9:131-141.
15. Eklind S, Mallard C, Leverin AL, et al. Bacterial endotoxin sensitizes the immature brain to hypoxic-ischaemic injury. *Eur J Neurosci*. 2001;13:1101-1106.
16. Kendall GS, Hristova M, Horn S, et al. TNF gene cluster deletion abolishes lipopolysaccharide-mediated sensitization of the neonatal brain to hypoxic ischemic insult. *Lab Invest*. 2011;91:328-341.
17. Mallard C. Innate immune regulation by toll-like receptors in the brain. *ISRN Neurol*. 2012;2012:701950.
18. Coumans AB, Middelanis JS, Garnier Y, et al. Intracisternal application of endotoxin enhances the susceptibility to subsequent hypoxic-ischemic brain damage in neonatal rats. *Pediatr Res*. 2003;53:770-775.
19. Eklind S, Mallard C, Arvidsson P, Hagberg H. Lipopolysaccharide induces both a primary and a secondary phase of sensitization in the developing rat brain. *Pediatr Res*. 2005;58:112-116.
20. Wang X, Hagberg H, Nie C, Zhu C, Ikeda T, Mallard C. Dual role of intrauterine immune challenge on neonatal and adult brain vulnerability to hypoxia-ischemia. *J Neuropathol Exp Neurol*. 2007;66:552-561.
21. Yang L, Sameshima H, Ikeda T, Ikenoue T. Lipopolysaccharide administration enhances hypoxic-ischemic brain damage in newborn rats. *J Obstet Gynaecol Res*. 2004;30:142-147.
22. Filgueiras CC, Manhaes AC. Increased lateralization in rotational side preference in male mice rendered acallosal by prenatal gamma irradiation. *Behav Brain Res*. 2005;162:289-298.

23. van Velthoven CT, van de Looij Y, Kavelaars A, et al. Mesenchymal stem cells restore cortical rewiring after neonatal ischemia in mice. *Ann Neurol*. 2012;71:785-796.
24. Dammann O, Leviton A. Inflammatory brain damage in preterm newborns--dry numbers, wet lab, and causal inferences. *Early Hum Dev*. 2004;79:1-15.
25. Hagberg H, Gressens P, Mallard C. Inflammation during fetal and neonatal life: implications for neurologic and neuropsychiatric disease in children and adults. *Ann Neurol*. 2012;71:444-457.
26. Volpe JJ. Brain injury in premature infants: a complex amalgam of destructive and developmental disturbances. *Lancet Neurol*. 2009;8:110-124.
27. Leviton A, Paneth N, Reuss ML, et al. Maternal infection, fetal inflammatory response, and brain damage in very low birth weight infants. Developmental Epidemiology Network Investigators. *Pediatr Res*. 1999;46:566-575.
28. Wu YW, Escobar GJ, Grether JK, Croen LA, Greene JD, Newman TB. Chorioamnionitis and cerebral palsy in term and near-term infants. *JAMA*. 2003;290:2677-2684.
29. Yoon BH, Park CW, Chaiworapongsa T. Intrauterine infection and the development of cerebral palsy. *BJOG*. 2003;110 Suppl 20:124-127.
30. Eklind S, Hagberg H, Wang X, et al. Effect of lipopolysaccharide on global gene expression in the immature rat brain. *Pediatr Res*. 2006;60:161-168.
31. Wang X, Stridh L, Li W, et al. Lipopolysaccharide sensitizes neonatal hypoxic-ischemic brain injury in a MyD88-dependent manner. *J Immunol*. 2009;183:7471-7477.
32. Degos V, Peineau S, Nijboer C, et al. G protein-coupled receptor kinase 2 and group I metabotropic glutamate receptors mediate inflammation-induced sensitization to excitotoxic neurodegeneration. *Ann Neurol*. 2013;73:667-678.
33. Nijboer CH, Heijnen CJ, Degos V, Willemen HL, Gressens P, Kavelaars A. Astrocyte GRK2 as a novel regulator of glutamate transport and brain damage. *Neurobiol Dis*. 2013;54:206-215.
34. Singh AK, Jiang Y. How does peripheral lipopolysaccharide induce gene expression in the brain of rats? *Toxicology*. 2004;201:197-207.
35. Xaio H, Banks WA, Niehoff ML, Morley JE. Effect of LPS on the permeability of the blood-brain barrier to insulin. *Brain Res*. 2001;896:36-42.
36. Donega V, van Velthoven CT, Nijboer CH, et al. Intranasal mesenchymal stem cell treatment for neonatal brain damage: long-term cognitive and sensorimotor improvement. *PLoS One*. 2013;8:51253.
37. van Velthoven CT, Kavelaars A, van Bel F, Heijnen CJ. Mesenchymal stem cell treatment after neonatal hypoxic-ischemic brain injury improves behavioral outcome and induces neuronal and oligodendrocyte regeneration. *Brain Behav Immun*. 2010;24:387-393.
38. Chang YS, Mu D, Wendland M, et al. Erythropoietin improves functional and histological outcome in neonatal stroke. *Pediatr Res*. 2005;58:106-111.
39. Juul SE, McPherson RJ, Bauer LA, Ledbetter KJ, Gleason CA, Mayock DE. A phase I/II trial of high-dose erythropoietin in extremely low birth weight infants: pharmacokinetics and safety. *Pediatrics*. 2008;122:383-391.
40. Welin AK, Svedin P, Lapatto R, et al. Melatonin reduces inflammation and cell death in white matter in the mid-gestation fetal sheep following umbilical cord occlusion. *Pediatr Res*. 2007;61:153-158.
41. Fan X, Heijnen CJ, van der KOOIJ MA, Groenendaal F, van Bel F. Beneficial effect of erythropoietin on sensorimotor function and white matter after hypoxia-ischemia in neonatal mice. *Pediatr Res*. 2011;69:56-61.
42. Tusor N, Wusthoff C, Smee N, et al. Prediction of neurodevelopmental outcome after hypoxic-ischemic encephalopathy treated with hypothermia by diffusion tensor imaging analyzed using tract-based spatial statistics. *Pediatr Res*. 2012;72:63-69.
43. Caldu X, Narberhaus A, Junque C, et al. Corpus callosum size and neuropsychologic impairment in adolescents who were born preterm. *J Child Neurol*. 2006;21:406-410.

44. VAN Kooij BJ, VAN Handel M, Uiterwaal CS, et al. Corpus callosum size in relation to motor performance in 9- to 10-year-old children with neonatal encephalopathy. *Pediatr Res*. 2008;63:103-108.
45. van Kooij BJ, de Vries LS, Ball G, et al. Neonatal tract-based spatial statistics findings and outcome in preterm infants. *AJNR Am J Neuroradiol*. 2012;33:188-194.
46. Ewing-Cobbs L, Prasad MR, Swank P, et al. Arrested development and disrupted callosal microstructure following pediatric traumatic brain injury: relation to neurobehavioral outcomes. *Neuroimage*. 2008;42:1305-1315.
47. Volpe JJ, Kinney HC, Jensen FE, Rosenberg PA. The developing oligodendrocyte: key cellular target in brain injury in the premature infant. *Int J Dev Neurosci*. 2011;29:423-440.
48. Dean JM, van de Looij Y, Sizonenko SV, et al. Delayed cortical impairment following lipopolysaccharide exposure in preterm fetal sheep. *Ann Neurol*. 2011;70:846-856.
49. Favrais G, van de Looij Y, Fleiss B, et al. Systemic inflammation disrupts the developmental program of white matter. *Ann Neurol*. 2011;70:550-565.
50. Segovia KN, McClure M, Moravec M, et al. Arrested oligodendrocyte lineage maturation in chronic perinatal white matter injury. *Ann Neurol*. 2008;63:520-530.
51. Xiong M, Li J, Ma SM, Yang Y, Zhou WH. Effects of hypothermia on oligodendrocyte precursor cell proliferation, differentiation and maturation following hypoxia ischemia in vivo and in vitro. *Exp Neurol*. 2013;247:720-729.
52. Buser JR, Maire J, Riddle A, et al. Arrested preoligodendrocyte maturation contributes to myelination failure in premature infants. *Ann Neurol*. 2012;71:93-109.
53. Billiards SS, Haynes RL, Folkerth RD, et al. Myelin abnormalities without oligodendrocyte loss in periventricular leukomalacia. *Brain Pathol*. 2008;18:153-163.
54. Hagberg H, Peebles D, Mallard C. Models of white matter injury: comparison of infectious, hypoxic-ischemic, and excitotoxic insults. *Ment Retard Dev Disabil Res Rev*. 2002;8:30-38.
55. Duncan JR, Cock ML, Scheerlinck JP, et al. White matter injury after repeated endotoxin exposure in the preterm ovine fetus. *Pediatr Res*. 2002;52:941-949.
56. Garnier Y, Berger R, Alm S, et al. Systemic endotoxin administration results in increased S100B protein blood levels and periventricular brain white matter injury in the preterm fetal sheep. *Eur J Obstet Gynecol Reprod Biol*. 2006;124:15-22.
57. Mallard C, Welin AK, Peebles D, Hagberg H, Kjellmer I. White matter injury following systemic endotoxemia or asphyxia in the fetal sheep. *Neurochem Res*. 2003;28:215-223.
58. Pang Y, Cai Z, Rhodes PG. Disturbance of oligodendrocyte development, hypomyelination and white matter injury in the neonatal rat brain after intracerebral injection of lipopolysaccharide. *Brain Res Dev Brain Res*. 2003;140:205-214.
59. Back SA, Tuohy TM, Chen H, et al. Hyaluronan accumulates in demyelinated lesions and inhibits oligodendrocyte progenitor maturation. *Nat Med*. 2005;11:966-972.
60. Kadhim H, Tabarki B, Verellen G, De Prez C, Rona AM, Sebire G. Inflammatory cytokines in the pathogenesis of periventricular leukomalacia. *Neurology*. 2001;56:1278-1284.
61. Pang Y, Campbell L, Zheng B, Fan L, Cai Z, Rhodes P. Lipopolysaccharide-activated microglia induce death of oligodendrocyte progenitor cells and impede their development. *Neuroscience*. 2010;166:464-475.
62. Selmaj K, Raine CS, Farooq M, Norton WT, Brosnan CF. Cytokine cytotoxicity against oligodendrocytes. Apoptosis induced by lymphotoxin. *J Immunol*. 1991;147:1522-1529.
63. Nijboer CH, Heijnen CJ, Groenendaal F, van Bel F, Kavelaars A. Alternate pathways preserve tumor necrosis factor-alpha production after nuclear factor-kappaB inhibition in neonatal cerebral hypoxia-ischemia. *Stroke*. 2009;40:3362-3368.
64. Nobuta H, Ghiani CA, Paez PM, et al. STAT3-mediated astrogliosis protects myelin development in neonatal brain injury. *Ann Neurol*. 2012;72:750-765.

65. Rodts-Palenik S, Wyatt-Ashmead J, Pang Y, et al. Maternal infection-induced white matter injury is reduced by treatment with interleukin-10. *Am J Obstet Gynecol*. 2004;191:1387-1392.

66. Brehmer F, Bendix I, Prager S, et al. Interaction of inflammation and hyperoxia in a rat model of neonatal white matter damage. *PLoS One*. 2012;7:49023.

67. Pang Y, Rodts-Palenik S, Cai Z, Bennett WA, Rhodes PG. Suppression of glial activation is involved in the protection of IL-10 on maternal E. coli induced neonatal white matter injury. *Brain Res Dev Brain Res*. 2005;157:141-149.

68. Barres BA, Schmid R, Sendnter M, Raff MC. Multiple extracellular signals are required for long-term oligodendrocyte survival. *Development*. 1993;118:283-295.

69. Wolswijk G, Riddle PN, Noble M. Platelet-derived growth factor is mitogenic for O-2Aadult progenitor cells. *Glia*. 1991;4:495-503.

70. Dean JM, Wang X, Kaindl AM, et al. Microglial MyD88 signaling regulates acute neuronal toxicity of LPS-stimulated microglia in vitro. *Brain Behav Immun*. 2010;24:776-783.

71. Lehnardt S, Massillon L, Follett P, et al. Activation of innate immunity in the CNS triggers neurodegeneration through a Toll-like receptor 4-dependent pathway. *Proc Natl Acad Sci U S A*. 2003;100:8514-8519.

72. Vroon A, Heijnen CJ, Lombardi MS, et al. Reduced GRK2 level in T cells potentiates chemotaxis and signaling in response to CCL4. *J Leukoc Biol*. 2004;75:901-909.

73. Vroon A, Kavelaars A, Limmroth V, et al. G protein-coupled receptor kinase 2 in multiple sclerosis and experimental autoimmune encephalomyelitis. *J Immunol*. 2005;174:4400-4406.

74. Hudome S, Palmer C, Roberts RL, Mauger D, Housman C, Towfighi J. The role of neutrophils in the production of hypoxic-ischemic brain injury in the neonatal rat. *Pediatr Res*. 1997;41:607-616.

75. Nijboer CH, Kavelaars A, Vroon A, Groenendaal F, van Bel F, Heijnen CJ. Low endogenous G-protein-coupled receptor kinase 2 sensitizes the immature brain to hypoxia-ischemia-induced gray and white matter damage. *J Neurosci*. 2008;28:3324-3332.

76. Palmer C, Roberts RL, Young PI. Timing of neutrophil depletion influences long-term neuroprotection in neonatal rat hypoxic-ischemic brain injury. *Pediatr Res*. 2004;55:549-556.

77. Azzopardi DV, Strohm B, Edwards AD, et al. Moderate hypothermia to treat perinatal asphyxial encephalopathy. *N Engl J Med*. 2009;361:1349-1358.

78. Johnston MV, Fatemi A, Wilson MA, Northington F. Treatment advances in neonatal neuroprotection and neurointensive care. *Lancet Neurol*. 2011;10:372-382.

79. Osredkar D, Thoresen M, Maes E, Flatebo T, Elstad M, Sabir H. Hypothermia is not neuroprotective after infection-sensitized neonatal hypoxic-ischemic brain injury. *Resuscitation*. 2014;85:567-572.

6

Inflammation in the context of neonatal hypoxic-ischemic brain injury decreases the neuroprotective efficacy of the JNK inhibitor D-JNKi

Hilde J.C. Bonestroo
Cora H. Nijboer
Frank van Bel
Cobi J. Heijnen

Submitted

Abstract

Background An antenatal infection dramatically increases the risk of severe encephalopathy and adverse outcome after a hypoxic-ischemic (HI) insult in human neonates and rodents. Previous results show that D-JNKi, a small peptide inhibitor of c-Jun N-terminal kinase (JNK), strongly reduced HI brain injury in neonatal rats. Here, we investigated the potential neuroprotective effect of D-JNKi in neonatal lipopolysaccharide (LPS)-sensitized HI animals.

Methods Postnatal-day-9 mice received LPS or saline 14 h before being subjected to unilateral carotid artery occlusion and systemic hypoxia (HI), followed by intraperitoneal treatment with D-JNKi, etanercept, D-JNKi+etanercept or vehicle. Brain damage was assessed by staining for MAP2 and MBP; JNK activation and apoptosis by Western blotting, and mRNA expression of TNF-α and TNF-receptor 1 and 2 by qRT-PCR.

Results D-JNKi treatment reduced brain injury after HI in mice. However, D-JNKi had no neuroprotective effect after LPS+HI using the same dose of D-JNKi. Higher doses of D-JNKi moderately reduced brain damage by 30% after LPS+HI. LPS+HI resulted in strong activation of caspase 3 but, in contrast to its effect in HI mice, did not significantly affect the intrinsic route of apoptosis: *i.e.* mitochondrial JNK phosphorylation, mitochondrial Bcl-2/Bcl-xL levels or cytochrome *c* release. Notably, LPS+HI led to increased TNF-α expression and caspase 8 activation (markers of the extrinsic route of apoptosis). These parameters were, however, not inhibited by D-JNKi. Moreover, inhibiting TNF-α by etanercept did not reduce cerebral damage after LPS+HI, and even nullified the neuroprotective effect of D-JNKi when given in combination.

Conclusion Our data indicate that under inflammatory conditions, cerebral cell death is mainly mediated by the extrinsic instead of the intrinsic route of apoptosis. We propose that the extrinsic apoptotic pathway is activated by other death receptor ligands than TNF-α. We previously showed that JNK-regulated mitochondrial damage is the key target of D-JNKi treatment after HI only. Due to switch in the use of apoptotic pathway in the presence of sensitization, treatment with D-JNKi loses its neuroprotective effect. The moderate protection observed when using high doses of D-JNKi after LPS+HI might be mediated via increased TNF-R2 expression known to promote cell survival instead of inhibiting intrinsic apoptosis.

Introduction

Neonatal encephalopathy due to perinatal asphyxia or neonatal hypoxia-ischemia (HI) is a severe condition associated with high mortality and morbidity, affecting 2-6 per 1000 live-born term newborns in Western countries.[1-5] Besides intrapartum sentinel events such as uterine rupture, placental abruption and cord prolapse, other well-known risk factors for neonatal HI are maternal fever and chorioamnionitis.[6-8] The combined exposure to neonatal HI and an antenatal infection dramatically increases the risk of a worse outcome such as spastic cerebral palsy.[9-12] The sensitizing effect of an infection on HI-induced brain damage has also been shown in animal studies in which lipopolysaccharide (LPS) is often used to induce the inflammatory response.[13-15] At this moment treatment options for neonates who face a HI insult are scarce. Importantly, it has been suggested that the only clinically-applied protective strategy for HI brain damage, hypothermia, has no or only a limited effect when the HI insult is preceded by inflammation.[16,17] Understanding the mechanisms involved in the sensitizing effect of inflammation on HI-induced brain damage is therefore crucial, since this may lead to development of new treatment options for neonates that face HI combined with inflammation.

Our previous studies showed that inhibition of the c-Jun N-terminal protein kinase (JNK) pathway results in a strong neuroprotective effect after HI in a neonatal rat model.[18-20] To inhibit JNK we used small peptides L-JNKi and D-JNKi coupled to the protein transduction sequence of HIV-TAT. Our study showed that D-JNKi treatment preserved mitochondrial integrity and thereby strongly reduced induction of apoptotic cell death and the cerebral inflammatory response after HI resulting in long-term anatomical and functional improvements. JNK is a serine/threonine protein kinase belonging to the mitogen-activated protein kinase (MAPK) family and is activated during stress and cellular damage. JNK activation results in the phosphorylation of its downstream substrates, including c-Jun, the dominant component of transcription factor activator protein (AP)-1. AP-1 regulates transcription of multiple genes involved in *e.g.* inflammation, cell survival and apoptosis. Furthermore, mitochondrial JNK can directly promote apoptosis via phosphorylation of pro- and anti-apoptotic mitochondrial proteins (*e.g.* Bcl-2, Bcl-xL, Bad, Bid). Moreover, there are indications that JNK is involved in stabilization of mitochondrial p53 leading to enhanced apoptosis.[21-25] We and others have shown that an inflammatory stimulus prior to HI greatly influences the pattern and timing of brain injury and the extent of neuroinflammation.[14] (Bonestroo et al. submitted). These data may imply that the efficacy of these promising neuroprotective strategies emerging from available animal studies involving HI, could be less when HI is preceded by inflammation.

The aim of the present study was to investigate the neuroprotective effect of D-JNKi and the underlying mechanisms on brain injury including the role of tumor necrosis factor-α (TNF- α) in a neonatal HI model using LPS-sensitized mice.

Materials and Methods

Animals

All experiments were performed according to international guidelines and were approved by the local experimental animal committee of the University Medical Center Utrecht (DEC-ABC, Utrecht, The Netherlands). At postnatal day 9 (P9), C57Bl/6 mice pups were anesthetized with isoflurane (4% induction, 2% maintenance) for <5 min during which the right common carotid artery was exposed and occluded by thermo-cauterization. Xylocaine (100 mg/ml, AstraZeneca, Zoetermeer, the Netherlands) was applied and incision was closed. Pups recovered for at least 1 h before undergoing systemic hypoxia for 45 min at 10% O_2 in N_2. Sham-control animals underwent anesthesia and incision only. LPS+HI animals received an intraperitoneal (i.p.) injection of lipopolysaccharide (LPS; List biological Laboratories, Campbell, CA) at a dose of 0.5 mg/kg 14 h before surgery. Pups of both sexes were used and we did not observe any sex differences in any of the measured parameters.

D-JNKi (dqsrpvqpflnlttprlpr-pp-rrrqrrkkrg: composed of all D-amino acids in *retro-inverso* form with underlined the amino acids representing the HIV-TAT shuttle domain) was synthesized at W.M. Keck facility (Yale University, New Haven, CT, USA). D-JNKi was dissolved in PBS and administered i.p. at 10 or 20 mg/kg direct after the HI insult (T0). The TNF-α inhibitor etanercept (Pfizer, Dublin, Ireland) was dissolved in saline and administered i.p. at 5 or 20 mg/kg at T0. PBS or saline were used as respective vehicle solutions.

Histology

Animals were sacrificed by pentobarbital overdose at 7 or 28 days after HI followed by transcardial perfusion with 4% paraformaldehyde (PFA) in PBS. Brains were post-fixed in PFA and embedded in paraffin. Coronal paraffin brain sections (8 µm) were cut at hippocampal level (equivalent to -1.28 mm from bregma in adult mice). Deparaffinized sections were incubated with mouse anti-microtubule-associated protein 2 (MAP2; Sigma-Aldrich, Steinheim, Germany) and mouse-anti-myelin basic protein (MBP; Sternberger Monoclonals Incorporated, Lutherville, MD) antibodies followed by biotinylated horse anti-mouse antibody (Vector Laboratories, Burlingame, CA). Visualization was performed using Vectastain ABC kit (Vector Laboratories) and diaminobenzamidine. Full-section images were captured with a Nikon D1 digital camera (Nikon, Tokyo, Japan). Brain areas were manually outlined using image processing tools in Adobe Photoshop CS5 (Adobe Systems Inc., San Jose, CA) or ImageJ software (Rasband WS, Image J, US National Institutes of Health, Bethesda, MD; http://rsb.info.nih.gov/ij/). Ipsilateral MAP2 or MBP loss was calculated as 1-(area ipsilateral positive staining/area contralateral positive staining) x 100%.

Western blotting

Animals were sacrificed by decapitation at 3, 24, 48 or 72 h post-insult. Cerebellum was removed and contra- and ipsilateral brain hemispheres were separately frozen in liquid

nitrogen. Hemispheres were pulverized using a liquid nitrogen-cooled mortar and pestle, and stored at -80 °C. Cytosolic and mitochondrial protein fractions were prepared from pulverized whole contra- and ipsilateral hemispheres as extensively described previously.[26] Similar amounts of protein for each sample were separated by SDS-PAGE, transferred to Hybond-C membranes (Amersham, Buckinghamshire, UK) and incubated with mouse-anti-HSP70 (Stressgen biotechnologies), mouse-anti-cytochrome *c* (BD Biosciences Pharmingen), rabbit-anti-cleaved-caspase 3, rabbit-anti-phospho (P)-JNK, rabbit-anti-JNK, rabbit-anti-Bcl-2, rabbit-anti-Bcl-xL (all Cell Signaling), rabbit-anti-cleaved-caspase 8 and goat-anti-β-actin (both Santa Cruz Biotechnology), followed by peroxidase-labeled secondary antibodies. Signal was visualized using chemiluminescence by WesternBright Quantum HRP substrate (Advanstra, Menlo Park, CA) and Proxima 2750T (Isogen life science, de Meern, The Netherlands) and was analyzed using image processing tools in ImageJ software. For loading control, cytosolic protein membranes were reprobed with β-actin. Previous results showed that mitochondrial-specific markers like COX-IV were affected by HI. Therefore we reprobed mitochondrial protein membranes with β-actin since β-actin staining correlated with protein loading observed by Ponceau S staining of the mitochondrial membranes.

Quantitative real time reverse transcriptase PCR

Total RNA was isolated from pulverized hemispheres (see above at Western blotting) using TRIzol® (Invitrogen, Paisley, UK) according to the manufacturer's protocol. cDNA was synthesized with SuperScript Reverse Transcriptase (Invitrogen). PCR was performed using the iQ5 Real-Time PCR Detection System (Bio-Rad Laboratories, Veenendaal, The Netherlands) using primers for TNF-α (forward: GCGGTGCCTATGTCTCAG; reverse: GCCATTTGGGAACTTCTCATC), TNF-receptor (R)1 (forward: TGAGGAGTGTATGAAGTTGTG; reverse: CTGATGAAGATAAAGGATAGAAGG) and TNF-R2 (forward: TCAGCCAGAGCCCACAAG; reverse: TTCACCAGTCCTAACATCAGC). To confirm appropriate amplification, the size of PCR products was verified on gel. Data were individually normalized to the mean of the relative expression of GAPDH (forward: TGAAGCAGGCATCTGAGGG; reverse: CGAAGGTGGAAGAGTGGGAG).

Statistical analysis

All analyses were performed in a blinded setup. All data are expressed as mean ± SEM and were analyzed by t-test or one-way ANOVA with Bonferroni post-tests.

Results

Short- and long-term effects of D-JNKi treatment on HI brain damage

We previously showed the neuroprotective effect of D-JNKi treatment in a neonatal *rat* model of severe HI brain damage.[18] Here we investigated whether D-JNKi was also neuroprotective in a neonatal *mouse* model of mild HI induced brain damage. HI was induced in P9 mice

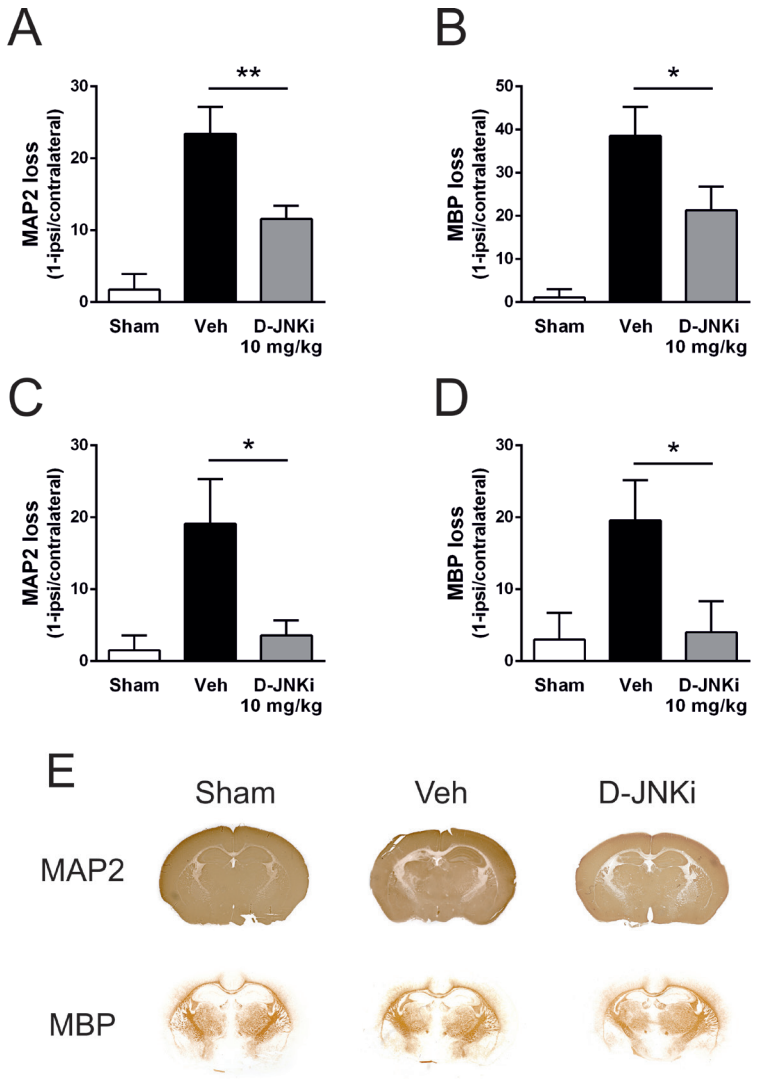

Figure 1: Effect of D-JNKi treatment on HI-induced gray and white matter damage in neonatal mice.

Mice were subjected to sham-operation (Sham) or HI at P9. HI mouse pups were treated with vehicle (Veh) or D-JNKi (10 mg/kg) at 0 h after HI. Cerebral gray and white matter injury were assessed by analyzing staining for microtubule-associated-protein 2 (MAP2) (**A**, **C, E**), and myelin basic protein (MBP) (**B, D**, **E**) respectively, in the contra- and ipsilateral hemisphere at 7 days (**A**, **B**, **E**) or 28 days (**C**, **D**) post-insult. No significant MAP2 or MBP loss was observed in the contralateral hemisphere of HI animals or in sham-operated animals. MAP2 and MBP loss are expressed as ratio ipsi-/contralateral MAP2- or MBP-positive area in the above described experimental groups. **E:** Representative photographs of MAP2 and MBP staining in sham-operated animals and HI animals after vehicle or D-JNKi treatment at day 7 post-insult. Sham n=8, Veh n=11-12, D-JNKi n=8-14 animals per group. Data were analyzed by one-way ANOVA with Bonferroni post-tests. Data represent mean ± SEM. * p <0.05, ** p <0.01 D-JNKi vs vehicle treated animals.

and resulted in neuronal damage limited to the ipsilateral hippocampal area with 23.4 ± 3.7% MAP2 loss and 38.5 ± 6.8% MBP loss at 7 days post-insult (Fig 1A, B, E). D-JNKi was administered i.p. in a dose of 10 mg/kg, based on the neuroprotective effects observed earlier in the rat model.[18] Treatment with 10 mg/kg of D-JNKi administered directly after HI significantly reduced short-term neuronal and white matter damage by 51% and 45% compared to vehicle-treated mice at 7 days post-insult (Fig 1A, B, E). Additionally, D-JNKi treatment resulted in long-lasting neuroprotection as it induced 81% and 80% reduction in MAP2 loss and MBP loss respectively compared to vehicle-treated mice at 28 days post-HI (Fig 1C, D).

Short- and long-term effects of D-JNKi treatment on HI brain damage in LPS-sensitized mice

Next, we determined whether D-JNKi treatment was also neuroprotective in mice subjected to LPS-sensitization in combination with HI. Mouse pups were injected with LPS (0.5 mg/kg) 14 h before HI and received an i.p. injection of D-JNKi (10 mg/kg) or vehicle directly after HI. Seven days after subjection of P9 mice to LPS+HI, we observed an increase in gray and white matter damage compared to mice subjected to HI only (39.4 ± 5.4% vs 23.4 ± 3.7% MAP2 loss and 53.1 ± 6.5% vs 38.5 ± 6.8 % MBP loss; LPS+HI vs HI) (Fig 1A, B vs 2A, B). Remarkably, D-JNKi treatment did not reduce cerebral MAP2 or MBP loss after LPS+HI as observed 7 days post-insult (Fig 2A, B, E). Also at 28 days post-insult, D-JNKi treatment did not improve histological outcome after LPS+HI (Fig 2C, D). Since LPS injection prior to HI increased the amount of brain damage, we increased the initial dosage of D-JNKi from 10 to 20 mg/kg. Treatment with this higher dose of D-JNKi showed moderate neuroprotective effects and reduced ipsilateral MAP2 and MBP loss by 29% compared to vehicle-treated animals at 7 days post-insult (Fig 3A-C).

Effect of D-JNKi treatment on the intrinsic apoptotic pathway in LPS-sensitized mice after HI

Next, we set out to investigate the underlying mechanism why D-JNKi was not effective in our LPS-sensitized HI model. First we investigated whether D-JNKi interfered in a different way with apoptosis. To study the effect of D-JNKi on cell death pathways after LPS+HI, we first assessed which time point after LPS+HI was optimal to determine the early cellular stress response and apoptotic cascade. The data in figure 4A and B together show that LPS+HI induced a strong increase in ipsilateral HSP70 levels at 24-48 h post-insult and induced clear cleavage of caspase 3 at 24 h post-insult compared to sham controls. HSP70 and cleaved caspase 3 levels in the contralateral hemispheres were equal to levels in sham-control animals (data not shown).

In our previous study we discovered that D-JNKi potently reduced cerebral apoptotic cell death by reducing HI-induced phosphorylation of mitochondrial JNK, which subsequently led to a preservation of mitochondrial integrity and inhibition of the intrinsic route of apoptosis

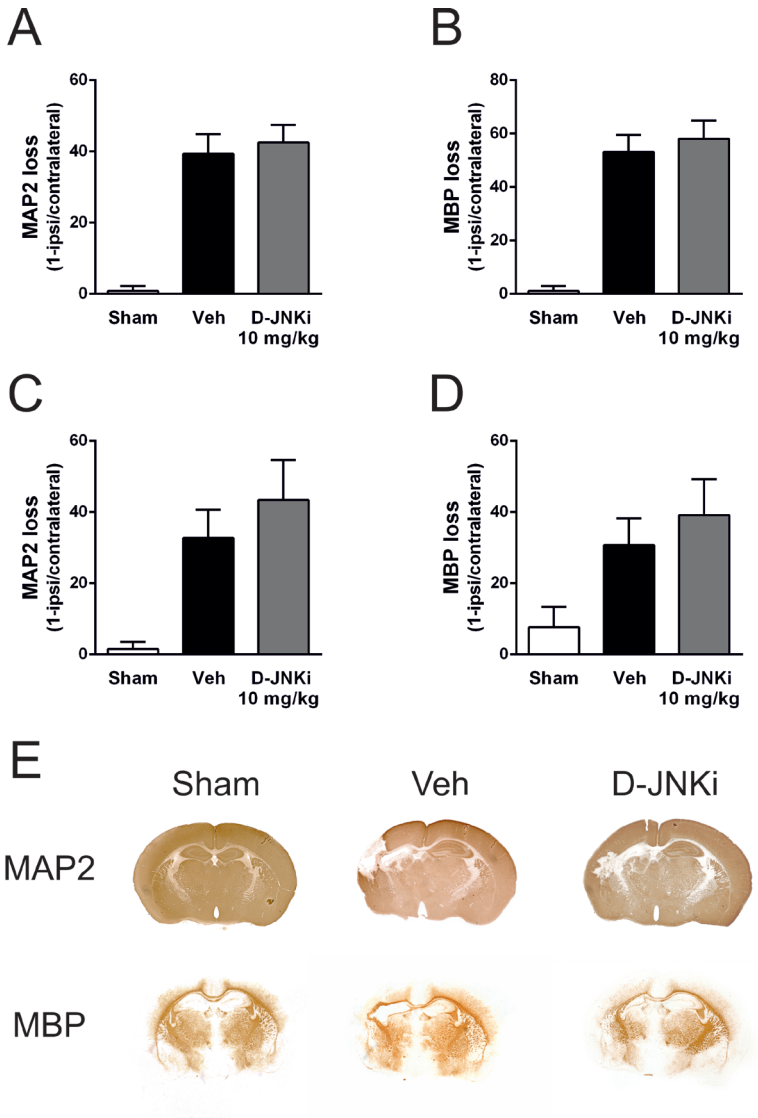

Figure 2: Effect of D-JNKi treatment on gray and white matter damage after LPS-sensitized neonatal HI.

Mice were subjected to sham-operation (Sham) or LPS+HI at P9. LPS was injected intraperitoneally 14 h before the HI insult. LPS+HI mouse pups were treated with vehicle (Veh) or D-JNKi (10 mg/kg) at 0 h post-insult. Cerebral gray and white matter injury were assessed by analyzing staining for microtubule-associated-protein 2 (MAP2) (**A**, **C**, **E**), and myelin basic protein (MBP) (**B**, **D**, **E**) respectively, in the contra- and ipsilateral hemisphere at 7 days (**A**, **B**, **E**) or 28 days (**C**, **D**) post-insult. No significant MAP2 or MBP loss was observed in the contralateral hemisphere of LPS+HI animals or in sham-operated animals. MAP2 and MBP loss are expressed as ratio ipsi-/contralateral MAP2- or MBP-positive area in the above described experimental groups. **E:** Representative photographs of MAP2 and MBP staining in sham-operated animals and LPS+HI animals after vehicle or D-JNKi treatment at day 7 post-insult. Sham n=8-12, Veh n=10-18, D-JNKi n=8-16 animals per group. Data were analyzed by one-way ANOVA with Bonferroni post-tests. Data represent mean ± SEM.

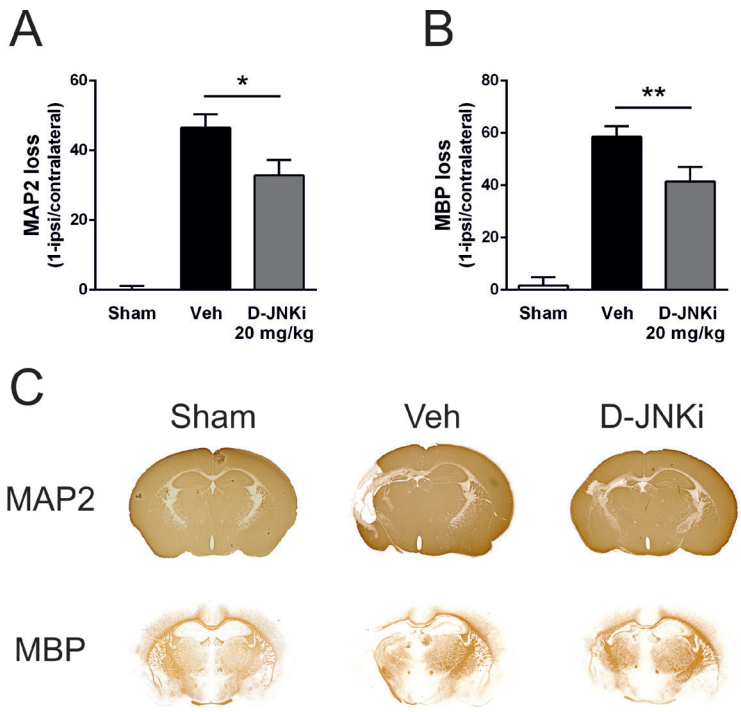

Figure 3: Effect of a higher dose D-JNKi treatment on brain damage after LPS-sensitized neonatal HI.
Mice were subjected to sham-operation (Sham) or LPS+HI at P9. LPS was injected intraperitoneally 14 h before the HI insult. LPS+HI mouse pups were treated with vehicle (Veh) or D-JNKi (20 mg/kg) at 0 h post-insult. Cerebral gray and white matter injury were assessed by analyzing staining for microtubule-associated-protein 2 (MAP2) (**A**). and myelin basic protein (MBP) (**B**) respectively, in the contra- and ipsilateral hemisphere at 7 days post-insult. No significant MAP2 or MBP loss was observed in the contralateral hemisphere of LPS+HI animals or in sham-operated animals. MAP2 and MBP loss are expressed as ratio ipsi-/contralateral MAP2- or MBP-positive area in the above described experimental groups. Sham n=10, Veh n=25, D-JNKi n=26 animals per group. Data were analyzed by one-way ANOVA with Bonferroni post-tests. Data represent mean ± SEM. * p <0.05, ** p <0.01 D-JNKi vs vehicle treated animals. **C:** Representative photographs of MAP2 and MBP staining in sham-operated animals and HI animals after vehicle or D-JNKi treatment.

(*e.g.* the release of cytochrome *c* and caspase 3 activation). Therefore we next assessed the effect of LPS+HI and D-JNKi treatment on mitochondrial phosphorylated (P-)JNK levels at 3 h post-insult (Fig 4C, D). The antibody we used against P-JNK1-3 detects both 46 and 54 kDa JNK isoforms. LPS+HI did not induce phosphorylation of mitochondrial JNK and did not affect total JNK levels compared to sham-control animals (Fig 4C, D). D-JNKi treatment had no effect on P-JNK or total JNK levels compared to vehicle treatment (Fig 4C, D).

Another protective mechanism contributing to neuroprotection after D-JNKi treatment in the HI model is the increase in mitochondrial expression of the anti-apoptotic proteins Bcl-2 and Bcl-xL.[18] Figure 4E and F show that LPS+HI did not affect the expression of mitochondrial

Bcl-2 or Bcl-xL proteins in the ipsilateral hemisphere at 24 h post-insult (Fig 4E, F). In addition, D-JNKi treatment did not affect mitochondrial Bcl-2 and Bcl-xL levels (Fig 4E, F).

Next, we determined the effect of D-JNKi treatment on two hallmarks of apoptosis: release of cytochrome *c* from the mitochondria into the cytosol and activation of caspase 3 *at 24 h* after LPS+HI (Fig 4G, H). LPS+HI resulted in a small, but non-significant (*p* 0.07) increase in cytosolic cytochrome *c* at 24 h after the insult compared to sham littermates (Fig 4G). D-JNKi treatment did not alter these low cytosolic cytochrome *c* levels after LPS+HI compared to vehicle treatment (Fig 4G). LPS+HI induced a clear activation/cleavage of caspase 3 which was not significantly reduced after D-JNKi treatment in the ipsilateral hemisphere at 24 h post-insult (Fig 4H).

The data presented in figure 4 indicate that when HI is preceded by inflammation the contribution of molecular pathways such as JNK to cell death and the development of HI-induced brain damage changes fundamentally.

Figure 4: Effects of LPS-sensitized HI and D-JNKi treatment on markers of cell damage and apoptosis. ➔

Mice were subjected to sham-operation (Sham) or LPS+HI at P9. LPS was injected intraperitoneally 14 h before the HI insult. **A**, **B**: Cytosolic fractions of ipsilateral hemispheres were analyzed by Western blotting for the expression of HSP70 (**A**) and cleaved caspase 3 (**B**) at 3, 24, 48 and 72 h post insult in LPS+HI and sham-control animals. **C**-**H**: LPS+HI mouse pups were treated with vehicle (Veh) or D-JNKi (20 mg/kg) at 0 h post-insult. **C**-**F**: Mitochondrial fractions of ipsilateral hemispheres were analyzed by Western Blot at 3 h post-insult for expression of phosphorylated (P)-JNK or total JNK 46 kDa (**C**) and 54 kDa (**D**) JNK isoform, and at 24 h post-insult for the expression of Bcl-2 (**E**) and Bcl-xL (**F**) in sham-operated, vehicle and D-JNKi treated LPS+HI animals. **G**-**H**: Cytosolic fractions of ipsilateral hemispheres were analyzed by Western Blot at 24 h post-insult for expression of cytochrome *c* (**G**) and cleaved caspase 3 (**H**) in sham-operated, vehicle and D-JNKi treated LPS+HI animals. There were no significant differences in the contralateral hemispheres levels of LPS+HI(-Veh) or LPS+HI-D-JNKi animals compared to sham control levels, for any of the measured parameters. Sham n=4-6, Veh n=4-8, D-JNKi n=4 animals per group. Data were analyzed by one-way ANOVA with Bonferroni post-tests. Data represent mean ± SEM. * p <0.05, ** p <0.01, *** p <0.001. Levels are relative to levels in sham-operated animals which were put at 1. A.U.: Arbitrary units; ns: non-significant.

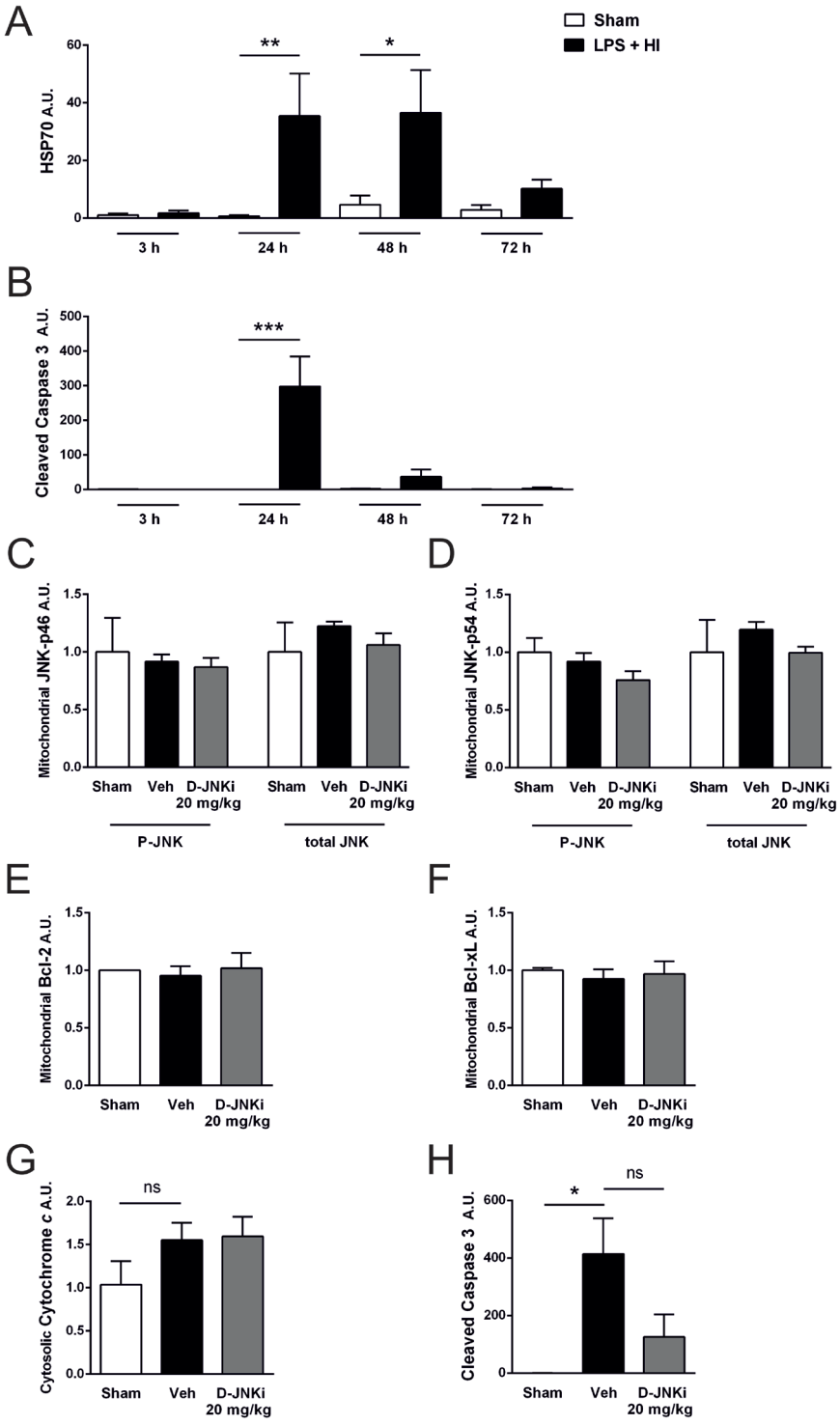
A
Sham
LPS + HI
HSP70 A.U.
60
40
20
0
**
*
3 h
24 h
48 h
72 h
B
Cleaved Caspase 3 A.U.
500
400
300
200
100
0
***
3 h
24 h
48 h
72 h
C
Mitochondrial JNK-p46 A.U.
1.5
1.0
0.5
0.0
Sham
Veh
D-JNKi 20 mg/kg
Sham
Veh
D-JNKi 20 mg/kg
P-JNK
total JNK
D
Mitochondrial JNK-p54 A.U.
1.5
1.0
0.5
0.0
Sham
Veh
D-JNKi 20 mg/kg
Sham
Veh
D-JNKi 20 mg/kg
P-JNK
total JNK
E
Mitochondrial Bcl-2 A.U.
1.5
1.0
0.5
0.0
Sham
Veh
D-JNKi 20 mg/kg
F
Mitochondrial Bcl-xL A.U.
1.5
1.0
0.5
0.0
Sham
Veh
D-JNKi 20 mg/kg
G
Cytosolic Cytochrome c A.U.
2.0
1.5
1.0
0.5
0.0
ns
Sham
Veh
D-JNKi 20 mg/kg
H
Cleaved Caspase 3 A.U.
600
400
200
0
*
ns
Sham
Veh
D-JNKi 20 mg/kg

Activation of the extrinsic route of apoptosis in LPS-sensitized mice after HI

Our data show that LPS+HI does not induce mitochondrial JNK activation and has no effect on the expression of mitochondrial anti-apoptotic proteins nor on the release of cytochrome c into the cytosol. Therefore we suggest that the high level of cerebral caspase 3 activation after LPS+HI might not result from activation of the *intrinsic* route of apoptosis, but may possibly involve activation of the *extrinsic* route of apoptosis. Hence, we determined expression of TNF-α, an important agonist of the death receptor TNF-R1, and cleaved caspase 8 which is activated directly downstream of the death receptors in animals exposed to LPS+HI vs sham control littermates. The data in figure 5A demonstrate that TNF-α mRNA expression was upregulated by app. 40 fold in the ipsilateral hemisphere after LPS+HI compared to levels in sham control littermates at 3 h post-insult (Fig 5A). The increased expression of TNF-α was still present at 72 h post-insult (Fig 5A). Additionally, LPS+HI induced a app. 5 fold increase in cleaved caspase 8 expression in the ipsilateral hemisphere at 3 h post-insult (Fig 5B), whereas HI alone resulted in a app. 3 fold increase in caspase 8 activation compared to sham-control levels (data not shown). Levels of TNF-α mRNA and cleaved caspase 8 in the contralateral hemisphere were equal to levels in sham-control animals (data not shown). The data in figure 5 indicate that the extrinsic route of apoptosis is operative in the brain after LPS+HI.

Importantly, however, figure 5C shows that treatment with D-JNKi did not affect the expression of TNF-α mRNA at 3 h post-insult compared to vehicle treatment. Also at 24 and 72 h post-insult, no significant changes in TNF-α expression were observed between D-JNKi- and vehicle-treated animals (data not shown). Moreover, D-JNKi treatment did not reduce caspase 8 activation at 3 h after LPS+HI (Fig 5D). Levels of cleaved caspase 8 and TNF-α mRNA in the contralateral hemisphere were equal to levels in sham-control animals (data not shown).

Role of TNF-α in LPS-sensitized HI-induced brain damage

To define the contribution of TNF-α and the *extrinsic* apoptotic pathway to the development of LPS-sensitized HI brain damage and the effect of D-JNKi, pups were treated i.p. directly after the HI insult with etanercept (5 or 20 mg/kg), or with a combination of etanercept and D-JNKi (20 mg/kg). Etanercept is a recombinant human IgG_1 TNF-receptor 2 fusion protein that binds TNF-α and competitively inhibits the binding of TNF-α to its receptors TNF-R1 and -R2. Figure 6A and B show that treatment with etanercept (5 or 20 mg/kg) directly post-insult did not significantly reduce cerebral gray or white matter injury after LPS+HI compared to vehicle treatment.

Interestingly, when animals were treated with a combination of etanercept (5 mg/kg) and D-JNKi peptide (20 mg/kg), the neuroprotective effect of the high dose D-JNKi was completely abolished (Fig 6C, D). These data indicate that the increased cerebral expression of TNF-α after LPS+HI contributes to the neuroprotective effect of D-JNKi treatment which may suggest that TNF-α is more a survival signal than a damage-inducing signal under these circumstances.

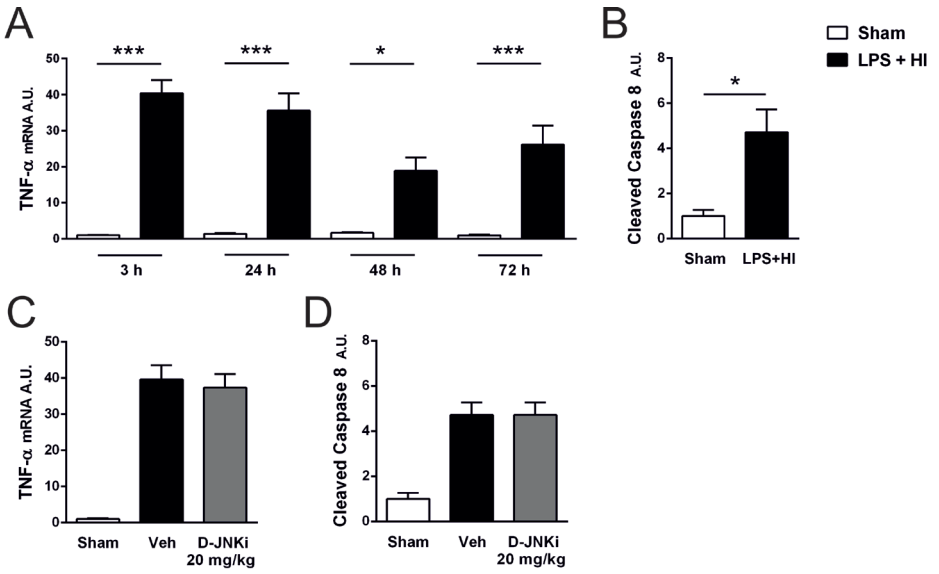

Figure 5: Effects of LPS-sensitized HI and D-JNKi treatment on TNF-α expression and caspase 8 activation.

Mice were subjected to sham-operation (Sham) or LPS+HI at P9. LPS was injected intraperitoneally 14 h before the HI insult. **A**, **C**: TNF-α mRNA expression was determined by quantitative real time RT-PCR in the ipsilateral hemisphere of LPS+HI animals and sham-controls at 3, 24, 48 and 72 h post-insult (**A**) and in LPS+HI mouse pups treated with vehicle (Veh) or D-JNKi (20 mg/kg) at 0 h post-insult (**C**). **B, D**: Cytosolic fractions of ipsilateral hemispheres were analyzed by Western blotting for the expression of cleaved caspase 8 at 3 h post-insult in LPS+HI and sham control animals (**B**) and in LPS+HI mouse pups treated with vehicle (Veh) or D-JNKi (20 mg/kg) at 0 h post-insult (**D**). There were no significant differences in the contralateral hemispheres levels of LPS+HI animals compared to sham control levels for TNF-α expression or caspase 8 activation. Sham n=4-6, Veh n=4-8, D-JNKi n=5 animals per group. Data were analyzed by one-way ANOVA with Bonferroni post-tests (**A**, **C**, **D**) and t-test (**B**) and Data represent mean ± SEM. * p <0.05, *** p <0.001 LPS+HI vs sham control animals. Levels are relative to levels in sham-operated animals which were put at 1. A.U.: Arbitrary units.

Binding of TNF-α to the death receptor TNF-R1 induces cell death, whereas binding of TNF-α to TNF-R2 results in neuronal survival. To assess the effect of LPS+HI on the TNF-R1 and -R2 balance, we determined the expression of both receptors from 3-72 h post-insult in vehicle-treated animals. LPS+HI increased ipsilateral TNF-R1 mRNA expression by 6-fold as early as 24 h post-insult which was maintained to at least 72 h post-HI compared to sham-controls (Fig 7A). The ipsilateral expression of TNF-R2 gradually increased over time; from a 5-fold increase at 24 h up to almost 10-fold increase at 72 h post-insult in LPS+HI vs sham-control littermates (Fig 7B).

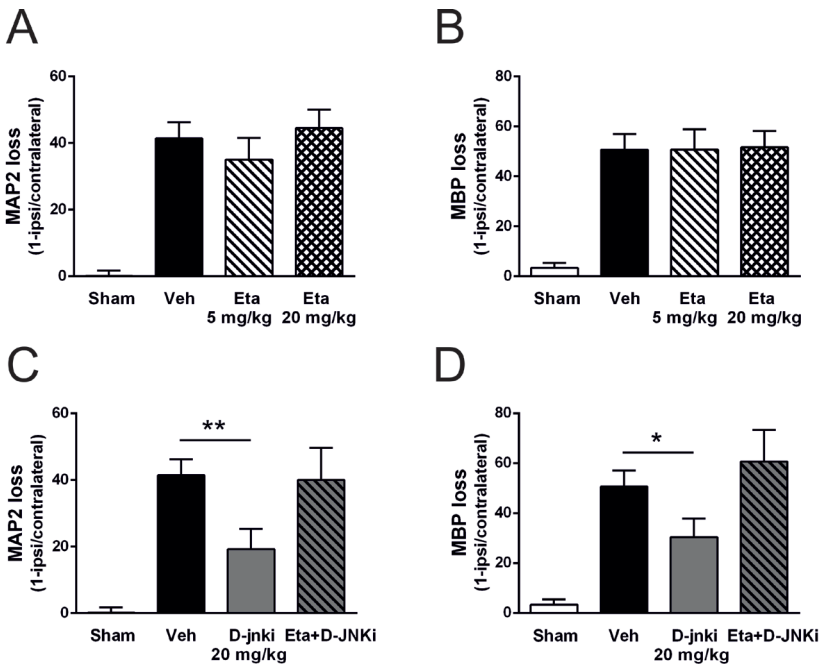

Figure 6: Effect of etanercept treatment on brain damage after LPS-sensitized neonatal HI. Mice were subjected to sham-operation (Sham) or LPS+HI at P9. LPS was injected intraperitoneally 14 h before the HI insult. LPS+HI mouse pups were treated with vehicle (Veh), etanercept (Eta) (5-20 mg/kg) (**A**, **B**), D-JNKi (20 mg/kg) or DJNKi+etanercept (5 mg/kg) (**C**, **D**) at 0 h post-insult. Cerebral gray and white matter injury were assessed by analyzing staining for microtubule-associated-protein 2 (MAP2) (**A**, **C**), and myelin basic protein (MBP) (**B**, **C**) respectively, in the contra- and ipsilateral hemisphere at 7 days post-insult. No significant MAP2 or MBP loss was observed in the contralateral hemisphere of LPS+HI animals or in sham-operated animals. MAP2 and MBP loss are expressed as ratio ipsi-/contralateral MAP2- or MBP-positive area in the above described experimental groups. Sham n=10, Veh n=10, Eta 5 mg/kg n=10, Eta 20 mg/kg n=8, D-JNKi n=7, D-JNKi+Eta n=7 animals per group. Data were analyzed by one-way ANOVA with Bonferroni post-tests. Data represent mean ± SEM. * p <0.05, ** p <0.01 D-JNKi vs vehicle treated animals.

Next, we determined whether D-JNKi treatment affected the expression of TNF-R1 and TNF-R2 at 24, 48 and 72 h after LPS+HI. D-JNKi treatment had no significant effect on TNF-R1 expression at 3, 24 or 72 h post-insult (Fig 7C, showing data of 24 h post-insult). D-JNKi increased TNF-R2 expression 2.4 fold (p 0.06) in the ipsilateral hemisphere compared to vehicle treatment at 72 h post-insult (Fig 7D). Expression levels of TNF-α, TNF-R1 and TNF-R2 in the contralateral hemisphere were equal to levels in sham-control animals (data not shown).

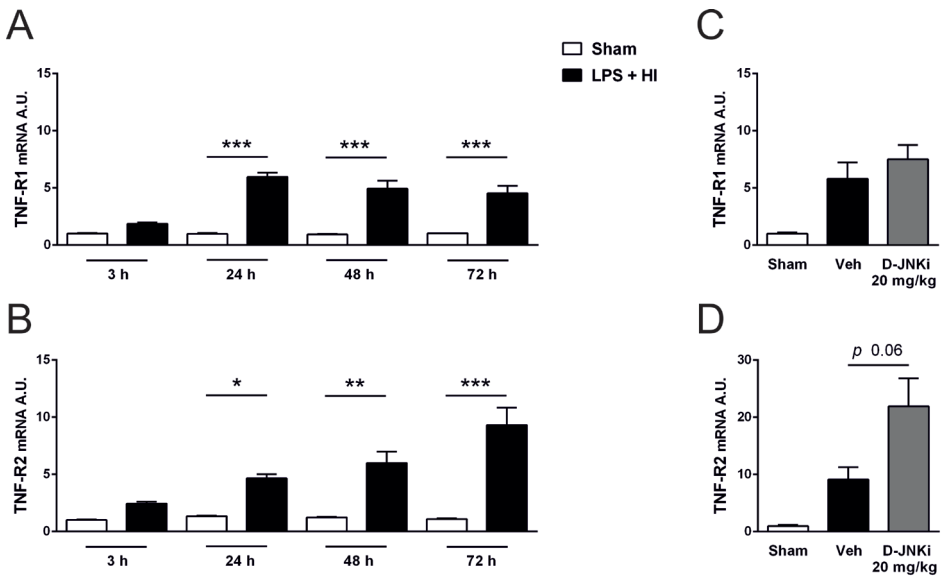

Figure 7: Effects of LPS-sensitized HI and D-JNKi treatment on expression of TNF-R1 and TNF-R2. Mice were subjected to sham-operation (Sham) or LPS+HI at P9. LPS was injected intraperitoneally 14 h before the HI insult. **A**, **B**: TNF-R1 and TNF-R2 mRNA expression was determined by quantitative real time RT-PCR in the ipsilateral hemisphere of LPS+HI animals and sham-controls at 3, 24, 48 and 72 h post-insult. **C**, **D**: LPS+HI mouse pups were treated with vehicle (Veh) or D-JNKi (20 mg/kg) at 0 h post-insult. The mRNA expression of TNF-α, TNF-R1 and -R2 were determined by quantitative real time RT-PCR in the ipsilateral hemisphere of sham operated, vehicle and D-JNKi treated LPS+HI animals. **C**, **D**: mRNA expression of TNF-R1 at 24 h (**C**) and TNF-R2 (**D**) at 72 h post-insult. There were no significant differences in the contralateral hemispheres levels of LPS+HI animals compared to sham control levels for TNF-α, TNF-R1 or TNF-R2 expression. Sham n=6, Veh n=4, D-JNKi n=6 animals per group. Data were analyzed by one-way ANOVA with Bonferroni post-tests. Data represent mean ± SEM. * p <0.05, ** p <0.01, *** p <0.001. Levels are relative to levels in sham-operated animals which were put at 1. A.U.: Arbitrary units.

Discussion

Apoptosis can be activated via two main routes: the intrinsic mitochondria-mediated route and the extrinsic death receptor-mediated pathway. Both pathways activate the proteolytic caspase cascade that eventually leads to the activation of caspase 3, the executioner of apoptosis which induces DNA fragmentation and degradation of nuclear and cytoskeletal proteins.[27] Cellular stress such as HI, activates the intrinsic apoptotic route via multiple intracellular signals which determine the delicate balance between pro- and anti-apoptotic proteins residing at the mitochondrial membrane. Disturbance of this balance leads to permeabilization of the outer mitochondrial membrane with the subsequent release of pro-apoptotic mitochondrial proteins, like cytochrome *c* into the cytosol. Cytochrome *c*, when released into the cytosol, binds to apoptosis protease activating factor (Apaf)-1 and pro-caspase 9 as part of the apoptosome, leading to activation of caspase 9 and of caspase 3.

The extrinsic route of apoptosis is activated by binding of death ligands *e.g.* TNF-α, Fas ligand, TNF related apoptosis-inducing ligand (TRAIL), Apo3 or 2L to death receptors TNF-R1, Fas, TRAIL1, death receptor (DR)3 and DR5 respectively.[28,29] Activation of the death receptors results in the formation of the intracellular death-inducing signaling complex (DISC), responsible for activation of caspase 8 with subsequent direct downstream activation of caspase 3.[27,30]

Previously we and others clearly showed that cerebral HI in the neonatal brain activates the intrinsic apoptotic route: mitochondrial integrity was affected (determined by reduction in ATP levels and free radical formation), mitochondrial proteins like cytochrome *c*, apoptosis-inducing factor (AIF) and Smac/DIABLO were released from the mitochondria, and caspase 9 and 3 were strongly activated after HI in neonatal rats and mice.[18-20,25,26,31-34]

Recently we demonstrated in a rat model that HI induces activation of the MAPK JNK at the mitochondrial membrane. Mitochondrial P-JNK was shown to be an important regulator of apoptotic cell death, presumably by disturbing the mitochondrial pro- and anti-apoptotic protein equilibrium. Our previous study clearly demonstrated that the protective mechanism of D-JNKi after HI was associated with complete inhibition of HI-induced phosphorylation of mitochondrial JNK and associated with an upregulation of the anti-apoptotic mitochondrial proteins Bcl-2 and Bcl-xL.[18] We proposed that D-JNKi protected mitochondrial integrity, reducing the release of cytochrome *c* and attenuating activation of apoptosis via the intrinsic pathway. Our study revealed that treatment of neonatal rats after HI with D-JNKi resulted in a >85% reduction in infarct volume.[18]

In the present study we confirm the neuroprotective effects of i.p. D-JNKi treatment (10 mg/kg) after HI in neonatal mice. Neuroprotection in mice was long-lasting as neuronal damage was diminished by app. 80% at 28 days post-insult. However, using the same dose of D-JNKi (10 mg/kg), we did not observe any neuroprotective effect of D-JNKi treatment when LPS was given 14 h before HI in neonatal mice. Increasing the D-JNKi dose from 10 to 20 mg/kg resulted in a moderate neuroprotective effect (app. 30% reduction infarct volume) in LPS+HI mice. To elucidate why D-JNKi treatment was less effective when the animal was in a pro-inflammatory state, we investigated whether pre-administration with LPS led to a switch in the use of the apoptotic pathways.

LPS injection prior to HI resulted in an exacerbation of cerebral damage and a clear activation of caspase 8 and caspase 3. Importantly, we observed a strong increase in cerebral expression of TNF-α from 3-72 h after LPS+HI. In our earlier paper we demonstrated that after HI, TNF-α expression was only slightly increased at 3 and 24 h and normalized to sham-control levels at 48 h post-insult (Bonestroo et al. submitted). The strong upregulation of cerebral TNF-α could be one of the factors responsible for the activation of death receptors, *i.e.* TNF-R1, and subsequently the downstream extrinsic apoptotic pathway after LPS+HI.[35-38] In contrast, TNF-R2 binding to TNF-R2 activates pro-survival signals by *e.g.* upregulating anti-apoptotic factors, increasing anti-inflammatory cytokines and antioxidant enzyme superoxide

dismutase.[36,39-44] A large number of studies have described that cerebral TNF-α expression after an insult is predominantly associated with aggravation of cerebral damage.[45,46] In line, different strategies to inhibit TNF-α have been shown to be neuroprotective in a range of adult and neonatal brain damage models.[20,46-54] Moreover, *in vitro* and *in vivo* studies that investigated inflammatory-sensitization in relation to HI-induced neuronal damage, described TNF-α as a key factor in mediating sensitization: deletion of the TNF gene or TNF-α blockade prevented the inflammation-induced increase in microglia and endothelial activation and neuronal damage.[40,55,56] However, in the literature also a number of studies observed neuroprotective properties of TNF-α.[20,36,38,39,57-63] The apparent discrepancy between the data is probably caused by the balance between activation of TNF-R1 and -R2 is in the various models used.[43,57-59]

To study a possible contribution of TNF-α to brain damage in our model, we investigated the effect of etanercept treatment on lesion size after LPS+HI. Etanercept is a well-described competitive inhibitor of TNF-α.[64] We could not detect a neuroprotective effect of 5 or 20 mg/kg etanercept treatment when the HI insult was preceded by LPS. In line with our current observations, Cai et al. (2003) described that inhibiting TNF-α had no effect on apoptosis or white matter injury in a LPS-induced white matter damage model.[65] In 2009 our group described that treatment with 5 mg/kg etanercept had a moderate neuroprotective effect in neonatal rats after HI only.[20] Adén et al. (2010) administered 20 mg/kg etanercept for multiple times in an inflammation-sensitized neonatal excitotoxic brain damage model and observed a 50% reduction in brain damage.[56] TNF-α is probably involved in the level of sensitization by LPS.[40,55,56] However, since we administered etanercept after the HI insult, we conclude that the direct contribution of TNF-α to neuronal death *after* the LPS+HI insult might be limited.

We initially expected that the increased TNF-α expression was responsible for activation of the extrinsic apoptotic pathway after LPS-sensitized HI. However, since etanercept did not reduce brain damage after LPS+HI other death receptors ligands must be responsible for the extrinsic apoptotic pathway activity, for example Fas ligand, TRAIL, APO2 or 3L. Further research is necessary to clarify the role of these death receptor ligands in the development of brain injury after LPS-sensitized HI.

The group of Yang et al. (2013) reported that LPS+HI results in a rapid and strong activation of nuclear factor κB (NF-κB), a transcription factor that regulates many inflammatory, cell death, and survival target genes.[66] The strong activation of NF-κB in the LPS+HI model might be responsible for the high TNF-α expression and possibly also increases other death receptor ligands after LPS+HI. Furthermore, it is known that the NF-κB pathway can inhibit the JNK pathway via different NF-κB regulated targets.[20, 67-69] Therefore, we suggest that relative high NF-κB activity after LPS+HI could be responsible for the fact that there is no activation of JNK at the mitochondria in this inflammatory model. The lack of mitochondrial

JNK activation after LPS+HI elucidates why inhibiting JNK by using D-JNKi (10 mg/kg) had no neuroprotective effect in this model.

How can we explain the fact that D-JNKi in a higher dose resulted in a moderate reduction in infarct volume after LPS+HI? We show that D-JNKi in this high dose influenced the TNF-receptor balance, by upregulating the expression of especially TNF-R2 at 72 h after LPS+HI. The switch towards an increased TNF-R2 expression might promote neuronal protection by TNF-α and we suggest that this could be one of the mechanisms through which D-JNKi treatment induced moderate neuroprotection after LPS+HI. We observed the D-JNKi induced an increase in TNF-R2 expression only at the late time point (*i.e.* 72 h post-HI), which might explain why this protective mechanism does not lead to strong neuroprotection after D-JNKi, since probably before this time point other detrimental pathways have already been initiated. Our observation that decreasing TNF-α (by etanercept) in D-JNKi-treated animals reduced neuroprotection by D-JNKi treatment is completely in line with the proposed protective mechanism of D-JNKi-induced upregulation of TNF-R2.

Conclusions

In conclusion, in the present study we show that when a HI insult is preceded by inflammation, a switch in cellular death routes may occur. We show here that LPS+HI resulted in activation of the extrinsic apoptotic pathway and hardly of the intrinsic apoptotic pathway. Inhibition of TNF-α, one of the activators of the extrinsic pathway, did not reduce brain damage, suggesting that other cell death ligands are responsible for the activation of the extrinsic apoptotic pathway. Moreover, it may indicate that once the system is sensitized, anti-inflammatory agents like etanercept are no longer effective to halt aggravation of brain damage due to inflammatory sensitization. Treatment with D-JNKi, an inhibitor of the intrinsic mitochondria-regulated pathway, showed only a very moderate protective effect in a high dose in the LPS+HI model. Our data suggest that D-JNKi treatment increased protective TNF-R2 expression thereby promoting TNF-α-induced cell survival after LPS-sensitized HI. Our study as have others, shows that the scarce promising protective treatment options currently investigated for HI brain damage, lose (most of their) effectiveness when inflammation is preceding the insult. These data emphasize the need for alternative therapies when hypoxia-ischemic is associated with inflammation. Hypoxic-ischemic events without inflammation may be treated efficiently with drugs blocking the intrinsic apoptotic pathway. When the patient is in an inflammatory state, alternative drugs such as inhibitors of the extrinsic pathway may be applied. Additional research to unravel the underlying mechanisms involved in the development of brain damage after inflammation-sensitized HI is urgently needed to make a breakthrough in the field of neonatal cerebral neuroprotection to improve quality of life of these vulnerable patients.

References

1. Perlman M, Shah PS. Hypoxic-ischemic encephalopathy: challenges in outcome and prediction. *J Pediatr*. 2011;158:51-4.
2. Ferriero DM. Neonatal brain injury. *N Engl J Med*. 2004;351:1985-1995.
3. Lawn JE, Cousens S, Zupan J, Lancet Neonatal Survival Steering Team. 4 million neonatal deaths: when? Where? Why? *Lancet*. 2005;365:891-900.
4. Spector JM, Daga S. Preventing those so-called stillbirths. *Bull World Health Organ*. 2008;86:315-316.
5. Thornberg E, Thiringer K, Odeback A, Milsom I. Birth asphyxia: incidence, clinical course and outcome in a Swedish population. *Acta Paediatr*. 1995;84:927-932.
6. Grether JK, Nelson KB. Maternal infection and cerebral palsy in infants of normal birth weight. *JAMA*. 1997;278:207-211.
7. Impey L, Greenwood C, MacQuillan K, Reynolds M, Sheil O. Fever in labour and neonatal encephalopathy: a prospective cohort study. *BJOG*. 2001;108:594-597.
8. Badawi N, Kurinczuk JJ, Keogh JM, et al. Antepartum risk factors for newborn encephalopathy: the Western Australian case-control study. *BMJ*. 1998;317:1549-1553.
9. Peebles DM, Wyatt JS. Synergy between antenatal exposure to infection and intrapartum events in causation of perinatal brain injury at term. *BJOG*. 2002;109:737-739.
10. Wu YW, Escobar GJ, Grether JK, Croen LA, Greene JD, Newman TB. Chorioamnionitis and cerebral palsy in term and near-term infants. *JAMA*. 2003;290:2677-2684.
11. Blume HK, Li CI, Loch CM, Koepsell TD. Intrapartum fever and chorioamnionitis as risks for encephalopathy in term newborns: a case-control study. *Dev Med Child Neurol*. 2008;50:19-24.
12. Nelson KB, Grether JK. Potentially asphyxiating conditions and spastic cerebral palsy in infants of normal birth weight. *Am J Obstet Gynecol*. 1998;179:507-513.
13. Eklind S, Mallard C, Leverin AL, et al. Bacterial endotoxin sensitizes the immature brain to hypoxic--ischaemic injury. *Eur J Neurosci*. 2001;13:1101-1106.
14. Mallard C. Innate immune regulation by toll-like receptors in the brain. *ISRN Neurol*. 2012;2012:701950.
15. Wang X, Stridh L, Li W, et al. Lipopolysaccharide sensitizes neonatal hypoxic-ischemic brain injury in a MyD88-dependent manner. *J Immunol*. 2009;183:7471-7477.
16. Wintermark P, Boyd T, Gregas MC, Labrecque M, Hansen A. Placental pathology in asphyxiated newborns meeting the criteria for therapeutic hypothermia. *Am J Obstet Gynecol*. 2010;203:579.1-579.9.
17. Osredkar D, Thoresen M, Maes E, Flatebo T, Elstad M, Sabir H. Hypothermia is not neuroprotective after infection-sensitized neonatal hypoxic-ischemic brain injury. *Resuscitation*. 2014;85:567-572.
18. Nijboer CH, Bonestroo HJ, Zijlstra J, Kavelaars A, Heijnen CJ. Mitochondrial JNK phosphorylation as a novel therapeutic target to inhibit neuroinflammation and apoptosis after neonatal ischemic brain damage. *Neurobiol Dis*. 2013;54:432-444.
19. Nijboer CH, van der Kooij MA, van Bel F, Ohl F, Heijnen CJ, Kavelaars A. Inhibition of the JNK/AP-1 pathway reduces neuronal death and improves behavioral outcome after neonatal hypoxic-ischemic brain injury. *Brain Behav Immun*. 2010;24:812-821.
20. Nijboer CH, Heijnen CJ, Groenendaal F, van Bel F, Kavelaars A. Alternate pathways preserve tumor necrosis factor-alpha production after nuclear factor-kappaB inhibition in neonatal cerebral hypoxia-ischemia. *Stroke*. 2009;40:3362-3368.
21. Fuchs SY, Adler V, Pincus MR, Ronai Z. MEKK1/JNK signaling stabilizes and activates p53. *Proc Natl Acad Sci U S A*. 1998;95:10541-10546.
22. Bogoyevitch MA, Ngoei KR, Zhao TT, Yeap YY, Ng DC. c-Jun N-terminal kinase (JNK) signaling: recent advances and challenges. *Biochim Biophys Acta*. 2010;1804:463-475.

23. Dhanasekaran DN, Reddy EP. JNK signaling in apoptosis. *Oncogene*. 2008;27:6245-6251.
24. Raivich G, Behrens A. Role of the AP-1 transcription factor c-Jun in developing, adult and injured brain. *Prog Neurobiol*. 2006;78:347-363.
25. Nijboer CH, Heijnen CJ, van der Kooij MA, et al. Targeting the p53 pathway to protect the neonatal ischemic brain. *Ann Neurol*. 2011;70:255-264.
26. Nijboer CH, Groenendaal F, Kavelaars A, Hagberg HH, van Bel F, Heijnen CJ. Gender-specific neuroprotection by 2-iminobiotin after hypoxia-ischemia in the neonatal rat via a nitric oxide independent pathway. *J Cereb Blood Flow Metab*. 2007;27:282-292.
27. Elmore S. Apoptosis: a review of programmed cell death. *Toxicol Pathol*. 2007;35:495-516.
28. Lavrik I, Golks A, Krammer PH. Death receptor signaling. *J Cell Sci*. 2005;118:265-267.
29. Kichev A, Rousset CI, Baburamani AA, et al. Tumor necrosis factor-related apoptosis-inducing ligand (TRAIL) signaling and cell death in the immature central nervous system after hypoxia-ischemia and inflammation. *J Biol Chem*. 2014;289:9430-9439.
30. Broughton BR, Reutens DC, Sobey CG. Apoptotic mechanisms after cerebral ischemia. *Stroke*. 2009;40:331-9.
31. Nijboer CH, Heijnen CJ, Groenendaal F, May MJ, van Bel F, Kavelaars A. Strong neuroprotection by inhibition of NF-kappaB after neonatal hypoxia-ischemia involves apoptotic mechanisms but is independent of cytokines. *Stroke*. 2008;39:2129-2137.
32. Nijboer CH, Kavelaars A, Vroon A, Groenendaal F, van Bel F, Heijnen CJ. Low endogenous G-protein-coupled receptor kinase 2 sensitizes the immature brain to hypoxia-ischemia-induced gray and white matter damage. *J Neurosci*. 2008;28:3324-3332.
33. Zhu C, Wang X, Huang Z, et al. Apoptosis-inducing factor is a major contributor to neuronal loss induced by neonatal cerebral hypoxia-ischemia. *Cell Death Differ*. 2007;14:775-784.
34. Wang X, Karlsson JO, Zhu C, Bahr BA, Hagberg H, Blomgren K. Caspase-3 activation after neonatal rat cerebral hypoxia-ischemia. *Biol Neonate*. 2001;79:172-179.
35. Wajant H, Pfizenmaier K, Scheurich P. Tumor necrosis factor signaling. *Cell Death Differ*. 2003;10:45-65.
36. Gupta S. A decision between life and death during TNF-alpha-induced signaling. *J Clin Immunol*. 2002;22:185-194.
37. Baud V, Karin M. Signal transduction by tumor necrosis factor and its relatives. *Trends Cell Biol*. 2001;11:372-377.
38. Hallenbeck JM. The many faces of tumor necrosis factor in stroke. *Nat Med*. 2002;8:1363-1368.
39. Sriram K, O'Callaghan JP. Divergent roles for tumor necrosis factor-alpha in the brain. *J Neuroimmune Pharmacol*. 2007;2:140-153.
40. Markus T, Cronberg T, Cilio C, Pronk C, Wieloch T, Ley D. Tumor necrosis factor receptor-1 is essential for LPS-induced sensitization and tolerance to oxygen-glucose deprivation in murine neonatal organotypic hippocampal slices. *J Cereb Blood Flow Metab*. 2009;29:73-86.
41. Fontaine V, Mohand-Said S, Hanoteau N, Fuchs C, Pfizenmaier K, Eisel U. Neurodegenerative and neuroprotective effects of tumor Necrosis factor (TNF) in retinal ischemia: opposite roles of TNF receptor 1 and TNF receptor 2. *J Neurosci*. 2002;22:216.
42. Scherbel U, Raghupathi R, Nakamura M, et al. Differential acute and chronic responses of tumor necrosis factor-deficient mice to experimental brain injury. *Proc Natl Acad Sci U S A*. 1999;96:8721-8726.
43. Heldmann U, Thored P, Claasen JH, Arvidsson A, Kokaia Z, Lindvall O. TNF-alpha antibody infusion impairs survival of stroke-generated neuroblasts in adult rat brain. *Exp Neurol*. 2005;196:204-208.
44. Becker D, Zahn N, Deller T, Vlachos A. Tumor necrosis factor alpha maintains denervation-induced homeostatic synaptic plasticity of mouse dentate granule cells. *Front Cell Neurosci*. 2013;7:257.
45. Pettigrew LC, Kindy MS, Scheff S, et al. Focal cerebral ischemia in the TNFalpha-transgenic rat. *J Neuroinflammation*. 2008;5:47-2094-5-47.

46. Martin-Villalba A, Hahne M, Kleber S, et al. Therapeutic neutralization of CD95-ligand and TNF attenuates brain damage in stroke. *Cell Death Differ*. 2001;8:679-686.
47. Meistrell ME,3rd, Botchkina GI, Wang H, et al. Tumor necrosis factor is a brain damaging cytokine in cerebral ischemia. *Shock*. 1997;8:341-348.
48. Barone FC, Arvin B, White RF, et al. Tumor necrosis factor-alpha. A mediator of focal ischemic brain injury. *Stroke*. 1997;28:1233-1244.
49. Nawashiro H, Martin D, Hallenbeck JM. Neuroprotective effects of TNF binding protein in focal cerebral ischemia. *Brain Res*. 1997;778:265-271.
50. Hosomi N, Ban CR, Naya T, et al. Tumor necrosis factor-alpha neutralization reduced cerebral edema through inhibition of matrix metalloproteinase production after transient focal cerebral ischemia. *J Cereb Blood Flow Metab*. 2005;25:959-967.
51. Lavine SD, Hofman FM, Zlokovic BV. Circulating antibody against tumor necrosis factor-alpha protects rat brain from reperfusion injury. *J Cereb Blood Flow Metab*. 1998;18:52-58.
52. Sumbria RK, Boado RJ, Pardridge WM. Brain protection from stroke with intravenous TNFalpha decoy receptor-Trojan horse fusion protein. *J Cereb Blood Flow Metab*. 2012;32:1933-1938.
53. Caso JR, Lizasoain I, Lorenzo P, Moro MA, Leza JC. The role of tumor necrosis factor-alpha in stress-induced worsening of cerebral ischemia in rats. *Neuroscience*. 2006;142:59-69.
54. Wang X, Feuerstein GZ, Xu L, et al. Inhibition of tumor necrosis factor-alpha-converting enzyme by a selective antagonist protects brain from focal ischemic injury in rats. *Mol Pharmacol*. 2004;65:890-896.
55. Kendall GS, Hristova M, Horn S, et al. TNF gene cluster deletion abolishes lipopolysaccharide-mediated sensitization of the neonatal brain to hypoxic ischemic insult. *Lab Invest*. 2011;91:328-341.
56. Aden U, Favrais G, Plaisant F, et al. Systemic inflammation sensitizes the neonatal brain to excitotoxicity through a pro-/anti-inflammatory imbalance: key role of TNFalpha pathway and protection by etanercept. *Brain Behav Immun*. 2010;24:747-758.
57. Lambertsen KL, Clausen BH, Babcock AA, et al. Microglia protect neurons against ischemia by synthesis of tumor necrosis factor. *J Neurosci*. 2009;29:1319-1330.
58. Gary DS, Bruce-Keller AJ, Kindy MS, Mattson MP. Ischemic and excitotoxic brain injury is enhanced in mice lacking the p55 tumor necrosis factor receptor. *J Cereb Blood Flow Metab*. 1998;18:1283-1287.
59. Marchetti L, Klein M, Schlett K, Pfizenmaier K, Eisel UL. Tumor necrosis factor (TNF)-mediated neuroprotection against glutamate-induced excitotoxicity is enhanced by N-methyl-D-aspartate receptor activation. Essential role of a TNF receptor 2-mediated phosphatidylinositol 3-kinase-dependent NF-kappa B pathway. *J Biol Chem*. 2004;279:32869-32881.
60. Turrin NP, Rivest S. Tumor necrosis factor alpha but not interleukin 1 beta mediates neuroprotection in response to acute nitric oxide excitotoxicity. *J Neurosci*. 2006;26:143-151.
61. Bruce AJ, Boling W, Kindy MS, et al. Altered neuronal and microglial responses to excitotoxic and ischemic brain injury in mice lacking TNF receptors. *Nat Med*. 1996;2:788-794.
62. Shohami E, Ginis I, Hallenbeck JM. Dual role of tumor necrosis factor alpha in brain injury. *Cytokine Growth Factor Rev*. 1999;10:119-130.
63. Pires PW, Girgla SS, Moreno G, McClain JL, Dorrance AM. Tumor necrosis factor-alpha inhibition attenuates middle cerebral artery remodeling but increases cerebral ischemic damage in hypertensive rats. *Am J Physiol Heart Circ Physiol*. 2014.
64. McCoy MK, Tansey MG. TNF signaling inhibition in the CNS: implications for normal brain function and neurodegenerative disease. *J Neuroinflammation*. 2008;5:45-2094-5-45.
65. Cai Z, Pang Y, Lin S, Rhodes PG. Differential roles of tumor necrosis factor-alpha and interleukin-1 beta in lipopolysaccharide-induced brain injury in the neonatal rat. *Brain Res*. 2003;975:37-47.
66. Yang D, Sun YY, Lin X, et al. Intranasal delivery of cell-penetrating anti-NF-kappaB peptides (Tat-NBD) alleviates infection-sensitized hypoxic-ischemic brain injury. *Exp Neurol*. 2013;247:447-455.

67. Liu J, Lin A. Wiring the cell signaling circuitry by the NF-kappa B and JNK1 crosstalk and its applications in human diseases. *Oncogene*. 2007;26:3267-3278.

68. Tang G, Minemoto Y, Dibling B, et al. Inhibition of JNK activation through NF-kappaB target genes. *Nature*. 2001;414:313-317.

69. Javelaud D, Besancon F. NF-kappa B activation results in rapid inactivation of JNK in TNF alpha-treated Ewing sarcoma cells: a mechanism for the anti-apoptotic effect of NF-kappa B. *Oncogene*. 2001;20:4365-4372.

7

The neonatal brain is not protected by osteopontin peptide treatment after hypoxia-ischemia

Hilde J.C. Bonestroo
Cora H. Nijboer
Cindy T.J. van Velthoven
Frank van Bel
Cobi J. Heijnen

Developmental Neuroscience **accepted for publication**

Abstract

Neonatal encephalopathy due to perinatal hypoxia-ischemia (HI) is a severe condition and current treatment options are limited. Expression of endogenous osteopontin (OPN), a multifunction glycoprotein, is strongly upregulated in the brain after neonatal HI. Intracerebrally administered OPN has been shown to be neuroprotective following experimental neonatal HI and adult stroke. In the present study we determined whether intranasal, intraperitoneal or intracerebral treatment with a smaller TAT-OPN peptide is neuroprotective in neonatal mice with HI brain damage.

The TAT-OPN peptide exerts bio-activity as it was as potent as full length OPN in inducing cell adhesion in an *in vitro* adhesion assay. Intranasal administration of TAT-OPN peptide immediately after HI (T0) or in a repetitive treatment schedule of T0, 3 h, D1, 2, 3 post-HI did not protect cerebral gray or white matter after HI. Intraperitoneal TAT-OPN treatment at T0 or in two extended treatment schedules (D5, 7, 9, 11, 13, 15 post-HI or T0, D1, 3, 5, 7, 9, 11, 13 and 15 post-HI) also did not result in neuroprotection. Moreover, no functional improvement (cylinder rearing test or adhesive removal task) was observed following TAT-OPN treatment in neither of the intraperitoneal treatment schedules. We validated that the TAT-OPN peptide reached the brain after intranasal or intraperitoneal administration by using a HIV-TAT staining. Finally, also intracerebral administration of TAT-OPN peptide at 1 h after HI did not reduce cerebral neuronal damage.

Our data show that administration of the TAT-OPN peptide did not exert neuroprotective effects on neonatal HI-induced brain injury or sensorimotor behavioral deficits.

Introduction

Neonatal encephalopathy due to perinatal hypoxia-ischemia (HI) is a severe clinical condition associated with high mortality and morbidity mainly characterized by long-term neurological deficits.[1-5] In developed countries, the prevalence of neonatal HI is about 1-3 per 1000 live term births.[2,6,7] Therapeutic options to improve the outcome of neonates with HI brain injury are still very limited. At the moment, hypothermia is the only established intervention with modest therapeutic efficacy which can only be used in term neonates if started within 6 h after the insult.[8-10] New therapeutic options to combat brain injury following neonatal HI are urgently needed.

The mechanisms underlying neonatal HI brain damage are only partially understood and consist of an intricate interplay between excitotoxicity, inflammation and apoptotic cell death. In animal models, it has been shown that expression of a large amount of inflammation- and growth factor-related genes are upregulated within the neonatal brain after exposure to HI.[11-17] We and others have previously shown that the expression of osteopontin (OPN), a multifunctional phosphorylated acidic glycoprotein secreted by various cells[18], is strongly upregulated in the brain after HI in neonatal mice and rats.[12,16,19] We described earlier that mRNA expression of OPN was already increased in the ipsilateral hemisphere at 12 h post-insult which further increased until day 5 after HI.[16] OPN binds to multiple integrin receptors and various isoforms and promotes a variety of cellular processes, *e.g.* cell adhesion, chemotaxis, angiogenesis, migration, differentiation, apoptosis and cell survival, the latter two via activation of the transcription factor NF-κB.[18,20-22]

In a previous study we have described that HI brain damage is exacerbated in neonatal mice deficient for OPN compared to wild type (WT) littermates.[16] Moreover, HI-induced cell proliferation/survival and oligodendrogenesis were decreased in OPN-deficient animals, strongly indicating that OPN is a pivotal factor for cerebral repair processes.[16]

A couple of experimental studies have described the neuroprotective effects of OPN treatment in models of adult stroke, adult subarachnoid hemorrhage and also after neonatal HI.[19,23-26] Importantly, in these studies, full length OPN was administered intracerebrally, which limits its value for clinical situations. The study by Doyle et al. (2008) is, to the best of our knowledge, the only study that has described the effect of *intranasal* OPN treatment in an adult stroke model.[23] Moreover, these authors showed that intranasal administration of the smaller N-terminal OPN-peptide provided a higher neuroprotective effect than administration of full length OPN.[23] The aim of the current study was therefore to investigate whether treatment with the small OPN peptide as described by Doyle et al. (2008), could exert neuroprotective effects on HI brain damage in neonatal mice, when applied via clinically-applicable (*i.e.* intranasally or intraperitoneally) routes of administration.[23] To facilitate cellular uptake in the brain, we coupled a HIV-TAT (Human immunodeficiency virus-transactivator of transcription) shuttle sequence to the OPN peptide as we have shown before for delivery of other small peptides in the brain.[27-31]

Material and methods

Animals

All experiments were performed according to international guidelines and approved by the local experimental animal committee of the University Medical Center Utrecht (DEC-ABC, Utrecht). Postnatal day 9 (P9) C57BL/6 mice pups of both genders were subjected to HI by permanent occlusion of the right common carotid artery under isoflurane anesthesia (4.0% induction, 2.0% maintenance), followed by systemic hypoxia for 50 min at 10% O_2. Sham-control animals underwent anesthesia and incision only. During the HI procedure hypothermia was actively prevented by placing animals on a heating mattress during and after surgery and during hypoxia. Furthermore, hypoxia was induced in a preheated, temperature-controlled incubator (37 °C) and the 10% O_2 gas mixture was humidified and pre-warmed. Pups from at least three different litters were used in each experimental group. At 4 weeks of age, animals were weaned and group-housed per gender on a reversed day-night cycle in order to perform the behavioral tests.

Animals were sacrificed by pentobarbital overdose at 6 h, or 7 or 65 days post-insult, and transcardial perfused with 4% paraformaldehyde in phosphate buffered salt (PBS). Brains were post-fixed in 4% paraformaldehyde and embedded in paraffin.

We did not observe any significant gender differences for any of the measured parameters.

OPN treatment

TAT-OPN peptide (YGRKKRRQRRR-IVPTVDVPNGRGDSLAYGLR; with HIV-TAT shuttle sequence underlined) (W.M. Keck Biotechnology, New Haven, CT) was dissolved in dimethyl sulfoxide (DMSO; 40 mg/ml), diluted in PBS and administered either intranasally at a dose of 350 ng/pup or 2100 ng/pup, or intraperitoneally at a dose of 10 mg/kg, 2.5% DMSO in PBS was used as vehicle solution. For intracerebral injection TAT-OPN was dissolved in NaCl 0.9% and administered in a dose of 100 ng/pup in 1.5 µl.

For intranasal administration, animals were treated directly after HI (T0); directly and at 3 h post-HI (T0+3); or in a repetitive schedule at T0+3 and D1, 2 and 3 after HI (T0+3, D1, 2, 3). For intraperitoneal administration, three different timeframes were used: animals were injected at T0; at D5, 7, 9, 11, 13 and 15 post-HI (late schedule); or at T0, D1, 3, 4, 7, 9, 11, 13 and 15 (total schedule).

For intracerebral administration, animals recovered for 1 h after the HI insult before placing them in a stereotaxic frame (Kopf instruments, Tujunga, CA, USA) under isoflurane anesthesia. TAT-OPN peptide was administered using a 26s-gauge Hamilton syringe. 1.5 µl of TAT-OPN peptide solution or NaCl 0.9% was infused in 2 min in the ipsilateral hemisphere (1 mm caudal to bregma, 1 mm right from midline and 2 mm below dural surface).

Cell adhesion assay

Cell adhesion assays were performed to examine the ability of mouse mesenchymal stem cells (MSCs) and HEK293 cells to specifically bind to full length OPN (Sigma-Aldrich) or TAT-OPN peptide (W.M. Keck Biotechnology). Ninety-six-wells plates were coated overnight at 4 °C with mouse recombinant full length OPN (2 or 20 µg/ml in PBS) or TAT-OPN peptide (equimolar dose to 2, 20 or 200 µg/ml full length OPN). Coating with 1% BSA/PBS was used a control. After coating the plates were washed three times with PBS before blocking with 1% BSA/PBS for 1 h at RT. HEK 293 cells and MSCs were plated (1 x 10^5 cells/well) in adhesion buffer (PBS containing 50 mM HEPES, 0.1% BSA, 0.1% glucose, and 0.05 mmol/L $MnCl_2$). Cells were allowed to adhere for 45 min at 37 °C followed by a gentle wash to remove non-adherent cells. Relative number of adherent cells was quantified by a MTT assay. In short 0.5 mg/ml MTT ((3-)4,5-dimethyl-2 tiazoyl)-2,5-diphenyl-tetrazolium-bromide) (Sigma-Aldrich) was added to the adherent cells for 3 h at 37 °C. MTT crystals were dissolved in DMSO and absorbance was measured at 550 nm. The assay was performed in 6-fold and was repeated 2 times.

Histology

Coronal paraffin sections (8 µm) were cut at hippocampal level (equivalent to -1.28 mm from bregma in adult mice) and incubated with mouse anti-microtubule-associated protein 2 (MAP2) (Sigma-Aldrich, Steinheim, Germany), mouse anti-myelin basic protein (MBP) (Sternberger Monoclonals, Lutherville, MD) or mouse anti-HIV1-TAT antibody (Abcam, Cambridge, UK) followed by biotinylated horse anti-mouse (Vector Laboratories, Burlingame, CA) antibody. Visualization was performed using Vectastain ABC kit (Vector Laboratories) and diaminobenzamidine.

For MAP2 staining, full section images were captured with a Nikon D1 digital camera (Nikon, Tokyo, Japan). The brain areas were outlined manually using image processing tools in Adobe Photoshop CS5 (Adobe Systems Inc., San Jose, CA). MBP-staining was quantified using image processing tools in ImageJ software (rasband WS, Image J, U.S. National Institutes of Health, Bethesda, MS; http://rsb.info.nih.gov/ij/, 1997-2006). Ipsilateral area loss was calculated as follows: [1 - (MAP2 or MBP-positive area in ipsilateral hemisphere / MAP2 or MBP-positive area in contralateral hemisphere)] x 100%. Photographs of the HIV1-TAT staining were taken with a Zeiss Axio Lab A1 microscope and Icc5 camera (Carl Zeiss, Oberkochen, Germany)

Functional outcome

To study long-term (sensori-)motor behavior, the cylinder rearing test (CRT) and adhesive removal task (ART) were performed. The CRT was used to assess forelimb use asymmetry at D14, 21 and 35 post-HI. Each animal was individually placed in a transparent cylinder (9 cm diameter; 15 cm high) for 3 min. The weight-bearing forepaw(s) to contact the wall during a full rear was recorded as left (impaired), right (non-impaired) or both. Paw preference was calculated as (non-impaired - impaired) / (non-impaired forepaw + impaired forepaw + both) x 100%.

During the ART the latency to sticker removal from the forepaws was measured at D60 post-HI. Stickers (tough-spots, Diversified Biotech, Boston, MA) were placed on the forepaws. The order for left/right forepaw sticker placement was alternated between and within animals. The task was performed in the dark and recorded on video. The time to remove the training sticker for both left and right forepaws was not analyzed but served to habituate the animal to the test. The time that it takes the animal to remove the sticker from its forepaw (‘total removal time’) was measured. In addition, the time to start removal of the sticker (‘exploring time’) was recorded as a measure of sensory function, as well as the time it takes the animal to actually remove the sticker after sensing it (‘effective removal time’) as a measure of motor function. The mean removal latency of three stickers placed per forepaw after one training sticker was determined.
Both tests were performed by a trained observer blinded to treatment.

Statistical analysis

All analyses were performed in a blinded setup. Data are presented as mean ± SEM and were analyzed by one-way ANOVA with Bonferroni post-tests. Cylinder rearing test was analyzed using two-way ANOVA with Fisher’s LDS post-tests. p <0.05 was considered statistically significant. With a sample size of 11, we were able to demonstrate a difference in cerebral damage with a power of 0.80.

Results

In vitro cell adhesion to full length OPN and the TAT-OPN peptide

To demonstrate that the TAT-OPN peptide exerts bioactivity, we performed an *in vitro* cell adhesion assay using murine mesenchymal stem cells (MSCs) and HEK293 cells as was described earlier.[23] Our data in figure 1 show that the TAT-OPN peptide was as potent as full length OPN in inducing adhesion of both MSCs (Fig 1A) and HEK293 cells (Fig 1B) in a dose-dependent manner.

The effect of intranasal treatment with TAT-OPN peptide on brain damage after neonatal HI

HI brain damage was induced in P9 mice by unilateral occlusion of the right carotid artery followed by 50 min of systemic hypoxia at 10% O_2. This experimental procedure resulted in unilateral brain damage primarily in the hippocampal area, with 28 ± 2.6% MAP2 loss at D7 post-HI without detectable damage in the contralateral hemisphere. The anesthesia procedure did not induce any brain damage since there was no MAP2 loss in sham-operated animals.

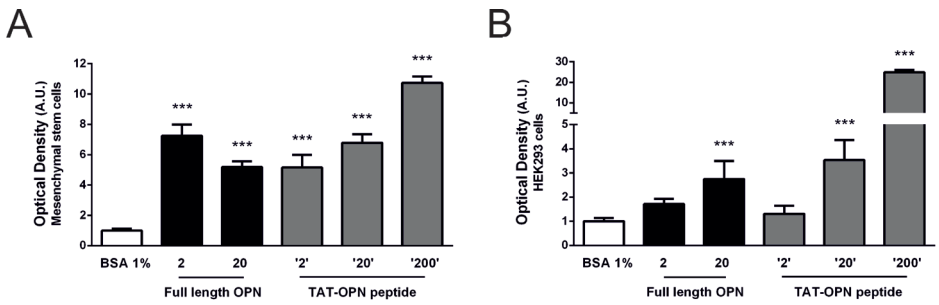

Figure 1: TAT-OPN peptide induces adhesion of MSCs and HEK293 cells.
Wells were coated with full length OPN (2 or 20 µg/ml) or TAT-OPN peptide (dose equimolar to 2, 20 or 200 µg/ml full length OPN) overnight. Mesenchymal stem cells (MSCs) (**A**) and HEK293 cells (**B**) were allowed to adhere for 45 min. Adherent cells were quantified by using a MTT assay. Optical density levels are presented relative to control levels in 1% BSA-coated wells which were put at 1. The dose of 200 ug/ml TAT-OPN peptide was added to the assay to obtain a clear dose-response of adhesion of cells to the TAT-OPN peptide. The assay was performed in 6-fold and was repeated twice. Data represent mean ± SEM. A.U.: Arbitrary units, BSA: Bovine serum albumin. *** $p < 0.001$ vs BSA.

In the first experiments the TAT-OPN peptide was administered intranasally. This non-invasive route of administration has been shown by Doyle et al. (2008) to be an effective way to reduce brain injury after adult stroke.[23] However, in our study when TAT-OPN peptide was administered in a dose of 350 ng directly (T0) or at T0+3 post-HI, no significant reduction in gray or white matter damage was observed compared to vehicle-treated animals as determined by both MAP2 and MBP staining respectively (Fig 2A, B and E).
To investigate whether a higher intranasal dose of TAT-OPN peptide or repetitive gifts of the peptide could result in neuroprotection, a 6 times higher dosage of 2100 ng TAT-OPN peptide was intranasally delivered at T0 post-HI or at T0+3 plus D1, 2 and 3 after HI. Increasing the dose and/or prolonging the treatment schedule of intranasal TAT-OPN peptide treatment however did not result in reduction of HI brain injury as determined at D7 post-HI (Fig 2C, D).

The effect of intraperitoneal treatment with TAT-OPN peptide on brain damage after neonatal HI

We next determined whether treatment with TAT-OPN peptide could be more efficient when administered via the intraperitoneal route. First, mouse pups were treated directly after HI with an intraperitoneal injection of the TAT-OPN peptide at a dose of 10 mg/kg (Fig 3A, B). Intraperitoneal treatment with TAT-OPN peptide at T0 did not result in a reduction of MAP2 loss or a reduction of MBP loss compared to vehicle-treated littermates at D7 post-HI (Fig 3A and B).
Our previous study showed that the HI-induced increase in endogenous cerebral OPN expression dropped rapidly between D5-D7 post-HI.[16] The subsequent rationale for the next experiments was to administer the TAT-OPN peptide from D5 to prevent the drop in endogenous OPN levels following neonatal HI. Thus, TAT-OPN treatment was started at the endogenous peak of OPN production (D5) and was repeated every other day for 15 days,

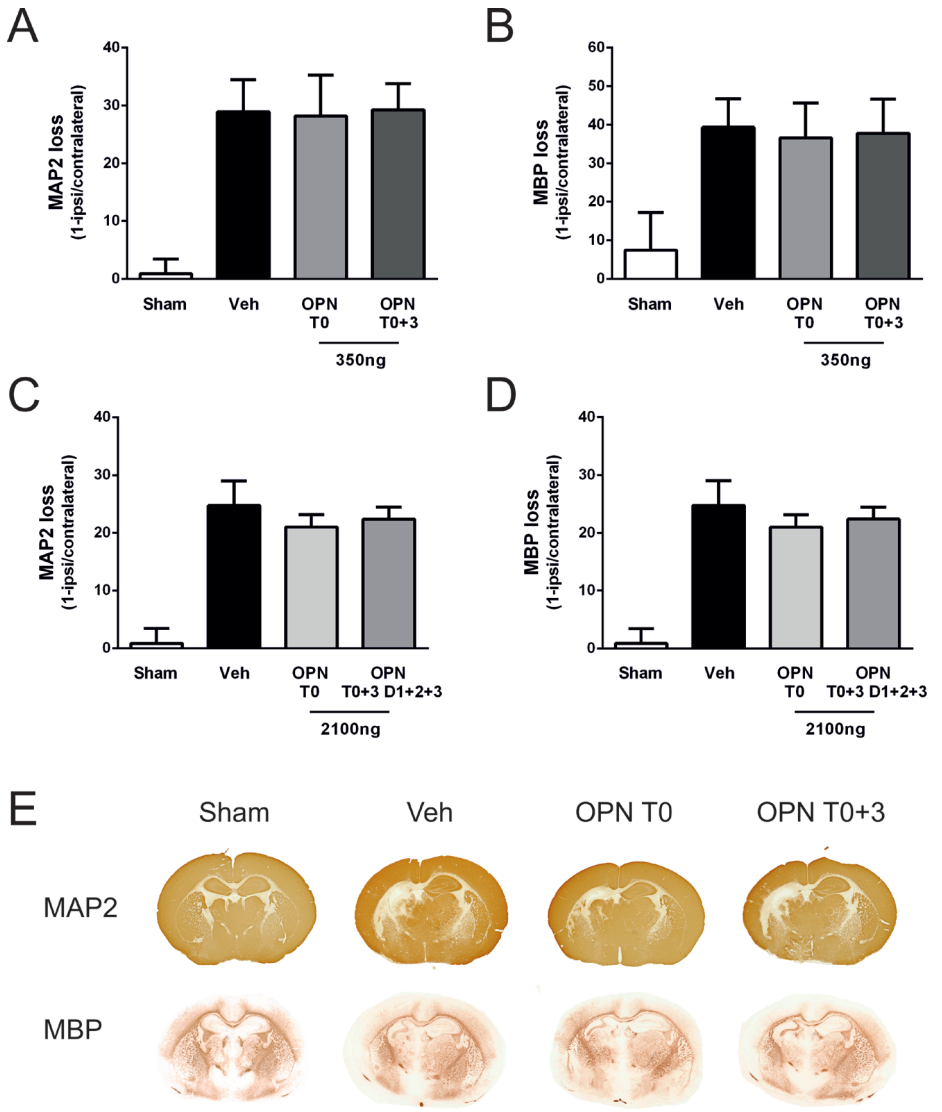

Figure 2: Effect of intranasal TAT-OPN peptide treatment on cerebral gray and white matter damage.

Mice were subjected to sham-operation (Sham) or HI at P9. HI mouse pups were treated intranasally with vehicle (Veh), TAT-OPN peptide (350 ng) at 0 h after HI (T0), at 0 and 3 h after HI (T0+3) (**A**, **B**) or with TAT-OPN peptide (2100 ng) at T0 or at T0+3 and D1, 2 and 3 (**C, D**).Neuronal damage and white matter damage were assessed by analyzing staining for microtubule-associated protein 2 (MAP2) and myelin basic protein (MBP) respectively, in the contra- and ipsilateral hemisphere at D7 post-HI. No significant MAP2 or MBP loss was observed in the contralateral hemisphere of HI animals or in sham-operated animals. (**A**, **C**) Quantification of MAP2 loss and (**B**, **D**) quantification of MBP loss expressed as ratio ipsi-/contralateral MAP2- or MBP-positive area in the above described experimental groups. (**E**) Representative examples of MAP2 and MBP staining in brains of sham-operated, vehicle and TAT-OPN peptide-treated animals as depicted in figure A and B. n=11-12 animals per group. Data represent mean ± SEM.

i.e. D5, 7, 9, 11, 13, 15 after HI (designated as 'OPN Late'). In a second set-up, TAT-OPN was injected intraperitoneally over a longer time period, starting directly following HI and every other day for 15 days, *i.e.* at T0 and D1, 3, 5, 7, 9, 11, 13 and 15 post-HI (designated as 'OPN Total'). Animals were followed until D65 post-HI to assess effects on gray and white matter damage and (sensori-)motor behavior. Both the 'OPN Late' and the 'OPN Total' treatment schedules did not result in anatomical improvements as no significant differences in the amount of HI-induced MAP2 or MBP loss could be detected between vehicle- and TAT-OPN peptide treated mice at D65 post-HI (Fig 3C, D).

The effect of intraperitoneal TAT-OPN peptide treatment on long-term (sensori-)motor behavior after neonatal HI

Neuroprotective treatments may sometimes not result in an overt reduction of anatomical brain injury but the treatment may be limited to improvement of functional performance. For this reason, sham-operated mice and HI mice treated intraperitoneally with vehicle or TAT-OPN peptide on D5, 7, 9, 11, 13, 15 ('OPN Late') or T0 and D1, 3, 5, 7, 9, 11, 13, 15 ('OPN Total') were subjected to two (sensori-)motor behavioral tasks (Fig 3E-H). In the cylinder rearing test (CRT), which was performed at D14, 21 and 35 post-HI, sham-operated animals showed symmetrical use of both forepaws, *i.e.* no preference for one of the forepaws (Fig 3H). Mice subjected to HI showed a marked preference (app. 30-35%) for use of the non-impaired (right) forepaw at all measured time points. No significant reduction in non-impaired paw preference was observed after 'Late' or 'Total' TAT-OPN peptide treatment at the measured time points compared to vehicle-treated HI animals (Fig 3H).

Next, mice were tested for sensorimotor behavior in the adhesive removal task (ART). HI animals showed a clear increased 'total removal time' for the left (impaired) forepaw compared to the right (non-impaired) forepaw (Fig 3E). Figure 3F clearly shows that HI induced sensory defects in the forepaw as 'exploring time' was clearly prolonged in the impaired forepaw, whereas the 'effective removal time' was not significantly different between left and right forepaws in HI animals (Fig 3F and G). Treatment with the 'Late' or 'Total' TAT-OPN peptide schedule did not improve sensorimotor behavior in the ART compared to vehicle-treatment (Fig 3E-G).

To investigate whether the lack of neuroprotection was due to impaired delivery of the TAT-OPN peptide to the brain after intranasal or intraperitoneal administration, we stained the mouse brains for the HIV1-TAT sequence at 6 h post-insult. Brains from both intranasally and intraperitoneally TAT-OPN peptide treated HI animals stained positively for HIV1-TAT throughout the brain (Fig 4). Brains of vehicle-treated HI animals did not stain for HIV1-TAT (Fig 4). Omitting the primary antibody resulted in negative staining of the brain sections of an intraperitoneally treated TAT-OPN mouse, indicating that the positive signal is due to the presence of HIV1-TAT sequence (Fig 4).

Figure 3: Effect of intraperitoneal TAT-OPN peptide treatment on cerebral gray and white matter damage and (sensori-)motor behavior. ➔

Mice were subjected to sham-operation (Sham) or HI at P9. HI mouse pups were treated intraperitoneally with vehicle (Veh), TAT-OPN peptide (10 mg/kg) at 0 h after HI (T0) (**A**, **B**). TAT-OPN peptide (10 mg/kg) at D5, 7, 9, 11, 13, 15 post-HI ('OPN Late') or at T0 and D1, 3, 5, 7, 9, 11, 13, 15 post-HI ('OPN Total') (**C**-**H**). Neuronal damage and white matter damage were assessed by analyzing staining for microtubule-associated protein 2 (MAP2) and myelin basic protein (MBP) respectively, in the contra- and ipsilateral hemisphere at D7 (**A**, **B**) or D65 post-HI (**C**, **D**). No MAP2 or MBP loss was observed in the contralateral hemisphere of HI animals or in sham-operated animals. Quantification of MAP2 loss (**A**, **C**) and quantification of MBP loss (**B**, **D**) expressed as ratio ipsi-/contralateral MAP2- or MBP-positive area in in the above described experimental groups. Representative examples of MAP2 and MBP staining in brains of sham-operated, vehicle- and TAT-OPN peptide-treated animals as depicted in figure A and B.Mice were tested in the adhesive removal task (ART) to quantify sensorimotor deficits at D60 post-HI. Stickers were placed on the forepaws and the latency to removal was recorded for the left (L: impaired) and right (R: non-impaired) forepaw. The mean removal latency of three stickers placed per forepaw was determined. Panel **E** Shows 'total removal time', *i.e.* the total time it takes the animals to remove the sticker from its paw. Panel **F** shows 'Exploring time', *i.e.* the time the animal spends exploring before it senses the sticker at its paw and starts removing it. Panel **G** shows 'effective removal time'. *i.e.* the time it takes the animal to remove the sticker after sensing the sticker on its paw. Mice were tested in the cylinder rearing test (CRT) to quantify laterizing motor deficits at D14, D21 and D35 post-HI (**H**). Use of right (non-impaired) and left (impaired) forepaw during full rears was recorded over a 3 min test period and preference (%) for using the non-impaired forepaw was depicted. **A**, **B**: n=11-12 animals per group. **C**-**H**: n=17-19 animals per group. Data represent mean ± SEM. * p <0.05, ** p <0.01, *** p <0.001 vs sham.

The effect of intracerebral treatment with TAT-OPN peptide on brain damage after neonatal HI

Next, we determined whether TAT-OPN peptide could exert neuroprotective effects when delivered directly into the brain by intracerebral administration, as was shown before by Chen et al. (2011) in neonatal HI rats.[19] Intracerebral treatment with TAT-OPN peptide at 1 h after induction of HI did not result in a reduction of MAP2 loss or MBP loss compared to vehicle-treated littermates (Fig 5A-C).

Discussion

In this study we demonstrate that administration of the TAT-OPN peptide via the intranasal, intraperitoneal or intracerebral route do not result in a neuroprotective effect on HI-induced histological brain injury or (sensori-)motor deficits in neonatal mice.

OPN is a protein expressed in various cell types. OPN possesses both pro- and anti-inflammatory properties, which makes it difficult to predict the exact role of OPN during injury.[18,21,22] Our group as well as others has shown a significant increase in OPN expression after ischemia in both the neonatal and adult brain.[12,19,32-34] These results indicate that OPN might fulfill an important role in the complex interplay of cascades activated by brain damage. Studies using OPN-deficient mice have demonstrated that decreased levels of OPN result in increased vulnerability to tissue damage following different types of injury. These data indicate a protective role for OPN, although it is important to keep in mind that mice

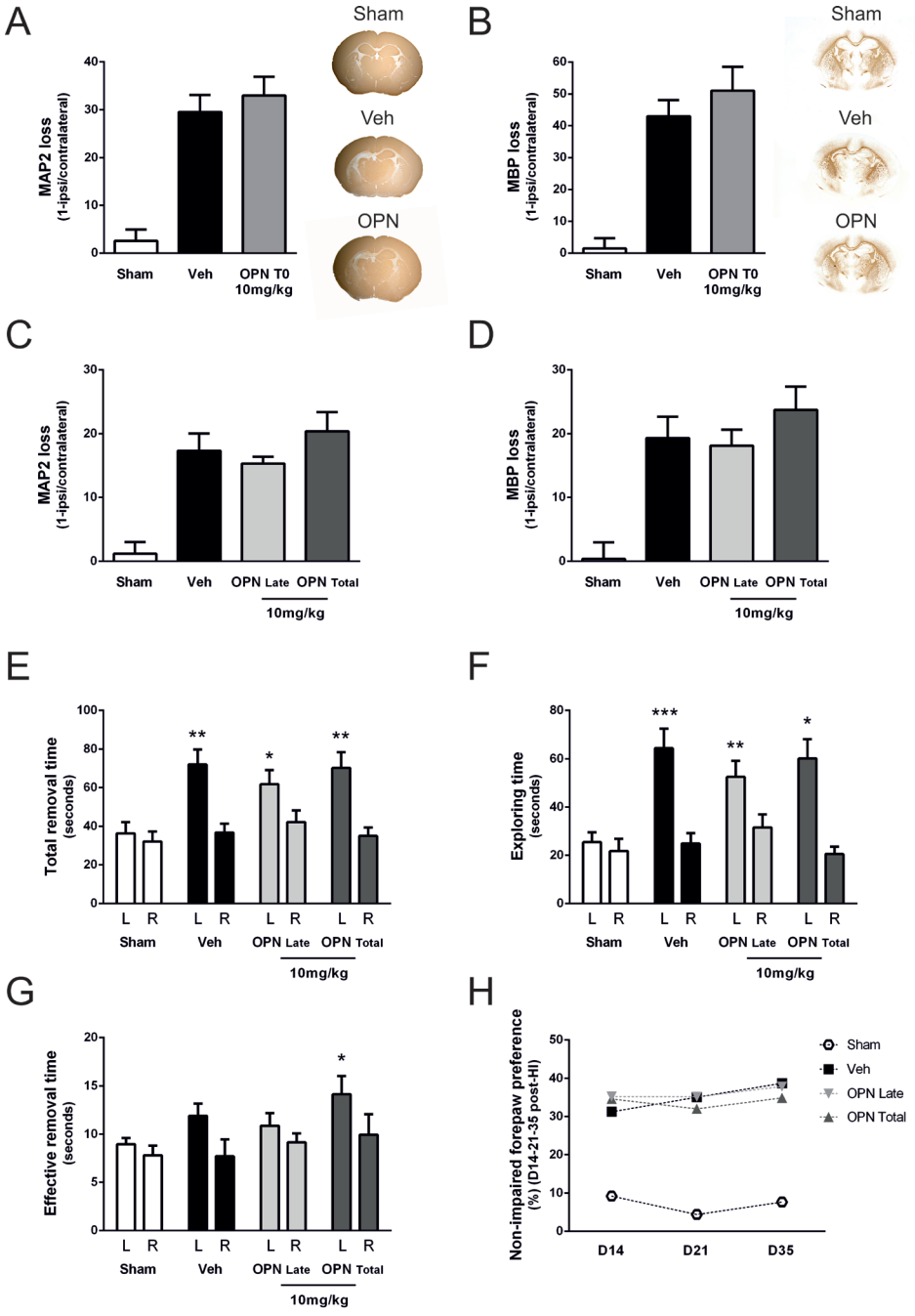
A
MAP2 loss
(1-ipsi/contralateral)
Sham
Veh
OPN T0
10mg/kg
Sham
Veh
OPN
B
MBP loss
(1-ipsi/contralateral)
Sham
Veh
OPN T0
10mg/kg
Sham
Veh
OPN
C
MAP2 loss
(1-ipsi/contralateral)
Sham
Veh
OPN Late
OPN Total
10mg/kg
D
MBP loss
(1-ipsi/contralateral)
Sham
Veh
OPN Late
OPN Total
10mg/kg
E
Total removal time
(seconds)
L R
Sham
Veh
OPN Late
OPN Total
10mg/kg
F
Exploring time
(seconds)
L R
Sham
Veh
OPN Late
OPN Total
10mg/kg
G
Effective removal time
(seconds)
L R
Sham
Veh
OPN Late
OPN Total
10mg/kg
H
Non-impaired forepaw preference
(%) (D14-21-35 post-HI)
D14
D21
D35
Sham
Veh
OPN Late
OPN Total

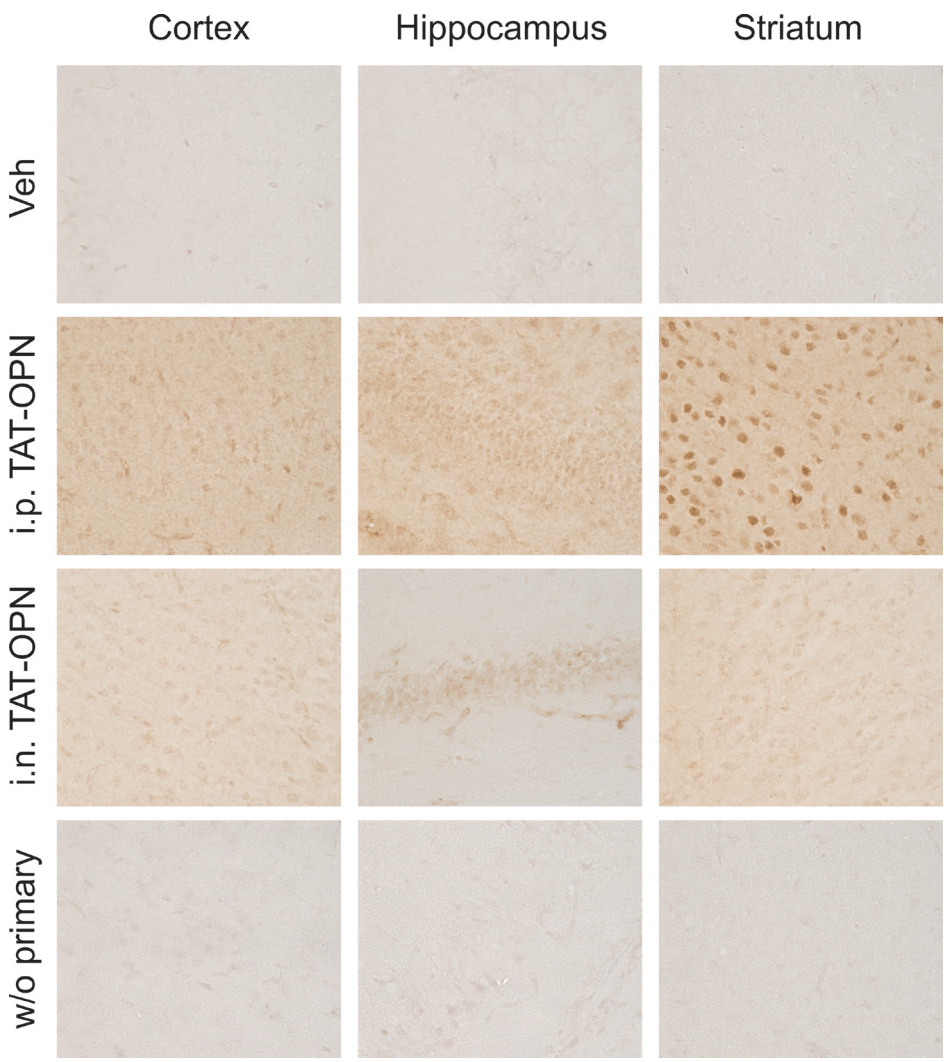

Figure 4: TAT-OPN reaches the brain after intranasal and intraperitoneal administration. Representative photographs of cortex, hippocampal and striatum areas stained for HIV1-TAT at 6 h post-HI to detect arrival of the TAT-OPN peptide in the brain. Mice were subjected to HI at P9, HI mouse pups were treated intranasally (i.n.) with TAT-OPN (2100 ng) or intraperitoneally (i.p.) with TAT-OPN (10 mg/kg) directly after HI. Brains of vehicle-treated (Veh) HI animals were used as a negative control. Additionally, first antibody was omitted (w/o primary) on brain sections of i.p. treated TAT-OPN animals to confirm specificity of the HIV1-TAT staining.

lacking whole-body expression of OPN have reduced OPN levels before induction of tissue injury, which might affect outcome.[16,35,36-38] In line, our previously study using OPN-deficient mice indicated that OPN might be an important factor for cell proliferation, survival and oligodendrogenesis after neonatal HI.[16]

Moreover, neuroprotection after OPN treatment has already been described in different *in vitro* and *in vivo* models for neurodegenerative pathologies.[23,24,25] *In vivo* intracerebral application

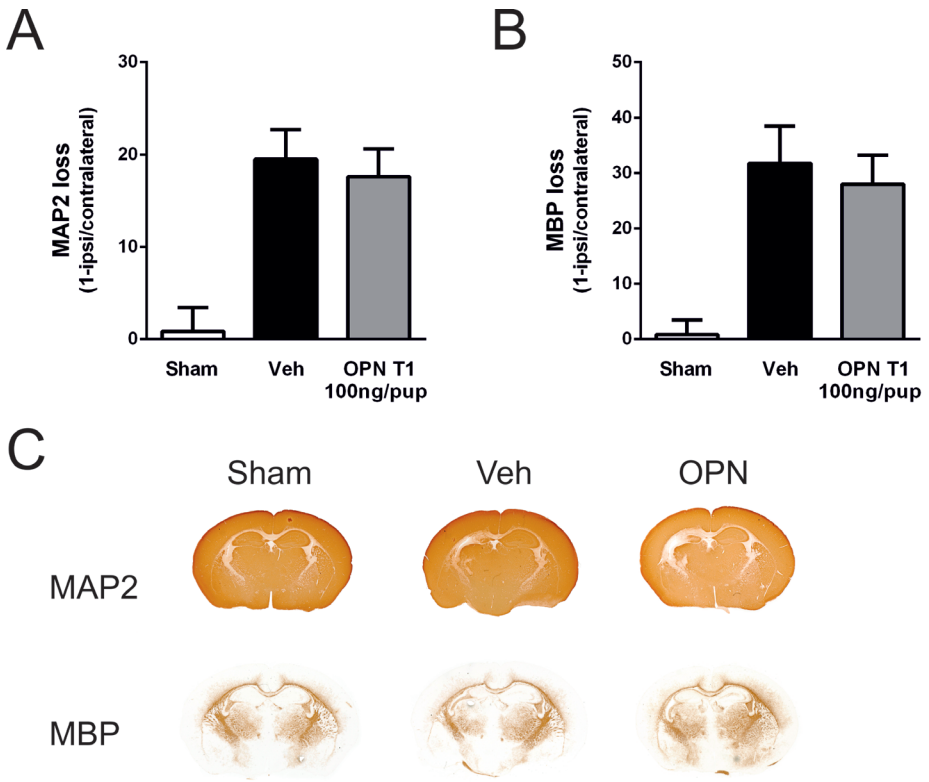

Figure 5: Effect of intracerebral TAT-OPN peptide treatment on cerebral gray and white matter damage.

Mice were subjected to sham-operation (Sham) or HI at P9. HI mouse pups were treated intracerebrally with vehicle (Veh), TAT-OPN peptide (100 ng) at 1 h after HI (T1) (**A**, **B**). Neuronal damage and white matter damage were assessed by analyzing staining for microtubule-associated protein 2 (MAP2) and myelin basic protein (MBP) respectively, in the contra- and ipsilateral hemisphere at D7 post-HI. No significant MAP2 or MBP loss was observed in the contralateral hemisphere of HI animals or in sham-operated animals.

(**A**) Quantification of MAP2 loss and (**B**) quantification of MBP loss expressed as ratio ipsi-/contralateral MAP2- or MBP-positive area in the above described experimental groups. n=7-8 animals per group. Data represent mean ± SEM. (**C**) Representative examples of MAP2 and MBP staining in brains of sham-operated, vehicle- and TAT-OPN peptide-treated animals as depicted in figure A and B.

of full length OPN protein caused a 45% reduction in infarct volume in an adult murine stroke model.[24] These authors suggested that OPN may mediate its effects through integrin receptors and via activation of Akt or the ERK1/2 MAPK cascade.[24] In a similar adult stroke model, intranasal administration of the small OPN peptide 'N-terminal 134-153' resulted in a 61% reduction of cerebral infarct volume.[23] Also, after subarachnoid hemorrhage in adult rats and HI in neonatal rats, full length OPN treatment prevented neurologic impairment.[25,19] In most of the previous studies, except the study of Doyle et al. (2008), OPN has been administered intracerebrally, which limits its value for clinical situations.[23] Therefore the main goal of our study was to investigate the possible neuroprotective effects of intranasal and intraperitoneal TAT-OPN peptide administration following neonatal HI.

Unexpectedly, our current data show no significant reduction in HI brain damage following TAT-OPN peptide administration. Chen and co-workers (2011) observed a significant neuroprotective effect after a single intracerebral injection of full length OPN (0.03 µg or 0.1 µg) at 1 h post-insult in a neonatal HI rat model.[19] A couple of possible explanations for the differences observed between our study and the one by Chen et al. (2011) can be offered. First of all, Chen et al. (2011) administered full length OPN whereas we used the smaller OPN peptide, containing amino acids 134-153.[19] We choose the small peptide since Doyle et al. (2008) observed improved integrin-binding and larger neuroprotective properties of this peptide compared to full length OPN *in vitro* and in a murine adult stroke model when administered intranasally with a time window up to 3 h post insult.[23] We used the OPN peptide described by Doyle et al. (2008) coupled to the HIV1-TAT sequence to facilitate cellular uptake. By performing an *in vitro* adhesion assay we demonstrate that addition of the TAT sequence did not affect the bio-activity of the OPN peptide. Secondly, Chen et al. (2011) administered OPN intracerebrally and we applied the TAT-OPN peptide via different administration routes, *i.e.* intranasally, intraperitoneally or intracerebrally as a control.[19] Previously, Doyle et al. (2008) elegantly showed the effectiveness of intranasal application of the OPN peptide, as the peptide could be detected in the brain within 2 h following administration to adult mice.[23] As far as we know, there is no evidence for a major difference in intranasal absorption between neonatal mice and adult mice and therefore we expect the OPN peptide to arrive at the site of damage after intranasal administration in neonatal mice following HI. Here we showed by using a HIV1-TAT staining that also in the neonatal HI model intranasally and intraperitoneally administered TAT-OPN peptide reaches the brain within 6 h. Also increasing the dose of the intranasally delivered TAT-OPN peptide by 6 times did not result in a protective effect on brain damage. Why treatment with the OPN peptide was neuroprotective after adult stroke and not in our neonatal HI model, might be explained by the difference in lesion site or the cellular, molecular or mechanistic nature of brain damage induced by adult stroke versus neonatal HI.

Next to the different administration routes of TAT-OPN peptide, we studied the effect of dose and kinetics of administration after neonatal HI. Recently, we showed that HI induced upregulation of endogenous OPN expression levels in the ipsilateral hemisphere within 12 h post-HI. OPN expression levels remained high until D5 followed by a sharp decrease in OPN expression after D7 post-HI.[16] To prevent this endogenous reduction in OPN levels we administered TAT-OPN in a 'late schedule', D5 up to D15 post-HI. Since the 'late schedule' did not result in neuroprotection, we further extended the administration schedule starting directly after HI up to D15 post-insult. However, even a treatment schedule that increases OPN levels for an extended time period did not result in a reduction of neuronal damage or improvement of functional outcome.

Taken our data together we cannot confirm the previously observed neuroprotective effects of OPN peptide in the adult stroke model, in our neonatal HI model using newborn mice.

Neither intranasal, nor intraperitoneal or intracerebral TAT-OPN peptide treatment resulted in anatomical reduction of the HI-induced brain insult or in improvement of motor behavior. Our data indicate that the development of brain damage after neonatal HI is not due to a lack of endogenous OPN. We would like to speculate that OPN is not a major neuroprotective factor in the injured neonatal brain.

References

1. Armstrong-Wells J, Bernard TJ, Boada R, Manco-Johnson M. Neurocognitive outcomes following neonatal encephalopathy. *Neuro Rehabilitation.* 2010;26:27-33.
2. de Haan M, Wyatt JS, Roth S, Vargha-Khadem F, Gadian D, Mishkin M. Brain and cognitive-behavioural development after asphyxia at term birth. *Dev Sci*. 2006;9:350-358.
3. Glass HC, Hong KJ, Rogers EE, et al. Risk factors for epilepsy in children with neonatal encephalopathy. *Pediatr Res*. 2011;70:535-540.
4. Gonzalez FF, Miller SP. Does perinatal asphyxia impair cognitive function without cerebral palsy? *Arch Dis Child Fetal Neonatal Ed*. 2006;91:F454-9.
5. van Handel M, Swaab H, de Vries LS, Jongmans MJ. Long-term cognitive and behavioral consequences of neonatal encephalopathy following perinatal asphyxia: a review. *Eur J Pediatr*. 2007;166:645-654.
6. Graham EM, Ruis KA, Hartman AL, Northington FJ, Fox HE. A systematic review of the role of intrapartum hypoxia-ischemia in the causation of neonatal encephalopathy. *Am J Obstet Gynecol*. 2008;199:587-595.
7. Wyatt JS, Gluckman PD, Liu PY, et al. Determinants of outcomes after head cooling for neonatal encephalopathy. *Pediatrics*. 2007;119:912-921.
8. Azzopardi DV, Strohm B, Edwards AD, et al. Moderate hypothermia to treat perinatal asphyxial encephalopathy. *N Engl J Med*. 2009;361:1349-1358.
9. Gluckman PD, Wyatt JS, Azzopardi D, et al. Selective head cooling with mild systemic hypothermia after neonatal encephalopathy: multicentre randomised trial. *Lancet*. 2005;365:663-670.
10. Shankaran S, Laptook AR, Ehrenkranz RA, et al. Whole-body hypothermia for neonates with hypoxic-ischemic encephalopathy. *N Engl J Med*. 2005;353:1574-1584.
11. Bonestroo HJ, Nijboer CH, van Velthoven CT, et al. Cerebral and hepatic inflammatory response after neonatal hypoxia-ischemia in newborn rats. *Dev Neurosci*. 2013;35:197-211.
12. Hedtjarn M, Mallard C, Eklind S, Gustafson-Brywe K, Hagberg HI. Global gene expression in the immature brain after hypoxia-ischemia. *J Cereb Blood Flow Metab*. 2004;24:1317-1332.
13. Hedtjarn M, Mallard C, Hagberg H. Inflammatory gene profiling in the developing mouse brain after hypoxia-ischemia. *J Cereb Blood Flow Metab*. 2004;24:1333-1351.
14. Hagberg H, Gilland E, Bona E, et al. Enhanced expression of interleukin (IL)-1 and IL-6 messenger RNA and bioactive protein after hypoxia-ischemia in neonatal rats. *Pediatr Res*. 1996;40:603-609.
15. Nijboer CH, Heijnen CJ, Groenendaal F, May MJ, van Bel F, Kavelaars A. A dual role of the NF-kappaB pathway in neonatal hypoxic-ischemic brain damage. *Stroke*. 2008;39:2578-2586.
16. van Velthoven CT, Heijnen CJ, van Bel F, Kavelaars A. Osteopontin enhances endogenous repair after neonatal hypoxic-ischemic brain injury. *Stroke.* 2011;42:2294-2301.
17. Vexler ZS, Ferriero DM. Molecular and biochemical mechanisms of perinatal brain injury. *Semin Neonatol*. 2001;6:99-108.
18. O'Regan A, Berman JS. Osteopontin: a key cytokine in cell-mediated and granulomatous inflammation. *Int J Exp Pathol*. 2000;81:373-390.
19. Chen W, Ma Q, Suzuki H, Hartman R, Tang J, Zhang JH. Osteopontin reduced hypoxia-ischemia neonatal brain injury by suppression of apoptosis in a rat pup model. *Stroke*. 2011;42:764-769.
20. Chakraborty G, Jain S, Behera R, et al. The multifaceted roles of osteopontin in cell signaling, tumor progression and angiogenesis. *Curr Mol Med*. 2006;6:819-830.
21. Denhardt DT, Noda M, O'Regan AW, Pavlin D, Berman JS. Osteopontin as a means to cope with environmental insults: regulation of inflammation, tissue remodeling, and cell survival. *J Clin Invest*. 2001;107:1055-1061.
22. Mazzali M, Kipari T, Ophascharoensuk V, Wesson JA, Johnson R, Hughes J. Osteopontin--a molecule for all seasons. *QJM*. 2002;95:3-13.

23. Doyle KP, Yang T, Lessov NS, et al. Nasal administration of osteopontin peptide mimetics confers neuroprotection in stroke. *J Cereb Blood Flow Metab*. 2008;28:1235-1248.
24. Meller R, Stevens SL, Minami M, et al. Neuroprotection by osteopontin in stroke. *J Cereb Blood Flow Metab*. 2005;25:217-225.
25. Suzuki H, Ayer R, Sugawara T, et al. Protective effects of recombinant osteopontin on early brain injury after subarachnoid hemorrhage in rats. *Crit Care Med*. 2010;38:612-618.
26. Suzuki H, Hasegawa Y, Kanamaru K, Zhang JH. Mechanisms of osteopontin-induced stabilization of blood-brain barrier disruption after subarachnoid hemorrhage in rats. *Stroke*. 2010;41:1783-1790.
27. Nijboer CH, Bonestroo HJ, Zijlstra J, Kavelaars A, Heijnen CJ. Mitochondrial JNK phosphorylation as a novel therapeutic target to inhibit neuroinflammation and apoptosis after neonatal ischemic brain damage. *Neurobiol Dis.* 2013;54:432-444.
28. Nijboer CH, Heijnen CJ, Groenendaal F, May MJ, van Bel F, Kavelaars A. Strong neuroprotection by inhibition of NF-kappaB after neonatal hypoxia-ischemia involves apoptotic mechanisms but is independent of cytokines. *Stroke*. 2008;39:2129-2137.
29. Yang D, Sun YY, Lin X et al. Intranasal delivery of cell-penetrating anti-NF-kappaB peptides (Tat-NBD) alleviates infection-sensitized hypoxic-ischemic brain injury. *Exp Neurol*. 2013;247:447-455.
30. Yin W, Cao G, Johnnides MJ. TAT-mediated delivery of Bcl-xL protein is neuroprotective against neonatal hypoxic-ischemic brain injury via inhibition of caspases and AIF. *Neurobiol Dis*. 2006;21:358-371.
31. Borsello T, Clarke PG, Hirt L, et al. A peptide inhibitor of c-Jun N-terminal kinase protects against excitotoxicity and cerebral ischemia. *Nat Med*. 2003;9:1180-1186.
32. Ellison JA, Velier JJ, Spera P, et al. Osteopontin and its integrin receptor alpha(v)beta3 are upregulated during formation of the glial scar after focal stroke. *Stroke*. 1998;29:1698-706.
33. Lee MY, Shin SL, Choi YS, et al. Transient upregulation of osteopontin mRNA in hippocampus and striatum following global forebrain ischemia in rats. *Neurosci Lett*. 1999;271:81-84.
34. Wang X, Louden C, Yue TL, et al. Delayed expression of osteopontin after focal stroke in the rat. *J Neurosci.* 1998;18:2075-2083.
35. Noiri E, Dickman K, Miller F, et al. Reduced tolerance to acute renal ischemia in mice with a targeted disruption of the osteopontin gene. *Kidney Int*. 1999;56:74-82.
36. Hashimoto M, Sun D, Rittling SR, Denhardt DT, Young W. Osteopontin-deficient mice exhibit less inflammation, greater tissue damage, and impaired locomotor recovery from spinal cord injury compared with wild-type controls. *J Neurosci*. 2007;27:3603-3611.
37. Liaw L, Birk DE, Ballas CB, Whitsitt JS, Davidson JM, Hogan BL. Altered wound healing in mice lacking a functional osteopontin gene (spp1). *J Clin Invest*. 1998;101:1468-1478.
38. Schroeter M, Zickler P, Denhardt DT, Hartung HP, Jander S. Increased thalamic neurodegeneration following ischaemic cortical stroke in osteopontin-deficient mice. *Brain*. 2006;129:1426-1437.

8

Summary and general discussion

At this moment, neuroprotective treatment options to combat brain damage after neonatal hypoxia-ischemia (HI) are scarce. Since multiple pathophysiological mechanisms are involved in the development of cerebral damage after a HI insult, it is hard to find one single potent protective treatment that targets all these pathways. Despite a long period of intensive research, there is still no effective neuroprotective treatment strategy available for neonates who face a severe HI insult. Besides supportive care, hypothermia is currently the only established intervention, with modest efficacy in protecting the neonatal brain after a HI insult. Unraveling the underlying pathophysiological mechanisms involved in the development of neonatal HI brain damage is indispensable for the discovery of new treatments for this vulnerable group of patients. In this thesis we reveal new promising therapeutic strategies to protect the neonatal brain after HI by preserving mitochondrial integrity. Furthermore, we focus on the contribution of apoptosis and inflammation to the development of HI brain damage in a neonatal mouse and rat model. In this chapter we will give an overview and discuss several facets of the most important results described in this thesis.

Mitochondrial targets

In the first part of this chapter we will focus on the role of apoptotic cell death focusing on the contribution of the mitochondria and two important mitochondrial targets *i.e.* the c-Jun N-terminal Kinase (JNK) and p53, in the development of neonatal HI brain injury. From the literature we know that disruption of the pro/anti-apoptotic balance in the brain upon neonatal HI is a major contributor to neuronal cell death.[1-8] We show in this thesis that besides regulating nuclear transcriptional activity, the JNK pathway and tumor suppressor p53 play a key role in regulating apoptosis by directly affecting mitochondrial integrity.

The JNK pathway as an orchestrator of HI brain damage

The JNK pathway is activated by different cellular stressors and regulates multiple cellular processes like apoptosis, DNA repair, inflammation, cell differentiation and proliferation. Previous studies reported the protective effects of inhibiting the JNK pathway in adult and neonatal ischemic brain damage models.[9-20] Several inhibitors of the JNK pathway have been described like ATP-competitors, including SP600125, but also small specific peptide inhibitors, like L-JNKi and D-JNKi. L- and D-JNKi competitively bind JNK kinase interacting motif (KIM) thereby preventing interaction with its scaffold protein, upstream activators (like MKK4/7) and downstream targets (like c-Jun).[21-25] Our group previously demonstrated that inhibition of the JNK pathway by intraperitoneal (i.p.) L-JNKi treatment had moderately protective effects after neonatal HI by preventing the activation of caspase 3.[26,27] D-JNKi is the D-isomer in *retro-inverso* form of L-JNKi with improved protease-resistance and therefore an enhanced half-life *in vivo*. In this thesis we show for the first time that D-JNKi is a very potent neuroprotective agent after neonatal HI in rats and mice (**chapter 3 and 6**). In **chapter 3** we

show the role of the JNK pathway in regulating apoptotic cell death and the neuroprotective effect and mechanism of D-JNKi treatment in a neonatal HI rat model. The HI insult induced an early (3 h) and late (24 h) peak of nuclear c-Jun/AP-1 activity in the brain, followed by an early increase in transcription of cerebral cytokines and chemokines. From the literature we expected c-Jun/AP-1 to be activated/phosphorylated by nuclear JNK. Yet, we describe for the first time that no activation of JNK in the cytosol or nuclear compartment was apparent in brains of rats subjected to HI. Surprisingly, strong activation of JNK was only observed at the mitochondria after neonatal HI (**chapter 3**). HI hampered mitochondrial integrity since we observed a decrease in ATP levels, an increase in lipid peroxidation, and a reduction in mitochondrial anti-apoptotic proteins with subsequent activation of the intrinsic apoptotic pathway.

We asked ourselves the question: what is the role of mitochondrial JNK activation in the development of HI-induced brain damage and how it is influenced by D-JNKi? Mitochondria play a key role in orchestrating cell death-promoting pathways, including calcium regulation, production of free radicals and harboring pro- and anti-apoptotic Bcl-2 family proteins.[28, 29] A number of *in vitro* and *in vivo* studies demonstrated that translocation of JNK to the mitochondria results in oxidative stress, mitochondrial dysfunction and eventually cell death in different cell types or tissues.[30-36] We demonstrated that one single i.p. injection of D-JNKi strongly reduced activation of JNK at the mitochondria. As a result, D-JNKi treatment preserved mitochondrial integrity, reduced apoptotic cell death, and almost completely protected the neonatal brain after HI-induced brain damage with a profound improvement in long-term motor and cognitive function (**chapter 3**) (Fig 1). The importance of *mitochondrial* JNK activation was further underlined by the finding that treatment with Sab_{KIM1}, a peptide that prevents JNK from binding to the mitochondrial scaffold Sab, also protected the brain after a HI insult (**chapter 3**). From the literature it is known that JNK can directly bind and phosphorylate both anti- and pro-apoptotic Bcl-2 family members; *e.g.* JNK-mediated phosphorylation of anti-apoptotic Bcl-2/-xL results in a decreased binding of these proteins to the pro-apoptotic counterparts, whereas JNK-mediated phosphorylation of pro-apoptotic Bad, BimL or Bax results in activation of these proteins.[31,37-40] In **chapter 3** we showed that D-JNKi treatment not only prevented the HI-induced reduction in anti-apoptotic mitochondrial proteins Bcl-2 and Bcl-xL but even *increased* the levels of these mitochondrial proteins in the brain (Fig 1). Upregulation of mitochondrial *anti-apoptotic* proteins (Bcl-2, Bcl-xL) seemed to be crucial for maintaining neuroprotection of D-JNKi treatment after the initial protective effects on mitochondrial integrity. Prolonged inhibition of JNK by D-JNKi treatment at 0+3 h prevented the upregulation of mitochondrial Bcl-2/Bcl-xL levels and was not neuroprotective, although it prevented the early phosphorylation of mitochondrial JNK. We showed that D-JNKi at 0+3 h inhibited both the early (3 h) and late AP-1 activation peak at 24 h post-insult (**chapter 3**). Our data indicate that D-JNKi might prevent JNK-mediated inhibitory effects on Bcl-2 and Bcl-xL at the mitochondrial membrane, but secondary AP-1-mediated de novo synthesis of Bcl-2 and Bcl-xL seems to be a crucial to counteract the disturbed apoptotic equilibrium at

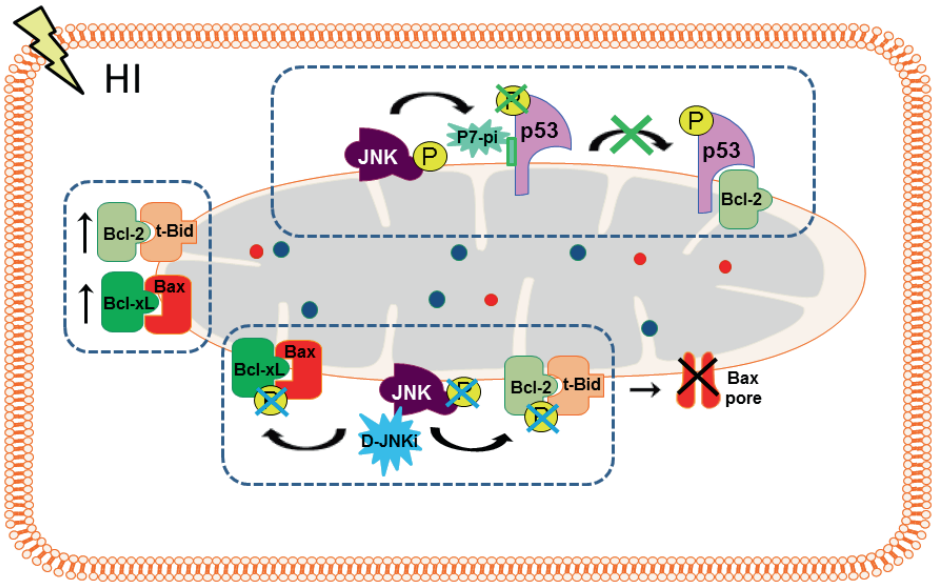

Figure 1 Schematic diagram illustrating mechanism of action of D-JNKi and TAT-P7-pi after HI.
D-JNKi is a small peptide inhibitor that inhibits the JNK pathway by preventing interaction of JNK with its scaffold protein, upstream activators and downstream targets. TAT-P7-pi is a small peptide inhibitor that blocks JNK-p53 interaction, thereby inhibiting JNK-mediated phosphorylation/stabilization of p53. In this thesis we show the potent neuroprotective effects of D-JNKi and TAT-P7-pi (both peptides are administered intraperitoneally at 10 mg/kg directly after the insult) on neonatal HI brain damage. A key mechanism of action of D-JNKi is preventing activation of JNK at the mitochondrial membrane. TAT-P7-pi is presumed to reduce the availability of p53 (hypothesized at the mitochondrial membrane). Moreover, both treatments not only prevent the HI-induced reduction in mitochondrial anti-apoptotic proteins Bcl-2/Bcl-xL but even increase the levels of these mitochondrial proteins, thereby restoring the disturbed apoptotic mitochondrial balance and preventing apoptosis via the intrinsic apoptotic pathway.
HI: hypoxia-ischemia; JNK: c-Jun N-terminal kinase; P: phosphorylation.

the mitochondrial interphase and maintain neuroprotection after neonatal HI. These data are in agreement with earlier findings by our group, demonstrating that neuroprotection is lost when cells are incapable of upregulating levels of anti-apoptotic proteins after prolonged or late inhibition of NF-κB.[41] We suggest that AP-1- and/or NF-κB-induced upregulation of the mitochondrial anti-apoptotic proteins that happens with a short delay of 12-24 h after HI, is an essential step in the decision whether a cell can survive a HI insult. The importance of increasing the levels of anti-apoptotic mitochondrial proteins in the brain for reduction of ischemic brain injury was also shown in other animal models of neuronal injury.[37,42-46]

In conclusion, the results described in **chapter 3** demonstrate that JNK activation at the mitochondria plays an important role in disturbance of the apoptotic balance after neonatal HI. We show that early protection of mitochondrial integrity results in strong long-lasting neuroprotection but only when anti-apoptotic proteins can be upregulated in a later phase.

A question that remained to be answered was: what is the role of the JNK pathway in other cellular compartments than the mitochondria after HI? We observed a clear activation of the nuclear c-Jun/AP-1 transcription factor, an important downstream target of JNK. But

interestingly, we did not observe JNK activation in the cytosolic or nuclear fraction after the HI insult (**chapter 3**). These data are in agreement with other studies that also reported activation of c-Jun without clear effects on JNK activity.[9,11,12,18,47,48] We suggest that alternative kinase pathways possibly activated after mitochondrial damage, are responsible for the activation of c-Jun/AP-1 at 3 h after HI.[49-51] Activation of nuclear AP-1 was functional, as we observed *e.g.* an increase in the cerebral inflammatory response after HI. D-JNKi treatment resulted in a complete and long-lasting inhibition of this increased cerebral inflammatory response, although D-JNKi only prevented the early and not the late peak of nuclear c-Jun/AP-1 activation. From our data it seems unlikely that D-JNKi treatment directly affects AP-1 activity. Therefore we propose that the early decrease in c-Jun/AP-1 activity and reduced transcription of inflammatory genes after D-JNKi treatment would probably be a downstream effect of preserving mitochondrial integrity. Notably, we determined activation of the JNK pathway at one single time point (3 h) post-HI. Therefore, it could still be that phosphorylation of JNK does take place in the cytosol or nucleus before 3 h post-HI which might regulate activation of the c-Jun/AP-1 transcription that already starts to increase at 30 min post-insult.[27] If this is the case, treatment with D-JNKi which is started directly after HI probably can affect both mitochondrial JNK as well as cytosolic/nuclear JNK. Interestingly, selective inhibition of binding of JNK to the mitochondria by Sab_{KIM1} was not as effective as D-JNKi treatment after neonatal HI (**chapter 3**), indicating that D-JNKi has some protective effects on structures outside the mitochondria. However, differences in mechanisms of action between Sab_{KIM1} and D-JNKi could also explain the differences in neuroprotection. D-JNKi prevents activation/phosphorylation of JNK that is already present at the mitochondrial membrane, whereas Sab_{KIM1} prevents binding of JNK to the mitochondrial scaffold Sab, and thereby reduces the availability of mitochondrial JNK that could be phosphorylated. Of interest, D-JNKi treatment had a stronger effect on reducing mitochondrial P-JNK levels than Sab_{KIM1}, which could also explain the differences in neuroprotection after HI. In conclusion, it remains unresolved whether the effects of D-JNKi on nuclear AP-1 and downstream pathways are direct effects of the inhibitor on nuclear pathways or an indirect effect of D-JNKi-mediated protection of the mitochondria.

In **chapter 6** we describe a possible additional non-mitochondrial effect of D-JNKi treatment. We investigated the effect of D-JNKi treatment in an inflammation-sensitized model of HI brain damage in neonatal mice. Interestingly, activation of mitochondrial JNK or a decrease in anti-apoptotic mitochondrial proteins was not observed after LPS-sensitized HI injury. In line, D-JNKi treatment in the LPS-sensitized HI injury model did not affect mitochondrial levels of JNK or Bcl-2/Bcl-xL. Treatment with a higher dose of D-JNKi under inflammatory conditions had a moderately protective effect after HI, probably by increasing the expression of TNF-R2 and promoting TNF-α dependent cell survival as discussed later (**chapter 6**). The fact that neuroprotective effects of D-JNKi were diminished when pathways including mitochondrial P-JNK and Bcl-2/xL regulation were not operative, highlight the contribution of these phenomena to D-JNKi-mediated neuroprotection after HI.

D-JNKi has been designed as the JNK-binding domain (JBD) of the JIP1 scaffold protein coupled to the HIV-TAT sequence to facilitate cellular uptake. Previous studies showed that the peptide can cross the blood-brain-barrier and penetrates neurons within 1 h after i.p. administration in a cerebral HI model.[11,18,47] This rapid distribution would allow D-JNKi to inhibit molecular pathways that are initiated very early after HI. In the brain, c-Jun is primarily activated in neurons (**chapter 3**) and in addition D-JNKi mainly localizes in neurons.[11,17,18,47,52,53] However, we cannot exclude that treatment with D-JNKi also influences other cell types within the brain. It has been demonstrated that JNK activation in microglia regulates activity and proliferation of these cells and leads to the expression of inflammatory molecules.[54-56] However, Benakis et al. (2010) showed that D-JNKi does not affect microglia activation or accumulation in a model of stroke.[52] It would be interesting to know what the role of the JNK pathway and the effect of D-JNKi treatment is in microglial cells in the LPS+HI model where these cells probably play a key role in aggravating brain damage after HI. Furthermore, we should keep in mind that rats with HI brain damage were treated i.p. with D-JNKi, so D-JNKi may also affect cells outside the central nervous system. It is known that in, for example neutrophils the JNK pathway plays an important role in chemotaxis and defense against microbial pathogens.[57] Whether D-JNKi affects the JNK pathway in neutrophils and if this might inhibit recruitment of peripheral cells to the injured brain is not clear yet and should be the focus of future research.

Interaction between JNK and p53: a deadly encounter

Besides activation at the mitochondrial membrane and regulation of the transcription of apoptotic genes, JNK can also influence apoptosis via phosphorylation of the tumor suppressor protein p53 that results in an increased stability and half-life of p53.[58] p53 is one of the most important death genes regulating the expression of different proteins involved in growth control, cell cycle checkpoints and apoptosis. Furthermore, p53 can translocate to the mitochondria where it promotes mitochondrial outer membrane permeabilization (MOMP) by activating pro-apoptotic and counteracting anti-apoptotic Bcl-2 family members.[59-62] Our group previously showed that neonatal HI triggers mitochondrial translocation of p53 which had detrimental effects on mitochondrial integrity.[26,41,63,64] Inhibition of mitochondrial p53 translocation by using the NF-κB inhibitor TAT-NBD or more specific with pifithrin (PFT)-μ reduced apoptotic cell death in the brain in the neonatal HI rat model.[41,63-65] In **chapter 4** we investigated the possible interaction between JNK and p53 after neonatal HI by using the TAT-P7-pi peptide. TAT-P7-pi is a peptide that mimics the P7 domain of p53 and thereby prevents binding of JNK to p53 and subsequent JNK-mediated phosphorylation of p53 at a specific threonine (Thr81) (Fig 1).[66,67] We describe for the first time in an *in vivo* model that one single i.p. gift of TAT-P7-pi resulted in a profound reduction in infarct volume and improvement in sensorimotor and cognitive function with a therapeutic window of at least 6 h after neonatal HI (**chapter 4**). We show that administration of TAT-P7-pi improved mitochondrial function, increased levels of mitochondrial anti-apoptotic proteins Bcl-2 and

Bcl-xL and reduced apoptotic cell death (Fig 1). Since inhibition of both mitochondrial located p53 and P-JNK results in potent neuroprotection after HI, while both treatments had no effect on the other molecule, we conclude that both JNK and p53 are needed to induce mitochondrial dysfunction and apoptotic cell death upon HI. With the results described in **chapter 4**, we show that the interaction between JNK and p53 plays a key role in setting off the apoptotic cascade.

What is the effect of JNK-p53 interaction? Under basal conditions, p53 is continuously ubiquitinated and has a half-life of less than 30 min.[68] After cellular stress JNK can bind p53 within the P7 domain, phosphorylate p53 at Thr81 and induce a conformational change that leads to suppressed binding of p53 to its endogenous inhibitor MDM2. In this way JNK can regulate ubiquitination of p53 and thereby facilitates prolonged availability of p53 within the cell (as a reduction in ubiquitination results in a strong increased half-life of p53). These modifications of p53 possibly induce mitochondrial translocation of p53 where it can bind and counteract the anti-apoptotic proteins Bcl-2 and Bcl-xL or directly activate pro-apoptotic members. Both of these actions strongly affect permeabilization of the mitochondrial membrane.[67-70] We demonstrated that inhibition of the JNK-p53 interaction by TAT-P7-pi strongly protects mitochondrial integrity (**chapter 4**). Although we did not yet determine the molecular location of the JNK-p53 interaction, we expect that this interaction happens at the mitochondrial level, since phosphorylated JNK is only present in this subcellular compartment after HI (**chapter 3**). Additional research is needed to confirm that the JNK-p53 interaction takes place at mitochondrial level. JNK and p53 both have an important nuclear role in regulating the transcription of multiple genes. It would be interesting to know if JNK and p53 interact within the nucleus and whether JNK-mediated p53 phosphorylation affects the transcriptional function of p53. Although TAT-P7-pi is capable of preventing p53-JNK interaction and reducing cell death *in vitro*,[67] we still have to investigate whether the neuroprotective effect of TAT-P7-pi is indeed induced by a reduction in JNK-p53 binding in the brain *in vivo*. Furthermore, it would be interesting to know whether TAT-P7-pi treatment results in the expected increased ubiquitination of p53 compared to vehicle treatment after neonatal HI.

Clinical translation of D-JNKi and TAT-P7-pi: a feasible and safe goal?

What are the possible side effects of D-JNKi or TAT-P7-pi treatment after HI? A relatively high basal level of JNK activation in the brain is necessary for the regulation of basal physiological processes.[10,71] One can therefore suppose that inhibition of such an important pathway is only feasible when regulated in a strictly controlled manner. Borsello et al. (2003) showed that D-JNKi is a highly specific inhibitor of the JNK pathway, since it had no effect on the activity of other kinases.[11] Noteworthy, we did not observe a downregulation in JNK activity in D-JNKi-treated animals lower than levels in sham controls (**chapter 3 and 6**). These data clearly indicate that treatment with D-JNKi only inhibited the HI-induced activation of the JNK pathway without affecting basal JNK levels that might play a physiological role.

Previously, we showed that prolonged inhibition of NF-κB activity or inhibition at a late time point (>12 h post-HI) after the insult aggravated the amount of brain damage which tampered the clinical usefulness of this treatment strategy.[41] In **chapter 3**, we show that one single injection of D-JNKi has short-lasting effects on JNK activity, since AP-1 activity at 24 h post-injection was restored. In addition, we demonstrate that after prolonged inhibition of the JNK pathway the protective effect of D-JNKi was lost, but most importantly, it did not exacerbate the amount of HI brain damage.

By using TAT-P7-pi treatment a crucial but very specific element of the JNK pathway is inhibited: the interaction between JNK and p53. Specific inhibition of JNK interaction with only one other molecule, *i.e.* leaving JNK interaction with all its other up- and downstream substrates undisturbed, diminishes the risk of negative side effects. Tumor suppressor p53, is important in preventing (suppressing) tumor formation. In a large part of human cancers mutations in p53 are observed.[60] However, for tumor formation a sustained inactivation of p53 is needed. When using TAT-P7-pi treatment we aimed at brief and selective inhibition of p53 stabilization by preventing interaction between JNK and p53. Importantly, we and others have shown that this interaction is only present after HI or upon cellular stress and is not operative under basal conditions (**chapter 4**).[69] These data indicate that TAT-P7-pi selectively inhibits the HI-induced JNK-p53 interaction that takes place at the damaged area. Therefore, we expect no side effects related to tumor formation. Importantly, all rats were followed for more than 9 weeks after D-JNKi and TAT-P7-pi treatment and within and after this period no adverse side effects or tumor formation were observed in any of the treated animals.

Another question is whether treatment with D-JNKi or TAT-P7-pi results in just preservation of damaged or dysfunctional neurons that should have died? In **chapter 3 and 4** we show that neuroprotection after D-JNKi and TAT-P7-pi was maintained over a time window of at least 9 weeks. From these findings we can conclude that treatment with D-JNKi or TAT-P7-pi not only postponed the onset of brain damage after HI, but really prevented neuronal damage that resulted in long-lasting neuroprotection. In addition, both treatments not only resulted in an anatomical improvement but the spared tissue was functional, as cognitive and sensorimotor function was preserved (**Chapter 3 and 4**). Before translation towards the clinical setting can be feasible both treatments should be tested in larger animal models (lamb, pig and/or monkey) to specifically address both the protective and possible adverse effects or toxicities of both peptides.

Several ways to die: apoptosis versus necrosis

In this thesis we mainly focused on the effect of D-JNKi, Sab_{KIM1} and TAT-P7-pi treatment on neuronal apoptotic cell death after neonatal HI. Besides apoptosis, HI-induced mitochondrial damage can also induce cell death via necrosis or an intermediate form of both, so called necroptosis.[72] Which route of cell death is activated depends on the nature of the stimulus, intensity and duration of the stimulus, type of cell, development stage and environmental factors such as the availability of caspases and ATP levels. Neonatal HI can lead to activation

of the calcium-dependent enzyme calpain, responsible for the cleavage of α-fodrin, resulting in membrane malfunction and necrotic cell death. We previously showed that treatment with L-JNKi in a neonatal HI rat model strongly reduced α-fodrin cleavage.[27] In line, Ginet et al. (2009) showed that D-JNKi decreased calpain activity after neonatal HI.[47] Furthermore, *in vitro* treatment with D-JNKi seemed to prevent necrotic cell death in cortical neurons exposed to high dose of NMDA.[73,74] Recently, it has been described that also mitochondrial-located p53 has an important role in regulating necrotic cell death by binding to cyclophilin D and opening of the mitochondrial permeability transition pore.[75, 76] In conclusion, treatment with D-JNKi and TAT-P7-pi might affect the role of JNK and/or p53 in both apoptotic and necrotic routes of cell death at once which would contribute to the potent neuroprotective effect observed after neonatal HI.

The research described in **chapter 3, 4 and 6** of this thesis emphasizes the importance of protecting the mitochondria to convey efficient neuroprotection after neonatal HI. Mitochondria are upstream key players involved in the early phase of cell death and damage to the mitochondrial outer membrane is described as a point of no return.[28,77] In this thesis, we show the potent neuroprotective effect of three small peptides, D-JNKi, Sab_{kim1} and TAT-P7-pi that prevent MOMP by targeting proteins that control the apoptotic balance at the mitochondrial membrane. Since mitochondrial integrity is affected in the early phase after the HI insult, treatment aimed at protecting the mitochondria should be started as soon as possible and at least within 6 h after the insult. The treatment strategies investigated in this thesis are promising therapeutic options for those neonates in whom a clear sentinel event is present just before or during birth. In cases of more chronic asphyxia other strategies, *i.e.* regenerative treatments, should be considered.

Inflammatory targets

In the second part of this chapter we focused on the role of inflammation in the development of neonatal HI brain damage. It is well known that after neonatal HI an inflammatory response evoked in the brain hallmarked by *e.g.* activation of microglia, increases cerebral expression of cytokine/chemokine and influx of neutrophils and macrophages from the periphery into the brain.[78-83] The purpose of inflammation is removal of harmful stimuli, stimulation of repair and healing, and restoration of homeostasis. However, the inflammatory response can also induce additional damage to surrounding cells and tissues.[84] Both the protective and destructive aspects of the cerebral and peripheral inflammatory response after neonatal HI-induced brain damage will be discussed below.

Polarization matters: M1 versus M2 microglia/macrophages

We confirm in **chapter 2** that neonatal HI induces an early neuroinflammatory response in P7 rats as illustrated by an increase in the expression of pro-inflammatory cytokines and chemokines and influx of neutrophils in the ipsilateral damaged hemisphere. Interestingly, we demonstrated for the first time that neonatal HI can induce polarization of microglia/macrophages towards a pro-inflammatory M1 phenotype early (starting at 3 h) post-HI whereas polarization to an anti-inflammatory M2 phenotype is observed at 24 h after HI in the damaged part of the brain (**chapter 2**). Since there are no clear differences in morphology or antigen markers between microglia and macrophages, these cell types are hard to distinguish in the damaged brain. Microglia cells are resident cells of the central nervous system and are first line immune defenders activated after brain damage, whereas macrophages first have to be recruited from the circulation towards the lesion site.[85-88] Since we investigated the effect of neonatal HI on the polarization early after HI (3-24 h) (**chapter 2**), we propose that the cell population observed in our study will prominently be microglia instead of infiltrating macrophages as the influx of macrophages probably contributes to damage in a later phase (2-3 days post-insult).[85-88] Microglia have a high plasticity and change their phenotype depending on environmental cues. To date, the exact role of microglia in the development of neonatal HI brain damage is still unclear; they appear to exert both protective and destructive properties. The polarization of microglia towards a pro-inflammatory M1 or anti-inflammatory/regenerative M2 phenotype may explain the different functional properties of these cells.[85-90] Polarization towards a M1 phenotype is predominantly induced by pro-inflammatory molecules like TNF-α and interferon-γ that are excreted in the early phase of brain damage, as observed in our study (**chapter 2**).[87,91] M1-like cells can excrete high levels of pro-inflammatory mediators (IL-1β, TNF-α, ROS) which, if not tightly controlled, can directly damage the surrounding tissue.[92] We suppose that polarization towards M1-like cells will be transient since the expression of one of the important stimuli (TNF-α) was short-lasting and decreased at 24 h post-HI, possibly facilitating a polarization switch towards the M2-like phenotype. In contrast, M2-like cells are believed to play a role in the healing process, by *e.g.* secretion of anti-inflammatory cytokines, suppressing nitrogen mono-oxide (NO) and cytokine production, facilitating phagocytosis of cell debris, influencing vascular permeability and angiogenesis.[88-90] Polarization towards the M2 phenotype is induced by anti-inflammatory factors such as IL-4, -10, -13, TGF-β. In **chapter 2** we show that cerebral expression of TGF-β is upregulated at 24 h after neonatal HI which would fit with the time point at which we observed polarization of microglia to the M2 phenotype. Important to note is that microglia/macrophages (especially of the M2 phenotype) are required for clearance of debris and phagocytosis of apoptotic and necrotic cells which dampens the inflammatory stimulus.[88-90,92] In this way impaired polarization towards the M2 phenotype could affect the protective phagocytotic function of microglia, resulting in an excessive neuroinflammatory response. We expect that a general inhibition of the function of the microglia/macrophage population as such does not necessarily has a beneficial effect on HI-induced brain damage.

For instance, as M2-like microglia/macrophages are involved in phagocytosis of cellular debris, these cells will aid in dampening the inflammatory reaction in the brain. Therefore, care should be taken in applying strategies to specifically inhibit polarization of microglia since these phenotypes have dual functions: damaging as well as protective. Investigating which factors are crucial to specific polarization of microglia/macrophage subtypes should be focus of future research.

Protecting the brain by targeting the periphery?

While the effects of neonatal HI on cerebral inflammation are quite well studied, less is known about the effects of HI brain injury on the peripheral inflammatory response and *vice versa*. In experimental studies using adult animals, local brain damage increases peripheral inflammation.[93-100] This peripheral response could support the cerebral inflammatory response and thereby aggravate brain damage. In this way specific targeting of the peripheral inflammatory response might become a strategy to protect the brain.

In **chapter 2** of this thesis we show that in contrast to adult animal studies, cerebral HI induces a short-lasting *decrease* in the peripheral inflammatory response. Noteworthy, although HI-induced brain damage resulted in decreased expression of almost all hepatic pro-inflammatory cytokines/chemokines, we observed a clear upregulation of hepatic CINC-1 expression at 3 h post-HI (**chapter 2**).

CINC-1 is an important chemokine for the recruitment of neutrophils. The hepatic CINC-1 could be essential for the recruitment of neutrophils from the bone marrow into the systemic circulation and secondly to the brain.[95,101,102] Within the brain neutrophils play an essential role in the clearance of cellular debris. However, activated neutrophils can also aggravate damage by producing and releasing substances like ROS, lysosomal enzymes, myeloperoxidase and pro-inflammatory cytokines that have clear adverse effects on neighboring cells. Importantly, neutrophils can cause additional brain damage by capillary plugging, obstructing the microvascular flow and impairing oxygen delivery to surrounding tissue. In line with these effects, several studies have shown that depletion of neutrophils, by using an antibody against polymorphonuclear cells, resulted in neuroprotection after experimental neonatal and adult HI.[78,103-109] From a clinical perspective it would be preferable to inhibit the increased influx of neutrophils to the lesion site instead of depleting the total neutrophil population, considering the increased risk of severe infections in neonates. We propose that early specific inhibition of peripheral CINC-1 after neonatal HI will reduce neutrophil influx from the bone marrow into the circulation and subsequently into the brain thereby preventing development of secondary brain damage by activated neutrophils. Reducing the HI-induced increase in peripheral CINC-1 expression could be a promising therapeutic target for neonates who face a HI insult.

Influence of systemic inflammation on HI brain damage: fuelling the fire

A maternal-fetal infection, for example chorioamnionitis, increases the risk of developing a neonatal HI insult. In addition, the combined exposure to an inflammatory environment *in utero* and a neonatal HI insult deteriorates neurodevelopmental outcome compared to HI alone.[110-112,112-117] The group of Mallard designed a mouse model to study the effect of systemic inflammation on HI-induced brain damage and nicely showed that a single, peripherally applied LPS injection aggravates HI-induced brain damage.[118-120]

Inflammatory mediators can directly damage the brain as for example observed after meningitis; the inflammatory reaction can also prime or sensitize the brain and make it more susceptible to a secondary event. LPS itself cannot cross the intact blood brain barrier (BBB),[121,122] is rapidly cleared from the circulation (half-life <30 min),[123] and on its own does not induce neuronal damage in a low dosage.[118,121,123,124] We therefore expect that systemic LPS aggravates HI-induced brain damage by sensitizing cells in the brain rather than directly affecting cerebral neuronal tissue.

The mechanisms of inflammatory sensitization of the brain are complex and far from being elucidated. One of the possible mechanisms is that peripheral inflammation induces stimulation of endothelial and epithelial cells of the BBB and choroid plexus, respectively. When these cells are activated, these cells produce immune signals that can activate and prime cells present in the brain (microglia, astrocytes, neurons) via activation of downstream signal pathways (*e.g.* MAPKs like ERK1/2, p38 and JNK as well as NF-κB) that stimulate the local production of inflammatory and apoptotic mediators. A second possible mechanism is that peripheral inflammation can increase BBB permeability thereby facilitating direct transport of peripheral inflammatory molecules across the BBB. A third possibility is that peripheral inflammation can influence signaling in the brain via stimulation of the vagal nerve by peripheral cytokines.[121,124,125] The complexity of this sensitizing effect is demonstrated by the fact that a single intraperitoneal LPS injection can change the expression of more than 1500 genes in the brain, of which the majority are involved in inflammation, cell death, phosphorylation and ion transport.[126]

Various studies suggest that a LPS-sensitized HI insult induces a faster and more intense activation of microglia and influx of macrophages compared to HI. Microglia are therefore described as the key cell type responsible for increased cerebral inflammation and tissue damage after sensitization.[120,127-129] We, however, did not observe a clear difference in number or morphology of Iba-1-positive microglia/macrophages present in the brain at 24 h post-insult between HI and LPS+HI animals (**chapter 5**). Based on this immunohistochemical staining's we concluded that in the early phase after LPS-sensitized HI, the increased cerebral inflammatory response is not induced by massive influx of macrophages. Nonetheless, microglia most likely play a key role in the early increased cerebral cytokine and chemokine expression after LPS+HI.[120,127-130]

We suggest that LPS-activated endothelial and epithelial cells prime microglia, resulting in an increased and prolonged production of inflammatory mediators and disturbance of the pro- and anti-inflammatory balance, without inducing a clear early change in the morphology of the microglia.

In **chapter 5 and 6** we show that systemic inflammation aggravates the severity of HI-induced brain damage. HI resulted in early neuronal damage that did not increase over time, whereas LPS-sensitized HI resulted in a gradual increase of neuronal damage up to day 15 post-insult, with the formation of an a-cellular cystic lesion in the ipsilateral hemisphere. The fact that cerebral damage still increases up to 15 days after the insult, possibly provides an extended window of opportunity to treat the exacerbation of brain damage after LPS+HI. For this purpose, it is crucial to elucidate which factors are responsible for the ongoing damage signal, so that specific treatments targeting these factors can be developed. Importantly, however, the development of an a-cellular lesion at 3-4 days after LPS+HI might be responsible for a diminished time-window for regenerative treatments, *e.g.* administration of mesenchymal stem cells (MSCs). MSCs regenerate the damaged brain when administered up to 10 day post-HI. However, MSCs need a matrix to reach the damaged area and accomplish their function. Therefore when the HI insult is preceded by inflammation MSC treatment should possibly be started before 3-4 days, as will be discussed in the last paragraph.

Of interest, we observed strong effects of LPS administration before HI on white matter integrity. We show that LPS+HI affected oligodendrocyte maturation, illustrated by a sharp decrease in mature oligodendrocytes after LPS+HI, decreased myelin production and induced white matter injury (**chapter 5**). TNF-α is known to damage oligodendrocytes directly or to inhibit maturation of oligodendrocytes.[128,131-133] Therefore, we suggest that the observed increased and prolonged cerebral expression of TNF-α could be responsible for impaired oligodendrocyte maturation and white matter injury after LPS+HI. Although inhibition of TNF-α by etanercept after the LPS+HI insult did not reduce white matter injury (**chapter 6**), TNF-α could still negatively influence oligodendrocyte maturation early after LPS injection or directly after HI. Unraveling which factors contribute to the maturational arrest of oligodendrocytes after LPS+HI is focus of our future research.

Systemic inflammation by LPS also changed the molecular pathways operative in the brain after HI. We describe in **chapter 6** that when HI is preceded by inflammation significant changes in the contribution of the JNK pathway and the intrinsic apoptotic pathway to the development of HI brain damage are observed. When HI was preceded by LPS, cell death was mainly regulated via the extrinsic apoptotic pathway, as observed by an increase in caspase 8 cleavage, and the JNK pathway and intrinsic apoptotic pathway had a minor role (**chapter 6**).

We propose that the reduced contribution of the JNK pathway is a result of increased activity of the NF-κB transcription factor, which has been shown to be potently activated after LPS+HI.[120,134] We and others have previously shown that activation of the NF-κB pathway can inhibit the JNK pathway via upregulation of different NF-κB-regulated target genes including

Gadd45β, XIAP, A20, Mn-Sod and FHC.[16,65,135,136] Increased NF-kB activity can in this way also be responsible for the upregulation of pro-inflammatory molecules and death receptor ligands that can activate the extrinsic apoptotic pathway.

From the results described in **chapter 5 and 6** we conclude that systemic inflammation does not only exacerbate HI-induced brain damage, but fundamentally changes some molecular mechanisms involved in the development of brain damage. Insight into these changes after inflammation-sensitized HI is very essential, since these changes might require adjustments in time window, dose or combination of different treatment strategies to achieve neuroprotection when a HI insult is preceded by systemic inflammation, as will be discussed later on.

Sensitization versus preconditioning

Although we observed a clear sensitizing (damaging) effect of inflammation on HI brain damage, inflammation can also induce tolerance or preconditioning of the brain, *i.e.* the brain is protected from a subsequent insult.[137-141] Whether inflammation induces a sensitizing or preconditioning effect depends on different factors, including the interval between inflammation and HI, duration of the secondary insult and the developmental stage of the brain. Studies have shown that LPS results in sensitization when administered 4-6 h, 14 h or 72 h before the HI insult, whereas a preconditioning effect is described when LPS is administered 24-48 h before the insult.[139-141] It is suggested that preconditioning needs a significant time delay between the primary and secondary insult since it requires the transcription of genes and protein synthesis.[137] Factors involved in preconditioning are: increased activation of NF-κB expression, upregulation of survival kinases, anti-apoptotic Bcl-2 proteins, the antioxidant enzyme superoxide dismutase, and upregulation of several inflammatory cytokines, among which TNF-α.[137,142,143] It is proposed that TNF-α produced in response to a mild preconditioning insult, increases the expression of negative feedback inhibitors (*e.g.* MnSOD, A20, cIAP, c-FLIP), responsible for suppressed TNF-α production during a secondary insult, in which TNF-α probably has damaging effects.[137,143-145] In the clinical setting it would be of great importance to know if an antenatal inflammatory response exerts a sensitizing or preconditioning effect on the brain; in other words if the child has an increased risk for the development of severe HI brain damage or if it is protected against. Ideally, the discovery of a specific biomarker that could differentiate between these conditions would be ideal to establish future clinical guidelines. A possible marker might be one of the negative feedback inhibitors of TNF-α as evidence of a preconditioning situation. In the next paragraph we will discuss in more detail the dual role of TNF-α during HI brain damage.

TNF-α: a double-edged sword

TNF-α is considered as a key mediator in neuroinflammation and is strongly upregulated in the brain after neonatal HI and LPS+HI (**chapter 2, 3 and 5**). TNF-α exerts a dual function, as it can induce both cell death and cell survival signals.[146] On the one hand, binding of TNF-α

to death receptor TNF-R1 can activate caspase 8 and apoptotic cell death via formation of the intracellular DISC or can lead to the activation of downstream pathways *i.e.* NF-κB, JNK and p38-MAPK. Activation of TNF-R2 on the other hand mainly initiates pro-survival signals via the PI3K cascade.[147,148] In the (damaged) brain TNF signaling via TNF-R1 is associated with: the polarization and activation of microglia/macrophages towards a M1 phenotype, activation of astrocytes and endothelial cells, direct toxic effects on neurons and oligodendrocytes, an increase in BBB permeability, an increase in glutamate excitotoxicity by preventing glutamate uptake by astrocytes, peripheral cellular recruitment, production of ROS, effects on coagulation cascades and stimulation of apoptosis.[128,130-133,146,149,150] Protective effects of TNF-α that have been described are for example beneficial effects on remyelination, synaptic plasticity, calcium homeostasis and membrane potential.[145,146,149,151-154] Whether TNF-α will exert protective or cytotoxic effects depends on different factors, for instance the amount of TNF-α, the brain regions were TNF-α is upregulated, microglial distribution and phenotype, and expression levels of the two TNF receptors.[146,154] We observed after LPS+HI that TNF-α expression was further increased and prolonged over time compared to HI alone, with a concomitant an early increase in the expression of TNF-R1 and later increase in TNF-R2 (**chapter 5 and 6**).

Initially we presumed that the increased TNF-α production after LPS+HI would have a predominant cytotoxic role, and could be responsible for setting off the apoptotic cascade via binding to death receptors. To investigate the role of TNF-α in the development of LPS-sensitized HI brain damage, we administered etanercept directly after the LPS+HI insult. Surprisingly, inhibition of TNF-α after the LPS+HI insult had no effect on cerebral damage after LPS+HI (**chapter 6**). Different studies showed that TNF-α might be key to inflammation-induced sensitization and activation of microglia and endothelial cells.[127,130,155] Therefore, we propose that TNF-α might be an important factor during early sensitization, yet the direct contribution of TNF-α to neuronal death after the LPS+HI insult is probably restricted.

In adult studies TNF-α production in the early phase (first 24 h) post-insult seems to have a damaging effect whereas it becomes involved in protection in the later phase.[156] This could also be the case in our neonatal HI model, since the expression of "protective" TNF-R2 occurred only after 1-3 days post-LPS+HI. Etanercept has a long-lasting inhibitory effect ($T_{1/2}$ app. 70 h) and will therefore probably inhibit the first, detrimental but also the second, protective phase of TNF-α. A (short-lasting) inhibitor that selectively reduces the early peak of TNF-α production without affecting the levels after 24 h or the use of a selective TNF-R1 antagonist would be a promising strategy to reduce HI brain injury.

In **chapter 6** we further describe that inhibition of TNF-α in D-JNKi-treated animals completely abolished the neuroprotective effect of D-JNKi after LPS+HI. Importantly, we observed that D-JNKi treatment causes an increase in TNF-R2 expression at 72 h after post-insult, further highlighting the importance of the TNF-R1 and -R2 balance in determining the destructive versus protective role of TNF-α.

Clinical perspectives and emerging concepts

To investigate the role of inflammation in HI brain damage, we used LPS as an activator of the innate immune system. LPS is a component of the cell wall of gram-negative bacteria, for example Escherichia coli, a pathogen often involved in maternal-fetal infection and early onset infections in especially prematurely born neonates. In the clinical setting, however, not only gram-negative bacteria are involved in fetal/neonatal inflammatory responses, but other micro-organisms such as Group B streptococcus, Listeria monocytogenes, Ureaplasma urealyticum, Mycoplasma hominis, Chlamydia trachomatis and Cytomegalovirus are also frequently involved.[157] These micro-organisms will activate other receptors than TLR4, which might result in activation of other downstream molecular cascades. At present it is unknown whether different specific pathogens might affect the development of HI brain damage differently.

We have discussed that inflammation not only aggravates HI brain damage, but also changes at least some of the pathophysiological mechanisms underlying HI brain damage. In **chapter 6** of this thesis we further illustrate the clinical relevance of these changes by demonstrating that two important protective treatment strategies in the experimental neonatal HI model (namely inhibiting the JNK pathway by D-JNKi and inhibiting TNF-α by etanercept) lose (most of) their protective effect when inflammation precedes HI. D-JNKi treatment had no effect on LPS+HI-induced cerebral damage in the effective dosage used in the HI model. Increasing the dosage of D-JNKi resulted in mild neuroprotection; app. 30% reduction in infarct volume compared to >80% reduction after the lower dosage in the HI only model. As described in the previous section, etanercept which has mild neuroprotective properties in the neonatal HI model, did not improve neuronal damage at all after LPS+HI (**chapter 6**). In line, Osredkar et al. (2014) recently described that hypothermia, the only clinically-applied protective treatment for full term neonates facing HI, seems to have no clear protective effect when inflammation is involved.[158] These data together show the emerging concept that potential treatment strategies for HI are less protective when inflammation comes into the equation.

The use of mesenchymal stem cells (MSC) as a neuroregenerative treatment is one of the most promising treatment strategies at this moment to repair neonatal HI brain damage in later stages after onset of HI, as the therapeutic window is at least 10 days.[159-161] Our preliminary data (which are not described in this thesis), however, indicate that treatment with MSC does not potently reduce cerebral damage when administered at 10 days after LPS-sensitized HI brain injury. As suggested in **chapter 5**, the changes in the timing of the damage response and formation of a cystic lesion from 4 days after LPS+HI, are possibly responsible for the decreased efficacy of MSC treatment.

In conclusion, we would like to emphasize that clinicians and researches have to be aware of the fact that (promising) treatment strategies might not be effective or might require modifications in therapeutic window, dose or combination of different treatments to achieve efficacious neuroprotection when neonates face a HI insult in combination with inflammation.

References

1. Nijboer CH, Bonestroo HJ, Zijlstra J, Kavelaars A, Heijnen CJ. Mitochondrial JNK phosphorylation as a novel therapeutic target to inhibit neuroinflammation and apoptosis after neonatal ischemic brain damage. *Neurobiol Dis*. 2013;54:432-444.
2. Nijboer CH, Heijnen CJ, Groenendaal F, May MJ, van Bel F, Kavelaars A. Strong neuroprotection by inhibition of NF-kappaB after neonatal hypoxia-ischemia involves apoptotic mechanisms but is independent of cytokines. *Stroke*. 2008;39:2129-2137.
3. Nijboer CH, Heijnen CJ, Groenendaal F, van Bel F, Kavelaars A. Alternate pathways preserve tumor necrosis factor-alpha production after nuclear factor-kappaB inhibition in neonatal cerebral hypoxia-ischemia. *Stroke*. 2009;40:3362-3368.
4. Nijboer CH, Heijnen CJ, van der Kooij MA, et al. Targeting the p53 pathway to protect the neonatal ischemic brain. *Ann Neurol*. 2011;70:255-264.
5. Nijboer CH, Kavelaars A, Vroon A, Groenendaal F, van Bel F, Heijnen CJ. Low endogenous G-protein-coupled receptor kinase 2 sensitizes the immature brain to hypoxia-ischemia-induced gray and white matter damage. *J Neurosci*. 2008;28:3324-3332.
6. Nijboer CH, van der Kooij MA, van Bel F, Ohl F, Heijnen CJ, Kavelaars A. Inhibition of the JNK/AP-1 pathway reduces neuronal death and improves behavioral outcome after neonatal hypoxic-ischemic brain injury. *Brain Behav Immun*. 2010;24:812-821.
7. Edwards AD, Mehmet H. Apoptosis in perinatal hypoxic-ischaemic cerebral damage. *Neuropathol Appl Neurobiol*. 1996;22:494-498.
8. Gill R, Soriano M, Blomgren K, et al. Role of caspase-3 activation in cerebral ischemia-induced neurodegeneration in adult and neonatal brain. *J Cereb Blood Flow Metab*. 2002;22:420-430.
9. Pirianov G, Brywe KG, Mallard C, et al. Deletion of the c-Jun N-terminal kinase 3 gene protects neonatal mice against cerebral hypoxic-ischaemic injury. *J Cereb Blood Flow Metab*. 2007;27:1022-1032.
10. Kuan CY, Whitmarsh AJ, Yang DD, et al. A critical role of neural-specific JNK3 for ischemic apoptosis. *Proc Natl Acad Sci U S A*. 2003;100:15184-15189.
11. Borsello T, Clarke PG, Hirt L, et al. A peptide inhibitor of c-Jun N-terminal kinase protects against excitotoxicity and cerebral ischemia. *Nat Med*. 2003;9:1180-1186.
12. Repici M, Mare L, Colombo A, et al. c-Jun N-terminal kinase binding domain-dependent phosphorylation of mitogen-activated protein kinase kinase 4 and mitogen-activated protein kinase kinase 7 and balancing cross-talk between c-Jun N-terminal kinase and extracellular signal-regulated kinase pathways in cortical neurons. *Neuroscience*. 2009;159:94-103.
13. Wiegler K, Bonny C, Coquoz D, Hirt L. The JNK inhibitor XG-102 protects from ischemic damage with delayed intravenous administration also in the presence of recombinant tissue plasminogen activator. *Cerebrovasc Dis*. 2008;26:360-366.
14. Esneault E, Castagne V, Moser P, Bonny C, Bernaudin M. D-JNKi, a peptide inhibitor of c-Jun N-terminal kinase, promotes functional recovery after transient focal cerebral ischemia in rats. *Neuroscience*. 2008;152:308-320.
15. Hirt L, Badaut J, Thevenet J, et al. D-JNKI1, a cell-penetrating c-Jun-N-terminal kinase inhibitor, protects against cell death in severe cerebral ischemia. *Stroke*. 2004;35:1738-1743.
16. Liu JR, Zhao Y, Patzer A, et al. The c-Jun N-terminal kinase (JNK) inhibitor XG-102 enhances the neuroprotection of hyperbaric oxygen after cerebral ischaemia in adult rats. *Neuropathol Appl Neurobiol*. 2010;36:211-224.
17. Michel-Monigadon D, Bonny C, Hirt L. c-Jun N-terminal kinase pathway inhibition in intracerebral hemorrhage. *Cerebrovasc Dis*. 2010;29:564-570.
18. Repici M, Centeno C, Tomasi S, et al. Time-course of c-Jun N-terminal kinase activation after cerebral ischemia and effect of D-JNKI1 on c-Jun and caspase-3 activation. *Neuroscience*. 2007;150:40-49.

19. Repici M, Chen X, Morel MP, et al. Specific inhibition of the JNK pathway promotes locomotor recovery and neuroprotection after mouse spinal cord injury. *Neurobiol Dis*. 2012;46:710-721.
20. Repici M, Borsello T. JNK pathway as therapeutic target to prevent degeneration in the central nervous system. *Adv Exp Med Biol*. 2006;588:145-155.
21. Bogoyevitch MA, Kobe B. Uses for JNK: the many and varied substrates of the c-Jun N-terminal kinases. *Microbiol Mol Biol Rev*. 2006;70:1061-1095.
22. Bogoyevitch MA, Ngoei KR, Zhao TT, Yeap YY, Ng DC. c-Jun N-terminal kinase (JNK) signaling: recent advances and challenges. *Biochim Biophys Acta*. 2010;1804:463-475.
23. Barr RK, Kendrick TS, Bogoyevitch MA. Identification of the critical features of a small peptide inhibitor of JNK activity. *J Biol Chem*. 2002;277:10987-10997.
24. Bonny C, Borsello T, Zine A. Targeting the JNK pathway as a therapeutic protective strategy for nervous system diseases. *Rev Neurosci*. 2005;16:57-67.
25. Bonny C, Oberson A, Negri S, Sauser C, Schorderet DF. Cell-permeable peptide inhibitors of JNK: novel blockers of beta-cell death. *Diabetes*. 2001;50:77-82.
26. Nijboer CH, Heijnen CJ, Groenendaal F, van Bel F, Kavelaars A. Alternate pathways preserve tumor necrosis factor-alpha production after nuclear factor-kappaB inhibition in neonatal cerebral hypoxia-ischemia. *Stroke*. 2009;40:3362-3368.
27. Nijboer CH, van der Kooij MA, van Bel F, Ohl F, Heijnen CJ, Kavelaars A. Inhibition of the JNK/AP-1 pathway reduces neuronal death and improves behavioral outcome after neonatal hypoxic-ischemic brain injury. *Brain Behav Immun*. 2010;24:812-821.
28. Hagberg H, Mallard C, Rousset CI, Thornton C. Mitochondria: hub of injury responses in the developing brain. *Lancet Neurol*. 2014;13:217-232.
29. Blomgren K, Zhu C, Hallin U, Hagberg H. Mitochondria and ischemic reperfusion damage in the adult and in the developing brain. *Biochem Biophys Res Commun*. 2003;304:551-559.
30. Chambers JW, Howard S, LoGrasso PV. Blocking c-Jun N-terminal kinase (JNK) translocation to the mitochondria prevents 6-hydroxydopamine-induced toxicity in vitro and in vivo. *J Biol Chem*. 2013;288:1079-1087.
31. Chambers JW, Pachori A, Howard S, Iqbal S, LoGrasso PV. Inhibition of JNK mitochondrial localization and signaling is protective against ischemia/reperfusion injury in rats. *J Biol Chem*. 2013;288:4000-4011.
32. Hanawa N, Shinohara M, Saberi B, Gaarde WA, Han D, Kaplowitz N. Role of JNK translocation to mitochondria leading to inhibition of mitochondria bioenergetics in acetaminophen-induced liver injury. *J Biol Chem*. 2008;283:13565-13577.
33. Zhao Y, Spigolon G, Bonny C, Culman J, Vercelli A, Herdegen T. The JNK inhibitor D-JNKI-1 blocks apoptotic JNK signaling in brain mitochondria. *Mol Cell Neurosci*. 2012;49:300-310.
34. Kharbanda S, Saxena S, Yoshida K, et al. Translocation of SAPK/JNK to mitochondria and interaction with Bcl-x(L) in response to DNA damage. *J Biol Chem*. 2000;275:322-327.
35. Schroeter H, Boyd CS, Ahmed R, et al. c-Jun N-terminal kinase (JNK)-mediated modulation of brain mitochondria function: new target proteins for JNK signalling in mitochondrion-dependent apoptosis. *Biochem J*. 2003;372:359-369.
36. Aoki H, Kang PM, Hampe J, et al. Direct activation of mitochondrial apoptosis machinery by c-Jun N-terminal kinase in adult cardiac myocytes. *J Biol Chem*. 2002;277:10244-10250.
37. Wang F, Jiang Y, Zhang S, Xiao W, Zhu S. Protective effects of overexpression of bcl-xl gene on local cerebral infarction in transgenic mice undergoing permanent occlusion of middle cerebral artery. *J Huazhong Univ Sci Technolog Med Sci*. 2008;28:56-59.
38. Yamamoto K, Ichijo H, Korsmeyer SJ. BCL-2 is phosphorylated and inactivated by an ASK1/Jun N-terminal protein kinase pathway normally activated at G(2)/M. *Mol Cell Biol*. 1999;19:8469-8478.
39. Fan M, Goodwin M, Vu T, Brantley-Finley C, Gaarde WA, Chambers TC. Vinblastine-induced phosphorylation of Bcl-2 and Bcl-XL is mediated by JNK and occurs in parallel with inactivation of the Raf-1/MEK/ERK cascade. *J Biol Chem*. 2000;275:29980-29985.

40. Han JY, Jeong EY, Kim YS, et al. C-jun N-terminal kinase regulates the interaction between 14-3-3 and Bad in ethanol-induced cell death. *J Neurosci Res*. 2008;86:3221-3229.
41. Nijboer CH, Heijnen CJ, Groenendaal F, May MJ, van Bel F, Kavelaars A. A dual role of the NF-kappaB pathway in neonatal hypoxic-ischemic brain damage. *Stroke*. 2008;39:2578-2586.
42. Yin W, Cao G, Johnnides MJ, et al. TAT-mediated delivery of Bcl-xL protein is neuroprotective against neonatal hypoxic-ischemic brain injury via inhibition of caspases and AIF. *Neurobiol Dis*. 2006;21:358-371.
43. Doeppner TR, Dietz GP, Weise J, Bahr M. Protection of hippocampal neurogenesis by TAT-Bcl-x(L) after cerebral ischemia in mice. *Exp Neurol*. 2010;223:548-556.
44. Kilic E, Dietz GP, Hermann DM, Bahr M. Intravenous TAT-Bcl-Xl is protective after middle cerebral artery occlusion in mice. *Ann Neurol*. 2002;52:617-622.
45. Wong LF, Ralph GS, Walmsley LE, et al. Lentiviral-mediated delivery of Bcl-2 or GDNF protects against excitotoxicity in the rat hippocampus. *Mol Ther*. 2005;11:89-95.
46. Lawrence MS, McLaughlin JR, Sun GH, et al. Herpes simplex viral vectors expressing Bcl-2 are neuroprotective when delivered after a stroke. *J Cereb Blood Flow Metab*. 1997;17:740-744.
47. Ginet V, Puyal J, Magnin G, Clarke PG, Truttmann AC. Limited role of the c-Jun N-terminal kinase pathway in a neonatal rat model of cerebral hypoxia-ischemia. *J Neurochem*. 2009;108:552-562.
48. Borsello T, Bonny C. Use of cell-permeable peptides to prevent neuronal degeneration. *Trends Mol Med*. 2004;10:239-244.
49. Besirli CG, Johnson EM,Jr. JNK-independent activation of c-Jun during neuronal apoptosis induced by multiple DNA-damaging agents. *J Biol Chem*. 2003;278:22357-22366.
50. Bessero AC, Chiodini F, Rungger-Brandle E, Bonny C, Clarke PG. Role of the c-Jun N-terminal kinase pathway in retinal excitotoxicity, and neuroprotection by its inhibition. *J Neurochem*. 2010;113:1307-1318.
51. Sevilla A, Santos CR, Barcia R, Vega FM, Lazo PA. c-Jun phosphorylation by the human vaccinia-related kinase 1 (VRK1) and its cooperation with the N-terminal kinase of c-Jun (JNK). *Oncogene*. 2004;23:8950-8958.
52. Benakis C, Bonny C, Hirt L. JNK inhibition and inflammation after cerebral ischemia. *Brain Behav Immun*. 2010;24:800-811.
53. Liu J, Lin A. Wiring the cell signaling circuitry by the NF-kappa B and JNK1 crosstalk and its applications in human diseases. *Oncogene*. 2007;26:3267-3278.
54. Hidding U, Mielke K, Waetzig V, et al. The c-Jun N-terminal kinases in cerebral microglia: immunological functions in the brain. *Biochem Pharmacol*. 2002;64:781-788.
55. Waetzig V, Czeloth K, Hidding U, et al. c-Jun N-terminal kinases (JNKs) mediate pro-inflammatory actions of microglia. *Glia*. 2005;50:235-246.
56. Kaminska B. MAPK signalling pathways as molecular targets for anti-inflammatory therapy--from molecular mechanisms to therapeutic benefits. *Biochim Biophys Acta*. 2005;1754:253-262.
57. Yeh MC, Mukaro V, Hii CS, Ferrante A. Regulation of neutrophil-mediated killing of Staphylococcus aureus and chemotaxis by c-jun NH2 terminal kinase. *J Leukoc Biol*. 2010;87:925-932.
58. Dhanasekaran DN, Reddy EP. JNK signaling in apoptosis. *Oncogene*. 2008;27:6245-6251.
59. Culmsee C, Mattson MP. P53 in Neuronal Apoptosis. *Biochem Biophys Res Commun*. 2005;331:761-777.
60. Vousden KH, Lu X. Live or let die: the cell's response to p53. *Nat Rev Cancer*. 2002;2:594-604.
61. Morrison RS, Kinoshita Y, Johnson MD, Guo W, Garden GA. P53-Dependent Cell Death Signaling in Neurons. *Neurochem Res*. 2003;28:15-27.
62. Green DR, Kroemer G. Cytoplasmic functions of the tumour suppressor p53. *Nature*. 2009;458:1127-1130.
63. Nijboer CH, Heijnen CJ, van der Kooij MA, et al. Targeting the p53 pathway to protect the neonatal ischemic brain. *Ann Neurol*. 2011;70:255-264.

64. Nijboer CH, Heijnen CJ, Groenendaal F, May MJ, van Bel F, Kavelaars A. Strong neuroprotection by inhibition of NF-kappaB after neonatal hypoxia-ischemia involves apoptotic mechanisms but is independent of cytokines. *Stroke*. 2008;39:2129-2137.

65. Nijboer CH, Heijnen CJ, Groenendaal F, van Bel F, Kavelaars A. Alternate pathways preserve tumor necrosis factor-alpha production after nuclear factor-kappaB inhibition in neonatal cerebral hypoxia-ischemia. *Stroke*. 2009;40:3362-3368.

66. Adler V, Pincus MR, Minamoto T, et al. Conformation-dependent phosphorylation of p53. *Proc Natl Acad Sci U S A*. 1997;94:1686-1691.

67. Buschmann T, Potapova O, Bar-Shira A, et al. Jun NH2-terminal kinase phosphorylation of p53 on Thr-81 is important for p53 stabilization and transcriptional activities in response to stress. *Mol Cell Biol*. 2001;21:2743-2754.

68. Moll UM, Petrenko O. The MDM2-p53 interaction. *Mol Cancer Res*. 2003;1:1001-1008.

69. Fuchs SY, Adler V, Buschmann T, et al. JNK targets p53 ubiquitination and degradation in nonstressed cells. *Genes Dev*. 1998;12:2658-2663.

70. Vaseva AV, Moll UM. The mitochondrial p53 pathway. *Biochim Biophys Acta*. 2009;1787:414-420.

71. Xu X, Raber J, Yang D, Su B, Mucke L. Dynamic regulation of c-Jun N-terminal kinase activity in mouse brain by environmental stimuli. *Proc Natl Acad Sci U S A*. 1997;94:12655-12660.

72. Northington FJ, Chavez-Valdez R, Martin LJ. Neuronal cell death in neonatal hypoxia-ischemia. *Ann Neurol*. 2011;69:743-758.

73. Centeno C, Repici M, Chatton JY, et al. Role of the JNK pathway in NMDA-mediated excitotoxicity of cortical neurons. *Cell Death Differ*. 2007;14:240-253.

74. Vaslin A, Puyal J, Borsello T, Clarke PG. Excitotoxicity-related endocytosis in cortical neurons. *J Neurochem*. 2007;102:789-800.

75. Vaseva AV, Marchenko ND, Ji K, Tsirka SE, Holzmann S, Moll UM. P53 Opens the Mitochondrial Permeability Transition Pore to Trigger Necrosis. *Cell*. 2012;149:1536-1548.

76. Kinnally KW, Peixoto PM, Ryu SY, Dejean LM. Is mPTP the gatekeeper for necrosis, apoptosis, or both? *Biochim Biophys Acta*. 2011;1813:616-622.

77. Hagberg H, Mallard C, Rousset CI, Xiaoyang W. Apoptotic mechanisms in the immature brain: involvement of mitochondria. *J Child Neurol*. 2009;24:1141-1146.

78. Palmer C, Roberts RL, Young PI. Timing of neutrophil depletion influences long-term neuroprotection in neonatal rat hypoxic-ischemic brain injury. *Pediatr Res*. 2004;55:549-556.

79. Silverstein FS, Barks JD, Hagan P, Liu XH, Ivacko J, Szaflarski J. Cytokines and perinatal brain injury. *Neurochem Int*. 1997;30:375-383.

80. Hedtjarn M, Mallard C, Hagberg H. Inflammatory gene profiling in the developing mouse brain after hypoxia-ischemia. *J Cereb Blood Flow Metab*. 2004;24:1333-1351.

81. Bona E, Andersson AL, Blomgren K, et al. Chemokine and inflammatory cell response to hypoxia-ischemia in immature rats. *Pediatr Res*. 1999;45:500-509.

82. Dammann O, O'Shea TM. Cytokines and perinatal brain damage. *Clin Perinatol*. 2008;35:643-63.

83. Hagberg H, Gilland E, Bona E, et al. Enhanced expression of interleukin (IL)-1 and IL-6 messenger RNA and bioactive protein after hypoxia-ischemia in neonatal rats. *Pediatr Res*. 1996;40:603-609.

84. Medzhitov R. Origin and physiological roles of inflammation. *Nature*. 2008;454:428-435.

85. Martinez FO, Sica A, Mantovani A, Locati M. Macrophage activation and polarization. *Front Biosci*. 2008;13:453-461.

86. Martinez FO, Helming L, Gordon S. Alternative activation of macrophages: an immunologic functional perspective. *Annu Rev Immunol*. 2009;27:451-483.

87. Martinez FO. Regulators of macrophage activation. *Eur J Immunol*. 2011;41:1531-1534.

88. Mosser DM, Edwards JP. Exploring the full spectrum of macrophage activation. *Nat Rev Immunol*. 2008;8:958-969.

89. Gordon S, Martinez FO. Alternative activation of macrophages: mechanism and functions. *Immunity*. 2010;32:593-604.

90. David S, Kroner A. Repertoire of microglial and macrophage responses after spinal cord injury. *Nat Rev Neurosci*. 2011;12:388-399.

91. Murray PJ, Wynn TA. Obstacles and opportunities for understanding macrophage polarization. *J Leukoc Biol*. 2011;89:557-563.

92. Kigerl KA, Gensel JC, Ankeny DP, Alexander JK, Donnelly DJ, Popovich PG. Identification of two distinct macrophage subsets with divergent effects causing either neurotoxicity or regeneration in the injured mouse spinal cord. *J Neurosci*. 2009;29:13435-13444.

93. Anthony DC, Couch Y, Losey P, Evans MC. The systemic response to brain injury and disease. *Brain Behav Immun*. 2012;26:534-540.

94. Wilcockson DC, Campbell SJ, Anthony DC, Perry VH. The systemic and local acute phase response following acute brain injury. *J Cereb Blood Flow Metab*. 2002;22:318-326.

95. Campbell SJ, Anthony DC, Oakley F, et al. Hepatic nuclear factor kappa B regulates neutrophil recruitment to the injured brain. *J Neuropathol Exp Neurol*. 2008;67:223-230.

96. Campbell SJ, Deacon RM, Jiang Y, Ferrari C, Pitossi FJ, Anthony DC. Overexpression of IL-1beta by adenoviral-mediated gene transfer in the rat brain causes a prolonged hepatic chemokine response, axonal injury and the suppression of spontaneous behaviour. *Neurobiol Dis*. 2007;27:151-163.

97. Campbell SJ, Hughes PM, Iredale JP, et al. CINC-1 is an acute-phase protein induced by focal brain injury causing leukocyte mobilization and liver injury. *FASEB J*. 2003;17:1168-1170.

98. Campbell SJ, Perry VH, Pitossi FJ, et al. Central nervous system injury triggers hepatic CC and CXC chemokine expression that is associated with leukocyte mobilization and recruitment to both the central nervous system and the liver. *Am J Pathol*. 2005;166:1487-1497.

99. Campbell SJ, Zahid I, Losey P, et al. Liver Kupffer cells control the magnitude of the inflammatory response in the injured brain and spinal cord. *Neuropharmacology*. 2008;55:780-787.

100. Chapman KZ, Dale VQ, Denes A, et al. A rapid and transient peripheral inflammatory response precedes brain inflammation after experimental stroke. *J Cereb Blood Flow Metab*. 2009;29:1764-1768.

101. Maher JJ, Scott MK, Saito JM, Burton MC. Adenovirus-mediated expression of cytokine-induced neutrophil chemoattractant in rat liver induces a neutrophilic hepatitis. *Hepatology*. 1997;25:624-630.

102. Wittwer AJ, Carr LS, Zagorski J, Dolecki GJ, Crippes BA, De Larco JE. High-level expression of cytokine-induced neutrophil chemoattractant (CINC) by a metastatic rat cell line: purification and production of blocking antibodies. *J Cell Physiol*. 1993;156:421-427.

103. Hudome S, Palmer C, Roberts RL, Mauger D, Housman C, Towfighi J. The role of neutrophils in the production of hypoxic-ischemic brain injury in the neonatal rat. *Pediatr Res*. 1997;41:607-616.

104. Nijboer CH, Kavelaars A, Vroon A, Groenendaal F, van Bel F, Heijnen CJ. Low endogenous G-protein-coupled receptor kinase 2 sensitizes the immature brain to hypoxia-ischemia-induced gray and white matter damage. *J Neurosci*. 2008;28:3324-3332.

105. Garcia JH, Liu KF, Yoshida Y, Lian J, Chen S, del Zoppo GJ. Influx of leukocytes and platelets in an evolving brain infarct (Wistar rat). *Am J Pathol*. 1994;144:188-199.

106. Matsuo Y, Onodera H, Shiga Y, et al. Correlation between myeloperoxidase-quantified neutrophil accumulation and ischemic brain injury in the rat. Effects of neutrophil depletion. *Stroke*. 1994;25:1469-1475.

107. Heinel LA, Rubin S, Rosenwasser RH, Vasthare US, Tuma RF. Leukocyte involvement in cerebral infarct generation after ischemia and reperfusion. *Brain Res Bull*. 1994;34:137-141.

108. Jiang N, Moyle M, Soule HR, Rote WE, Chopp M. Neutrophil inhibitory factor is neuroprotective after focal ischemia in rats. *Ann Neurol*. 1995;38:935-942.

109. Doycheva DM, Hadley T, Li L, Applegate RL,2nd, Zhang JH, Tang J. Anti-neutrophil antibody enhances the neuroprotective effects of G-CSF by decreasing number of neutrophils in hypoxic ischemic neonatal rat model. *Neurobiol Dis*. 2014;69:192-199.

110. Wu YW, Escobar GJ, Grether JK, Croen LA, Greene JD, Newman TB. Chorioamnionitis and cerebral palsy in term and near-term infants. *JAMA*. 2003;290:2677-2684.

111. Blume HK, Li CI, Loch CM, Koepsell TD. Intrapartum fever and chorioamnionitis as risks for encephalopathy in term newborns: a case-control study. *Dev Med Child Neurol*. 2008;50:19-24.

112. Nelson KB, Dambrosia JM, Grether JK, Phillips TM. Neonatal cytokines and coagulation factors in children with cerebral palsy. *Ann Neurol*. 1998;44:665-675.

113. Grether JK, Nelson KB. Maternal infection and cerebral palsy in infants of normal birth weight. *JAMA*. 1997;278:207-211.

114. Bartha AI, Foster-Barber A, Miller SP, et al. Neonatal encephalopathy: association of cytokines with MR spectroscopy and outcome. *Pediatr Res*. 2004;56:960-966.

115. Shalak LF, Laptook AR, Jafri HS, Ramilo O, Perlman JM. Clinical chorioamnionitis, elevated cytokines, and brain injury in term infants. *Pediatrics*. 2002;110:673-680.

116. Aly H, Khashaba MT, El-Ayouty M, El-Sayed O, Hasanein BM. IL-1beta, IL-6 and TNF-alpha and outcomes of neonatal hypoxic ischemic encephalopathy. *Brain Dev*. 2006;28:178-182.

117. Impey L, Greenwood C, MacQuillan K, Reynolds M, Sheil O. Fever in labour and neonatal encephalopathy: a prospective cohort study. *BJOG*. 2001;108:594-597.

118. Eklind S, Mallard C, Leverin AL, et al. Bacterial endotoxin sensitizes the immature brain to hypoxic--ischaemic injury. *Eur J Neurosci*. 2001;13:1101-1106.

119. Wang X, Rousset CI, Hagberg H, Mallard C. Lipopolysaccharide-induced inflammation and perinatal brain injury. *Semin Fetal Neonatal Med*. 2006;11:343-353.

120. Wang X, Stridh L, Li W, et al. Lipopolysaccharide sensitizes neonatal hypoxic-ischemic brain injury in a MyD88-dependent manner. *J Immunol*. 2009;183:7471-7477.

121. Singh AK, Jiang Y. How does peripheral lipopolysaccharide induce gene expression in the brain of rats? *Toxicology*. 2004;201:197-207.

122. Banks WA, Robinson SM. Minimal penetration of lipopolysaccharide across the murine blood-brain barrier. *Brain Behav Immun*. 2010;24:102-109.

123. Mathison JC, Ulevitch RJ. The clearance, tissue distribution, and cellular localization of intravenously injected lipopolysaccharide in rabbits. *J Immunol*. 1979;123:2133-2143.

124. Xaio H, Banks WA, Niehoff ML, Morley JE. Effect of LPS on the permeability of the blood-brain barrier to insulin. *Brain Res*. 2001;896:36-42.

125. Mallard C. Innate immune regulation by toll-like receptors in the brain. *ISRN Neurol*. 2012;2012:701950.

126. Eklind S, Hagberg H, Wang X, et al. Effect of lipopolysaccharide on global gene expression in the immature rat brain. *Pediatr Res*. 2006;60:161-168.

127. Aden U, Favrais G, Plaisant F, et al. Systemic inflammation sensitizes the neonatal brain to excitotoxicity through a pro-/anti-inflammatory imbalance: key role of TNFalpha pathway and protection by etanercept. *Brain Behav Immun*. 2010;24:747-758.

128. Kadhim H, Tabarki B, Verellen G, De Prez C, Rona AM, Sebire G. Inflammatory cytokines in the pathogenesis of periventricular leukomalacia. *Neurology*. 2001;56:1278-1284.

129. Dean JM, Wang X, Kaindl AM, et al. Microglial MyD88 signaling regulates acute neuronal toxicity of LPS-stimulated microglia in vitro. *Brain Behav Immun*. 2010;24:776-783.

130. Kendall GS, Hristova M, Horn S, et al. TNF gene cluster deletion abolishes lipopolysaccharide-mediated sensitization of the neonatal brain to hypoxic ischemic insult. *Lab Invest*. 2011;91:328-341.

131. Pang Y, Campbell L, Zheng B, Fan L, Cai Z, Rhodes P. Lipopolysaccharide-activated microglia induce death of oligodendrocyte progenitor cells and impede their development. *Neuroscience*. 2010;166:464-475.

132. Volpe JJ, Kinney HC, Jensen FE, Rosenberg PA. The developing oligodendrocyte: key cellular target in brain injury in the premature infant. *Int J Dev Neurosci*. 2011;29:423-440.

133. Selmaj K, Raine CS, Farooq M, Norton WT, Brosnan CF. Cytokine cytotoxicity against oligodendrocytes. Apoptosis induced by lymphotoxin. *J Immunol*. 1991;147:1522-1529.

134. Yang D, Sun YY, Lin X, et al. Intranasal delivery of cell-penetrating anti-NF-kappaB peptides (Tat-NBD) alleviates infection-sensitized hypoxic-ischemic brain injury. *Exp Neurol*. 2013;247:447-455.

135. Tang G, Minemoto Y, Dibling B, et al. Inhibition of JNK activation through NF-kappaB target genes. *Nature*. 2001;414:313-317.

136. Javelaud D, Besancon F. NF-kappa B activation results in rapid inactivation of JNK in TNF alpha-treated Ewing sarcoma cells: a mechanism for the anti-apoptotic effect of NF-kappa B. *Oncogene*. 2001;20:4365-4372.

137. Mallard C, Hagberg H. Inflammation-induced preconditioning in the immature brain. *Semin Fetal Neonatal Med*. 2007;12:280-286.

138. Jenster M, Bonifacio SL, Ruel T, et al. Maternal or neonatal infection: association with neonatal encephalopathy outcomes. *Pediatr Res*. 2014;76:93-99.

139. Tasaki K, Ruetzler CA, Ohtsuki T, Martin D, Nawashiro H, Hallenbeck JM. Lipopolysaccharide pre-treatment induces resistance against subsequent focal cerebral ischemic damage in spontaneously hypertensive rats. *Brain Res*. 1997;748:267-270.

140. Wang X, Hagberg H, Nie C, Zhu C, Ikeda T, Mallard C. Dual role of intrauterine immune challenge on neonatal and adult brain vulnerability to hypoxia-ischemia. *J Neuropathol Exp Neurol*. 2007;66:552-561.

141. Eklind S, Mallard C, Arvidsson P, Hagberg H. Lipopolysaccharide induces both a primary and a secondary phase of sensitization in the developing rat brain. *Pediatr Res*. 2005;58:112-116.

142. Bordet R, Deplanque D, Maboudou P, et al. Increase in endogenous brain superoxide dismutase as a potential mechanism of lipopolysaccharide-induced brain ischemic tolerance. *J Cereb Blood Flow Metab*. 2000;20:1190-1196.

143. Rosenzweig HL, Minami M, Lessov NS, et al. Endotoxin preconditioning protects against the cytotoxic effects of TNFalpha after stroke: a novel role for TNFalpha in LPS-ischemic tolerance. *J Cereb Blood Flow Metab*. 2007;27:1663-1674.

144. Lastres-Becker I, Cartmell T, Molina-Holgado F. Endotoxin preconditioning protects neurones from in vitro ischemia: role of endogenous IL-1beta and TNF-alpha. *J Neuroimmunol*. 2006;173:108-116.

145. Cheng B, Christakos S, Mattson MP. Tumor necrosis factors protect neurons against metabolic-excitotoxic insults and promote maintenance of calcium homeostasis. *Neuron*. 1994;12:139-153.

146. Sriram K, O'Callaghan JP. Divergent roles for tumor necrosis factor-alpha in the brain. *J Neuroimmune Pharmacol*. 2007;2:140-153.

147. Gupta S. A decision between life and death during TNF-alpha-induced signaling. *J Clin Immunol*. 2002;22:185-194.

148. Wajant H, Pfizenmaier K, Scheurich P. Tumor necrosis factor signaling. *Cell Death Differ*. 2003;10:45-65.

149. McCoy MK, Tansey MG. TNF signaling inhibition in the CNS: implications for normal brain function and neurodegenerative disease. *J Neuroinflammation*. 2008;5:45-2094-5-45.

150. Hallenbeck JM. The many faces of tumor necrosis factor in stroke. *Nat Med*. 2002;8:1363-1368.

151. Houzen H, Kikuchi S, Kanno M, Shinpo K, Tashiro K. Tumor necrosis factor enhancement of transient outward potassium currents in cultured rat cortical neurons. *J Neurosci Res*. 1997;50:990-999.

152. Carlson NG, Bacchi A, Rogers SW, Gahring LC. Nicotine blocks TNF-alpha-mediated neuroprotection to NMDA by an alpha-bungarotoxin-sensitive pathway. *J Neurobiol*. 1998;35:29-36.

153. Turrin NP, Rivest S. Tumor necrosis factor alpha but not interleukin 1 beta mediates neuroprotection in response to acute nitric oxide excitotoxicity. *J Neurosci*. 2006;26:143-151.

154. Plant SR, Arnett HA, Ting JP. Astroglial-derived lymphotoxin-alpha exacerbates inflammation and demyelination, but not remyelination. *Glia*. 2005;49:1-14.

155. Markus T, Cronberg T, Cilio C, Pronk C, Wieloch T, Ley D. Tumor necrosis factor receptor-1 is essential for LPS-induced sensitization and tolerance to oxygen-glucose deprivation in murine neonatal organotypic hippocampal slices. *J Cereb Blood Flow Metab*. 2009;29:73-86.

156. Scherbel U, Raghupathi R, Nakamura M, et al. Differential acute and chronic responses of tumor necrosis factor-deficient mice to experimental brain injury. *Proc Natl Acad Sci U S A*. 1999;96:8721-8726.

157. Levy O. Innate immunity of the newborn: basic mechanisms and clinical correlates. *Nat Rev Immunol*. 2007;7:379-390.

158. Osredkar D, Thoresen M, Maes E, Flatebo T, Elstad M, Sabir H. Hypothermia is not neuroprotective after infection-sensitized neonatal hypoxic-ischemic brain injury. *Resuscitation*. 2014;85:567-572.

159. van Velthoven CT, Sheldon RA, Kavelaars A, et al. Mesenchymal stem cell transplantation attenuates brain injury after neonatal stroke. *Stroke*. 2013;44:1426-1432.

160. Donega V, van Velthoven CT, Nijboer CH, et al. Intranasal mesenchymal stem cell treatment for neonatal brain damage: long-term cognitive and sensorimotor improvement. *PLoS One*. 2013;8:51253.

161. Bennet L, Tan S, Van den Heuij L, et al. Cell therapy for neonatal hypoxia-ischemia and cerebral palsy. *Ann Neurol*. 2012;71:589-600.

9

Nederlandse samenvatting

Summary in Dutch

Zuurstofgebrek rondom de geboorte, in dit proefschrift beschreven als *perinatale asfyxie* of neonatale *hypoxie-ischemie* (HI), is een ernstig ziektebeeld dat ontstaat na een periode van onvoldoende zuurstof uitwisseling voor, tijdens of kort na de geboorte. Perinatale asfyxie is wereldwijd een van de belangrijkste oorzaken van babysterfte binnen de eerste levensmaand (de neonatale periode). In de Westerse wereld komt perinatale asfyxie voor bij 2-6 op de 1000 levendgeborenen, in ontwikkelingslanden ligt dit aantal vele malen hoger. Door het zuurstofgebrek lopen verschillende organen schade op; zo kunnen er problemen ontstaan aan o.a. het hart, de longen, darmen, nieren en de bloedstolling. Doordat het brein een hoge energie- en zuurstofbehoefte heeft en relatief weinig herstellend vermogen, is dit een van de meest kwetsbare organen voor zuurstofgebrek. Perinatale asfyxie kan hierdoor leiden tot ernstige hersenschade, ook wel *neonatale encefalopathie* genoemd. Uiteindelijk overlijdt 20% van de aangedane baby's aan de gevolgen van perinatale asfyxie. Van de overlevenden houdt een groot gedeelte levenslange lichamelijke en/of geestelijke beperkingen, waarbij men kan denken aan spasticiteit, ernstige ontwikkelingsachterstand, mentale retardatie, gedragsproblemen, doofheid, blindheid en/of epilepsie.

Ondanks het vele onderzoek verricht naar perinatale asfyxie, zijn de behandelingsmogelijkheden voor deze kwetsbare groep patiënten tot op heden zeer beperkt. Momenteel wordt alleen koeling (hypothermie) als standaard behandeling gegeven na ernstig zuurstofgebrek en tekenen van hersenschade; deze behandeling zorgt voor enige verbetering van de hersenschade in een gedeelte van de aangedane baby's.

Onderzoek naar de onderliggende factoren die bijdragen aan het ontstaan van hersenschade na perinatale asfyxie zijn van groot belang, omdat dit uiteindelijk kan leiden tot de ontwikkeling van nieuwe behandelingsstrategieën om hersenschade en levenslange beperkingen te voorkomen of te herstellen. We starten dit hoofdstuk met enige achtergrond informatie over reeds bekende pathofysiologische mechanismen betrokken bij het ontstaan van hersenschade na perinatale asfyxie en informatie over de experimentele diermodellen die we gebruikt hebben in dit proefschrift. Daarna volgt een samenvatting van de in dit proefschrift beschreven resultaten en eindigt dit hoofdstuk met een conclusie.

Het ontstaan van hersenschade na HI

Primaire fase

Meerdere mechanismen dragen bij aan het ontstaan van hersenschade na perinatale asfyxie. Direct na het incident is er een daling in zuurstof en energie niveau (ATP), hierdoor worden energiebronnen zoals glucose op een alternatieve manier verbrand, waarbij afvalstoffen vrijkomen (bijvoorbeeld lactaat) en er een zuur milieu ontstaat (acidose). Door een daling in ATP niveau worden energie-afhankelijke functies van de hersencellen verstoord, waaronder het behoud van een negatieve membraanpotentiaal. Verandering van deze membraanpotentiaal heeft belangrijke gevolgen; het veroorzaakt o.a. een instroom van

bepaalde ionen zoals natrium, chloride en calcium in de cel, gevolgd door water waardoor de cel opzwelt en kan barsten. Een toename in intracellulair calcium kan meerdere enzymen activeren, waaronder proteasen, lipasen en endonucleasen die zorgen voor de afbraak van verschillende belangrijke celstructuren. Daarnaast is calcium betrokken bij de vorming van schadelijke zuurstofradicalen. Membraan depolarisatie zorgt tevens voor een verhoogde afgifte van de neurotransmitter glutamaat door de zenuwcellen, waardoor glutamaat buiten de cel ophoopt. Glutamaat bindt en activeert receptoren waardoor andere zenuwcellen extra worden gestimuleerd; dit verhoogt het risico op het ontstaan van epilepsie en verdere verstoringen van het metabolisme. Glutamaat verhoogt daarnaast de instroom van natrium en calcium ionen in de cel, wat zorgt voor verdere zwelling van de cel en vorming van zuurstofradicalen. De hierboven beschreven factoren dragen allen bij aan de ontwikkeling van hersenschade, echter de grootste golf van celdood treedt pas op in een latere fase (6-48 uur na het incident) tijdens de zogenaamde *secundaire fase*.

Secundaire fase

In de secundaire fase is er vaak herstel van zuurstofaanbod en bloeddoorstroming in het brein, zogenaamde *reperfusie*. Reperfusie is van groot belang om de initiële schade te beperken, echter is het ook geassocieerd met een toename van schade doordat de aanvoer van zuurstof de vorming van vrije zuurstofradicalen versterkt. Hypoxie, calcium instroom en zuurstofradicalen zijn factoren die intracellulaire cascades en transcriptiefactoren kunnen activeren, zoals nuclear factor-κB (NF-κB) en c-Jun N-terminal kinase (JNK), wat zorgt voor een verhoogde expressie van verschillende genen betrokken bij ontsteking (inflammatie). Inflammatie is een complex proces waarbij vele immuuncellen *betrokken* zijn. Binnen 3 uur na het HI incident treedt er een duidelijke inflammatoire reactie op in het brein, gekenmerkt door activatie van lokale immuuncellen zoals microglia en astrocyten, instroom van perifere immuuncellen zoals neutrofiele granulocyten, macrofagen en T-cellen, en de productie van cytokinen en chemokinen door geactiveerde en beschadigde cellen. Microglia/macrofagen en neutrofiele granulocyten spelen een belangrijke rol bij het opruimen van beschadigde cellen en het stimuleren van weefselherstel. Echter wanneer deze cellen ongecontroleerd of overmatig worden geactiveerd, scheiden ze stoffen uit (o.a. cytokinen/chemokinen, zuurstofradicalen en proteasen) welke schadelijk kunnen zijn voor omliggende cellen. Verschillende studies hebben aangetoond dat het verminderen van het aantal neutrofiele granulocyten en bepaalde pro-inflammatoire cytokinen na neonatale HI, het ontstaan van hersenschade kan beperken in een diermodel. Echter de exacte invloed van het remmen van microglia/macrofagen en andere pro-inflammatoire cytokinen en chemokinen is nog onbekend. De inflammatoire reactie lijkt in ieder geval zowel een beschermende als een beschadigende werking te kunnen hebben in het brein na een neonataal HI incident.

Apoptose

Uiteindelijk resulteert een ernstig neonataal HI incident in celdood. Cellen kunnen dood gaan via 1) apoptose; een geprogrammeerde en gecontroleerde vorm van celdood, 2) necrose; een ongecontroleerde vorm van celdood waarbij de celinhoud vrijkomt en een inflammatoire reactie veroorzaakt, 3) necroptose; een tussenvorm van apoptose en necrose. In dit proefschrift hebben we ons met name gericht op de apoptotische vorm van celdood. Apoptose kan geactiveerd worden via een *intrinsieke* of een *extrinsieke* route (zie figuur 1 in hoofdstuk 1). Binnen de intrinsieke route spelen de mitochondriën een belangrijke rol. Mitochondriën zijn de energiecentrales van een cel, echter wanneer mitochondriën beschadigd raken, zijn ze betrokken bij het aanzetten van apoptose. Aan het mitochondriële buitenmembraan kunnen moleculen binden die apoptose stimuleren (pro-apoptotische eiwitten zoals Bid, Bax, Bak, Bad) of apoptose remmen (anti-apoptotische eiwitten zoals Bcl-2, Bcl-xL). Na een HI incident wordt de balans tussen de pro- en anti-apoptotische eiwitten verstoord, met een verlaging van anti-apoptotische en een verhoging van pro-apoptotische eiwitten tot gevolg. De pro-apoptotische eiwitten vormen een kanaal in het mitochondriële membraan, waardoor moleculen, zoals cytochrome c en Smac/Diablo, uit de mitochondriën in het cytosol lekken. Deze moleculen zorgen voor de activatie van caspase 9 en uiteindelijk activatie van caspase 3, die het DNA in de celkern kan beschadigen en apoptotische celdood induceert. De extrinsieke route wordt geactiveerd na binding van specifieke 'dood'-factoren (o.a. TNF-α, FasL en TRAIL) aan 'dood'-receptoren op de buitenkant van de celmembraan, waardoor er in de cel een complex wordt gevormd (de DISC) welke zorgt voor de activatie van caspase 8 en uiteindelijk caspase 3. Daarnaast kan caspase 8 ook de intrinsieke apoptotische route activeren door activatie van het pro-apoptotische eiwit Bid (zie figuur 1 in hoofdstuk 1).

p53 en JNK

Tijdens en na een neonataal HI incident worden meerdere transcriptiefactoren geactiveerd die de expressie van verschillende genen betrokken bij apoptose reguleren. In dit proefschrift hebben we ons met name gericht op de rol van transcriptiefactor p53 en MAP kinase eiwit JNK in het brein na neonatale HI.

p53 is een tumor-suppressor eiwit dat sterk verhoogd is in de kern en mitochondriën na HI. In de kern zorgt p53 voor de regulatie van verschillende eiwitten die een rol spelen bij celgroei en apoptose. Op mitochondrieel niveau activeert p53 pro-apoptotische eiwitten en heeft het een remmend effect op anti-apoptotische eiwitten, waardoor het zorgt voor de activatie van de intrinsieke apoptotische route.

De JNK cascade wordt geactiveerd na cellulaire stress. JNK kan vervolgens meerdere moleculen in de kern, cytosol en mitochondriën fosforyleren. Een van de belangrijkste effecten van JNK in de kern is fosforylatie/activatie van c-Jun. c-Jun is een onderdeel van transcriptiefactor AP-1, welke zorgt voor de regulatie van genen betrokken bij o.a. inflammatie en apoptose. Op mitochondrieel niveau zorgt JNK voor activatie van pro-apoptotische eiwitten en remming van anti-apoptotische eiwitten. Daarnaast kan JNK p53 binden en fosforyleren, waardoor

p53 minder snel wordt afgebroken en apoptotische celdood verder wordt gestimuleerd (voor een schematisch overzicht van de effecten van JNK, zie figuur 2, hoofdstuk 1).

Diermodel

Om onderliggende mechanismen betrokken bij het ontstaan van hersenschade na perinatale asfyxie en de werkzaamheid van nieuwe behandelstrategieën te onderzoeken is het gebruik van experimentele diermodellen tot op heden onmisbaar. In dit proefschrift hebben we gebruik gemaakt van 9 dagen oude muizen en 7 dagen oude ratten als model voor de pasgeboren baby's. Er is gekozen voor deze leeftijdstermijn omdat de hersenontwikkeling rond deze termijn in knaagdieren het meest overeenkomt met humane neonaten geboren na een zwangerschapsduur van ongeveer 34-36 weken). Het HI incident werd geïnduceerd volgens de methode beschreven door *Rice* en *Vannucci*. In het kort: er wordt een kleine incisie gemaakt rechts in de hals onder algehele en lokale anesthesie, waarna de rechter halsslagader (arterie carotis) wordt vrij geprepareerd en doorgebrand (ischemie) en de incisie middels 1-2 hechtingen wordt gesloten. Na een herstel periode van minimaal 1 uur, worden de pups in een afgesloten bak in een voorverwarmde couveuse geplaatst. Hypoxie wordt geïnduceerd door de toevoer van gas met een lage zuurstofconcentratie (muizen ondergaan 45-50 min hypoxie met 10% O_2, ratten 90-120 min met 8% O_2). Dit model resulteert in de muis in milde en in de rat in ernstige HI hersenschade, die beperkt blijft tot de rechter hemisfeer van het brein.

Een infectie gedurende de zwangerschap, bijvoorbeeld een baarmoederontsteking (chorioamnionitis), is een bekende risicofactor voor het ontstaan van perinatale asfyxie. Daarnaast heeft het gecombineerd voorkomen van een infectie met een neonataal HI incident een veel slechtere prognose dan wanneer neonatale HI op zichzelf staand voorkomt. Om deze situatie na te bootsen hebben we in **hoofdstuk 5 en 6** het neonatale HI model zoals hierboven beschreven gecombineerd met een inflammatoire stimulus. Een intra-peritoneale injectie met lipopolysaccharide (LPS) werd 14 uur voor de operatie gegeven aan neonatale muizen. LPS is afkomstig van een gramnegatieve bacterie (Escherichia coli) en wordt frequent gebruikt om een infectie na te bootsen. Het combineren van LPS met een HI incident zorgt voor een verergering van de HI-geïnduceerde hersenschade. Dit gecombineerde model is uiterst geschikt om het effect van infectie/inflammatie op het ontstaan van hersenschade na HI te onderzoeken en te kijken of veelbelovende behandelingen voor HI ook werkzaam zijn wanneer een inflammatie voorafgaat aan het incident.

Ook al is de situatie in een muis of rat vele malen meer simplistisch dan de humane situatie, het is een uiterst geschikt model om onderliggende pathofysiologische mechanismen te onderzoeken, de werking van potentieel nieuwe therapieën te testen, onderzoek te doen naar lange-termijn gevolgen en effecten op gedrag en functioneren, en een dosis-respons curve en therapeutisch window te onderzoeken. Voordat veelbelovende experimentele therapieën vanuit een knaagdiermodel in de klinische setting kunnen worden toegepast

zullen de werkzaamheid, mogelijke nadelige bijwerkingen en toxiciteit onderzocht moeten worden in een groter diermodel. Men kan hierbij denken aan een big, lam of primaat model.

Doel van dit proefschrift

In dit proefschrift hebben we in een neonataal HI muis en rat model onderzoek gedaan naar 1) de rol van apoptose en inflammatie bij het ontstaan van hersenschade na HI, en 2) nieuwe behandelmogelijkheden om hersenschade te voorkomen na neonatale HI, door de mitochondriën te beschermen middels behandeling met D-JNKi, Sab_{KIM1} of TAT-P7-pi.

De rol van de mitochondriën en apoptose

In **hoofdstuk 3 en 6** hebben we de rol van de JNK cascade in neonatale HI hersenschade onderzocht in een rat en muis model. We beschrijven voor het eerst dat de intracellulaire kinase (enzym) JNK na een neonataal HI incident alleen geactiveerd wordt aan de mitochondriën en niet in de kern of in het cytosol. Activatie van mitochondrieel gelokaliseerd JNK zorgt voor een disbalans tussen de mitochondriële anti- en pro-apoptotische eiwitten. Dit resulteert in activatie van de intrinsieke apoptotische route met afgifte van cytochrome *c* vanuit de mitochondriën naar het cytosol, dat uiteindelijk zorgt voor activatie van caspase 3 (**hoofdstuk 3**). Het remmen van de JNK cascade middels een klein peptide D-JNKi, zorgde voor een spectaculaire afname in apoptose en hersenschade, met >85% reductie in infarct volume en verbetering van sensorisch en motorisch gedrag en cognitie. De behandeling met D-JNKi kon tenminste 6 uur na het incident worden gestart (therapeutisch window) om nog een beschermend effect te hebben (**hoofdstuk 3 en 6**). Het sterke neuroprotectieve effect van D-JNKi behandeling bleek gebaseerd op 1) het remmen van de activatie van mitochondrieel JNK en 2) het verhogen van mitochondrieel gelokaliseerde anti-apoptotische eiwitten Bcl-2 en Bcl-xL. De combinatie van deze twee mechanismen resulteerde uiteindelijk in het beschermen van de mitochondriële functionaliteit en het voorkomen van activatie van apoptose via de intrinsieke route (**hoofdstuk 3**). De belangrijke rol van mitochondrieel gelokaliseerd JNK in het ontstaan van HI hersenschade werd verder onderstreept doordat behandeling met Sab_{KIM1}, een peptide dat specifiek mitochondrieel JNK remt en niet JNK in het cytosol of de kern, ook een beschermend effect had na een neonataal HI incident (**hoofdstuk 3**).

In voorgaande studies is aangetoond dat naast activatie van JNK, een neonataal HI incident ook zorgt voor mitochondriële translocatie van het tumor-suppressor eiwit p53. Remmen van mitochondriale translocatie van p53 middels pifithrin-μ zorgde eveneens voor een indrukwekkende afname in apoptotische celdood en hersenschade. *In vitro* studies hebben laten zien dat er een binding plaats kan vinden tussen JNK en p53 in het zogenoemde P7 domein van p53, waarna JNK p53 kan fosforyleren en hiermee de stabiliteit van p53 verhoogt. In **hoofdstuk 4** hebben we onderzocht of het remmen van deze p53-JNK interactie, die waarschijnlijk plaatsvindt op mitochondrieel niveau, een beschermend effect

zou kunnen hebben op HI hersenschade in een neonataal rat model. Hiervoor hebben we gebruik gemaakt van het kleine peptide TAT-P7-pi. We laten zien dat TAT-P7-pi een zeer potent middel is om hersenschade na HI te voorkomen, met een therapeutisch window van minimaal 6 uur (**hoofdstuk 4**). TAT-P7-pi zorgt voor een sterke afname in grijze en witte stof schade in het brein, het voorkomt de afname in anti-apoptotische mitochondriële eiwitten, het zorgt voor bescherming van de mitochondriële integriteit, voorkomt apoptotische celdood, en verbetert motorisch, sensori-motorisch en cognitief gedrag. Verder onderzoek is nodig om aan te tonen of de interactie tussen JNK en p53 inderdaad plaatsvindt en in welk compartiment van de cel, of TAT-P7-pi deze interactie remt en wat de invloed van deze remming is op de stabiliteit van p53.

De rol van inflammatie

In **hoofdstuk 2** hebben we de inflammatoire respons in de lever en het brein in kaart gebracht na een neonataal HI incident in de rat. We beschrijven dat er na neonatale HI een sterk verhoogde expressie is van pro-inflammatoire cytokinen/chemokinen in de beschadigde kant van het brein, met een sterke instroom aan perifere neutrofiele granulocyten in het brein. We laten voor het eerst zien dat er na neonatale HI in het brein polarisatie plaatsvindt van microglia/macrofagen naar een pro-inflammatoir M1 fenotype dat start op 3 uur, en naar een anti-inflammatoir M2 fenotype dat start op 24 uur na het incident. De precieze rol van microglia/macrofagen in het brein na neonatale HI is nog niet bekend, ze kunnen zowel een beschermende als destructieve werking hebben. Verschillende stimuli in de omgeving van microglia/macrofagen kunnen ervoor zorgen dat ze snel veranderen van fenotype en functie. Polarisatie van microglia/macrofagen naar een M1 fenotype wordt gestimuleerd door inflammatoire factoren als interferon-γ, LPS en TNF-α. M1 cellen kunnen zorgen voor de uitstoot van pro-inflammatoire factoren, waarmee ze omliggende cellen kunnen beschadigen. De anti-inflammatoire factoren IL-4, -13, -10 kunnen polarisatie naar het M2 fenotype induceren, deze M2 cellen proberen inflammatie te remmen en genezing te stimuleren. Omdat microglia/macrofagen ook een belangrijke beschermende immuunfunctie hebben zal het aspecifiek remmen van de microglia/macrofagen niet voordelig zijn. Echter het remmen van het ontstaan van een M1 fenotype of het stimuleren van polarisatie naar een M2 fenotype zou wel een mogelijk beschermende strategie kunnen zijn.

In tegenstelling tot wat beschreven is in volwassen studies, laten wij in **hoofdstuk 2** zien dat er na neonatale HI geen sterke inflammatoire respons plaatsvindt buiten het centrale zenuwstelsel. Neonatale HI resulteert in een verlaging van de meeste pro-inflammatoire cytokinen en chemokinen in de lever op 3 uur na het incident. Echter is er in de lever wel een sterke toename in de expressie van CINC-1, een belangrijk chemokine betrokken bij het aantrekken van neutrofiele granulocyten. Neutrofiele granulocyten zijn belangrijke immuuncellen, die een prominente rol spelen tijdens het opruimen van celresten. Echter geactiveerde neutrofiele granulocyten zorgen ook voor een toename van celschade doordat ze schadelijke stoffen zoals vrije zuurstofradicalen, pro-inflammatoire cytokinen en enzymen

uitscheiden. We speculeren dat de verhoogde CINC-1 expressie in de lever zou kunnen zorgen voor het aantrekken van neutrofielen vanuit het beenmerg naar de systemische circulatie en vervolgens naar het brein waar deze cellen zorgen voor een toename in inflammatie en hersenschade (**hoofdstuk 2**). Verder onderzoek is nodig om te achterhalen of het specifiek remmen van CINC-1 in de perifere circulatie kan zorgen voor een afname van neutrofiele granulocyten in het brein en daarmee een vermindering van hersenschade.

Uit klinische gegevens weten we dat het risico op het ontstaan van een neonataal HI incident groter is wanneer er een infectie, inflammatie of koorts aanwezig is vlak voor of gedurende de bevalling. Daarbij komend hebben deze neonaten vaak een slechtere prognose. In **Hoofdstuk 5** hebben we in een neonataal HI muis model onderzocht wat het effect is van een inflammatie voorafgaand aan een HI incident op grijze en witte stofschade, het aantal oligodendrocyten (cellen die zorgen voor de productie van witte stof) en de inflammatoire respons in het brein. We beschrijven voor het eerst dat een inflammatoire reactie, geïnduceerd met LPS 14 uur voor het HI incident, niet alleen resulteert in een toename in neuronale schade maar ook in een toename in hersenschade over tijd: tot 15 dagen na het incident ontwikkelde de hersenschade zich met de zichtbare ontwikkeling van een cysteuze laesie na 3-4 dagen. Na HI alleen is de neuronale schade al maximaal op 3 uur na het incident en ontstaat er geen cysteuze laesie. LPS+HI dieren hadden tevens meer witte stof schade in en buiten het infarct gebied, met een afname in het aantal rijpe oligodendrocyten. De combinatie van LPS+HI zorgde voor een verhoogde inflammatoire respons in het brein met een toename in 1) de expressie van cytokinen en chemokinen tot 3 dagen na het HI incident, 2) instroom van het aantal neutrofiele granulocyten en 3) en verhoogde activatie van microglia/macrofagen op 2 dagen na het incident (**hoofdstuk 2**). Aan de hand van deze resultaten concluderen we dat wanneer HI vooraf wordt gegaan door een inflammatie dit grote gevolgen zou kunnen hebben voor de werkzaamheid, effectieve dosering en/of therapeutisch window van veelbelovende experimentele therapieën, gezien de verandering van timing en toename in inflammatoire respons en hersenschade na LPS+HI.

De resultaten beschreven in **hoofdstuk 6** tonen dat er na inflammatie en HI niet alleen een verandering optreedt in de timing van en hoeveelheid aan hersenschade, maar dat er daadwerkelijk een verandering plaatsvindt in enkele onderliggende pathofysiologische mechanismen. Door het analyseren van verschillende apoptotische markers hebben we in **hoofdstuk 6** ontdekt dat apoptotische celdood na LPS+HI niet verloopt via de intrinsieke route, maar voornamelijk verloopt via de extrinsieke route. Waar er na HI in het brein sprake is van duidelijke activatie van JNK op mitochondrieel niveau met een afname in mitochondriële anti-apoptotische eiwitten en een sterke afgifte van cytochrome c vanuit de mitochondria naar het cytosol (**hoofdstuk 3**), vonden we na LPS+HI geen duidelijke veranderingen in deze parameters (**hoofdstuk 6**). LPS+HI zorgde wel voor activatie van caspase 8, een van de belangrijkste factoren binnen de extrinsieke apoptotische route.

Dat de verandering in betrokken intracellulaire cascades na LPS+HI vergaande gevolgen kan hebben, wordt verder duidelijk gemaakt in **hoofdstuk 6**. We tonen aan dat twee veelbelovende experimentele behandelingsstrategieën voor HI (het remmen van de JNK cascade en het remmen van TNF-α) niet effectief zijn in LPS+HI dieren. Eerdere studies hebben ook al aangetoond dat hypothermie, de enige klinisch beschikbare behandeling van neonatale HI op dit moment, geen of een verminderd effect heeft wanneer een inflammatie voorafgaat aan het HI incident. Verder onderzoek is hard nodig om te achterhalen welke factoren verantwoordelijk zijn voor de langdurige toename in hersenschade en inflammatoire respons na de combinatie van inflammatie en HI, zodat nieuwe therapeutische strategieën ontwikkelt kunnen worden voor neonaten waarin een HI incident vooraf wordt gegaan door een inflammatie.

In **hoofdstuk 5 en 6** laten we zien dat er na een inflammatie en HI incident sprake is van een sterke en langdurige toename in de expressie van TNF-α in de beschadigde zijde van het brein. TNF-α is in de literatuur vaak beschreven als een pro-inflammatoir cytokine dat o.a. directe schade kan veroorzaken aan oligodendrocyten en neuronen, zorgt voor activatie van lokale (immuun)cellen en dat de extrinsieke apoptotische route kan aanzetten via de 'dood'receptoren. Daarnaast wordt TNF-α beschreven als een van de belangrijkste factoren die zorgt voor de toename in hersenschade na LPS+HI. Om deze redenen hadden we verwacht dat remmen van TNF-α een veelbelovende therapie zou kunnen zijn voor neonaten wanneer een inflammatie voorafgaat aan een HI incident. Echter in **hoofdstuk 6** tonen we aan dat het remmen van TNF-α middels etanercept, geen neuroprotectieve werking heeft na LPS+HI. Onverwachts vonden we zelfs dat het remmen van TNF-α in D-JNKi-behandelde dieren een toename in hersenschade veroorzaakte, wat duidt op een mogelijk beschermend effect van TNF-α onder condities waarin JNK geremd wordt (**hoofdstuk 6**). We suggereren dat de balans tussen TNF-receptor 1 en 2 belangrijk is voor het ofwel nadelige ofwel beschermende effect van TNF-α. Activatie van TNF-receptor 1 induceert celdood en een inflammatoire reactie in tegenstelling tot activatie van TNF-receptor 2 welke zorgt voor celoverleving. Behandeling met een hoge dosering D-JNKi in LPS+HI dieren zorgde voor een verhoogde expressie van met name TNF-receptor 2, waardoor TNF-α in deze dieren dus mogelijk een beschermende werking, in plaats van nadelige werking heeft. TNF-α lijkt in het LPS+HI model niet de verantwoordelijke factor te zijn voor de activatie van de extrinsieke apoptotische route. Verder onderzoek is nodig om te achterhalen welke factoren verantwoordelijk zijn voor de activatie van (de extrinsieke route van) apoptose wanneer een HI incident vooraf wordt gegaan door inflammatie. Verder zou het specifiek remmen van TNF-receptor 1 of stimuleren van TNF-receptor 2 een mogelijke behandeloptie zijn.

In **hoofdstuk 7** hebben we uitgebreid onderzocht of osteopontine (OPN) een potentiële behandeloptie zou kunnen zijn voor neonatale HI hersenschade. OPN is een eiwit dat vele functies vervult en invloed heeft op o.a. celadhesie, migratie, differentiatie, apoptose en

overleving. Voorafgaand onderzoek binnen onze onderzoeksgroep heeft aangetoond dat de expressie van OPN sterk verhoogd is in het brein na neonatale HI. We konden verder aantonen dat OPN knock-out muizen (genetisch gemanipuleerde muizen die geen OPN bezitten) meer hersenschade ontwikkelen dan normale muizen na HI. Deze bevindingen gecombineerd met enkele studies die een neuroprotectief effect van OPN behandeling beschreven in verschillende diermodellen, leidde tot de studie in **hoofdstuk 7** waarin we hebben gekeken naar de mogelijke therapeutische effecten van OPN behandeling in ons neonataal HI model. We tonen aan in **hoofdstuk 7** dat behandeling met een klein OPN peptide niet zorgt voor een afname in hersenschade na neonatale HI in 9 dagen oude muizen. OPN werd gegeven via verschillende toedieningsroutes (intraperitoneaal (in de buikholte), intranasaal (via de neus) en intracerebraal (in het brein)), in verschillende doseringen en op verschillende tijdstippen na HI, echter geen van deze behandelingsstrategieën resulteerde in een beschermend effect van het OPN peptide. De endogene verhoging van OPN heeft waarschijnlijk een belangrijke beschermende functie in het brein na neonatale HI, maar het verder verhogen of langdurig hooghouden van de OPN concentratie lijkt geen verdere toegevoegde waarde te hebben voor HI hersenschade.

Conclusies

In dit proefschrift tonen we aan dat de eiwitten JNK en p53 aan de mitochondriën een belangrijke rol spelen in het verstoren van de apoptotische balans en zo in het ontstaan van hersenschade na neonatale HI (**hoofdstuk 3, 4 en 6**). We hebben uitgebreid laten zien dat drie zeer veelbelovende behandelingen, gericht op het remmen van de activatie van JNK of de interactie tussen JNK en p53, zorgen voor een bescherming van de mitochondriële integriteit en een spectaculaire afname in hersenschade na neonatale HI (**hoofdstuk 3, 4 en 6**). De behandelingen met D-JNKi, Sab_{KIM1} en TAT-P7-pi zijn beschermend tot tenminste 6 uur na het HI incident, en zouden daarmee een mogelijke therapie kunnen vormen voor neonaten waarbij er duidelijke acute tekenen zijn van perinatale asfyxie vlak voor of gedurende de geboorte en waarbij er na de geboorte snel gestart kan worden met de behandeling. Voordat deze behandelingen daadwerkelijk in de klinische setting toegepast kunnen worden, moet er nog wel uitgebreid onderzoek plaatsvinden naar de beschermende effecten, mogelijk bijwerkingen en toxiciteit in grotere diermodellen.

In **hoofdstuk 2, 5 en 6** van dit proefschrift hebben we de nadruk gelegd op mogelijke voor- en nadelige effecten van de inflammatoire reactie die plaatsvindt in het brein en perifere organen na een neonataal HI incident. We hebben in kaart gebracht wat de omvangrijke gevolgen zijn als inflammatie voorafgaat aan een HI incident (**hoofdstuk 5 en 6**). Naast een ernstige toename in hersenschade over tijd, de ontwikkeling van een cysteuze laesie en een versterkte cerebrale inflammatoire respons, laten we zien dat onderliggende mechanismen betrokken bij het ontstaan van hersenschade significant veranderen na een inflammatie,

zoals de rol van de JNK cascade en het verloop van apoptotische celdood (**hoofdstuk 5, 6**). Het is van groot belang dat zowel onderzoekers als clinici zich bewust zijn van het feit dat (veelbelovende) behandelingen mogelijk niet effectief zijn of aanpassing vereisen wat betreft dosering, therapeutisch window of combinatie van behandelingen om een beschermende werking te hebben in neonaten wanneer inflammatie voorafgaat aan een HI incident.

10

Authors and affiliations

List of abbreviations

List of publications

Dankwoord - Acknowledgements

Curriculum Vitae

Bel, Frank
Department of Neonatology, University Medical Center Utrecht, Utrecht, The Netherlands.

Bonestroo, Hilde J.C.
Laboratory of Neuroimmunology and Developmental Origins of Disease (NIDOD), University Medical Center Utrecht, Utrecht, The Netherlands.

Groenendaal, Floris
Department of Neonatology, University Medical Center Utrecht, Utrecht, The Netherlands.

Hack, Erik C.
Department of Immunology, University Medical Center Utrecht, Utrecht, The Netherlands.

Heijnen, Cobi J.
Laboratory of Neuroimmunology, Department of Symptom Research, Division of Internal Medicine, The University of Texas MD Anderson Cancer Center, Houston, USA and Laboratory of Neuroimmunology and Developmental Origins of Disease (NIDOD), University Medical Center Utrecht, Utrecht, The Netherlands.

Kavelaars, Annemieke M.A.A.
Laboratory of Neuroimmunology, Department of Symptom Research, Division of Internal Medicine, The University of Texas MD Anderson Cancer Center, Houston, USA.

Nijboer, Cora H.
Laboratory of Neuroimmunology and Developmental Origins of Disease (NIDOD), University Medical Center Utrecht, Utrecht, The Netherlands.

van Velthoven, Cindy T.J.
Laboratory of Neuroimmunology and Developmental Origins of Disease (NIDOD), University Medical Center Utrecht, Utrecht, The Netherlands.

Zijlstra, Jitske
Laboratory of Neuroimmunology and Developmental Origins of Disease (NIDOD), University Medical Center Utrecht, Utrecht, The Netherlands.

10

ADHD	Attention-deficit hyperactivity disorder
aEEG	Amplitude-integrated electroencephalogram
AIF	Apoptosis-inducing factor
AMPA	α-amino-3-hydroxy-5-methyl-4-isoxazole-propionic acid
ANOVA	Analysis of variance
AP-1	Activator protein 1
Apaf-1	Apoptotic protease activating factor 1
ART	Adhesive removal task
ATP	Adenosine triphosphate
A.U.	Arbitrary units
Bad	Bcl-2 associated death promotor
Bak	Bcl-2 homologous antagonist/killer
Bax	Bcl-2 associated protein
BBB	Blood-brain-barrier
BCA	Bicinchoninic acid
Bcl-2	B-cell leukemia/lymphoma 2
Bcl-xL	B-cell leukemia/lymphoma extra long
BDNF	Brain-derived neurotrophic factor
bFGF	basis fibroblast growth factor
BHT	Butylated hydroxytoluene
(t-)Bid	(truncated) BH-3 interacting domain death agonist
BSA	Bovine serum albumin
c	Contralateral
Ca^{2+}	Calcium
CAD	Caspase activated DNAse
CC	Corpus callosum
CINC-1	Cytokine-induced neutrophil chemoattractant 1
Cl^-	Chloride
CNPase	2′-3′-cyclic nucleotide 3′-phosphodiesterase
CNS	Central nervous system
CNTF	Ciliary-neurotrophic factor
COX	Cyclooxygenase
COX IV	Cytochrome *c* oxidase complex IV
CRT	Cylinder rearing test
CSF-1	Colony-stimulating factor 1
CTAC	Cetyltrimethylammonium chloride
Cyto	Cytosol
DAPI	4′,6-diamidino-2-phenylindole
DIABLO	Direct inhibitor of apoptosis protein-binding protein with low PI
DISC	Death-inducing signaling complex

D-JNKi	D-isomer of the JNK inhibiting peptide
DMSO	Dimethylsulfoxide
DNA	Deoxyribonucleic acid
DR	Death receptor
ELISA	Enzyme linked immunosorbent assay
EMSA	Electromobility shift assay
EPO	Erythropoietin
Eta	Etanercept
Fas	First apoptosis signal
FasL	Fas ligand
FGF	Fibroblast growth factor
GAPDH	Glyceraldehyde 3-phosphate dehydrogenase
GFAP	Glial fibrillary acidic protein
H_2O	Water
H_2O_2	Hydrogen peroxide
H_2SO_4	Sulfuric acid
HE	Hematoxylin-eosin
HI	Hypoxia-ischemia
HIE	Hypoxic-ischemic encephalopathy
HIF-1	Hypoxia inducible factor 1
HIV	Human immunodeficiency virus
HPA	Hypothalamic pituitary adrenal
HPRT	Hypoxanthine-guanine phosphoribosyltransferase
HSP70	Heat shock protein 70
i	Ipsilateral
IAP	Inhibitor of apoptosis protein
Iba-1	Ionized calcium binding adaptor molecule 1
i.c.	Intracranial
ICAM-1	Inter-cellular adhesion molecule 1
IFN	Interferon
IGF	Insulin-like growth factor
IL	Interleukin
i.n.	Intranasal
i.p.	Intraperitoneal
IRF-1	Interferon regulatory factor 1
JBD	JNK binding domain
JIP	JNK-interacting protein
JNK	c-Jun N-terminal kinase
K^+	Potassium
KIM	Kinase-interaction motif

L	Left
LPS	Lipopolysaccharide
L-JNKi	L-isomer of the JNK inhibiting peptide
MAP2	Microtubule-associated protein 2
MAPK	Mitogen activated protein kinase
MBP	Myelin basic protein
MCAO	Middle cerebral artery occlusion
MCP-1	Monocyte chemotactic protein 1
MDA	Malondialdehyde
MEK	MAPK/ERK kinase
MIP-2	Macrophage inflammatory protein 2
Mitoch	Mitochondrial
MKK	Mitogen activated protein kinase kinase
MOMP	Mitochondrial outer membrane permeabilization
MPO	Myeloperoxidase
MRI	Magnetic resonance imaging
(m)RNA	(messenger) Ribonucleic acid
MRS	Magnetic resonance spectroscopy
MSC	Mesenchymal stem cells
MUT	Mutant
n	Number
N_2	Nitrogen gas
N_2O	Nitrous oxide
Na^+	Sodium
NBD	NEMO binding domain
NC	Negative control
NEMO	NF-κB essential modulator
NeuN	Neuronal nuclei
NF-κB	Nuclear factor kappa B
NGF	Nerve growth factor
NIDOD	Neuroimmunology and developmental origins of disease
NIRS	Near-infrared spectroscopy
NMDA	N-methyl-D-aspartate
NO	Nitric oxide
NORT	Novel object recognition task
NOS	Nitric oxide synthase
ns	Non-significant
NSC	Neural stem cell
Nucl	Nuclear
O_2	Oxygen

OD	Optical density
$OH^{\cdot}$	Hydroxyl radical
Olig2	Oligodendrocyte lineage transcription factor 2
$ONOO^{-}$	Peroxynitrite
OPN	Osteopontin
P(7)	(7)-day-old/postnatal day (7)
PARP-1	Poly (ADP-ribose) polymerase 1
PBS	Phosphate buffered saline
PCA	Perchloric acid
P-c-Jun	Phosphorylated c-Jun
PDGF	Platelet-derived growth factor
PFA	Paraformaldehyde
PFT	Pifithrin
P-JNK	Phosphorylated JNK
PMN	Polymorphonuclear granulocytes
PTP	Permeability transition pore
PVHI	Periventricular hemorrhagic infarction
R	Right
RIP	Receptor interacting protein
ROS	Reactive oxygen species
RT	Room temperature
RT-PCR	Reverse transcriptase polymerase chain reaction
RTR	Rota-Rod
SCR	Scrambled sequence
SEM	Standard error of mean
SH	Sham-operated
Smac	Second mitochondria-derived activator of caspases
TAT	Transactivator of transcription
TBARS	Thiobarbituric acid reactive substances
TGF-β	Transforming growth factor beta
Thr	Threonine
TLR	Toll-like receptor
TNF-α	Tumor necrosis factor alpha
TNF-R	TNF-receptor
TRAIL	TNF-related apoptosis-inducing ligand
UMC	University medical center
VEGF	Vascular endothelial growth factor
VEH	Vehicle-treated
VRK-1	Vaccinia related kinase 1
WT	Wild type

10

Bonestroo HJ, Nijboer CH, Groenendaal F, van Bel F, Heijnen CJ. Development of cerebral gray and white matter injury and cerebral inflammation over time after inflammatory perinatal asphyxia. *Dev Neurosci.,* accepted for publication.

Bonestroo HJC, Nijboer CH, van Velthoven CTJ, van Bel F, Heijnen CJ. The neonatal brain is not protected by osteopontin peptide treatment after hypoxia-ischemia. *Dev Neurosci.,* accepted for publication.

Alderliesten T, Lemmers PM, van Haastert IC, de Vries LS, **Bonestroo HJC**, Bearts W, van Bel F. Hypotension in preterm neonates: low blood pressure alone does not affect neurodevelopmental outcome. *J Pediatr.* 2014;164:986-91.

Bonestroo HJ, Nijboer CH, van Velthoven CT, Kavelaars A, Hack CE, van Bel F, Heijnen CJ. Cerebral and hepatic inflammatory response after neonatal hypoxia-ischemia in newborn rats. *Dev Neurosci.* 2013;35:197-211.

Nijboer CH, **Bonestroo HJ**, Zijlstra J, Kavelaars A, Heijnen CJ. Mitochondrial JNK phosphorylation as a novel therapeutic target to inhibit neuroinflammation and apoptosis after neonatal ischemic brain damage. *Neurobiol Dis.* 2013;54:432-44.

Bonestroo HJ, Lemmers PM, Baerts W, van Bel F. Effect of antihypotensive treatment on cerebral oxygenation of preterm infants without PDA. *Pediatrics* 2011;128:1502-10.

Bonestroo HJ, de Winter-de Groot KM, van der Ent CK, Arets HG. Upper and low airway cultures in children with cystic fibrosis: do not neglect the upper airways. *J Cyst Fibros.* 2010;9:130-4.

Bonestroo HJ, Slieker MG, Arets HG. No positive effect of rhDNAse on the pulmonary colonization in children with cystic fibrosis. *Monaldi Arch Chest Dis.* 2010;73:12-7.

10

BAM! Na vier jaar hard knallen is het dan "opeens" klaar. De afgelopen jaren hebben veel mensen mij bijgestaan en geholpen op weg naar dit proefschrift. Zonder jullie enthousiasme, inspiratie, wetenschappelijke kennis en inzichten, helpende hand en begeleiding, vertrouwen, collegialiteit, maar vooral ook gezelligheid en humor was dit boekje er niet gekomen. In het bijzonder wil ik bedanken:

Promotoren prof.dr. Cobi Heijnen en prof.dr. Frank van Bel.

Copromotor comama dr. Cora Nijboer.

Leescommissie en opponenten prof.dr. Erik Hack, prof.dr. Annemieke Kavelaars, prof.dr. Linda de Vries, prof.dr. Boris Kramer, prof.dr. Marian Joëls, prof.dr. Gunnaer Naulaers en dr. Floris Groenendaal.

Collega's NIDOD lab Niels, Hanneke, Elke, Emiel, Erik, Luca, Marijke, Karima, Mirjam, Sabine. Oud-collega's: Lotte, Vanessa, Mariska, Marcel, Cindy, Huijing, Jitske, Maike, Mirjam, Annibal en Debby.

Collega's neonatologie Karina, Thomas, Kristin, Inge-Lot, Manon en Petra. Oud-collega's: Margaretha, Niek, Johanneke, Joppe en Britt.

Alle collega's arts-onderzoekers, arts-assistenten en kinderartsen uit het WKZ.

GDL medewerkers en in het bijzonder Helma, Anja, Paul, Norma, Romy en Jan.

Oud-collega's Gelderse Vallei Ede: dr. Gert van Enk, kinderartsen en lieve verpleging.

Vrienden Marieke, Jan-Willem, Marjolein, Timo, Nienke, Fiona en Manik.

Familie Papa en Mama, Tijmen en Aafke, Floor en Jasper, Tinus en Oukje, en natuurlijk ook de "schone" familie.

Mijn twee helden Nick en Jeske.

10

Hilde Bonestroo was born on October 9th 1984 in Heerlen, the Netherlands. She grew up with two brothers and one sister in Susteren. In 2003 she graduated from secondary school and started Medical school at Utrecht University. During her Medical training she was involved in two research projects at the Department of Pediatric Pulmonology at the Wilhelmina Children's Hospital in 2007 and 2008 under supervision of dr. Bert Arets. An internship in Pediatrics/Tropical Medicine was performed in the Igogwe Mission Hospital in Tanzania. She carried out her Research internship at the Department of Neonatology at the Wilhelmina Children's Hospital under supervision of dr. Petra Lemmers and prof. dr. Frank van Bel. After graduating from Medical school in 2009 she started working as a resident at the Department of Pediatrics at Gelderse Vallei Hospital in Ede under supervision of dr. Gert van Enk.

In August 2010 she started working as a PhD student on the project described in this thesis at the Laboratory of Neuroimmunology and Developmental Origins of Disease (NIDOD) and Department of Neonatology at the Wilhelmina Children's Hospital under supervision of prof. dr. Cobi Heijnen, prof. dr. Frank van Bel and dr. Cora Nijboer.

In December 2014 she will start her training in Pediatrics at the Wilhelmina Children's Hospital under supervision of dr. Joost Frenkel. The first one and a half year she will work at the Department of Pediatrics at Gelre Hospital in Apeldoorn under supervision of dr. Bianca van Maldegem.

Hilde is married to Nick, and together they have a daughter, named Jeske.